Mechanisms of Exercise Intolerance in Heart Failure

Sophie Alexandrea Hampson

Submitted in accordance with the requirements for the degree of Doctor of Philosophy

The University of Leeds
School of Biomedical Sciences
Faculty of Biological Sciences

December, 2018

The candidate confirms that the work submitted is her own and that appropriate credit has been given where reference has been made to the work of others.

Acknowledgements

I would like to express my sincere gratitude to my supervisors; Drs Al Benson, Carrie Ferguson, Klaus Witte and Harry Rossiter for their continued support and guidance. In addition, I would like to thank Drs Bryan Taylor, Scott Bowen, Dan Cannon and Professor Stuart Egginton, for their helpful comments, questions, and constructive feedback throughout. Also, thanks to Dr Bruno Grassi, who provided me with data to validate my model.

Thank you to my fellow lab mates, Said, Molly, Nick, Matt C, Tim, Abby, Marcelle, and especially Drs Matthew Davies and Gemma Lyall for all the help and support you have given me; and to Matthew Davies and Jack Graham who I carried out part of my data collection with.

I would like to thank all my friends and family, past and present, who have helped me become the person I am today. To my mum, for her unwavering faith in me, my dad, for his words of wisdom, and to Emma, Chloe, Jack and the Gavin's for all their love and support.

Finally, to my partner Mike (who knows far more about $\dot{V}O_2$ kinetics than he ought to); thank you for not only putting up with all my crazy ambitions, but for supporting and encouraging me to fulfil them!

This work was funded by a Medical Research Council-Doctoral Training studentship.

Abstract

Heart failure is a complex clinical syndrome where the heart is unable to maintain adequate cardiac output to meet the metabolic demands of tissues. This leads to a cascade of events that act to impair the oxygen transport system, giving rise to symptoms of fatigue and/or dyspnoea on exertion and, in more severe cases, at rest. Accordingly, exercise intolerance is a cardinal symptom of heart failure, and is a strong predictor of prognosis and mortality. As such, an individual's tolerance to exercise is inextricably linked to diagnosis in heart failure. The mechanisms for this exercise intolerance are still not fully understood and currently there is a debate surrounding whether exercise tolerance is governed primarily by impairments in cardiac function (i.e. oxygen delivery), or impairments at the skeletal muscle level (i.e. oxygen utilisation), or both. Resolving this issue has implications for improving and tailoring effective treatment in heart failure.

The work presented in this thesis fulfils two major aims: (i) the development and validation of a computational model of circulatory and oxygen uptake dynamics, that is able to predict oxygen uptake measurements that are experimentally measured at the lungs, and at the skeletal muscle, for ramp incremental exercise and; (ii) the assessment of the clinical utility of using near infrared spectroscopy as a non-invasive tool to determine the locus of exercise intolerance in heart failure patients.

The computational model of circulatory and oxygen uptake dynamics demonstrated that cardiopulmonary breath-by-breath gas exchange measurements alone are not sufficient to identify the locus of exercise intolerance in heart failure patients. However, with the addition of a model output that gives specific information on the skeletal muscle oxygenation dynamics, insights into the mechanisms governing exercise tolerance can be gained.

Near infrared spectroscopy was utilised under two different experimental conditions. During ramp incremental exercise, it was shown that near infrared spectroscopy can provide specific information regarding the locus of exercise intolerance in heart failure, particularly, those with oxygen delivery limitations. In addition, using a novel technique to assess oxidative capacity, it was established that near infrared spectroscopy can be used to produce reliable assessment of skeletal muscle function and, thereby, proves a promising technique to identify those with skeletal muscle dysfunction.

Contents

List of tables

List of figures

Abbreviations

$(a\text{-}v)O_2$	arterio-venous oxygen content
$\Delta\dot{V}O2/\Delta\dot{Q}$	change in oxygen uptake per change in blood flow
$\Delta\dot{V}O2/\Delta WR$	change in oxygen uptake per Watt change in work rate
ADP	adenosine diphosphate
AIC	Akaike Information Criterion
AICc	corrected Akaike Information Criterion
ATP	adenosine triphosphate
BP	blood pressure
$C\bar{v}O_2$	mixed venous oxygen concentration
C_aO_2	arterial oxygen concentration
C_{Hb}	Hüfners constant
CO	cardiac output
CO_2	carbon dioxide
CRT	cardiac resynchronisation therapy
C_vO_2	venous oxygen concentration
C_vO_{2b}	body venous oxygen concentration
C_vO_{2m}	muscle venous oxygen concentration
CWS	continuous wave spectroscopy
DO_{2m}	muscle oxygen diffusing capacity
DPF	differential path length factor
e	exponential term
f_a	arterial blood fraction in muscle
f_b	blood fraction in muscle
f_c	capillary blood fraction in muscle
f_i	tissue fraction in muscle
fv	venous blood fraction in muscle
G_{fibre}	muscle fibre gain
H^+	hydrogen ions
Hb	haemoglobin
$HbMbO_2$	oxygenated haemoglobin + myoglobin
$HbMbO_{2,\ norm}$	normalised haemoglobin + myoglobin signal
HbO_2	oxygenated haemoglobin
$HbO_{2,a}$	oxyhaemoglobin concentration arterial blood
$HbO_{2,c}$	oxyhaemoglobin concentration capillary blood
$HbO_{2,v}$	oxyhaemoglobin concentration venous blood
HF	heart failure
HHb	deoxygenated haemoglobin
$HHb_{,a}$	deoxygenated haemoglobin concentration arterial blood
$HHb_{,c}$	deoxygenated haemoglobin concentration capillary blood

$HHb_{,v}$	deoxygenated haemoglobin concentration venous blood
HHbMb	deoxygenated heamoglobin + myoglobin
$HHbMb_{,norm}$	normalised deoxygenated haemoglobin + myoglobin signal
HMb	deoxygenated myoglobin
$HMb_{,i}$	concentration deoxygenated myoglobin in tissue
HR	heart rate
k	proportionality constant
LVEF	left ventricular ejection fraction
Mb	myoglobin
MbO_2	oxygenated myoglobin
$MbO_{2,i}$	concentration of oxygenated myoglobin in tissue
MCM	multi compartment model
M_{Hb}	molar haemoglobin
M_{Mb}	molar myoglobin
MRT	mean response time
$m\dot{V}O_2$	muscle oxygen consumption
N_{fibres}/W	number of muscle fibres recruited per watt of exercise
NIRS	near infrared spectroscopy
NYHA	New York Heart Association
O_2	oxygen
P_{50}	myoglobin half saturation pressure
PCO_2	partial pressure carbon dioxide
PcO_2	capillary oxygen partial pressure
PCr	phosphocreatine
Pi	inorganic phosphate
P_iO_2	tissue oxygen partial pressure
$PmVO_2$	microvascular partial pressure oxygen
PO_2	partial pressure oxygen
$\dot{Q}$	blood flow
$\dot{Q}_b$	baseline blood flow
$\dot{Q}_{fib}$	steady state change in muscle fibre blood flow
$\dot{Q}_m$	muscle blood flow
$\dot{Q}_m\,\boldsymbol{\tau}$	muscle blood flow kinetics
$\dot{Q}_{tot}$	total blood flow
$\dot{Q}\boldsymbol{\tau}$	blood flow kinetics
RISE	ramp incremental step exercise
S_aO_2	arterial oxygen saturation
S_cO_2	capillary oxygen saturation
S_iO_2	tissue oxygen saturation
SRS	spatially resolved spectrometry
SS	steady state
SV	stroke volume
S_vO_2	venous oxygen saturation

t	time
TD	time delay
TOI	tissue oxygenation index
$t_{recruit}$	fibre recruitment time
V_a	arterial volume
V_b	blood volume
V_c	capillary volume
V_i	tissue volume
V_m	muscle volume
$\dot{V}O_2$	oxygen uptake
$\dot{V}O_{2,b}$	baseline oxygen uptake
$\dot{V}O_{2,max}$	maximal oxygen uptake
$\dot{V}O_{2,peak}$	peak oxygen uptake
$\dot{V}O_{2A}$	alveolar oxygen uptake
$\dot{V}O_{2fib}$	steady state change in muscle fibre oxygen uptake
$\dot{V}O_{2m}$	muscle oxygen uptake
$\dot{V}O_{2m}$ $\boldsymbol{\tau}$	muscle oxygen uptake kinetics
$\dot{V}O_{2m,b}$	baseline muscle oxygen uptake
$\dot{V}O_{2p}$	pulmonary oxygen uptake
$\dot{V}O_2\boldsymbol{\tau}$	Phase II oxygen uptake kinetics
Vv	venous volume
W	watts
WR	work rate
α_b	solubility coefficient of oxygen in blood
$\boldsymbol{\tau}$	time constant

Overview

Heart failure (HF) is considered a global pandemic, affecting approximately 26 million people worldwide and rising in prevalence with an increasing aging population (Ponikowski et al., 2014). Despite the significant advances in therapies and prevention, mortality and morbidity rates are still high and quality of life poor (Savarese and Lund, 2017).

HF is a complex clinical syndrome, where the heart is unable to maintain adequate cardiac output to meet the metabolic demands of tissues (Kemp and Conte, 2012). The clinical sequelae of this results in symptoms of fatigue or dyspnoea on exertion and, in more severe cases, at rest. Accordingly, exercise intolerance is one of the main symptoms experienced by heart failure patients, and is often a principal reason for seeking medical care (Piña et al., 2003; Kitzman and Groban, 2008). Lower exercise capacity is also associated with mortality in both health and heart failure (Mancini et al., 1991; Myers et al., 2002). Furthermore, heart failure is often classified based upon the functional capacity of the patient (Weber et al., 1982; Kemp and Conte, 2012; Bredy et al., 2018). Therefore, exercise intolerance is inextricably linked to the diagnosis of heart failure (Kitzman and Groban, 2008).

Exercise intolerance occurs when an individual is unable to sustain a rate of external work for a duration sufficient to complete the required task (Rossiter, 2011). It is logical to think that indices of cardiac function would be strongly related to exercise tolerance in heart failure. However, evidence shows this is not the case (Franciosa et al., 1981; Weber et al., 1984; Lipkin and Poole-Wilson, 1986; Witte et al., 2004). As such, many studies have sought mechanisms to explain the source of exercise intolerance present in heart failure patients.

There is evidence to suggest impairments at the skeletal muscle level are related to a reduced exercise capacity in heart failure (Hepple et al., 1999; Bowen et al., 2012). However, the exact mechanisms of this are still not completely understood. In addition, identifying the primary source (i.e. whether a patient is primarily limited by cardiac related issues or by skeletal

muscle related issues) of the exercise intolerance in a given patient poses an even bigger challenge.

Detailed knowledge of the pathophysiological mechanisms underlying exercise intolerance has implications for tailoring and optimising treatments on an individual patient level, as well as for the development of new therapeutic interventions, and evaluation of the effectiveness of current interventional strategies. In turn, a thorough understanding of the mechanisms determining exercise intolerance may help to reduce the burden that heart failure places on NHS resources, and improve the quality of life in patients suffering with heart failure.

This thesis aims to explore these issues, with a particular attention paid to impairments at the skeletal muscle level as the primary source of exercise intolerance. This will be achieved using a combined computational and experimental approach. There are two major aims of this thesis: (i) *computational approaches* to develop and validate a previously published computational model of circulatory and oxygen uptake dynamics for constant-intensity work rate exercise, that is able to predict oxygen uptake measurements that are experimentally measured at the lungs (i.e. pulmonary oxygen uptake), and at the skeletal muscle (i.e. muscle oxygen uptake) for changing-intensity work rate exercise and; (ii) *experimental approaches* to test the clinical utility of using near infrared spectroscopy as a non-invasive tool to identify individuals with skeletal muscle oxygen delivery limitations, and/or skeletal muscle oxygen utilisation impairment, in order determine the primary locus of exercise intolerance in heart failure patients.The major aim of chapter 1 is to provide an overview of the key physiological concepts that underpin this thesis and are important in understanding model development. This will include a detailed overview of oxygen uptake kinetics, as well as one the key relationships governing them: the oxygen delivery-to-oxygen utilisation relationship. Chapter 1 will also describe the physiology of the oxygen uptake response to exercise, defining key physiological markers of exercise intensity, how oxygen uptake is measured, how its kinetics are determined, and their clinical importance. The concepts described in Chapter 1 are central to this thesis and will be referred to throughout subsequent chapters. Chapter 2 contains the experimental methodology for each study including data collection, exercise protocols, measurements and equipment used and data analysis.

The major aim of chapter 3 is to validate a computational model of circulatory and oxygen uptake dynamics for ramp incremental exercise. In Chapter 4 this model is developed further to include an assessment of muscle oxygenation dynamics. One of the key concepts presented in Chapter 1 is the use of near infrared spectroscopy, a measurement technique that is key to this thesis and will feature throughout subsequent chapters. Chapter 2 will describe the key studies that have utilised near infrared spectroscopy, and that are relevant to this thesis. The chapter will then go on to describe the model development and model validation process, before describing the results from a sensitivity analysis of the model.

The following chapters will focus on model application and experimental approaches. This includes utilising three different approaches to measuring, non-invasively, impairments at a skeletal muscle level.

Chapter 5 will focus on 'whole body' approaches, where separating circulatory, pulmonary and muscle factors can prove challenging. Chapter 5 will utilise a combination of the models presented in chapters 3 and 4, and experimental data collected in healthy and heart failure participants. Its major aim is to quantify what the pulmonary oxygen uptake measurements in heart failure patients truly represent.

Chapters 6 and 7 will present two further different methods of non-invasively investigating skeletal muscle function. Chapter 6 will focus on the dynamic relationship between oxygen delivery and oxygen utilisation, while Chapter 7 aims to investigate, solely, muscle oxygen utilisation (i.e. in isolation from oxygen delivery). In Chapter 6, the main aim is to characterise and quantify muscle oxygenation dynamics in response to ramp incremental in heart failure patients.

The major aim of Chapter 7 is to test the reproducibility of a non-invasive method of assessing skeletal muscle function, without the confounding influences of oxygen delivery. Chapter 7 will begin by providing an overview of the oxidative capacity technique, as well as the current evidence behind it. Chapters 4-7 explore non-invasive methods of determining the locus of exercise intolerance in heart failure, with increasing specificity with each chapter. Chapter 5 utilises a whole-body approach, whilst Chapter 6 looks at

oxygen delivery in relation to oxygen utilisation and Chapter 7 looks solely at oxygen utilisation.

Chapter 1 General Introduction

1.1 Oxygen uptake kinetics

At the onset of exercise there is an increased demand on the body to deliver and utilise oxygen to provide the required energy to support the activity. This requires the effective co-ordination of the pulmonary, cardiovascular, and neuromuscular systems. The rate at which the body can adapt from one metabolic state to another (its kinetics) determines, in part, how well an individual copes with the increased work load (Rossiter, 2011). The uptake of oxygen by biological tissue can be described by the Fick principle:

$$\dot{V}O_2 = \dot{Q}\left(C_aO_2 - C_vO_2\right), \quad (1)$$

where $\dot{V}O_2$ is oxygen uptake (with units of L/min), $\dot{Q}$ is blood flow (L/min), and C_aO_2 and C_vO_2 are arterial and venous oxygen concentrations, respectively (L O_2 per L blood), with C_aO_2 typically remaining constant during exercise (Grassi et al., 1998). By rearranging the Fick equation:

$$C_vO_2 = C_aO_2 - (\dot{V}O_2 / \dot{Q}), \quad (2)$$

and noting that C_aO_2 is typically constant, such that:

$$C_vO_2 \propto \dot{V}O_2 / \dot{Q}, \quad (3)$$

muscle oxygenation (as reflected in C_vO_2) is proportional to the ratio of O_2 delivery (i.e. $\dot{Q}$) to O_2 utilisation (i.e. $\dot{V}O_2$). A drop in the $\dot{Q}/\dot{V}O_2$ ratio (i.e. a decrease in O_2 delivery, an increase in O_2 utilisation, or both) can reduce muscle oxygenation and inhibit peripheral O_2 exchange. However, both $\dot{Q}$ and $\dot{V}O_2$ change during exercise, and so it is the *kinetics* of the changes in $\dot{Q}$

and $\dot{V}O_2$ that determine muscle oxygenation during exercise: as such, the *transient dynamics* of the $\dot{Q}/\dot{V}O_2$ relationship (reflected in the C_vO_2 profile) are key determinants for maintaining oxidative phosphorylation during exercise (Whipp and Ward, 1992; Koga et al., 2014). Understanding the complicated dynamics of the $\dot{Q}/\dot{V}O_2$ relationship during exercise (which are determined by their steady state relationship, and their kinetics) can therefore provide a window into understanding metabolic control (O_2 delivery and utilisation, and muscle oxygenation) at the working muscle at the onset of, during and after exercise (Poole et al., 2008). Before exploring $\dot{V}O_2$ kinetics in relation to their influence upon exercise tolerance, it is important to first understand this $\dot{V}O_2/\dot{Q}$ relationship, one of the key relationships governing oxygen uptake.

1.2 The $\dot{V}O_2/\dot{Q}$ relationship

The *steady state* relationship between $\dot{V}O_2$ and $\dot{Q}$ is linear and is approximately 5-6 (Saltin et al., 1968; Faulkner et al., 1977; Richardson et al., 1993). Figure 1 shows this steady state linear relationship between $\dot{V}O_2$ and $\dot{Q}$ at the exercising muscle (i.e. $\dot{V}O_{2m}$ and $\dot{Q}_m$ respectively). The figure shows the theoretical $\dot{V}O_{2m}/\dot{Q}_m$ relationship of an individual during steady state exercise. In this case (i.e. under the steady state condition), the way an individual “travels”’ from their starting point (Point A) to their end point (Point B) is linear (blue line).

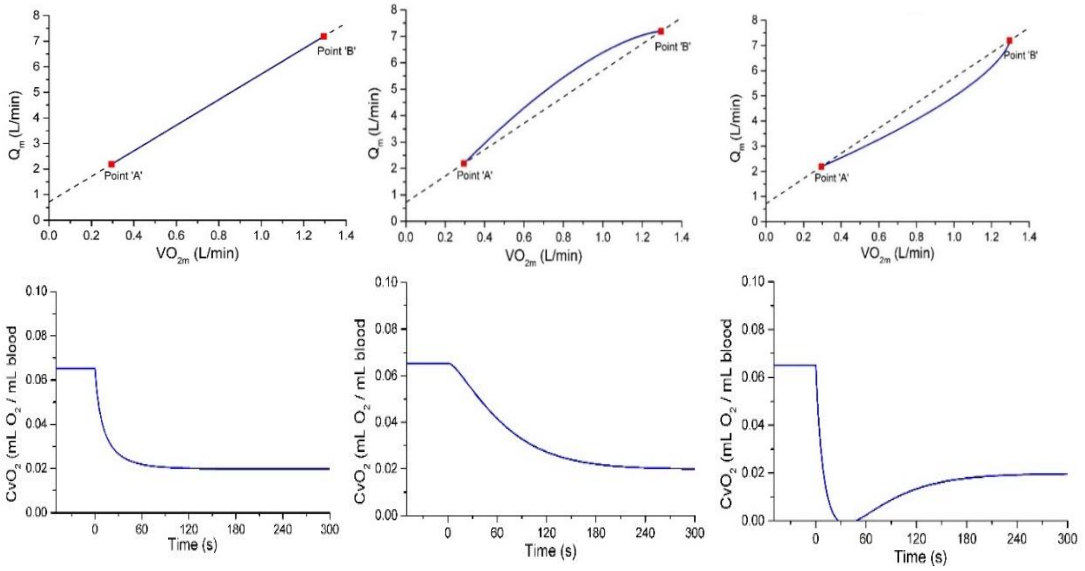

Figure 1: Top panel (left) The $\dot{V}O_{2m}/\dot{Q}_m$ relationship during steady state conditions. The dashed line shows this steady state relationship, with an increase in $\dot{Q}_m$ of 5 L/min for every 1 L/min increase in $\dot{V}O_{2m}$. The red squares represent start and end points. Blue solid line represents how an individual "travel" from point A to point B with time constants of 30s for both $\dot{V}O_{2m}$ and $\dot{Q}_m$**.** Middle: $\dot{V}O_{2m}$-$\dot{Q}_m$ relationship with time constants of 30s for $\dot{Q}_m$ and 45s for $\dot{V}O_{2m}$ (i.e. $\dot{V}O_{2m}$ kinetics are slow relative to $\dot{Q}_m$ kinetics). (Right) $\dot{V}O_{2m}/\dot{Q}_m$ relationship with time constants of 45s for $\dot{Q}_m$ and 30s for $\dot{V}O_{2m}$ (i.e. $\dot{V}O_{2m}$ kinetics are fast relative to $\dot{Q}_m$ kinetics).In both conditions the $\dot{V}O_{2m}/\dot{Q}_m$ relationship no longer follows a linear profile but rather overshoots (when $\dot{Q}_m$ kinetics fast relative to $\dot{V}O_{2m}$ kinetics; top middle) or undershoots (when $\dot{Q}_m$ kinetics slow relative to $\dot{V}O_{2m}$ kinetics; top right) the steady state increase, to get from point A to point B. Bottom panel**:** Muscle C_vO_2 profile during the steady state with time constants for $\dot{V}O_{2m}$ and $\dot{Q}_m$ of 30 s (left), and during exercise transition in which $\dot{Q}_m$ kinetics are fast relative to $\dot{V}O_{2m}$ kinetics, where time constant of $\dot{Q}_m$ is 30 s and $\dot{V}O_{2m}$ 45 s (middle), and where $\dot{Q}_m$ kinetics are slow relative to $\dot{V}O_{2m}$ kinetics, with time constants of 45 s for $\dot{Q}_m$ and 30 s for $\dot{V}O_{2m}$ (right). During steady state conditions muscle C_vO_2 decreases hyperbolically, however in conditions where $\dot{Q}_m$ kinetics are slowed muscle C_vO_2 undershoots its steady state values. NB: it is recognized that CvO_2 = 0 mL/O_2/mL blood is a theoretical artefact of the model not possible under physiological conditions but is used here to demonstrate the influence of $\dot{V}O_2$ and $\dot{Q}$ kinetics on oxygen extraction.

This relationship only holds true however, in the steady state. Therefore, during exercise transitions (i.e. when an individual is no longer in a steady state), how an individual "travels" to and from point A to point B can change. For example, Figure 1 also shows the $\dot{V}O_{2m}/\dot{Q}_m$ relationship under conditions where $\dot{Q}_m$ kinetics are faster than $\dot{V}O_{2m}$ kinetics (left). As shown, The $\dot{V}O_{2m}$-$\dot{Q}_m$ relationship is no longer linear, but rather overshoots the steady state line to get from point A to point B (blue line). Conversely, if $\dot{V}O_{2m}$ kinetics are faster than $\dot{Q}_m$ kinetics (right), the $\dot{V}O_{2m}$-$\dot{Q}_m$ relationship undershoots its steady state line to get from point A to point B.

This is important to consider as how an individual "travels" from point A to point B determines the muscle oxygenation profile (i.e. how much oxygen is extracted from the muscle). As such, the extent to which $\dot{V}O_{2m}$ and $\dot{Q}_m$ kinetics are speeded or slowed relative to each other influences muscle oxygenation also. This is shown in Figure 1: a linear increase in the $\dot{V}O_{2m}/\dot{Q}_m$ relationship (i.e. top panel, left) necessitates a hyperbolic decrease in C_vO_2 (bottom panel, left), whereas faster $\dot{Q}_m$ kinetics in relation to $\dot{V}O_{2m}$ kinetics reduces the extent to which the muscle is drained of O_2 during the transient (middle). Finally, in situations where $\dot{V}O_{2m}$ kinetics are fast relative to $\dot{Q}_m$ kinetics, there is an undershoot in muscle C_VO_2 before returning to its steady state, causing the muscle to be completely drained of O_2 in this simulation (right). This is pertinent in diseases which act to slow $\dot{Q}_m$ kinetics, such as heart failure.

1.3 $\dot{V}O_2$ kinetics in relation to exercise tolerance

Directly measuring exercising $\dot{V}O_{2m}$ and $\dot{Q}_m$ kinetics is technically challenging. For example, Grassi et al. (1996) used constant-infusion thermodilution techniques in combination with arterial and femoral venous blood sampling to measure leg blood flow and arteriovenous difference to calculate muscle $\dot{V}O_2$ using the Fick principle (Equation 1) during moderate intensity cycling in healthy young individuals. However, this method is extremely invasive and complex. Nevertheless, the study by Grassi et al. (1996) demonstrated that the kinetics of skeletal muscle $\dot{V}O_2$ and pulmonary $\dot{V}O_2$ (i.e. O_2 uptake measured non-invasively at the mouth, and O_2 uptake measured simultaneously at the skeletal muscle level) closely matched, to

within 2-3 seconds; these empirical findings confirmed previous modelling predictions that pulmonary $\dot{V}O_2$ kinetics are a close approximation of muscle oxygen consumption following exercise onset (Barstow et al., 1990). Therefore, a more commonly used and non-invasive method is to infer muscle $\dot{V}O_2$ ($\dot{V}O_{2m}$) and its kinetics indirectly from breath-by-breath measurements of pulmonary $\dot{V}O_2$ ($\dot{V}O_{2p}$). This non-invasive method of inferring $\dot{V}O_{2m}$ kinetics from $\dot{V}O_{2p}$ kinetics has led to a large focus on $\dot{V}O_{2p}$ kinetics, and their relation to exercise tolerance (Rossiter, 2011).

Faster $\dot{V}O_{2p}$ kinetics reflect a rapidly functioning (and therefore effective) physiological system; trained (versus untrained) individuals typically have faster $\dot{V}O_{2p}$ kinetics. Conversely, $\dot{V}O_{2p}$ kinetics are typically slowed in disease states such as heart failure (Belardinelli et al., 1997; Sperandio et al., 2009; Kemps et al., 2010; Bowen et al., 2012; Mezzani et al., 2013), suggesting that these patients have impairments at some point along the O_2 transport pathway that inhibits the body's ability to adjust to the new requirements for O_2 delivery and utilisation. Slowed $\dot{V}O_{2p}$ kinetics are strongly correlated to exercise intolerance (Sperandio et al., 2009) and, as such, are a highly prognostic indicator of morbidity and mortality in in diseases such as heart failure (Schalcher et al., 2003). The consequence of a slower $\dot{V}O_{2p}$ response is a greater reliance on anaerobic energy generating pathways, which are limited in their capacity. An increased reliance on anaerobic energy generating pathways results in reductions in phosphocreatine (PCr), adenosine triphosphate (ATP) and glycogen, as well as the formation of lactate. In addition, there is a build-up of metabolites detrimental to muscle function, such as adenosine diphosphate (ADP), inorganic phosphate (Pi), and hydrogen ions (Allen et al., 2008), all of which contribute to increased muscle fatigue and, consequently, exercise intolerance.

The mechanisms contributing to the slowed $\dot{V}O_{2p}$ kinetics in heart failure are still not completely understood, but have been suggested to be as a result of: (i) a reduced O_2 delivery (Hughson and Morrissey, 1982; Hughson, 1984) due to a reduction in cardiac output (Cerretelli et al., 1988) and/or impairments in blood flow distribution to the exercising skeletal muscle (Richardson et al., 2003); and (ii) O_2 utilisation limitations in the exercising skeletal muscle (Grassi et al., 1997, 1998; Bowen et al., 2012; Richardson et al., 2015) due to mitochondrial dysfunction, and/or a reduction in the number

of mitochondria due to muscle atrophy, or a shift in muscle fibre type distribution away from type I and towards type II (less oxidative) fibres (Drexler et al., 1992; Kemps et al., 2010). Resolution of this issue is essential for understanding the mechanistic bases for the impaired $\dot{V}O_{2p}$ kinetics found in patient populations (Poole et al., 2008) which, in turn, may help to target future therapeutic interventions to improve exercise tolerance, and explain the variance often seen in treatment effectiveness. Understanding the characteristics and different components of the $\dot{V}O_{2p}$ response is therefore a necessary first step in understanding $\dot{V}O_{2p}$ kinetics and its role in exercise, health and disease.

1.4 Exercise intensity domains

In addition to its kinetics, the $\dot{V}O_{2p}$ profile during constant work rate exercise has been utilised to define the 'exercise intensity' at which an individual is working. Exercise intensity is a key concept in exercise physiology, as it allows appropriate normalisation for exercise stressors between individuals (Rossiter, 2011). Exercise performed at the same intensity should have a common stress response profile between individuals. However, defining exercise intensity based on single physiological parameters (such as percentage of maximal oxygen uptake; $\%\dot{V}O_{2,max}$) could result in markedly different physiological responses amongst different individuals. This was demonstrated by Rossiter (2011), who assigned two individuals the same absolute work rate and percentage $\dot{V}O_{2,max}$ (85%) during constant work rate cycle-ergometry exercise. Despite this normalisation, one of the individuals was only able to sustain the work rate for around ten minutes (where they reached the limit of tolerance), whereas the other individual was able to attain a steady state and maintain the exercise for 30 minutes, resulting in markedly different physiological responses. An alternative method of assigning exercise intensity is by using other physiological markers such as lactate threshold, critical power and $\dot{V}O_{2,max}$ (Figure 2). The lactate threshold can be described as the level of work or O_2 uptake just below that at which metabolic acidosis and associated changes in gas exchange occur, and exercise performed below lactate threshold can be sustained for long periods of time (Wasserman et al., 1973). Critical power can be defined as the highest work rate at which a steady state in $\dot{V}O_2$, blood lactate, phosphocreatine, and inorganic phosphates can be achieved, representing

the asymptote of the hyperbolic relationship between work rate and time to intolerance for a given individual (Rossiter, 2011). Within a given 'intensity domain' different components of the $\dot{V}O_{2p}$ response to constant load exercise can be identified; that is, $\dot{V}O_{2p}$ profiles show different characteristics depending on the intensity domain the individual is exercising in (Whipp, 1994) as shown in Figure 2.

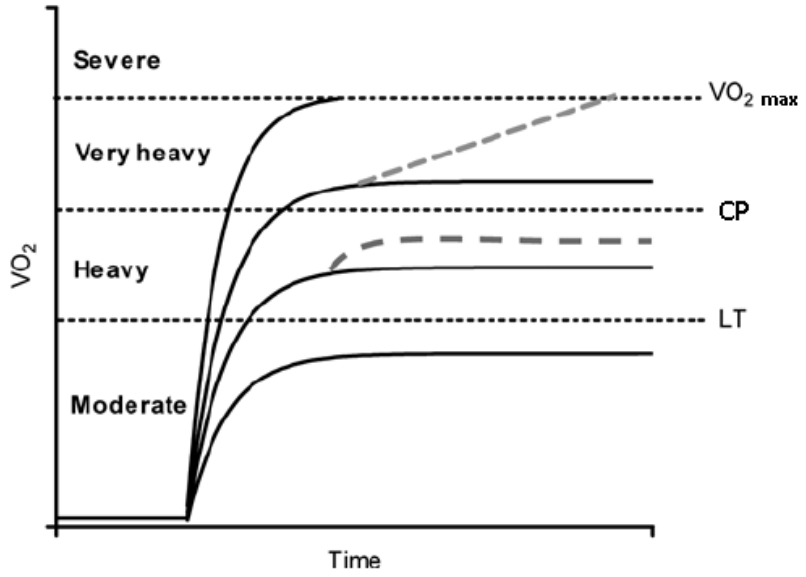

Figure 2: Intensity domains of muscular exercise and their associated $\dot{V}O_2$ responses. The horizontal dashed lines represent the physiological boundaries demarcating the moderate, heavy, very heavy and severe exercise intensity domains. The solid black curves show the $\dot{V}O_{2p}$ response in each exercise intensity domain. The grey dashed lines represent the $\dot{V}O_2$ slow component, causing $\dot{V}O_2$ to rise above that predicted by the sub LT $\dot{V}O_2$ work-rate relationship. CP, critical power; LT, lactate threshold. Adapted from Rossiter (2011).

Exercise performed below the lactate threshold has been termed 'moderate' intensity exercise (Whipp et al., 1982). In the moderate intensity domain there is no sustained metabolic acidosis, and an early steady state in $\dot{V}O_{2p}$ is attained (usually within three minutes in healthy adults). For all work rates in the moderate intensity domain, once a steady state has been attained, 100% of ATP resynthesis requirements can be met by oxidative metabolism (Özyener et al., 2001). Exercise performed above the lactate threshold, but below critical power can be defined as 'heavy' intensity exercise. Exercise in this domain becomes more complex (Whipp and Wasserman, 1972; Whipp, 1994; Gerbino et al., 1996) with the development of a delayed increase in

$\dot{V}O_2$, known as the “slow component”. The slow component is generated principally in the exercising muscles (Poole et al., 1991), and is thought to represent reduced work efficiency by mechanisms related to; increased ATP requirement, and/or reduced power contribution from fatiguing muscle fibers, necessitating an increased power production from already recruited fibers or recruitment of additional fibers (Jones et al., 2011). Nevertheless, a (delayed) steady state is still achieved in the heavy intensity exercise domain, as such exercise in this domain is still sustainable. ‘Very heavy’ intensity exercise (between critical power and $\dot{V}O_{2,max}$) is characterised by a $\dot{V}O_{2p}$ response with a slow component that continues to increase throughout the test towards $\dot{V}O_{2,max}$. A steady state in $\dot{V}O_{2p}$ is not achieved in this domain (Özyener et al., 2001); instead, there is a progressive rise until $\dot{V}O_{2,max}$ is reached. During ‘severe’ intensity exercise, the limit of tolerance is reached before a $\dot{V}O_{2p}$ slow component can develop, or be clearly distinguishable (Özyener et al., 2001). Work rates in this domain can usually only be sustained for a few minutes.

Despite the usefulness of the $\dot{V}O_{2p}$ response in characterising exercise intensity, exercise capacity, and health status, it is important to note that the $\dot{V}O_{2p}$ response is a ‘whole body’ measure. As such, when it comes to its kinetics, inferring $\dot{V}O_{2m}$ kinetics from $\dot{V}O_{2p}$ kinetics needs to be done carefully. $\dot{V}O_{2p}$ kinetics not only reflect $\dot{V}O_{2m}$ kinetics, but are influenced by muscle-to-lung transit time delays, and changes in vascular O_2 concentrations which can complicate estimation of $\dot{V}O_{2m}$ from cardiopulmonary measurements (Barstow et al., 1990). According to equation 2 and, as C_aO_2 is typically constant in healthy humans throughout exercise (Grassi et al., 1996), the O_2 content in the venous effluent of the contracting muscle is determined by the ratio between $\dot{V}O_{2m}$ and $\dot{Q}_m$ through the exercise transient (as described earlier). Any value of muscle C_vO_2, therefore, is dependent on the ratio of muscle $\dot{V}O_{2m}$ to muscle $\dot{Q}_m$. However, the muscle C_vO_2 profile (and therefore the muscle $\dot{V}O_2$ profile) is distorted as it travels to the lungs. The muscle venous effluent from the exercising muscle is at some point mixed with venous effluent from other, non-exercising, tissues in a flow-weighted manner. These venous effluents (both before and after mixing) must also travel through a series of venous volumes (Vv) to the lungs, that results in a transit delay between the C_vO_2 profile appearing at the muscle and appearing at the lungs. However, the muscle-to-lung transit delay *is not constant* during the exercise transient, but varies with blood flow, and the size of the venous volumes (Bangsbo et al., 2000).

$\dot{V}O_{2p}$ transients are, therefore, non-linear distorted variants of $\dot{V}O_{2m}$ (Benson et al., 2013; Hoffmann et al., 2013). The muscle-to-lung transit delay is typically thought to be around 20s at rest and can fall to about 10s during exercise (Krustrup et al., 2009). The greater the increment in blood flow to the exercising tissue at the onset of exercise, the larger the reduction in the transit delay (Rossiter, 2011). This is demonstrated in Figure 3 (left), which shows muscle-to-lung transit time during a step increase in work rate from 0 W to 50 W (red line), 0 W to 100 W (black line) and 0 W to 150 W (blue line). When the increment in blood flow to the exercising muscle is increased (achieved by increasing the work rate by a greater amount), the transit time is shorter, and vice versa. The *baseline* blood flow will also affect the muscle-to-lung transit delay, as shown in Figure 3 (Right). When baseline blood flow is decreased (red line) compared to control (black line), the initial (steady state) transit delay, plus the subsequent exercise time delays, become longer, and when baseline blood flow is increased (blue line) the transit delays are shorter.

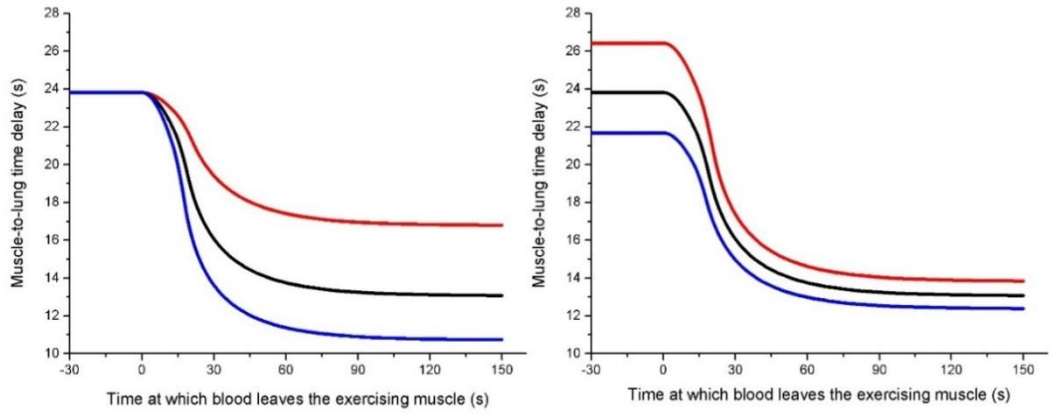

Figure 3: Left: The muscle-to-lung transit delay during simulations of a work rate step from: 0 to 50W (red line); 0 to 100W (black line); and 0 to 150W (blue line). The higher the step in work rate, the larger the increment in blood flow to the exercising tissues, resulting in a smaller muscle-to-lung transit delay during the exercise bout. Right: The muscle-to-lung transit delay during simulations of a work rate step from 0 to 100 W, for three different baseline blood flows: 8.01 L/min (red line), 8.89 L/min (black line) and 9.77 L/min (blue line). When baseline blood flow is increased (causing an increased blood flow throughout subsequent exercise), the transit delay is smaller.

Note, in this simulation the increment in blood flow stays the same, and only the baseline blood flow is altered. Furthermore, the rate of the mixing of the muscle and non-exercising effluents is also dependent on blood flow and the size of the venous volumes. The effluent which has a higher fraction of blood will have a bigger influence on the mixing and, moreover, the effluent which reaches the mixing point first will have a bigger influence on the mixing. As both these factors are not constant, flow weighted mixing also varies with time. As a consequence of this, the C_vO_2 profile at the lungs during the exercise bout may markedly differ from the C_vO_2 profile generated at the muscle (Hoffmann et al., 2013). This highlights the importance of taking due care and consideration when estimating $\dot{V}O_2$ kinetics from breath-by-breath pulmonary exchange measurements.

1.5 Characteristics of the pulmonary oxygen uptake response

The dynamics of the $\dot{V}O_{2p}$ response at the onset of exercise have been well characterised (Whipp and Wasserman, 1972; Whipp et al., 1982). Figure 4 shows that, at the onset of constant work-rate exercise, there is an initial abrupt increase of $\dot{V}O_{2p}$, termed “phase I.” This is due to an increase in pulmonary blood flow along with a constant venous O_2 content (as the venous effluent from the exercising muscle, with reduced O_2 content, has yet to reach the lungs). The duration of this phase therefore reflects the initial muscle-to-lung transit time (Poole and Jones, 2012), and lasts approximately 20 seconds in young and healthy individuals (De Cort et al., 1991; Benson et al., 2017). The ensuing component of the response (phase II) is an exponential increase (Grassi et al., 1996) which closely reflects the increase in muscle oxygen consumption (i.e. the increased O_2 extraction in the contracting muscle). An exponential function has an amplitude, and a time constant (τ) on which the duration of phase II depends. This is approximately 20-45 seconds in young and healthy humans (Richardson et al., 2015), and this time constant represents the time taken to reach ~63% of the steady state response. Phase II can therefore be described with the equation:

$$\dot{V}O_2(t) = \dot{V}O_{2,b} + A\left(1 - e^{-(t-TD)/\tau}\right) \quad (4)$$

where $\dot{V}O_2(t)$ is the $\dot{V}O_2$ at any time point, $\dot{V}O_{2,b}$ is the baseline $\dot{V}O_2$ before the onset of the transition to a higher work rate, *A* is the amplitude of the $\dot{V}O_2$ response, and $(1 - e^{-(t-TD)/\tau})$ is the exponential function that describes the rate at which $\dot{V}O_2$ is rising towards the steady state, where t is time, TD is the time delay before the start of the exponential term and τ is the time constant.

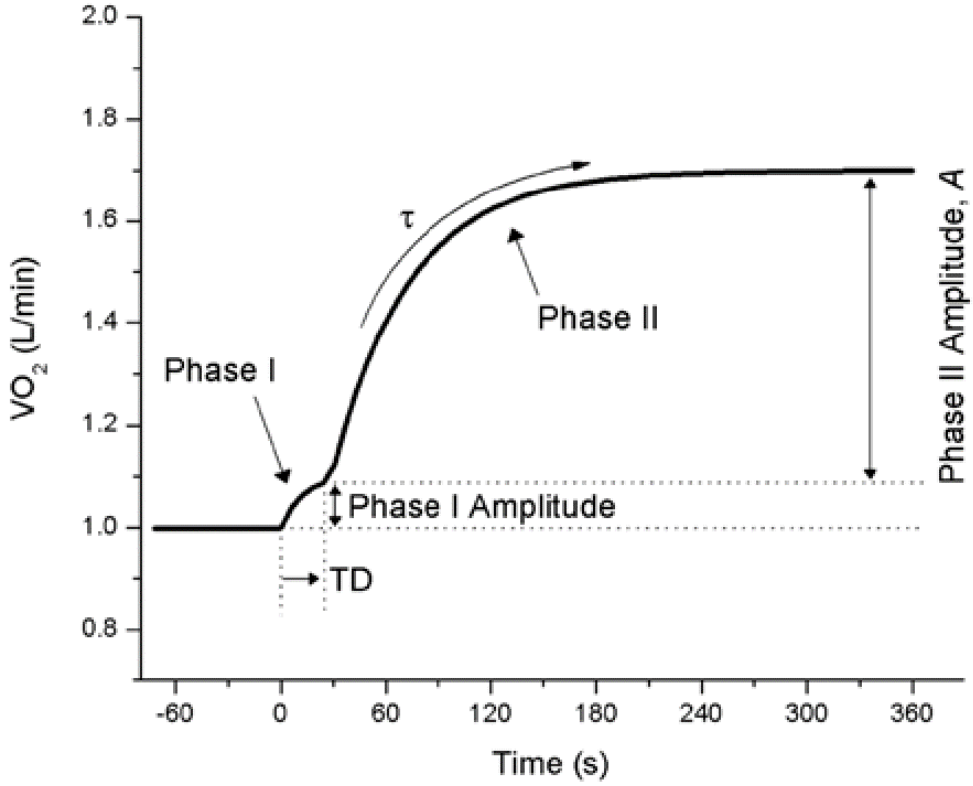

Figure 4: Breath-by-breath $\dot{V}O_2$ response following the onset of constant work rate exercise. Adapted from Manns et al. (2010).

A smaller time constant (i.e. faster kinetics) reflects the ability to respond rapidly to a stressor, such as exercise, and is a major feature of an effectively functioning physiological system (Rossiter, 2011). When both phases are complete a 'steady state' is attained where all the energy required by the body is met by aerobic metabolism. This is termed phase III (Whipp and Ward, 1992). Note that exponential processes never technically reach a steady state but approach the asymptote i.e. ($\dot{V}O_{2,b}$ + A) as $t \rightarrow \infty$ (as time approaches infinity). However, in reality, because of the noise on

experimentally-measured $\dot{V}O_2$ it can be assumed that the process reaches a steady state after ~4 time constants (Jones and Poole, 2005). The faster phase III is achieved, the smaller the "O_2 deficit", which is the sum of energy derived from anaerobic sources (i.e. phosphocreatine breakdown and glycolysis), will be. Hence, the time constant of the $\dot{V}O_{2p}$ response ($\tau\dot{V}O_{2p}$) is a fundamental parameter of aerobic performance, and may provide an insight into the broad range of exercise capabilities across populations (Poole and Jones, 2012).

1.6 The pulmonary oxygen uptake response to incremental exercise

So far, the $\dot{V}O_{2p}$ response to constant work rate exercise has been described. However, normal day-to-day activity and exercise is seldom of the "step" protocol type, where a constant work load is added at a single time point. Instead, day-to-day exercise tends to involve a constantly changing work load, and the physiological response to a given activity therefore tends to span multiple exercise intensity domains. Because of this, cardiopulmonary exercise testing using step exercise protocols tends to be limited to specialised research studies, and instead an incremental exercise protocol to the limit of tolerance, where work rate is gradually increased until the individual can no longer exercise, is the most widely used test of the efficiency of the integrated functioning of the cardiopulmonary and neuromuscular systems (Rossiter, 2011). Unlike a constant work rate test, incremental exercise spans the range of exercise intensity domains; as such, a steady state in $\dot{V}O_{2p}$ is not attained, requiring the body to continuously adapt to changing metabolic demands. The incremental exercise protocol can vary, increasing either (i) in small progressive work rate increases (e.g., 20 W) for a fixed period (e.g., every minute) in a staircase fashion, termed "step incremental", or (ii) in a smooth linear fashion where work rate is constantly and smoothly increased at a given rate (e.g., 20 W per minute), termed "ramp incremental". The $\dot{V}O_{2p}$ response to ramp incremental exercise of optimum duration (Buchfuhrer et al., 1983) is, following an early exponential phase, typically linear with increasing work rate and can be described by the equation:

$$\dot{V}O_2(t) = \Delta\dot{V}O_2(ss) \cdot [t - \tau \cdot (1 - e^{-t/\tau})] \quad (5)$$

where $\dot{V}O_2$ (t) is the $\dot{V}O_2$ at any given time, $\Delta\dot{V}O_2$(ss) is the steady state increase in $\dot{V}O_2$ above the baseline value required for the work rate at time *t*, and τ is the time constant of the response (Whipp et al., 1981). During ramp exercise however, it is not possible to distinguish between phase I and phase II. As such, τ represents both phase I and II of the response and is commonly referred to as the mean response time (MRT). The ramp incremental test allows determination of other important parameters of aerobic function, such as the $\dot{V}O_{2,peak}$, lactate threshold, and $\dot{V}O_2$ gain (the 'cost' of O_2 per Watt of exercise). The linearity of the $\dot{V}O_2$ response to incremental exercise is somewhat unexpected, considering that during constant-load/ power exercise at exercise intensities above lactate threshold the $\dot{V}O_2$ slow component drives $\dot{V}O_2$ above the expect value. This is typically not the case during incremental exercise (i.e. the emergence of a slow component above lactate threshold is not seen), and this is suggested to be the result of a slowly developing inefficiency (rise in $\dot{V}O_2$ gain) coupled with a progressive slowing of $\dot{V}O_2$ kinetics (Rossiter, 2011). However, during ramp incremental tests in which the duration is prolonged (i.e. if the work rate increments are relatively slow) nonlinearities in the $\dot{V}O_{2p}$ response have been reported (Davis et al., 1982; Hansen et al., 1988) possibly allowing time for a $\dot{V}O_2$ slow component to emerge.

1.7 Exercise tolerance and heart failure

Heart failure (HF) is a multifaceted syndrome in which one of the main symptoms is exercise intolerance, often due to muscular fatigue and dyspnoea, linked to structural and functional aberrations in the O_2 transport pathway (Nilsson et al., 2008; Poole et al., 2011). As a result of this, patients with HF in many cases have a reduced quality of life. Heart failure has a poor prognosis with 30-40% of patients diagnosed with HF dying within one year. Furthermore, the prevalence of HF is on the rise with an increasingly ageing population. It is a current and growing health concern that accounts for 2% of inpatient bed days, and 5% of emergency hospital admissions (Cowie, 2000; Owan et al., 2006; Hobbs et al., 2007).

Exercise tolerance is a principal predictor of hospital readmissions in HF (Hirai et al., 2015). However, the exact mechanisms leading to impaired exercise tolerance in this patient population are still not completely understood (Nilsson et al., 2008). Whilst an impaired cardiac function (which acts to impair cardiac output and consequently O_2 delivery) certainly plays

an important role in determining exercise tolerance (Hughson et al., 2001; MacDonald et al., 2001), there is *no* strong correlation between indices of cardiac function [i.e. left ventricular ejection fraction (Figure 5) and resting cardiac output] and exercise capacity (Franciosa et al., 1981; Weber et al., 1984; Lipkin and Poole-Wilson, 1986; Witte et al., 2004). There is, however, convincing evidence that skeletal muscle O_2 utilisation (i.e. a dysfunction at the skeletal muscle level) may also contribute to poor exercise tolerance in heart failure patients (Grassi et al., 2003; Bowen et al., 2012).

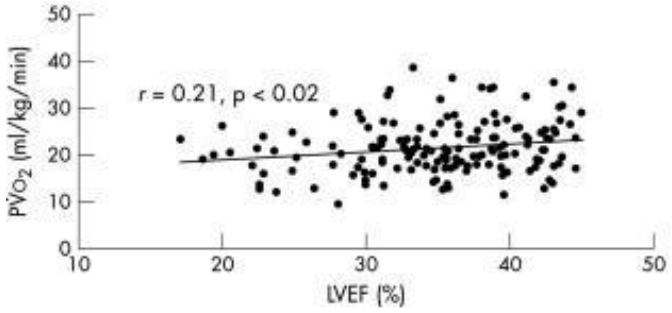

Figure 5: Relationship between $\dot{V}O_{2,peak}$ ($p\dot{V}O_2$; a measure of exercise capacity) and left ventricular ejection fraction (LVEF; a measure of cardiac function) in heart failure patients. Taken from Witte et al. (2004).

What is unclear, is whether one or both of these impairments (i.e. O_2 delivery or O_2 utilisation), is the primary cause of exercise intolerance in a given heart failure patient. For example, interventions aimed solely at improving cardiac output (such as cardiac resynchronisation therapy; CRT) may not be effective in improving symptoms associated with exercise intolerance (such as breathlessness and fatigue) in a patient who is also limited at the skeletal muscle level. Resolution of this issue is essential in understanding the patient-specific mechanisms of exercise intolerance in heart failure, to allow for better targeting of therapeutic interventions.

1.8 Oxygen delivery and exercise capacity

Cells rely on a continuous supply of oxygen to maintain aerobic respiration (Treacher and Leach, 1998). Within the mitochondrial inner membrane, oxygen acts as the terminal acceptor at the end of the electron transport chain whereby oxidative phosphorylation results in the synthesis of

adenosine triphosphate (ATP), the co-enzyme that supplies energy to all active metabolic processes. Delivery of oxygen around the body occurs though convective (i.e. the movement of oxygen within the circulation) and diffusive (the passive movement of oxygen down a concentration gradient) transport (Dunn et al., 2016). Convective delivery can be described by the Fick principle: $\dot{V}O_2 = \dot{Q} \times (C_aO_2 - C_vO_2)$, and diffusive delivery by Ficks law of diffusion: $\dot{V}O_2 = DO_{2m} \times (P_m\dot{V}O_2 - P_iO_2)$, where DO_{2m} is the muscle O_2 diffusing capacity, $P_m\dot{V}O_2$ is the microvascular partial pressure and P_iO_2 is the intracellular partial pressure. The integration of these two equations determines an individual's maximal oxygen capacity ($\dot{V}O_{2,max}$), which measures the upper ceiling of the O_2 transport/utilisation system and thus a person's capacity for exercise (Wagner, 1996). As such, in a clinical setting $\dot{V}O_{2,max}$ can be utilised as a physiological marker to evaluate exercise capacity and the severity of diseases that affect components of the O_2 transport chain (e.g. pulmonary, cardiovascular, neural and skeletal muscle systems), such as HF (Weber et al., 1982). Any impairments in the convective and/or diffusive O_2 transport system may reduce an individual's exercise tolerance.

1.9 Convective oxygen delivery

At the onset of, and during exercise the increased demand for oxygen is facilitated by an increase in cardiac output (CO), at least in healthy individuals (De Cort et al., 1991). Cardiac output is the product of stroke volume (SV) and heart rate (HR) such that: CO = SV * HR. At exercise onset the increase in cardiac output is achieved by an immediate increase in stroke volume and heart rate. Stroke volume increases during low levels of exercise via the Frank-Starling mechanism and during higher levels of exercise, stroke volume increases predominantly due to increased contractility, and may even decline slightly due to tachycardia and limited filling time (Kitzman and Groban, 2008). Heart rate increases in a linear fashion due to a decreased vagal tone and an increase in sympathetic nervous system stimulation. As exercise continues, stroke volume plateaus and remains relatively constant and further increases in cardiac output are primarily achieved by an increase in heart rate (Higginbotham et al., 1986).

In heart failure, there is a plethora of structural, mechanical and functional impairments that act to constrain blood flow to the exercising muscle during exercise in heart failure (Poole et al., 2011; Kemp and Conte, 2012). Impairments in ejection fraction (the proportion of blood ejected from the ventricles during ventricular contraction), stroke volume (the amount of blood ejected by the ventricle per heartbeat), and the heart rate response contribute to a reduced cardiac output (Sullivan et al., 1989). Additionally, the initial rapid increase in cardiac output seen in healthy individuals may be attenuated in HF; the result is a lower and slower cardiac output response (Zelis et al., 1968, 1974, 1988). When cardiac output cannot be maintained to meet the demands of the body, compensatory mechanisms are employed to maintain systemic arterial pressure; while initially beneficial, the long-term effects of these mechanisms serve to worsen heart failure in a vicious cycle (Poole et al., 2011). In HF elevated sympathetic nervous system activation and increased levels of circulating humoral mediators (i.e. norepinephrine, and angiotensin II), combined with a reduction in endothelial nitric oxide (Kubo et al., 1991; Ferreira, Hageman, et al., 2006; Chaggar et al., 2009) contribute to global vasoconstriction which, when maintained over time, leads to impairments in the ability of the body to distribute cardiac output to and within the skeletal muscle (Zelis et al., 1981).

1.10 Diffusive oxygen delivery

At the onset of exercise in healthy humans, red blood cell (RBC)-muscle mitochondrial O_2 flux increases rapidly (Hirai et al., 2015). As demonstrated by Fick's law of diffusion, that flux is determined by the O_2 pressure differential between the capillary (i.e. microvascular PO_2; $P_m\dot{V}O_2$) and the intramyocyte milieu (intracellular PO_2; P_iO_2) operating against a finite O_2 diffusing capacity (Hirai et al., 2015). $P_m\dot{V}O_2$ is determined by the O_2 delivery-to-O_2 utilisation ratio (i.e. $\dot{V}O_{2m}/\dot{Q}_m$; Figure 6)

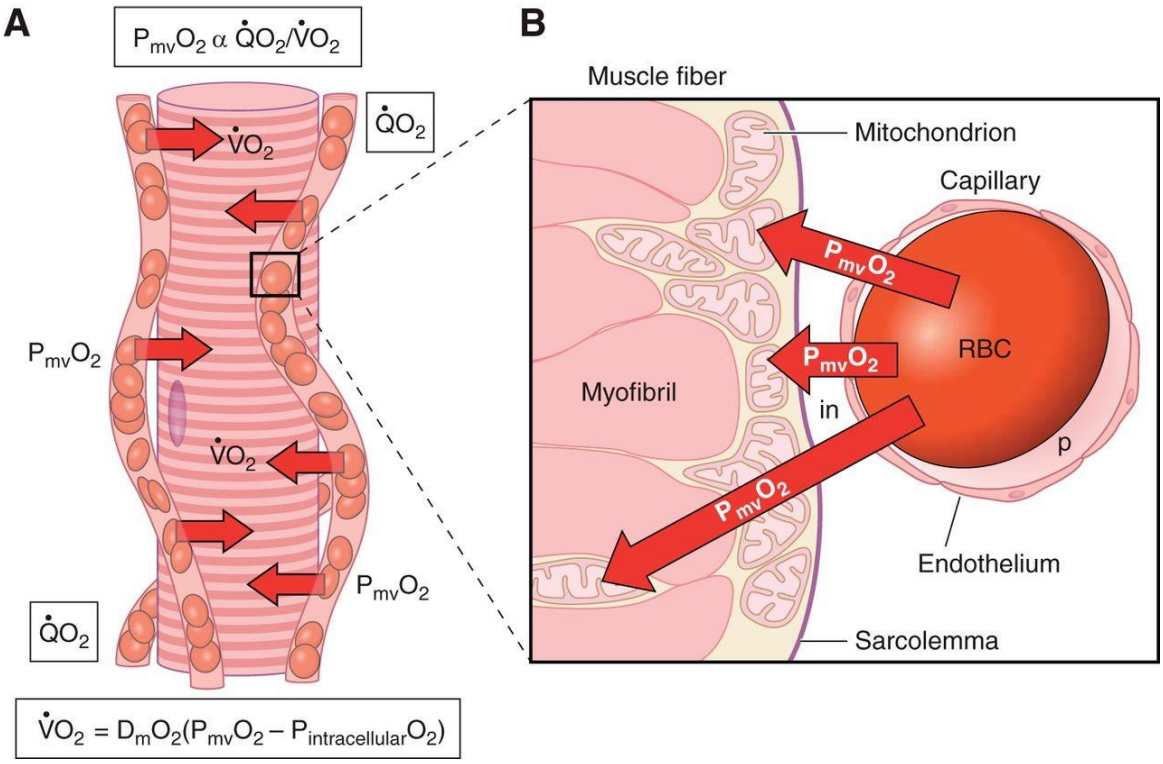

Figure 6: (A) Skeletal muscle fibre with adjacent capillaries and flowing red blood cells. (B). Schematic illustration showing O_2 flux from blood to mitochondria. Taken from Hirai et al. (2015).

In heart failure, diffusive O_2 delivery may be compromised consequent to structural and functional impairments. At the muscle capillary level there is a reduced capillarity and an increase in the proportion of capillaries that do not support red blood cell flux (Kindig et al., 1999; Richardson et al., 2003), resulting in fewer oxygenated red blood cells in the capillary bed at any given moment that are available to contribute to blood-to-myocyte O_2 flux, thereby placing a low limit on DO_{2m} (Poole et al., 2011). In addition, within the skeletal muscle there is muscle wasting (Mancini et al., 1992) and reduced mitochondrial volume density, in addition to a generalised shift away from type I (highly oxidative) fibres and towards type II and type IIb (less oxidative) fibres (Lipkin et al., 1988; Mancini et al., 1989; Sullivan et al., 1990; Drexler et al., 1992). These impairments to the O_2 transport system in heart failure give way to alterations in the $\dot{V}O_{2m}/\dot{Q}_m$ ratio and as $P_m\dot{V}O_2$ is a direct consequence of the $\dot{V}O_{2m}/\dot{Q}_m$ ratio, $P_m\dot{V}O_2$ is typically lower than normal at rest and during contractions in heart failure (Diederich et al., 2002; Behnke et al., 2004). The dynamics of this decrease in $P_m\dot{V}O_2$ vary according to disease severity (Diederich et al., 2002). As (according to the

Fick's law of diffusion) $P_m\dot{V}O_2$ is a key determinant of the blood-muscle O_2 flux, alterations in $P_m\dot{V}O_2$ will have a direct impact on muscle metabolism (Heinonen et al., 2015). Specifically, a lower microvascular PO_2 will impair blood–myocyte O_2 flux, compromising mitochondrial control and increasing reliance of non-oxidative metabolism. This increase in the reliance on non-oxidative metabolism contributes to exercise intolerance in HF (Wilson et al., 1984) and, therefore, understanding the mechanisms that contribute to the reduced $P_m\dot{V}O_2$ (i.e. alterations in the $\dot{V}O_{2m}/\dot{Q}_m$ ratio) is crucial to understanding exercise intolerance in HF.

1.11 Principles of near infrared spectroscopy

Near infrared (NIR) spectroscopy (NIRS) is an imaging technique used clinically and in research laboratories to measure and quantify the oxygenation status of human tissue. The basis of NIRS relies on two principles; (i) that tissue is relatively transparent to NIR light and, (ii) that there are compounds in the tissue in which absorption of light is dependent on the oxygenation status of the tissue. The propagation of light though tissue is dependent on the absorption, scattering and reflection properties of photons. The primary light absorbing compounds in the tissue within the NIR range are called chromophores. The absorption of these chromophores by NIR light, occurs at specific wavelengths determined by the molecular properties of the materials in the NIR light path (Jöbsis, 1977). The attenuation of light through a tissue can be related to the concentration of chromophores in the tissue by the Beer-Lambert Law:

$$A = \log\left(\frac{I}{I_0}\right) = \varepsilon \cdot C \cdot d, \qquad (6)$$

where, A (attenuation) is the logarithmic ratio of two intensities, I: the incident light (i.e. the light inputted), and I_0: the transmitted light (i.e. the light outputted), which is equal to ε: the molar extinction coefficient (which describes how strongly a substance absorbs light at a particular wavelength), C: is the concentration of the chromophore, and d: is the path length of the photon from the emitting to receiving light source (i.e. how far light has to travel through a substance).

According to the Beer-Lambert Law, a more concentrated solution absorbs more light than a more dilute solution, and therefore the NIR absorption changes will predominately reflect the smaller vessels (arterioles, capillaries, and venules (Mancini et al., 1994)). In larger vessels (veins and arteries) the NIR light is almost completely absorbed due to the comparatively high haem concentrations (Chance et al., 1992). In the muscle tissue, the primary absorbing chromophores are haemoglobin (Hb), myoglobin (Mb), and cytochrome c oxidase. However, the contribution of cytochrome c oxidase to the NIRS signal is thought to be very low at around 2-5% (Boushel et al., 2001). As such, the main chromophores of interest in monitoring skeletal muscle oxygenation by NIRS are haemoglobin and myoglobin.

Haemoglobin

A haemoglobin molecule (Figure 7) is made up of 4 amino acid chains (two α polypeptide globin chains and two β polypeptide globin chains). Each chain has a haem group containing an iron (Fe) ion at its center, which acts as the binding site for oxygen. Each haemoglobin molecule therefore has four major O_2 binding sites (Thomas and Lumb, 2012).

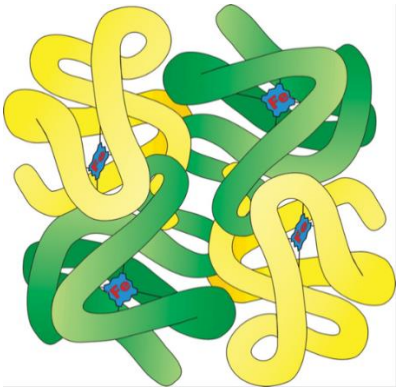

Figure 7: Schematic diagram showing the basic structure of a single adult haemoglobin molecule, including two α-globin chains (green), two β-globin chains (yellow), each containing a haem–iron complex (blue). Fe: iron. Taken from Thomas and Lumb (2012).

Haemoglobin has several functions, a major function being transporting, delivering, and removing oxygen and carbon dioxide throughout the body. To achieve this, haemoglobin molecules have several properties that make it good at binding to, and dissociating from, oxygen. For example,

haemoglobin is allosteric; as such, the binding of oxygen to one haem group increases the binding affinity of oxygen to the remaining haem groups. Similarly, the binding of CO_2 decreases its oxygen affinity and, as such, in the presence of high CO_2, O_2 becomes dissociated. This co-operative, reversible binding of oxygen to haemoglobin results in the sigmoidal shape of the oxyhaemoglobin dissociation curve (Figure 8). The oxyhaemoglobin dissociation curve shows that, at very low O_2 partial pressures (PO_2), the slope of the oxyhaemoglobin curve is almost flat. Each subsequent oxygen molecule binds to haemoglobin more easily and, therefore, the slope increases. As PO_2 increases, the binding sites become occupied and the curve flattens out again (Thomas and Lumb, 2012).

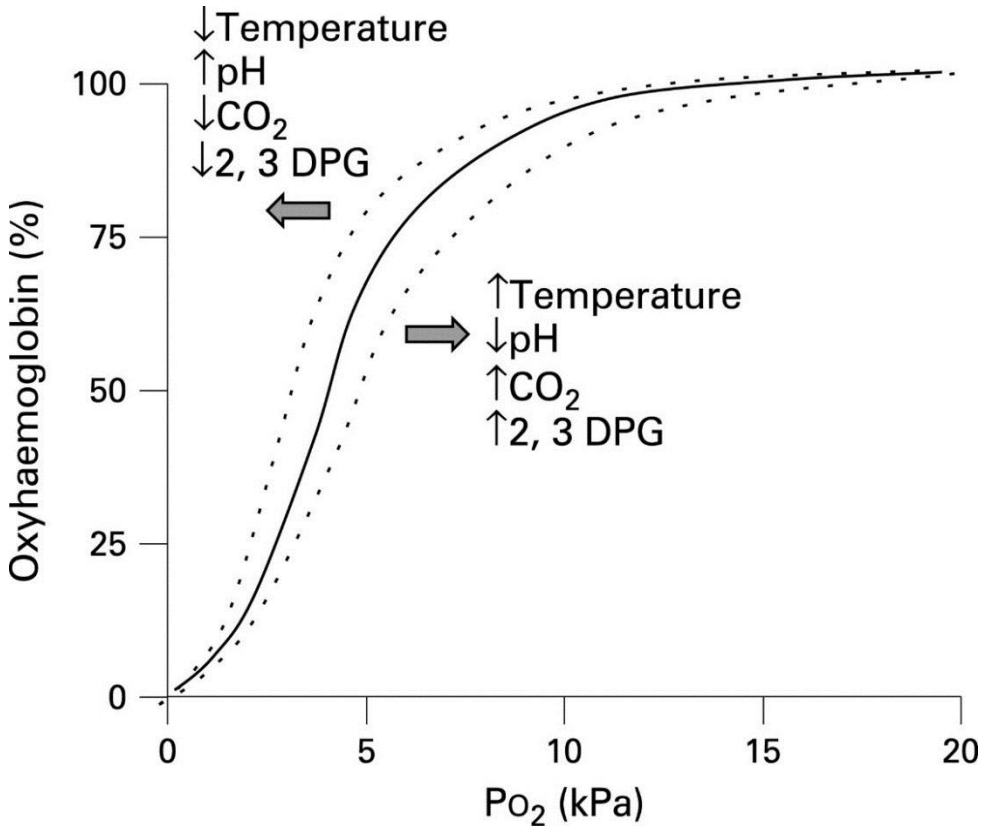

Figure 8: The oxyhaemoglobin dissociation curve (solid line). The curve can be shifted to the left or right (dashed lines), by factors listed in the figure. PO_2, partial pressure oxygen. Taken from O'Driscoll et al. (2008).

In acidic environments (e.g., areas in of high CO_2, such as in the exercising muscle) the oxyhaemoglobin dissociation curve is shifted to the right (called

the Bohr effect) consequently favouring the dissociation of oxygen from haemoglobin (i.e. lower oxygen affinity) in the metabolically active tissues. Conversely, areas of lower CO_2 (such as in the lungs), have a higher affinity for oxygen and thus favour the loading of oxygen to haemoglobin. This shift is advantageous during exercise, as it allows more O_2 to be delivered to the tissues for energy production.

Myoglobin

Unlike haemoglobin, with its four chains carrying oxygen, myoglobin consists of one molecule of haem and one polypeptide chain; myoglobin therefore binds only one molecule of O_2 per molecule of protein. Myoglobin has two main functions. It acts as a small O_2 store that can temporarily provide O_2 when blood O_2 delivery isn't sufficient, such as during periods of intense muscular activity. In addition, it acts as an O_2 carrier, thereby enhancing diffusion of O_2 through the cytosol.

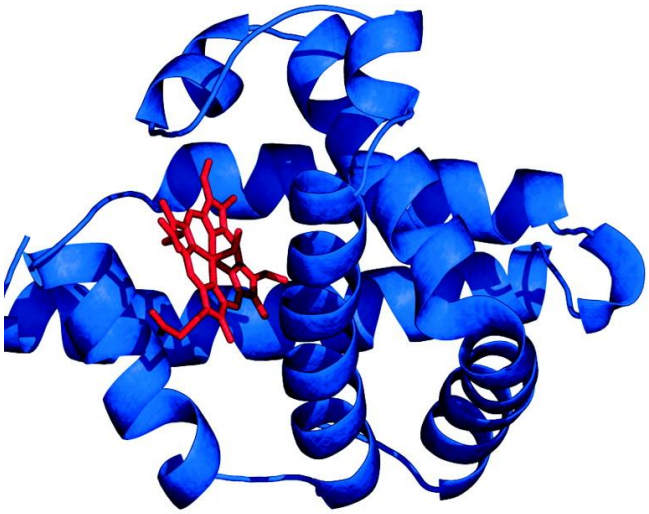

Figure 9: Myoglobin consists of one polypeptide chain and a haem-binding domain. The polypeptide chain consists of eight α-helices (blue) that wrap around a central pocket containing a haem group (red), which is capable of binding oxygen, carbon monoxide and nitric oxide.

Its dissociation curve is left of that of haemoglobin and has a hyperbolic profile (Figure 10), thus myoglobin has a high affinity for O_2, and only releases O_2 in areas of very low PO_2.

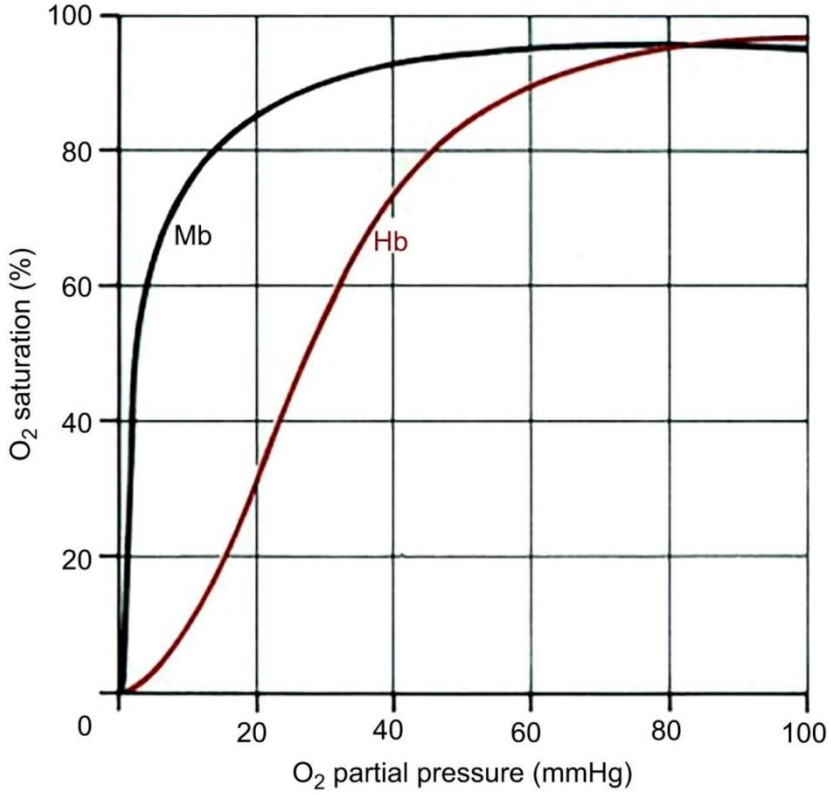

Figure 10: Haemoglobin and myoglobin dissociation curves. The Myoglobin curve lies to the left of the haemoglobin curve and has a hyperbolic profile, with a high affinity for O_2, thus O_2 is only dissociated in areas of very low O_2. Taken from Blix (2018). See equations 40 and 43 for formulations.

1.12 Absorption of haemoglobin and myoglobin by NIRS

Due to their similar absorption spectra, it is not possible to distinguish between haemoglobin and myoglobin by NIRS. Studies reporting the contribution of myoglobin to the NIRS signal have yielded inconsistent results, with estimates of the contribution of myoglobin to the NIRS signal ranging from ~10% (Chance et al., 1992; Mancini et al., 1994) to greater than 50% (Lai et al., 2009; Davis and Barstow, 2013). Therefore, changes in tissue saturation measured by NIRS are attributed to both changes in

haemoglobin *and* myoglobin (see limitations section for further details). It is possible to distinguish between the two major forms of haemoglobin and myoglobin; oxygenated haemoglobin plus oxygenated myoglobin ($HbMbO_2$) and deoxygenated haemoglobin plus deoxygenated myoglobin (HHbMb) due to differences in their absorbance spectra of ~850 nm and 760 nm respectively. For example, at wavelengths of 800 nm the oxygenated and deoxygenated forms of haemoglobin and myoglobin exhibit similar absorption coefficients and, therefore, absorption of light at this wavelength is proportional to the *total* amount of haemoglobin and myoglobin in the muscle under examination. However, at wavelengths of 760 nm, absorption is predominantly by the deoxygenated forms and so changes in light absorption at this wavelength provide assessment in changes of deoxygenated haemoglobin and myoglobin (Wilson et al., 1989). The difference in absorption between these wavelengths is an index of the balance between oxygen delivery and oxygen removal at the level of the small blood vessels (Pereira et al., 2007). As such, NIRS allows a non-invasive insight into local muscle oxidation status during rest and exercise.

1.13 Types of NIRS device

There are several types of NIRS devices, the simplest being a continuous-wave (CW) spectrometer which measures the attenuation of light through the tissue of interest (Boushel et al., 2001). A standard NIRS device (Figure 11) consists of a light source, emitting two or more wavelengths of light into the near-infrared region of the tissue of interest, and a light detector placed at a known distance from the light source(s). The NIR light travels in a banana shaped curve through tissue and, therefore, the path length (d) is longer than the geometric distance between the light source and detector. In addition, the amount of light scattering in unknown. In a highly scattering medium, photons will travel a mean distance that is far greater than d, this have been defined as the differential path-length and represents the true distance between optodes. To account for this, a differential path-length factor (DPF) is applied to the Beer-Lambert Law for continuous wave spectrometry (Delpy et al., 1988) such that:

$$A = \log\left(\frac{I}{I_0}\right) = \varepsilon \cdot C \cdot d \cdot DPF + G \qquad (7)$$

where G is the scattering coefficients of the tissue along with the geometry of the optodes. G is unknown and as such, continuous wave spectroscopy can only provide relative changes in $HbMbO_2$ and HHbMb (Boushel et al., 2001). More complex NIRS devices, such as time-resolved and frequency-resolved spectrometers, estimate the distribution of path lengths travelled in the tissue, and are therefore able to provide absolute measurements of $HbMbO_2$ and HHbMb. Consequently, time and frequency resolved spectrometer are typically costlier, and as such continuous wave spectrometers are more widely used (Pereira et al., 2007; Ferrari et al., 2011).

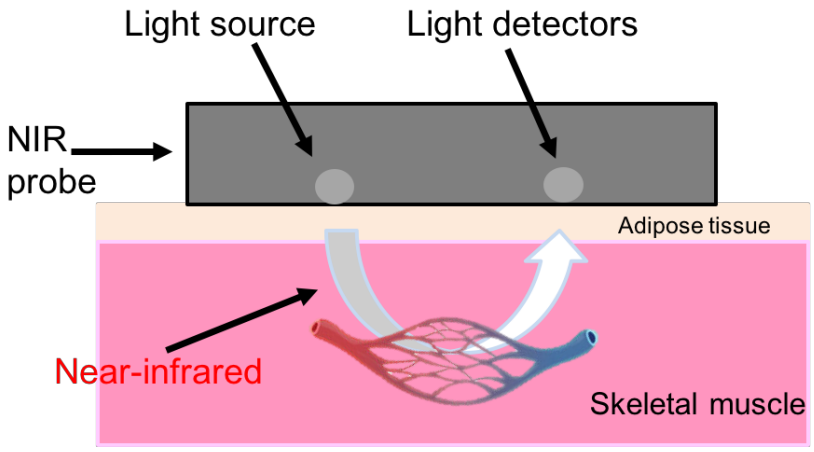

Figure 11: Schematic of a basic NIRS device, placed over skeletal muscle.

1.14 Physiological variables measured by NIRS

1.14.1 Oxygenated haemoglobin and myoglobin

Mancini et al. (1994) demonstrated a correlation between venous haemoglobin oxygen saturation measured by venous plethysmography and muscle deoxygenation measured by NIRS during forearm exercise in humans. Further, they showed: (i) the NIRS signal was sensitive to changes in limb blood flow (ii) by laser flow Doppler, the NIRS signal was minimally affected by skin blood flow and (iii) using ^{1}H-magnetic resonance spectroscopy, the contribution of myoglobin to the NIRS signal was minimal. However, some cycling studies have shown a dissociation between NIRS

muscle oxygenation and femoral O_2 saturation (Costes et al., 1996; MacDonald et al., 1999). For example, it was observed that at exercise onset, NIRS muscle oxygenation decreased with a corresponding decrease in venous femoral O_2 saturation, however, as exercise continued there appeared to be a muscle $HbMbO_2$ 're-oxygenation' which was not paralleled in venous O_2 saturation. A similar pattern in $HbMbO_2$ (but not in HHbMb) was observed by Grassi et al. (2003); the authors of this study suggested the $HbMbO_2$ re-oxygenation was likely a consequence of increased skin blood flow.

1.14.2 Deoxygenated haemoglobin

It has been demonstrated that the NIRS muscle deoxygenation signal is well correlated to venous O_2 saturation in exercising humans (Boushel et al., 1998, 2001; Esaki et al., 2005; Vogiatzis et al., 2015). Further, whilst interpretation of the $HbMbO_2$ signal appears to be dependent on changes in skin blood flow, the HHbMb signal appears to be less influenced by changes in skin blood flow, as it is primarily dependent on O_2 extraction (Grassi *et al.*, 2003). As such, of the NIRS derived parameters, relative changes in HHbMb can be considered a proxy for the arterio-venous O_2 difference (i.e. proportional to $C_aO_2 - C_vO_2$), and thus microvascular O_2 extraction (DeLorey et al., 2003; Grassi et al., 2003).

1.14.3 Tissue oxygenation index

In addition to changes in $HbMbO_2$ and HHbMb, most NIRS systems provide continuous monitoring of tissue O_2 saturation as the tissue oxygenation index (TOI), which represents the ratio of oxygenated haem to total haem, i.e. $HbMbO_2/(HbMbO_2+HHbMb)$ (Bowen et al., 2012). Characterisation of TOI uses spatially resolved spectroscopy, which utilises several light detectors within the same NIRS probe. When light is sent through a tissue the reflection of light is dependent on the absorption coefficient and the reduced scattering coefficient. In spatially resolved spectrometry, measuring the spatial variation of the intensity of retro-reflected light as a function of distance between light source detectors allows estimation of light attenuation (Matcher et al., 1995). The combination of the multi-distance measurements of optical attenuation allows calculation of the relative contributions of

oxygenated and deoxygenated haemoglobin in the illuminated tissue (Matcher et al., 1995; Suzuki et al., 1999).

1.15 The oxygen extraction response during exercise

As discussed in Chapter 1, there is a linear relationship between $\dot{Q}$ and $\dot{V}O_2$ during steady state exercise, this relationship can be described by the equation:

$$\dot{Q} = m \cdot \dot{V}O_2 + c, \quad (8)$$

where m is the slope and c is the y-axis (i.e. $\dot{Q}$ L/min) intercept of the relationship (Whipp et al., 1982). The slope of the relationship is approximately 5-6 (Saltin et al., 1968; Faulkner et al., 1977; Richardson et al., 1993), and has been demonstrated to be similar during different exercise modalities (Faulkner et al., 1977; Knight et al., 1992; Richardson et al., 1993). The linear relationship has a positive intercept on the y (or $\dot{Q}$) axis and, therefore, necessitates a hyperbolic increase in the arterio-venous O_2 difference (i.e. greater oxygen extraction) as $\dot{V}O_2$ and Q increase. This has been demonstrated by (Ferreira, McDonough, et al., 2006) who modelled these important relationships (Figure 12).

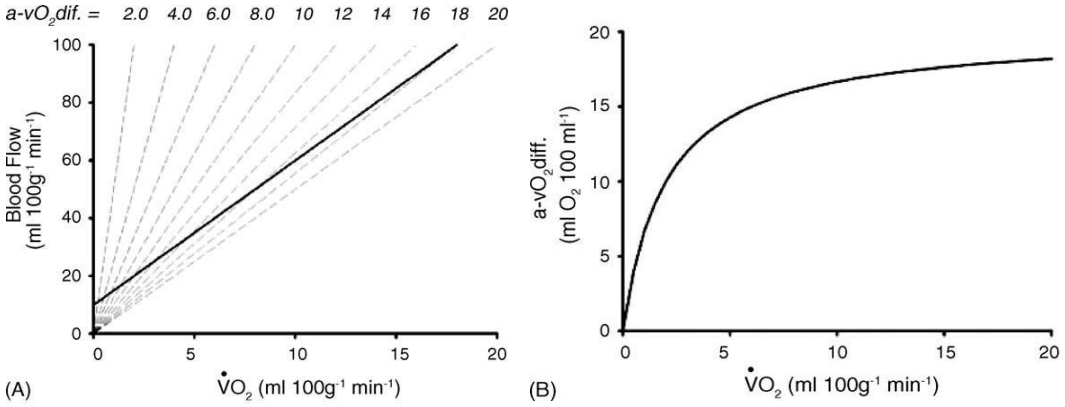

Figure 12: Schematic of the relationship between (A) blood flow and (B) arteriovenous O_2 difference (a-v_{O2} diff) vs. oxygen uptake ($\dot{V}O_2$) during steady-state exercise. Adapted from Ferreira et al., (2006). Solid line depicts an illustrative $\dot{Q}$ to $\dot{V}O_2$ relationship, where $\dot{Q}$ = 10+5($\dot{V}O_2$). Dashed lines represent isopleths of a-vO_2diff.(in ml O_2 (100 ml blood)$^{-1}$) assuming an

arterial O_2 content of 20 ml O_2 100 ml^{-1}. As a-vO_2diff.= $\dot{V}O_2$/ $\dot{Q}$, the lines pass through the origin. The slope ($\dot{Q}/\dot{V}O_2$) describing each constant a-vO_2diff. decreases hyperbolically with increasing a-vO_2diff. Importantly, the slope is the inverse of a-vO_2diff. ($\dot{V}O_2/\dot{Q}$); therefore, a-vO_2diff. increases hyperbolically as a function of $\dot{V}O_2$.

In Figure 12, the solid line shows a $\dot{V}O_2/\dot{Q}$ relationship where $\dot{Q}$ = 10 + 5$\dot{V}O_2$. The dashed lines represent isopleths of the (a-v)O_2 difference [ml O_2 (100 ml blood)$^{-1}$]. For a given (a-v)O_2 difference (i.e. at the top of panel A, from 2.0 - 20), the $\dot{V}O_2/\dot{Q}$ slope decreases hyperbolically as (a-v)O_2diff. increases. This slope is the inverse of the (a-v)O_2 difference: therefore, the (a-v)O_2 difference increases hyperbolically as a function of $\dot{V}O_2$. This (a-v)O_2-$\dot{V}O_2$ relationship (Figure 12; right) is best described by a rectangular hyperbola of the form:

$$(a\text{-}v)O2\ diff = \frac{ax}{(b+x)} \qquad (9)$$

where a is the maximal y value and b = the x value corresponding to 0.5a (Whipp et al., 1982; Ferreira et al., 2006).

The notion of a linear $\dot{V}O_2/\dot{Q}$ relationship during ramp incremental exercise (i.e. during non-steady state exercise) however, has been challenged. Stringer et al., (1997) observed a linear relationship between (a-v)O_2 difference and $\dot{V}O_{2m}$ during ramp exercise, and later demonstrated that $\dot{Q}_m$ does not increase linearly with $\dot{V}O_{2m}$; rather, $\dot{Q}_m$ increases faster relative to $\dot{V}O_{2m}$ but the rate of increase gets progressively slower (i.e. $\dot{V}O_{2m}$ and $\dot{Q}_m$ become better matched) as exercise intensity increases (Stringer et al., 2005). This change in the relationship between $\dot{V}O_{2m}$ and $\dot{Q}_m$ during ramp incremental exercise should then influence O_2 extraction. Accordingly, it has been demonstrated that the pattern of ΔHHbMb (i.e. proportional to O_2 extraction) during ramp incremental exercise does not follow a hyperbolic profile (as with steady state exercise). Rather, Ferreira et al., (2007) found that the ΔHHbMb response to ramp exercise followed a sigmoidal profile (Figure 13), supporting the notion of a non-linear relationship between $\dot{V}O_{2m}$ and $\dot{Q}_m$ during ramp incremental exercise.

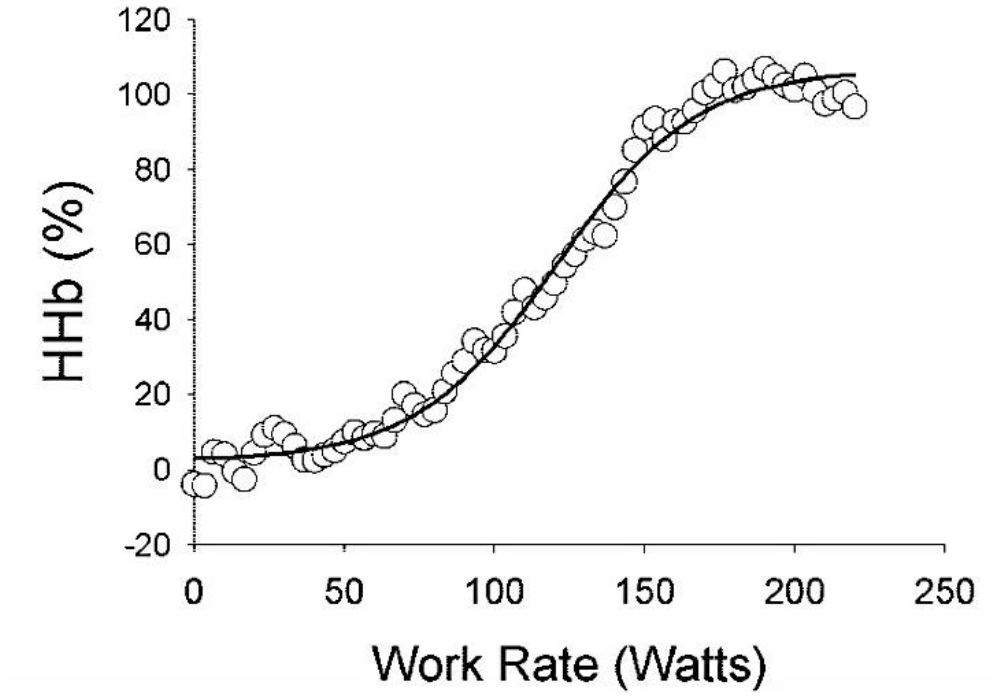

Figure 13: Increase in deoxygenated haemoglobin+ myoglobin (HHb) during incremental exercise. Solid line represents best fit from sigmoidal function**.** Taken from Ferreira et al., (2007).

The sigmoidal model suggests that at very low work rates $\dot{Q}_m$ kinetics are faster than $\dot{V}O_{2m}$ kinetics, resulting in a relatively larger increase in O_2 delivery compared to O_2 extraction and, therefore, a slow increase in fractional O_2 extraction. Following this initial slow response, HHbMb increases more steeply, indicating that fractional O_2 extraction is much greater relative to the increase in O_2 delivery during higher work rates, until in most subjects a plateau is reached, indicating that there is a tight coupling between $\dot{V}O_{2m}$ and $\dot{Q}_m$.

Muscle oxygenation dynamics (and their corresponding NIRS responses; namely TOI and deoxygenated haemoglobin + myoglobin) in health have been well characterised. However, they are still not completely understood in heart failure, where the implications for understanding control of O_2 delivery and utilisation are even greater (Poole and Jones, 2012). Experimental studies during moderate-intensity constant work rate (step) exercise in heart failure patients (Sperandio et al., 2009; Bowen et al., 2012) have demonstrated a transient overshoot in the HHbMb signal by NIRS (or

corresponding undershoot in TOI), implying that estimated fractional O_2 extraction increases above the steady state level because of impaired O_2 delivery relative to O_2 requirements at the onset of exercise. However, the step protocol is rarely used in a routine clinical setting, as information on the cardiopulmonary responses pertinent to disease states (i.e. lactate threshold, $\dot{V}O_{2,peak}$ and work efficiency) is obtained using a ramp incremental protocol, where work rate is progressively increased until the patient can no longer exercise (Whipp et al., 1981). Although a ramp incremental exercise test is the most widely used cardiopulmonary exercise test to assess exercise function in the clinic, the muscle oxygenation profile during such exercise has been investigated much less in heart failure. Further, as effective adjustment to constant changes in metabolic demand (as in a ramp incremental test) is an important determinant of exercise tolerance (Boone et al., 2016), and heart failure patients rarely spend time in a ‘steady state’ as seen at the end of step exercise protocols, understanding control of O_2 delivery and utilisation during such exercise will give us insights into mechanisms underlying exercise intolerance in heart failure.

Chapter 2 General methods

2.1 Experimental data collection

2.1.1 Protocol 1

Participants

Six healthy male competitive or amateur cyclists (mean ± SD: age, 22.8 ± 4.4 years; height, 181.0 ± 4.2 cm; body mass, 73.7 ± 6.1 kg) performed a step incremental exercise test to the limit of tolerance on a cycle ergometer. Note that the methods and the data used described in this protocol were taken (with permission) from Grassi et al. (1996).

Equipment and measurements

Subjects performed a 4-minute warm-up period at 100 W proceeded by an increase in work rate of 25 W each minute. Mean maximal $\dot{V}O_2$ was 4.35 ± 0.46 L/min (absolute) or 59.1 ± 5.3 mL/kg/min (relative). Breath-by-breath gas exchange was measured during all tests using an OUR system (Consentuis Technologies, Sandy, USA), with inspired and expired flows measured by a pneumotach (Fleisch no. 3) and gas concentrations measured by a mass spectrometer (model MGA 1100, Perkin-Elmer, Waltham, USA). Subsequently, subjects performed a series of 5 constant work rate exercise tests. For the constant work rate tests, subjects performed 4-6 minutes of unloaded pedalling, followed by 5 minutes of moderate intensity constant work rate exercise for 5 minutes. Work rates were determined from the incremental test, mean power output was 183 ± 20 W. Muscle blood flow, $\dot{Q}_{m,}$ was determined during three of the constant work rate tests by a constant-infusion thermodilution technique. This involved the placement of two catheters, one in the radial artery (for arterial blood sampling), one in the femoral vein (for venous blood sampling), and a thermocouple in the left femoral vein (for injection of sterile cold normal saline and blood gas sampling). Values for $\dot{Q}_m$ calculated during the three

constant work rate bouts were determined over 3s discrete time intervals throughout the transient. During the other two constant work rate bouts, 3-4 ml samples of arterial and venous blood were drawn anaerobically for measurement of PO_2, PCO_2, pH, O_2 saturation, and Hb concentration by a gas analyser and CO oximeter (model IL 1306 and IL282, Instrumentation Laboratories). Samples were drawn at rest and approximately every 5-8 s during the transient. $\dot{V}O_{2A}$ in the leg was calculated using the Fick principle (Equation 1). Model input parameters are shown below in Table 1.

Table 1: Pre-optimised model input parameters (middle column) with sensitivity analysis model input values)

Parameter	Parameter value		
	Minus 10%	**Pre-optimised**	**Plus 10%**
C_aO_2 (L O_2/ L blood)	0.18	0.20	0.22
Venus volumes, litres			
Muscle	0.63	0.70	0.77
Body	0.09	0.10	0.11
Mixed	2.07	2.30	2.53
Baseline (unloaded pedalling) values			
$\dot{V}O_{2A}$, L/min	0.78	0.87	0.96
Fraction from muscle[a]	0.51	0.57	0.63
$\dot{Q}_{tot}$, L/min	8.00	8.89	9.78
Fraction to muscle[a]	0.51	0.57	0.63
Exercise $\dot{V}O_2$ and $\dot{Q}$ parameters			
$\Delta\dot{V}O_{2m}$ /ΔWR, (L/min/W)	0.01	0.01	0.01
$\Delta\dot{Q}$ / $\Delta\dot{V}O_{2m}$	5.40	6.00	6.60
Muscle $\dot{V}O_2$ and blood flow kinetics			
$\tau\dot{Q}_m$ (s)	21.60	24.00	26.40
$\tau\dot{V}O_{2m}$ (s)	19.80	22.00	24.20

Table parameters: $\dot{Q}$ denotes blood flow. The subscripts 'tot' and 'm' denote total and muscle components, respectively. [a]The remainder of the baseline $\dot{V}O_{2p}$ (and $\dot{Q}_{tot}$) comes from (and goes to) the body compartment. All pre-optimised parameters are experimentally collected data from Grassi et al. (1996). NB: Pre-optimsed values are mean values from Grassi data, SD have been removed for clarity

Data analysis

$\dot{V}O_{2A}$ data from the incremental test was averaged over 30 s time intervals and plotted as a function of time. Because, for the model validation at least, the mechanisms causing any plateau in $\dot{V}O_{2A}$ at or near the limit of tolerance are not of primary concern (indeed, the model does not contain the appropriate components to be able to predict such phenomena), and the primary interest is the dynamics of the $\dot{V}O_{2A}$ response during the initial and fundamental (increasing) portions of the test, any plateau $\dot{V}O_{2A}$ data that occurred at the end of each test were removed before comparing with model data.

2.1.2 Protocol 2

Participants and ethics

11 young healthy participants (mean ± SD: age, 26 ± 5 years; body mass, 74 ± 14 kg; Height 1.7 ± 0.7 m) volunteered to take part in the study and provided informed written consent. The investigation was approved by the Faculty of Biological Sciences ethical review committee. Health screening and readiness for physical activity (PAR-Q) questionnaires were completed prior to any exercise.

Equipment and measurements

Gas exchange measurements: Pulmonary gas exchange was measured breath-by-breath throughout exercise for measurement of key variables associated with exercise tolerance. The breath-by-breath system (MedGraphics D-Series, MedGraphics Medical Graphics Corporation, St Paul, MN, USA) was calibrated before each test. The flow sensor was calibrated using 3-litre syringe; ten strokes passed through the pneumotach, at different flow rates. The calibration values were validated, and calibration was accepted when the standard deviation of the mean volume values was less than 0.02 L. O_2 and CO_2 analysers were calibrated using two different calibration gases of known concentrations (O_2, 12.0% and 21%, and CO_2, 5% and 0%).

Muscle oxygenation dynamics: Oxygenation of the left quadriceps muscle was measured by a wireless, portable continuous-wave, spatially-resolved spectroscopy (SRS) NIRS device (PortaMon, Artinis, The Netherlands), which consists of three light emitting diodes at wavelengths of 760 and 850 nm corresponding to the absorption wavelengths of oxygenated haemoglobin and deoxygenated haemoglobin. The distances between receiver and transmitter were set at 30, 35, and 40mm. NIRS data were collected at a sampling frequency of 10 Hz. Relative concentrations of oxygenated and deoxygenated haemoglobin and myoglobin were measured throughout. In addition, TOI was measured using the SRS approach. The NIRS probe was placed over the vastus lateralis muscle, and a black cloth was placed over the device to occlude ambient light. The NIRS probe and black cloth was secured with adhesive tape and an elastic bandage.

Haemodynamic assessments: Heart rate was determined from each R-R interval obtained from a 12-lead electrocardiogram. Cardiac output was estimated non-invasively via photoplethysmography (Finometer, FinaPres Medical Systems BV). This method continuously measures beat-to-beat finger blood pressure waveforms, to construct mean brachial arterial pressure. Stroke volume, heart rate, and cardiac output were calculated using Modelflow® algorithms. The FinaPres device was fitted to the left arm, with the cuff positioned on the medial phalanx of the middle or index finger (depending on best fit). The device contains a height correction unit to compensate for the hand position according to the position of the heart. Prior to the onset of exercise, participants remained at rest for physiological calibration which is performed automatically using the Physiocal software in the device.

Exercise protocols

All tests were performed on a computer-controlled electromagnetically braked cycle ergometer (Excalibur Sport PFM, Lode, BV, Groningen, NL). Participants attended the Leeds integrative exercise physiology laboratory on three separate occasions described below.

Visit 1: Ramp-Incremental Step Exercise test

On visit one participants performed a symptom limited ramp incremental step exercise (RISE) test (Rossiter et al., 2006). A RISE test consists of a standard ramp incremental exercise test to the limit of tolerance, followed by a constant work rate (step) exercise bout to the limit of tolerance, the work rate of which was set at 95% of the maximum work rate achieved during the ramp portion of the test. The ramp and step exercise bouts were separated by 6 minutes of unloaded pedalling. Each test was preceded and followed with at least 4 min unloaded pedalling at 20 W. Ramp rates (which ranged from 15-35 W/min) were individually targeted to produce a test duration of 8-12 minutes (Buchfuhrer et al., 1983). The ramp and step portions of the test were terminated when the pedal cadence could no longer be maintained above 50 rpm despite strong verbal encouragement.

Visit 2 and 3: Moderate-intensity constant load step tests

Visits two and three were identical. On both visits participants performed two moderate intensity constant load step exercise tests (4 step tests in total) at a work rate determined from the ramp incremental exercise test corresponding to 90% of lactate threshold. Each step test was 6 minutes in duration and was separated by 6 minutes of unloaded pedalling at 20 W. Each test was preceded with and followed with at least 4 min unloaded pedalling at 20 W.

Data analysis

Breath-by-breath data: Lactate threshold was estimated using the V-slope method, with confirmatory analysis of end tidal O_2 and CO_2, ventilatory equivalents for O_2 and CO_2, and the respiratory exchange ratio (Whipp et al., 1986). Baseline $\dot{V}O_2$ was taken as an average of breaths during the last 60 s unloaded pedalling, $\dot{V}O_{2,peak}$ was taken as the highest 12-breath average from the final 24 breaths (~20 s) of exercise during the ramp test. $\dot{V}O_2$ data from each individual test was edited to eliminate any errant breaths that may have been caused by swallows or coughs etc. 99.7% prediction bands were fitted to the data, and any breaths that fell outside these bands (~4 SD from the local mean) were considered to be uncharacteristic of the underlying physiological response, and were therefore eliminated to improve the confidence of the fit (Lamarra et al., 1987; Benson et al., 2017). For healthy participants breath-by-breath $\dot{V}O_2$ responses (from the step exercise tests)

for each subject were time aligned at the onset of exercise for each exercise bout and interpolated to second-by-second values. The four exercise bouts were then averaged to create one mean data set that incorporated all the repeated step tests. This process yielded one value for time and $\dot{V}O_2$ (Benson et al., 2017). Each $\dot{V}O_2$ response profile was fit with an exponential of the form:

$$y_0 + A * (1 - \exp(^{-(x-TD)/\tau})) \quad (10)$$

where $y_0$is baseline, A is the amplitude, TD is the time delay, and τ is the time constant. The first 20s of data was disregarded during the fitting procedure to isolate phase II kinetics.

Haemodynamic measurements: Baseline cardiac output was taken as the final 60 s of unloaded pedalling. Data from the first and third step were time aligned and averaged to reduce signal-to-noise ratio, where possible (NB: in 4 participants, FinaPres calibration was lost at exercise onset during one of the step exercise bouts, preventing accurate kinetic estimation; therefore, in these participants only one step bout was used). Each cardiac output response was then fitted with an exponential function [using the same equation used to fit the $\dot{V}O_2$ kinetics (Equation 10)] from time 0 (i.e. no time delay) for determination of cardiac output kinetics. All fitting was carried out in OriginLab (OriginLab Corporation, Northampton, MA, USA).

NIRS measurements: (Chapter 4) HHbMb was normalised from baseline to peak HHbMb (0-100%). Baseline HHbMb was taken as an average of the final 60 s unloaded pedalling, peak HHbMb was taken as the final HHbMb value during the ramp test. HHbMb amplitude was determined by peak HHbMb minus baseline HHbMb. Peak HHbMb was taken as the final HHbMb value (rather than the peak HHbMb during the whole ramp) to maintain the profile of the response following normalisation procedures.

(Chapter 6) NIRS data were averaged into one second bins. These second-by-second responses were then normalised to the total amplitude of the response from baseline (0%) to peak (100%) exercise. Baseline HHbMb was determined as the mean of the last 60 seconds of unloaded pedalling, and peak HHbMb was taken as the mean of the final HHbMb data point of the ramp exercise (Boone et al., 2009). The final data point was chosen as the

peak value (rather than taken as an average of the final data points) to maintain the dynamic profile of the response following normalisation procedures. The amplitude of ΔHHbMb was taken as peak HHbMb minus baseline HHbMb. Normalised ΔHHbMb (ΔHHbMb %) was plotted as a function of increasing work rate (W). Two inflection points were identified from the raw signal. Point A corresponded to the work rate after exercise onset at which HHbMb started to systematically increase. Point B corresponded to the point at which there was a systematic departure from linearity. Linear regression was applied from point A to point B and from point B to point C (peak exercise). The response was then split into three phases. Phase 1 represented the portion of the response from onset of the ramp up until point A. Phase 2 corresponded to the mid-portion of the response (i.e. from point A to point B), and phase 3 included the data from point B onwards (Figure 14). Finally, the slope of the linear regression of phase 2 was calculated in addition to the HHbMb difference between points B and C. Due to probe displacement during exercise, two heart failure patient's NIRS data were eliminated from data analysis.

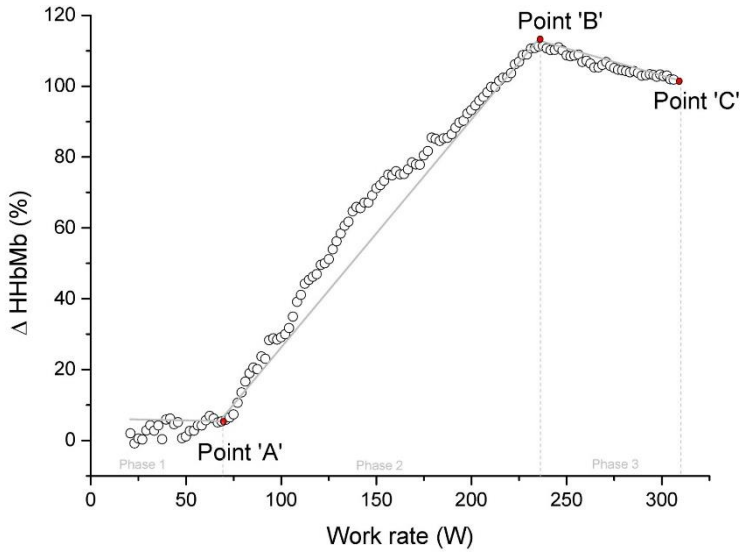

Figure 14: Representative deoxygenated haemoglobin-myoglobin (ΔHHbMb) response profile plotted as a function of increasing work rate (W) in a healthy control. Points 'A' and 'B' correspond to the first and second inflection points. Point 'C' is the peak work rate (W).

Comparing sigmoidal vs double linear functions

For a subset of 8 patients, sigmoidal and double linear function fits to the data were compared. For these patients NIRS data were averaged and normalised using the same method described above. In addition to the above, normalised HHbMb (ΔHHbMb %) was plotted as both a function of absolute work rate and normalised work rate. The averaged, normalised data were then fit with a piecewise linear function of the form:

$$y = \begin{cases} \dfrac{y_1(x_3 - x) + y_3(x - x_1)}{x_3 - x_1}, & x < x_3 \\ \dfrac{y_3(x_2 - x) + y_2(x - x_3)}{x_2 - x_3}, & x \geq x_3 \end{cases} \quad (11)$$

where x_1 and x_2 are x values of the curve endpoints; x_3 is the intersection of the two segments (the break point), and y_1, y_2 and y_3 are y values at x_1, x_2 and x_3 respectively. This double linear analysis yields:

$$y = \begin{cases} b_1 x + a_1, & x < x_3 \\ b_2 x + a_2, & x \geq x_3 \end{cases} \quad (12)$$

where *b* represents the slope, and a is the y-intercept value.

The data were also fit with a sigmoidal model of the form:

$$y = y_0 + A/\left[1 + e^{-(-c + dx)}\right] \quad (13)$$

where y_0 is baseline, A is the amplitude, c is a constant dependant on d, the slope of the sigmoid, where c/d gives the x value corresponding to 50% of the total amplitude.

Fitting model comparisons

The Akaike Information Criterion (AIC) compares the quality of model (the function in this case) fits to data, relative to each other. The sigmoid and double linear function were compared by calculating the change in corrected Akaike Information Criterion (ΔAIC_C) scores (Akaike, 1974; Spencer et al., 2012). As described in detail in Spencer et al. (2012), for each model:

$$AIC_C = N \ln\left(\frac{RSS}{N}\right) + 2K + \left[\frac{2K(K+1)}{N-K-1}\right] \quad (14)$$

where N is the number of data points used in the analysis for that subject, RSS is the residual sum of squares from the regression analysis, and K is the number of parameters in the fitted model + 1.

The AIC_C score was calculated by subtracting the AIC_C score from the double-linear function with the AIC_C score from the sigmoid function; as the model with the lower AIC_C score is most likely to describe the underlying data more accurately, a positive ΔAIC_C score favours the double-linear model.

Statistical analyses

Fitting was carried out in OriginLab (OriginLab Corporation, Northampton, MA, USA). The model parameters were estimated by least-squares regression (sigmoid) or linear regression (double linear). Persons product moment correlation was calculated to quantify the relationship between key variables, and a student's t-test was used to determine significant difference between means. Significance was accepted when $p < 0.05$.

Key experimentally measured baseline, exercise, and peak exercise values obtained from this protocol are shown in Table 2.

Table 2: Key baseline, exercise, and peak exercise values (n=11)

Parameter	Mean ± SD
Baseline values	
$\dot{V}O_{2p}$ (L/min)	0.96 ± 0.21
$\dot{Q}$ (L/min)	8.47 ± 1.51
Exercise values	
$\dot{V}O_{2p}\tau$ (L/min)	24.40 ± 6.80
$\dot{Q}\tau$ (L/min)	29.60 ± 15.30
$\dot{V}O_{2m}\tau$(s)	26.60 ± 4.20
$\Delta\dot{V}O_2/\Delta$WR (L/min/W)	0.01 ± 0.00
$\dot{Q}$-$\dot{V}O_2$ slope	5.43 ± 1.16
$\dot{Q}$ (L/min)	11.49 ± 2.93
Total time (s)	691.80 ± 76.00
Ramp rate (W/min)	23.30 ± 5.57
Peak exercise values	
$\dot{V}O_{2p}$ (L/min)	3.57 ± 0.97
TOI amp (%)	14.39 ± 7.20
Peak work rate (W)	290.00 ±75.00

Parameters shaded in grey were determined from the ramp incremental exercise test. Remaining parameters were determined from step exercise tests (see methods section). Baseline values were determined from an average of the last 60s unloaded pedalling; $\dot{V}O_{2m}\tau$(s) was back-calculated in the model from pulmonary $\dot{V}O_2$ measurements; $\dot{Q}$-$\dot{V}O_2$ slope was determined from moderate step exercise by ($\Delta\dot{Q}/\Delta\dot{V}O_2$); $\dot{V}O_{2p}$ was taken as the highest 12 breath average during the last 30 seconds of ramp exercise. Table parameters: $\dot{V}O_{2p}$ pulmonary oxygen uptake; $\dot{Q}$ blood flow; $\dot{V}O_{2p}\tau$ oxygen uptake kinetics; $\dot{Q}\tau$ blood flow kinetics; TOI amp tissue oxygenation index amplitude

2.1.3 Protocol 3

Subjects and ethics were the same as for protocol 2.

Equipment, measures and protocols

Subjects were placed supine on a padded table with their legs fully extended. The NIRS probe was placed longitudinally on the belly of the right medial gastrocnemius and secured with adhesive tape and an elastic bandage. A 13 cm x 85 cm blood pressure cuff was placed on the proximal thigh of same leg, attached to a rapid cuff inflator, and a cushioned pad was

placed under the ankle of the participant such that the lower leg was elevated (~50-75 mm), and the NIRS probe was suspended above the table, to limit potential movement artefacts from the NIRS probe touching the table during the assessment. The participant was first familiarised with cycles of plantar flexion-relaxation exercise (at roughly one per second) against a manually applied (hand) resistance. Participants were instructed to keep their knee joint straight and focus on only using the gastrocnemius to perform the exercise. Repeated cuff inflations from low (~50 mmHg) to high (~250 mmHg) were also performed during familiarisation phase, and arterial occlusion (AO) was determined from a tolerated cuff pressure within the range of 200-300 mmHg that resulted in HHbMb rise, $HbMbO_2$ fall, and an approximately constant tHbMb over ~15-20 s. Following familiarisation and a 2-3-minute resting period (to allow the NIRS signals to return to a resting state), the measurement protocol began. The participant was instructed to execute 10-12 cycles of plantar flexion exercise (this was approx. 10 – 15 s), which was followed immediately by sustained arterial occlusion (SAO), which was applied until a steady state in TOI (%) was reached. When a steady state in TOI was reached, the cuff was deflated, and muscle 're-oxygenation' was recorded until a steady state was reached. This procedure (the physiological normalization; PN) identifies the functional range of TOI under resting conditions, from minimum TOI at the end of the sustained arterial occlusion to maximum TOI at the peak of the reactive hyperaemia. Next, the participant performed two oxidative capacity assessments. Here, the participant performed cycles of plantar flection exercise to desaturate the muscle to a target of 50% of the physiological normalization amplitude (Figure 15). This was immediately followed by a series of intermittent arterial occlusions (5 occlusions for 5 s, and 10 occlusions for 10 s, each separated by 5-20 s recovery). The occlusion protocol was designed to maximise the ability to characterise the kinetics changes in $m\dot{V}O_2$ whilst minimising any discomfort to participants. The oxidative capacity assessment was then repeated for a second time once a resting steady state was re-established.

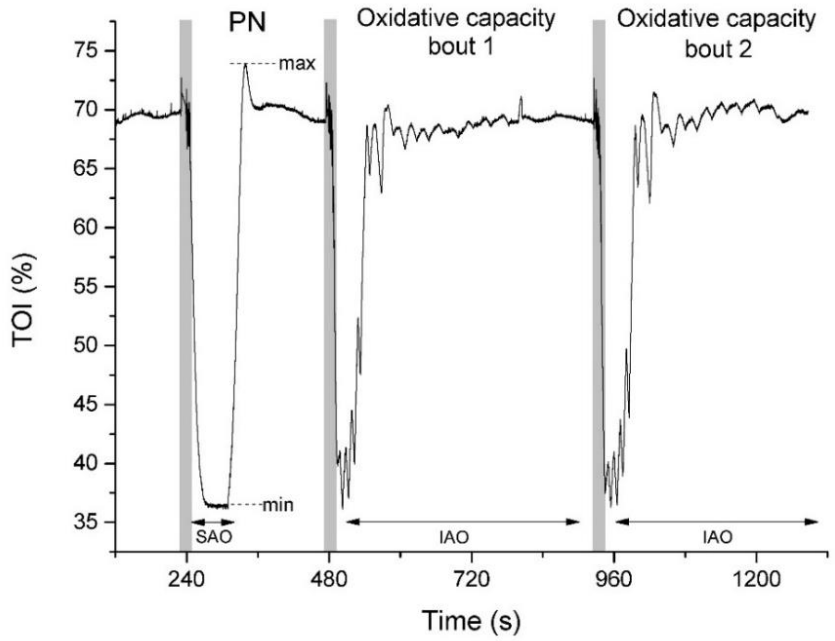

Figure 15: Raw tissue oxygenation index (TOI) trace from one complete visit in a representative subject. PN is the physiological normalisation procedure. “min” and “max” mark minimum [at the end of the sustained arterial occlusion (SAO)] and maximum (at peak reactive hyperaemia) TOI respectively. IOA represents periods of intermittent arterial occlusions, from which the kinetics of $m\dot{V}O_2$ recovery are calculated (see methods section for details).

Data analysis

Raw HHbMb, $HbMbO_2$, and TOI was averaged into second-by-second data. HHbMb and $HbMbO_2$ were then corrected for changes in blood volume using the following equations (Ryan et al., 2012).

$$\beta(t)= \frac{HbMbO2(t)}{[HbMbO2(t)]+[HHbMb(t)]} \quad (15)$$

where β is the blood volume correction factor, and t represents time. A value for β was calculated for each data point. Each data point was then corrected using its corresponding β such that:

$$HbMbO_{2c}=HbMbO2-[tHbMb \times (1- \beta)] \quad (16)$$

and

$$HHbMb_c = HHbMb - (tHb - \beta) \quad (17)$$

where $HbMbO_{2c}$ and $HHbMb_c$ are corrected oxygenated and deoxygenated haemoglobin and myoglobin respectively (Figure 16). This gives a $HbMbO_2$ signal that is corrected by subtracting the proportion of the blood volume change attributed to $HbMbO_2$, giving a corrected $HbMbO_2$ that represents the $HBMbO_2$ signal minus the oxygenated blood volume change. Similarly, the raw HHbMb signal is corrected by subtracting the proportion of the blood volume change attributed to HHbMb, giving a corrected HHbMb signal that represents the HHbMb signal minus the deoxygenated blood volume change (Ryan et al., 2012). During the repeated oxidative capacity tests, for each intermittent arterial occlusion the negative slope of corrected HbO_{2c} was fitted with a simple linear regression to estimate relative $m\dot{V}O_2$. The time constant (τ, with units of seconds) and the $m\dot{V}O_2$ exponential recovery rate constant *k* were estimated using non-linear least-squares regression. The rate constant *k* (where *k* (min^{-1}) = [1/ τ]* 60) for the recovery of $m\dot{V}O_2$ is directly related to the muscles oxidative capacity, while the time constant τ (i.e. τ = [1/*k*]*60) is inversely related to muscle oxidative capacity.

Statistical analysis

All data are presented as mean ± SD unless otherwise stated. A Bland-Altman analysis was performed for repeated measurements to assess the agreement between the $m\dot{V}O_2$ recovery kinetics. Coefficient of variance (CV) and intra class correlation coefficient (ICC) was used to assess within subject test-retest variability. Where within the same day tests (i.e. bout one and bout two) were found to be reproducible, these tests were averaged and compared in the same manner described above for between day (i.e. day 1 and day 2) test-retest reproducibility.

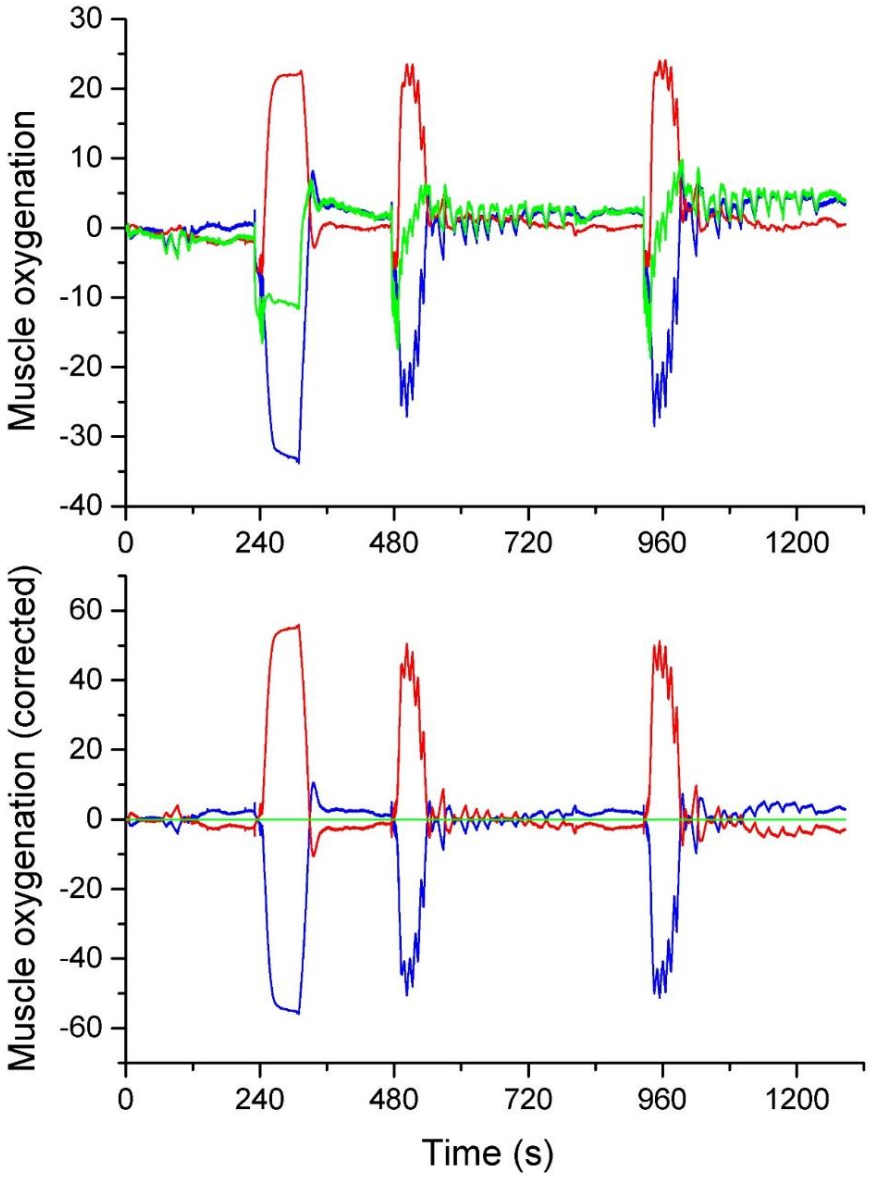

Figure 16: Raw HHbMb (red line), $HbMbO_2$ (blue line) and tHbMb (green line) during physiological normalisation and two oxidative capacity tests in a representative subject before (top panel) and after (bottom panel) correcting for blood volume changes.

2.1.4 Protocol 4

Subjects and ethics

8 Heart failure patients (mean ± SD: age, 59 ± 10 years; body mass, 82 ± 13 kg; Height 1.7 ± 0.7 m; LVEF 33 ± 9 %; NYHA classes II-III) attended Leeds Clinical Research Facility on three occasions.

Equipment and measures

Pulmonary gas exchange measurements were collected as described in protocol 2.

Exercise protocols

Visit 1: Ramp incremental exercise test

Patients performed a symptom limited ramp incremental exercise test to the limit of tolerance as described above. Ramp rates ranged from 5-15 W/min and were individually targeted to produce a test duration of 8-12 minutes. The test was terminated when the pedal cadence could no longer be maintained above 50 rpm despite strong verbal encouragement, or at the discretion of the cardiac physiologist overseeing the test. Before each bout, the ergometer flywheel was manually accelerated to 50 rpm to eliminate inertial influence at exercise onset. Pedal cadence was maintained between 50 and 60 rpm during exercise.

Visit 2 and 3: Moderate intensity step exercise test

Patients performed a constant load moderate intensity exercise tests at a work rate determined from the ramp incremental exercise test corresponding to 90% of lactate threshold. Patients performed at least 4 minutes of warm-up exercise at 10 W, followed by a constant work load bout lasting 6 minutes in duration, and followed with at least 6 minutes of rest with the patient sat on the ergometer. All tests were conducted at the same time of day for each patient, with 7 days between visits.

Data analysis

Data analysis was the same as described in protocol 2 (for healthy participants) with the exception of hemodynamic measurements. For heart failure patients it was not possible to obtain baseline cardiac output from the exercise protocol used. As such, baseline cardiac output was estimated by using a scaling factor determined from previously published cardiac output and $\dot{V}O_2$ measurements in two hundred and nineteen heart failure patients (Williams et al., 2001). From Williams et al. (2001) the ratio of baseline

cardiac output to baseline $\dot{V}O_2$ was 4.8:0.33 (L/min) respectively. Therefore, a scaling factor of 14.5 was used for baseline cardiac output estimation (i.e. baseline cardiac output = baseline $\dot{V}O_2$ * 14.5).

2.1.5 Protocol 5

Subjects and ethics

33 heart failure patients (mean ± SD: age, 65 ± 10 years; body mass, 85 ± 16 kg; Height 1.2 ± 0.8 m; LVEF 30 ± 8 %; NYHA classes I-III) volunteered to take part in the study and provided informed written consent. The investigation was approved by the National Institute for Health Research, Leeds Clinical Facility research committee.

Equipment and measures

Pulmonary gas exchange measurements and NIRS were collected as described in protocol 2.

Exercise protocols

Patients attended Leeds Clinical Research Facility on one occasion. On arrival, prior to any exercise, a resting echocardiogram was performed for measurement of key cardiac function parameters. Participants then performed a symptom limited ramp incremental exercise test to the limit of tolerance. Each test was preceded and followed with at least 4 minutes of unloaded pedalling at 10 W. Ramp rates (which ranged from 5-15 W/min) were individually targeted to produce a test duration of 8-12 minutes. The test was terminated when the pedal cadence could no longer be maintained above 50 rpm despite strong verbal encouragement, or at the discretion of the cardiac physiologist overseeing the test.

Data analysis

Data was analysed according to the methods described in protocol 2.

Chapter 3 A validated model of muscle oxygen uptake and circulatory dynamics during incremental exercise

3.1 Introduction

Exercise capacity is determined, largely, by the balance between oxygen supply and oxygen demand, and is a reliable predictor of prognosis in diseases the affect the cardio-respiratory system, such as heart failure (Cahalin et al., 1996; Stelken et al., 1996; Francis, 2000). An in-depth understanding of the mechanisms governing the control of muscular blood flow ($\dot{Q}_m$) and oxygen uptake ($\dot{V}O_{2m}$) is therefore important and may provide useful insights into the mechanisms determining exercise capacity in heart failure. Computational models have been useful in this regard but have predominantly been utilised for constant work rate (i.e. a constant metabolic demand) exercise (Barstow and Molé, 1987; Barstow et al., 1990; Lai et al., 2007; Zhou et al., 2008; Benson et al., 2013). During exercise in which the work-rate is continually increasing (incremental) exercise, the metabolic demands are constantly changing, and consequently, the relationship between $\dot{Q}_m$ and $\dot{V}O_{2m}$ must also adapt to meet these demands. This is important to consider as activities of daily living rarely occur at one metabolic rate and so assessing these dynamics during incremental exercise may be more applicable to everyday life. A computational model of oxygen transport and utilisation for incremental exercise may therefore be useful in aiding our current understanding of muscle blood flow and oxygen uptake in health failure patients.

3.1.1 A model of muscle and pulmonary O_2 uptake and circulatory dynamics during exercise

Computational modelling is an indirect method of estimating physiological variables where direct measurements are not feasible. By integrating mechanistic models of O_2 transport, circulatory dynamics, O_2 uptake and metabolism in skeletal muscle with experimental measures, factors which cannot be readily measured or altered *in vivo* can be explored. Further, the

effects of variation in parameters that are difficult to measure or manipulate *in vivo* can be quantitatively assessed (Barstow et al., 1990; Lai et al., 2009; Benson et al., 2013; Hoffmann et al., 2013). Barstow et al. (1990) developed a computational model to simulate circulatory and metabolic responses to exercise. The model is composed of three compartments; the exercising muscle, a lumped compartment for the rest of the body, and the pulmonary system through which all the cardiac output passes. A single venous volume (Vv) connected the compartments on the venous side (Figure 17).

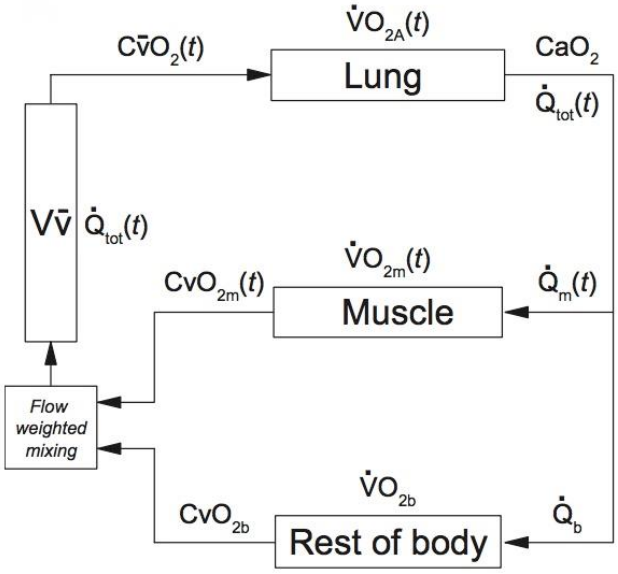

Figure 17: Schematic of the model developed by Barstow et al. (1990) that links exercising "muscle" and non-exercising "rest of body" compartments to the pulmonary circulation. The subscripts 'tot', 'm' and 'b' denote total, muscle and body components, respectively. The macron denotes "mixed venous". Taken from Benson et al. (2013).

This purposely simple model assumes the muscle to be a single homogenous compartment, where $\dot{V}O_2$ and $\dot{Q}$ were modelled to increase exponentially in response to a step increase in work rate. Equation 2 can be expanded to include the descriptions of $\dot{V}O_{2m}$ and $\dot{Q}$ such that:

$$C_vO_2 = C_aO_2 - \frac{\dot{V}O_{2b} + \Delta\dot{V}O_2 \cdot \left(1 - e^{-\frac{t}{\tau\dot{V}O_{2m}}}\right)}{\dot{Q}_b + \Delta\dot{Q} \cdot \left(1 - e^{-\frac{t}{\tau\dot{Q}}}\right)}, \quad (18)$$

where $\dot{V}O_{2m,b}$ and $\dot{Q}_b$ are baseline values, $\tau\dot{V}O_{2m}$ and $\tau\dot{Q}$ are muscle $\dot{V}O_2$ and cardiac output time constants respectively, and $\Delta\dot{V}O_2$ and $\Delta\dot{Q}$ are the steady state increases. During cycle ergometry exercise (where external work rate can be controlled) $\Delta\dot{V}O_2$ can be determined by:

$$\Delta\dot{V}O_2 = G \cdot WR , \tag{19}$$

where G is the $\dot{V}O_2$ functional gain with units of L/min/W (i.e. the O_2 cost of exercise). For cycle ergometry exercise, G is approximately 10 mL/min/W, and this is relatively constant across different genders, training status, and health status (Demarle et al., 2001). The steady-state change in blood flow, $\Delta\dot{Q}$, is defined as a function of the $\Delta\dot{V}O_2$, based on the linear relationship between $\dot{Q}$ and $\dot{V}O_2$. The $\dot{Q}/\dot{V}O_2$ relationship can be described mathematically by the equation:

$$\dot{Q} = m \cdot \dot{V}O_2 + c , \tag{20}$$

where m is the slope and c is the intercept of the linear relationship (Whipp et al., 1982). Therefore, $\Delta\dot{Q}$ during exercise is given as the product of $\Delta\dot{V}O_2$ and the slope of the $\dot{Q}/\dot{V}O_2$ relationship, i.e. a 5 L/min increase in $\dot{Q}$ for every 1 L/min increase in $\dot{V}O_2$, giving a slope of 5. The kinetics of cardiac output and muscle $\dot{V}O_2$ were modelled to increase to their steady-state values in an exponential manner. Finally, resting cardiac output ($\dot{Q}_{tot}$) and resting alveolar $\dot{V}O_2$ ($\dot{V}O_{2A}$) was divided so that a fraction was directed to the 'muscle' compartment, and the remainder going to the 'rest of the body' compartment. Note that the model predicts alveolar, rather than pulmonary, $\dot{V}O_2$ as the experimental data against which the model was validated were measures of alveolar $\dot{V}O_2$. However, there is minimal difference between these two measures (Beaver et al., 1981) and so $\dot{V}O_{2A}$ and $\dot{V}O_{2p}$ can be considered synonymous, as least for the concepts discussed here. The fractions of total $\dot{Q}$ to and $\dot{V}O_2$ from the exercising muscle compartment at rest were set to 57%, with the remainder going to/coming from the rest-of-body compartment, and C_aO_2 was kept constant throughout.

Effects of different time constants for $\dot{Q}_m$ and $\dot{V}O_{2m}$ on the C_vO_2 profile at exercise onset showed that, if $\tau\dot{Q}$ is less than or equal to $\tau\dot{V}O_{2m}$ muscle C_vO_2 falls to a new steady state without an overshoot. When $\tau\dot{Q}$ is longer than $\tau\dot{V}O_{2m}$ (i.e. blood flow kinetics are slower) muscle C_vO_2 transiently undershoots its steady state value, i.e. when the $\dot{V}O_{2m}/\dot{Q}_m$ ratio is increased, muscle C_vO_2 reaches some 'critical value' or in some scenarios, all O_2 is

extracted from the muscle. This ratio is also affected by venous O_2 capacitances [i.e. a healthy individual may store approximately 450 ml O_2 in the venous vasculature (Rossiter, 2011)] which sets the limits for the allowable discrepancy between $\dot{Q}_m$ and $\dot{V}O_{2m}$ kinetics during the exercise transient (Barstow et al., 1990). This could be significant in cases where $\dot{Q}$ kinetics are compromised, such as in heart failure patients. Under conditions where the model values were set to replicate those of healthy humans, however, oxygen delivery rises more rapidly than oxygen extraction, and hence, is not limiting to muscle $\dot{V}O_2$ kinetics during moderate exercise (i.e. in this situation CvO_2 does not undershoot its steady state value. In addition, another key finding of the model was that, despite some "kinetic dissociation" due to circulatory effects, phase II $\dot{V}O_{2p}$ kinetics closely reflected $\dot{V}O_{2m}$ kinetics to within a couple of seconds, a finding later confirmed experimentally (Grassi et al., 1996) in healthy young adults [although this may not be true in disease states such as heart failure, where cardiac function can be impaired, acting to slow cardiac output kinetics (Matsumoto et al., 1999)].

3.1.2 The multi-compartment model (MCM)

This model was recently optimised by Benson et al. (2013) where further complexity was added to the model, including the addition of separate venous volumes for the muscle and rest of body compartments, in order that the model more closely matched experimentally-recorded measures of $\dot{Q}$, C_vO_2 and $\dot{V}O_2$ (Figure 18; left). As the venous volumes were not directly measured experimentally, their values were determined by selecting, on an individual basis, the three venous volume values that gave the minimum kinetic difference of Δphase I, phase I time delay (i.e. initial muscle-to-lung time transit time), and phase II $\dot{V}O_{2A}$ τ between the model output and the experimental data. This optimised model accounted for changes in blood flow and $\dot{V}O_2$ (and therefore the $\dot{Q}_b/\dot{V}O_{2,b}$ ratio and $C_vO_{2,b}$) in the non-exercising tissues, which the original model was unable to appropriately account for. These changes allowed phase I and phase II alveolar oxygen uptake ($\dot{V}O_{2A}$) kinetics to be accurately predicted from knowledge of circulatory and respiratory dynamic interactions at the onset of exercise (Figure 18, right). The model was validated against data from the only study to date that directly and simultaneously measured pulmonary ventilation and

gas exchange, leg blood flow, blood gases and lactate concentration, and $\dot{V}O_2$ at the leg during moderate intensity cycle-ergometer exercise in healthy young men (Grassi et al., 1996).

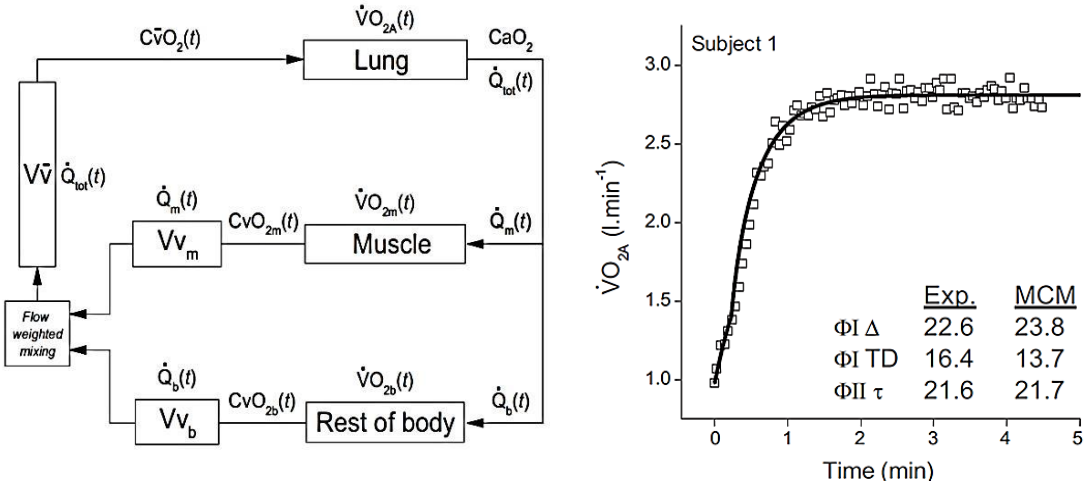

Figure 18: Left: schematic of the optimised model developed by Benson et al. (2013) named the multi-compartment model (MCM) due to its separate venous volumes for muscle and rest of body compartments. See Figure 17 for definitions. Right: the predicted $\dot{V}O_{2A}$ output from the optimized MCM for a representative subject (solid line), superimposed on the experimental $\dot{V}O_{2A}$ measurements from that subject (open squares). $\phi I\Delta$, phase I amplitude; ϕI, phase I time delay; $\phi II\tau$, phase II time constant; TD, time delay. Taken from Benson et al. (2013).

A key finding from the MCM was that the kinetics of $\dot{V}O_{2A}$ during exercise are very sensitive to pre-exercise conditions such as resting or unloaded exercise blood flow distributions. Model input values (i.e. $\dot{Q}_{tot}$, fraction $\dot{Q}$ to muscle) assumed by Barstow et al. (1990) were significantly less than the experimentally derived values. As such, simulations of the C_vO_2 profile using the input values from Barstow et al. (1990) in comparison to the experimental values, resulted in a 50% undershoot in C_vO_{2m} (Figure 19), which would result in all available muscle O_2 being extracted, this is despite the only differences being the absolute values of $\dot{Q}_m$ and $\dot{V}O_{2m}$ at unloaded pedalling. Moreover, the C_vO_2 undershoot does not just shift downwards, but is more pronounced under conditions where the muscle is poorly perfused at rest or unloaded pedalling (Benson et al., 2013). This is because, where C_aO_2 is constant, the C_vO_2 profile is determined by the ratio of the $\dot{V}O_{2m}/Q_m$ relationship (see Equation 3), which has a positive $\dot{Q}_m$ intercept. In this

context, larger discrepancies between $\dot{V}O_{2m}/\dot{Q}_m$ [in the values assumed by Barstow (1990)], resulted in a larger $\dot{V}O_2/\dot{Q}$ ratio, causing a CvO_2 undershoot whereas, closer $\dot{V}O_{2m}/\dot{Q}_m$ values measured experimentally (Grassi et al., 1996), resulted in a lower $\dot{V}O_{2m}/\dot{Q}_m$ ratio and thus reduced the CvO_2 undershoot (Benson et al., 2013).

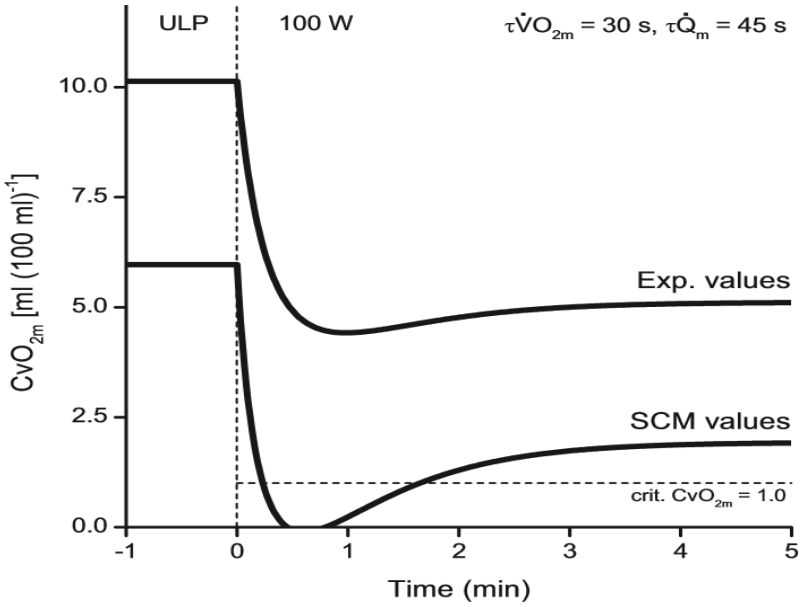

Figure 19: Simulated C_vO_2 profiles for a 100-W step change in work rate from unloaded pedalling (ULP) with use of SCM parameter values or experimentally measured values. Taken from Benson et al. (2013). SCM, single compartment model: model of Barstow et al. (1990) named the single compartment model due to having one venous volume compartment.

Experimentally, this important $\dot{V}O_2/\dot{Q}$ relationship may partially explain the transient overshoot in muscle deoxygenation (Sperandio et al., 2009) or transient undershoot in tissue oxygenation (Bowen et al., 2012) measured by near infrared spectroscopy at exercise onset seen in heart failure patients (where sluggish cardiac function may act to slow $\dot{Q}_m$ kinetics). Sperandio et al. (2009) observed a transient overshoot in the deoxygenated haemoglobin + myoglobin signal, implying that estimated fractional O_2 extraction increased above the steady state level because of impaired blood flow relative to $\dot{V}O_2$ causing C_vO_2 (or capillary PO_2) to reach some critical value,

that likely reduces the diffusion gradient from capillary to mitochondria, causing impaired O_2 flux and limiting the rate of increase in muscle $\dot{V}O_2$.

3.2 MCM model: current state and projections

The models of Barstow et al. (1990) and Benson et al. (2013) have shown that computational approaches can be beneficial in helping to understand the kinetics of oxygen uptake and the availability of O_2 at the skeletal muscle during exercise. This has implications for understanding the mechanisms underlying the changes to $\dot{V}O_{2p}$ kinetics seen in heart failure: are changes to measured pulmonary $\dot{V}O_2$ direct reflections of changes to muscle $\dot{V}O_2$, or can changes to resting blood flow, for example, influence $\dot{V}O_{2p}$ kinetics?

Computational models integrating muscle oxygen uptake and circulatory dynamics have demonstrated how impairments in oxygen transport (i.e. poor cardiac function) and/or utilisation can lead to distortions of key physiological relationships (e.g. slowed $\dot{V}O_2$ kinetics), that ultimately lead to exercise intolerance (Benson et al., 2013). To date, models of oxygen uptake and circulatory dynamics have been predominately developed for constant work rate (step) exercise (Barstow et al., 1990; Lai et al., 2009; Benson et al., 2013), where valuable inferences can be made during the transition from rest or unloaded pedalling to the prescribed work rate. The model of Benson et al. (2013) has only been validated for moderate intensity exercise during the on-transient (i.e. at the start of sub-lactate threshold constant-load exercise), and not for higher intensity domains (above lactate threshold). It is therefore unclear whether the model can reproduce the physiological characteristics seen across exercise intensities and during different exercise protocols such as ramp incremental exercise to the limit of tolerance. This is pertinent in disease states such as heart failure, as activities of daily living are rarely performed at one exercise intensity (or metabolic steady state). Additionally, ramp incremental tests (requiring continuous adjustment to changes in metabolic demand) are the most commonly used cardio-pulmonary exercise test in clinical settings (Weisman, 2003). As such, its use as a diagnostic tool is limited, at least until such a validation is carried out. The aim for this chapter was to develop and validate the MCM for incremental exercise by adding new components to the model. This chapter consists of the addition of these components and parameterisation to the data. The new components are described below (see section “developing the model for incremental exercise”) and can be summarised by equations

25-27. NB: This chapter was a collaborative piece of work with Dr Al Benson. Contributions as follows: Sophie Hampson; model development & formulation of equations, data collection, data analysis, model validation, and all write up. Dr Al Benson: model development & formulation of equations, all model coding.

3.3 Methods

Experimental methods

The experimental data used in this chapter were taken (with permission) from Grassi et al. (1996). Experimental methods are described in the general methods section under sub-heading “Protocol 1”

Computational methods

3.3.1 The MCM model

The MCM developed by Benson et al. (2013) was based on the original model of Barstow et al. (1990). It is composed of three compartments; ‘muscle’ ‘rest of body’ and ‘pulmonary’, with venous volume effluents from the muscle and rest of body compartment, and a third venous volume which both effluents flow through, in a flow-weighted mixing manner. As in the Barstow et al. (1990) model, $\dot{Q}_m$ and $\dot{V}O_{2m}$ increased exponentially (see Equation 4) towards their steady state which was determined by their assigned work rate profile. O_2 concentrations of the muscle (C_vO_{2m}) and rest of body (C_vO_{2b}) effluents were calculated by utilising the Fick equation:

$$C_vO_{2x}(t) = C_aO_2 - VO_{2x}(t) / \dot{Q}_x(t), \quad (21)$$

where the subscript x represents either muscle or rest of body. Flow weighted mixing was calculated by:

$$C_vO_{2,m+b} = C_vO_{2m}\left(\frac{\dot{Q}_m}{\dot{Q}_{tot}}\right) + C_vO_{2b}\left(\frac{\dot{Q}_b}{\dot{Q}_{tot}}\right), \quad (22)$$

where all variable are functions of time. The blood with the now mixed venous O_2 concentration then travels down a single venous volume to the

pulmonary compartment the variable flow in the venous volume is determined by $\dot{Q}_{tot}$. This results in a muscle-to-lung transit time delay (TD) that is determined by the values of Vv, $\dot{Q}_{tot}$, and t. The TD for the venous effluents being mixed at any given time is calculated by integrating $\dot{Q}_{tot}$ from t until the integral is equal to V_v, conforming to the equation:

$$V_v = \int_t^{t+TD(t)} Q_{tot}(t)dt \, . \quad (23)$$

Integration was carried out using the trapezoid rule. Mixed C_vO_2 ($C\bar{v}O_2$) at the lung and at time t+TD(t) is given by C_vO_{2m+b} at time t, with $C\bar{v}O_2$ remaining at its unloaded pedalling (baseline) value for when t is less than the initial muscle-to-lung time delay. $\dot{V}O_{2A}$ at each time t is then solved using the Fick principle:

$$\dot{V}O_{2A}(t) = \dot{Q}_{tot}(t)[C_aO_2 - C\bar{v}O_2(t)] \quad (24)$$

3.3.2 Developing the MCM for incremental exercise

To simulate incremental exercise, some important changes to the MCM were required. This involved (i) the inclusion of "muscle fibre recruitment" and (ii) changing the profile of the $\dot{V}O_2$ and $\dot{Q}$ responses following exercise onset.

During increasing work rate exercise, muscle fibres are sequentially recruited to meet the increasing work rate requirements of the task, in order to increase the metabolic rate to generate the required energy (Burnley et al., 2002). The MCM developed to reproduce responses to step exercise (Benson et al., 2013; henceforth referred to as "MCM_{step}") contained a single homogeneous muscle compartment. In order to reproduce responses to incremental exercise, it was therefore necessary to develop a model that contained separate "muscle fibres" that could be sequentially recruited as work rate increased (this version of the model will be referred to as "MCM_{inc}"): During an exercise simulation, the MCM_{inc} gradually recruits these individual muscle fibres as the exercise protocol progresses and the work rate increases, with a given number of muscle fibres recruited per watt increase in work rate. Each muscle fibre has its own $\dot{V}O_2$ gain (G_{fibre}) that is determined by whole body $\dot{V}O_2$ gain and the number of fibres recruited per watt of exercise – for example, if whole body $\dot{V}O_2$ gain is 10 mL/min/W and 5

muscle fibres are recruited per watt of exercise, then the individual G_{fibre} = 10/5 = 2 mL/min/W. (Note that, if required, the parameters associated with each individual "muscle fibre" can be set individually to produce a heterogeneous muscle compartment. For these studies, however, gain and other parameters in each fibre were set to be identical, producing a homogeneous muscle compartment.) The $\dot{V}O_2$ of each muscle fibre increases in an exponential manner to a steady state, as described by Equation 27. These muscle fibres are sequentially recruited and their $\dot{V}O_2$ responses are summed. Thus, the $\dot{V}O_2$ response profile of individual muscle fibres is a mono-exponential increase (exponential decay) to steady-state, while the whole-muscle $\dot{V}O_2$ response shows a short exponential phase followed by a linear increase (assuming the gain of each recruited muscle fibre is identical) typical of whole-muscle/whole-body $\dot{V}O_2$ responses to ramp incremental exercise.

The change in $\dot{Q}$ and $\dot{V}O_2$ during the ramp for each individual muscle fibre and body compartment was therefore calculated by:

$$\Delta\dot{V}O_{2fib} = (\Delta\dot{V}O_2/\Delta W_{mus})/N_{fibres/W}, \quad (25)$$

and,

$$\Delta\dot{Q}_{fib} = \Delta\dot{V}O_{2fib} \cdot (\Delta\dot{Q}/\Delta\dot{V}O_{2mus}), \quad (26)$$

where $\Delta\dot{V}O_{2fib}$ is the steady state change in muscle fibre $\dot{V}O_2$ (L/min), $\Delta\dot{V}O_2/\Delta W_{mus}$ is the change in muscle compartment $\dot{V}O_2$ per watt of exercise (i.e. the $\dot{V}O_2$ gain of the muscle; L/min/W), $N_{fibres/W}$ is the number of muscle fibres recruited per watt of exercise (W), $\Delta\dot{Q}_{fib}$ is the steady state change in muscle fibre blood flow (L/min), and $\Delta\dot{Q}/\Delta\dot{V}O_{2mus}$ is the change in muscle compartment blood flow per litre change in muscle $\dot{V}O_2$ (L/min).

Cardiac output to muscle fibres, and $\dot{V}O_2$ from muscle fibres, were modelled to increase monoexponentially, conforming to the equation:

$$fibre_x(t) = fibre_{x,base} + \Delta fibre_x \cdot (1 - e^{-(t-t_{recruit,x})/\tau_x}), \quad (27)$$

where the subscript x denotes $\dot{Q}$ or $\dot{V}O_2$, $fibre_{x,base}$ is baseline or starting fibre value, $\Delta fibre_x$ is the steady state change in muscle fibre required for a given work rate, and $t_{recruit,x}$ is the fibre recruitment time for fibre x.

Oxygen concentrations in the blood draining the muscle and rest of body compartments, flow weighted mixing, transit delays and pulmonary $\dot{V}O_2$ was calculated in the same manner as the MCM for step exercise (described above, and see Benson et al. (2013). Mean response time was calculated as the time delay between the end of the simulation and the time at which the end-simulation $\dot{V}O_{2p}$ would have occurred if the $\dot{V}O_{2p}$ response increased linearly with no kinetics according to $\dot{V}O_2 = G \times t \times$ ramp slope. Model $\dot{V}O_{2p}$ outputs were averaged into 30s bins in the same manner as the experimental data and plotted as functions of increasing work rate before being superimposed over experimental $\dot{V}O_{2p}$ data. 99% percent prediction bands (equal to 3 standard deviations from the mean, where 1 SD on the $\dot{V}O_{2p}$ noise is 0.1 L/min (Lamarra et al., 1987; Rossiter et al., 2000) were applied to the model $\dot{V}O_{2p}$ data, indicating the regions in which one would expect 99% of experimental breaths to fall. The accuracy of the model was determined by the percentage of data points that fell within these 99% prediction bands. Models were coded in C and were compiled to run on a Windows PC using Code::Blocks IDE (integrated development environment) software (open-source software available at http://www.codeblocks.org) The model was validated against $\dot{V}O_{2p}$ data from the same subjects in which the original MCM (for moderate intensity constant work rate exercise) was developed against (Grassi et al., 1996).

3.4 Results and discussion

3.4.1 Initial model validation

The pulmonary $\dot{V}O_2$ output from the MCM_{inc} were validated, on a subject-by-subject basis, against the ramp data from the Grassi study (Grassi et al., 1996) using the subject-specific parameters from the original (i.e. pre-optimised) MCM_{step} (Benson et al., 2013) as inputs to the model. Table 3 shows the level of agreement between experimental data and the MCM_{inc} with pre-optimised parameters, presented as percentage of experimental data points that lie within the model 99% prediction bands (i.e. the model $\dot{V}O_{2p}$ output ± 0.3 L/min, which equates to ± 3 standard deviations of the noise expected on $\dot{V}O_{2p}$ (Lamarra et al., 1987; Rossiter et al., 2000).

Table 3: Level of agreement between pre-optimised model values and experimental data for individual subjects

Subject	Level of agreement (%)
1	88
2	94
3	94
4	63
5	72
6	76

The mean overall agreement between our experimental data and the pre-optimised model parameters was 81% (i.e. on average 81% of the experimental $\dot{V}O_{2p}$ data lay within 3 standard deviations from the mean of the model $\dot{V}O_{2p}$ data). Figure 20 shows the (30s) averaged experimental data with 3 SD error bars, and the pre-optimised model values averaged in the same manner as the experimental data. As shown, the model did not always lie in the 3 standard deviations of expected noise, this is especially true towards the end of the ramp where the $\dot{V}O_{2p}$ starts to plateau in some subjects (despite obvious plateau data at or near the limit of tolerance being removed from the experimental dataset before comparison). Figure 21 shows the time series pre-optimised model $\dot{V}O_{2p}$ data superimposed with experimental data. As with the averaged data, not all the experimental data fell within 99% prediction bands.

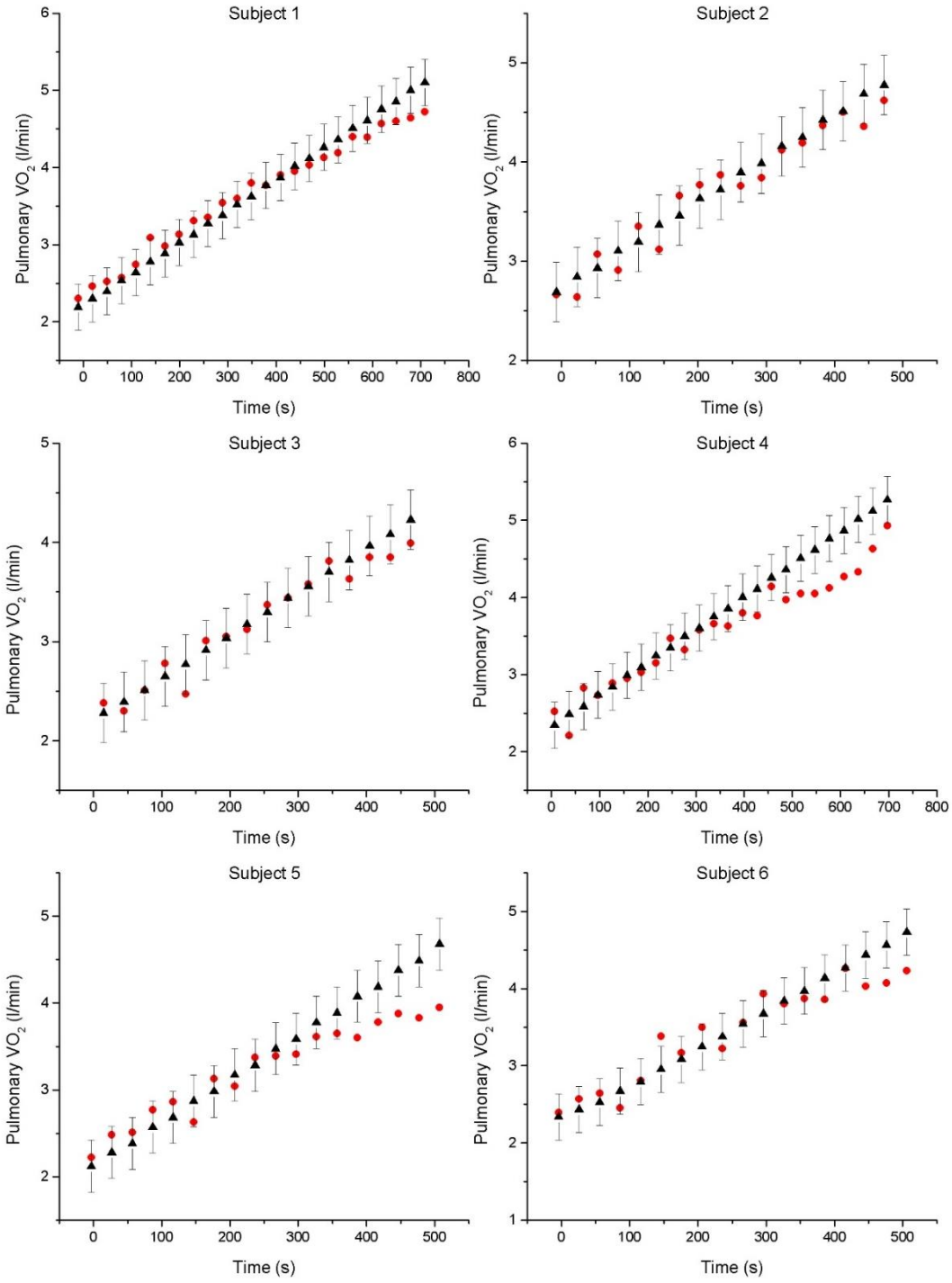

Figure 20: Averaged pre-optimised model $\dot{V}O_{2p}$ values (black triangles) with y-error bars marking 3 standard deviations from the mean, superimposed on experimental data (red circles).

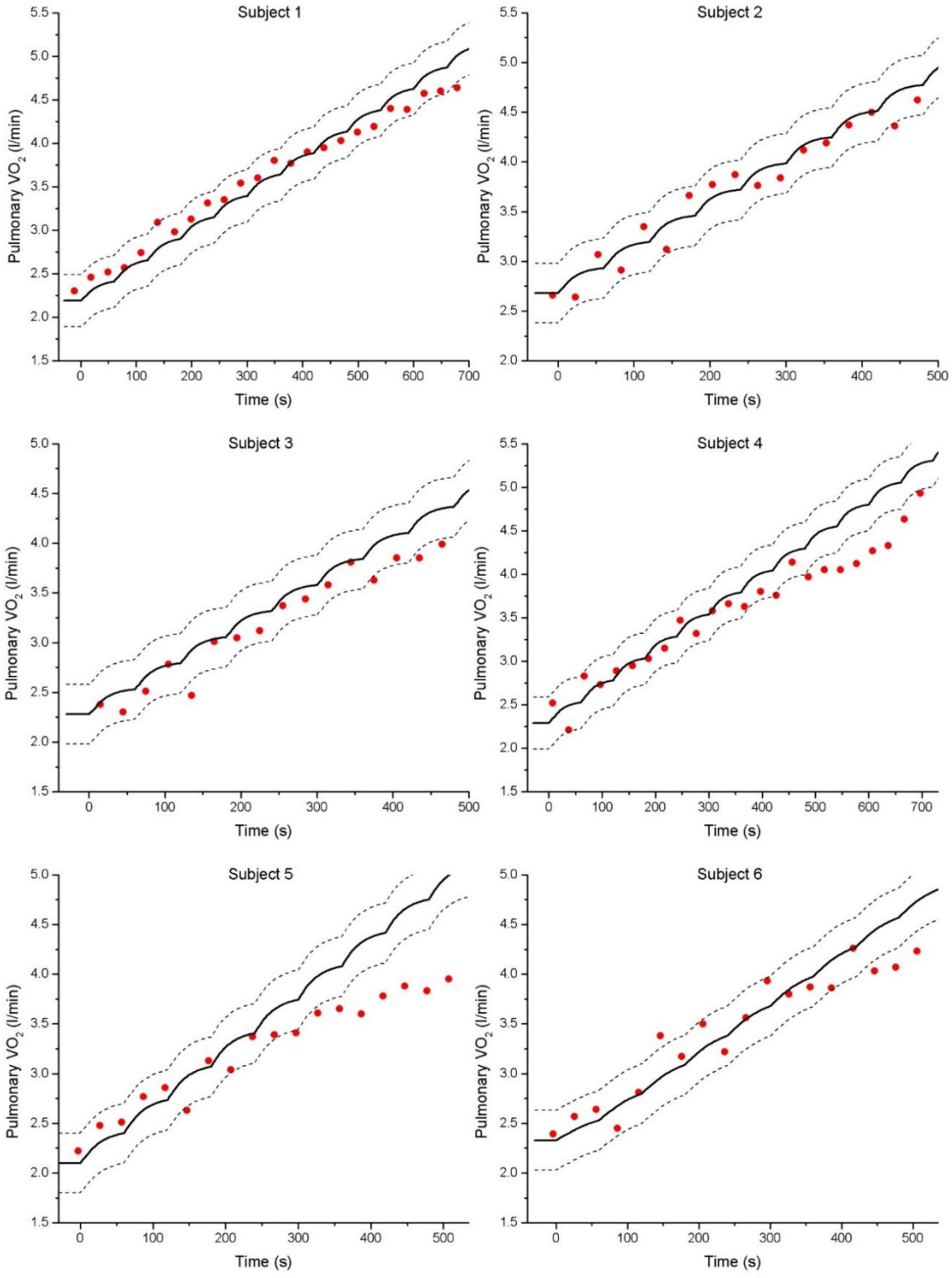

Figure 21: Time series pre-optimised_model (solid black line) with 99% prediction bands (dashed black lines) superimposed with 30s averaged experimental $\dot{V}O_{2p}$ data.

3.4.1 Model optimisation

Next, it was explored whether normal expected physiological variability in parameters could account for the discrepancy between the model and the experimental data. To identify model parameters that have a significant effect on the model output (and thus help us streamline its optimisation) a sensitivity analysis was performed on the MCM_{inc}. Model parameters were changed by ± 10% from their pre-optimised_values (see Table 1 and Table 4 for sensitivity analysis input and output values). Any parameter that caused a >1% change in the baseline $\dot{V}O_2$, the slope of the $\dot{V}O_2$ response, the peak $\dot{V}O_2$, or the kinetics of the $\dot{V}O_2$ response (see Table 5) was considered a parameter that could be modified in order to optimise the MCM_{inc}. The search identified baseline cardiac output ($\dot{Q}_b$), baseline pulmonary $\dot{V}O_2$ ($\dot{V}O_{2p,b}$), functional gain ($\Delta\dot{V}O_2/\Delta WR$), the slope of the $\dot{V}O_2$-$\dot{Q}$ relationship ($\Delta\dot{V}O_2/\Delta\dot{Q}$), and muscle $\dot{V}O_2$ kinetics ($\tau\dot{V}O_{2m}$) to be most important parameters in terms of modifying the model outputs under observation (see Table 5). Subsequently, these key parameters were modified, on a subject-by-subject basis, to find the combination of parameter values that gave the best fit between the MCM_{inc} output and the experimental data. Of the five key parameters identified, $\dot{Q}_b$, $\Delta\dot{V}O_2/\Delta WR$, $\Delta\dot{V}O_2/\Delta\dot{Q}$, and $\tau\dot{V}O_{2m}$ were changed. Baseline oxygen uptake ($\dot{V}O_{2p,b}$) was not changed, as this parameter value was measured directly from the experimental data, and so was not an unknown. As $\dot{V}O_{2m}$ kinetics were modified, to avoid kinetic mismatch (where O_2 delivery is unphysiologically slow compared to O_2 utilisation, or vice versa) $\dot{Q}$ kinetics ($\tau\dot{Q}$) were also modified to maintain the $\tau\dot{Q}/\tau\dot{V}O_{2m}$ ratio at a suitable level. To avoid unphysiological best-fit parameter values, any changed parameter values were constrained to lie in the range of mean ± 3 SDs of the values from Grassi et al. (1996) and Benson et al. (2013): $5.95 \leq \dot{Q}_b \leq 12.24$ s; $6.92 \leq \Delta\dot{V}O_2/\Delta WR \leq 12.02$ ml.min^{-1}.W^{-1}; $4.44 \leq \Delta\dot{V}O_2/\Delta\dot{Q} \leq 7.62$; $13.81 \leq \tau\dot{V}O_{2m} \leq 30.93$ s; $0.84 \leq \tau\dot{Q}/\tau\dot{V}O_{2m} \leq 1.32$. Because of the complexity of the model and the fact that analytical solutions to the equations are not possible (thus precluding the use of the gold-standard Levenberg-Marquardt algorithm for parameter fitting), a custom “alternating variable search” (Press, 2007) was employed to find the combination of parameter values (for parameters identified as key in the sensitivity analysis) that reduced the sum-of-squares between binned and experimental data to a minimum (where model output data were binned and averaged to match the experimental data). The alternating variable search starts by increasing then decreasing one parameter ($\dot{Q}_b$ in this case) by

10%: if either change resulted in a model output with a better fit to the experimental data, that parameter change was kept and the parameter took on the new value (i.e. its previous value plus or minus 10%, depending on whether increasing or decreasing the parameter value resulted in the better fit); if neither increasing nor decreasing the parameter value resulted in a better fit between model output and experimental data, the old parameter value was kept. The algorithm then works through the remaining parameters in turn ($\Delta\dot{V}O_2/\Delta WR$, followed by $\Delta\dot{V}O_2/\Delta\dot{Q}$, $\tau\dot{V}O_{2m}$ and finally $\tau\dot{Q}/\tau\dot{V}O_{2m}$) performing the same ±10% parameter value change as described above. Once the algorithm had changed each parameter by ±10%, the process was repeated, again looping through each parameter in turn and changing the parameter value by ±10%. When changing any parameter by ±10% no longer resulted in a better fit between model output and experimental data, the entire process described above was repeated but with ±1% parameter changes. Again, once changing any parameter by ±1% no longer resulted in a better fit between model output and experimental data, the entire process was repeated a final time using ±0.1% parameter changes. Note that, because of the large muscle-pulmonary kinetic dissociation seen with Subject 6 and the probability that this occurred because of complicated bi-exponential cardiac output and muscle blood flow kinetics (Grassi et al., 1996; Benson et al., 2013), subject 6 was omitted from the current optimisation procedure.

Table 4: Pre-optimised model output parameters (top line) and model output parameters following sensitivity analysis

	Minus 10%				Plus 10%			
		$\dot{V}O_2$				$\dot{V}O_2$		
	Baseline (L/min)	τ (s)	**Slope** (L/min/min)	**Peak** (L/min)	**Baseline** (L/min)	**MRT** (s)	**Slope** (L/min/min)	**Peak** (L/min)
Pre-optimised:	0.87	23.40	0.20	2.79	0.87	23.40	0.20	2.79
C_aO_2	0.87	23.40	0.20	2.79	0.87	23.39	0.20	2.79
Venus volumes, litres								
Muscle	0.87	23.37	0.20	2.79	0.87	23.44	0.20	2.79
Body	0.87	23.40	0.20	2.79	0.87	23.40	0.20	2.79
Mixed	0.87	23.29	0.20	2.79	0.87	23.52	0.20	2.79
Baseline (unloaded pedalling) values								
$\dot{V}O_{2A}$	0.78	23.62	0.20	2.70	0.96	23.17	0.20	2.88
Fraction from muscle[a]	0.87	23.45	0.20	2.79	0.87	23.35	0.20	2.79
$\dot{Q}_{tot}$	0.87	23.12	0.20	2.79	0.87	23.62	0.20	2.79
Fraction to muscle[a]	0.87	23.33	0.20	2.79	0.87	23.45	0.20	2.79
Exercise $\dot{V}O_2$ and $\dot{Q}$ parameters								
$\Delta\dot{V}O_{2m}$ / ΔWR	0.87	23.60	0.18	2.60	0.87	23.23	0.22	2.98
$\Delta\dot{Q}$ / ΔWR	0.87	23.85	0.20	2.79	0.87	23.03	0.20	2.79
Muscle $\dot{V}O_2$ and blood flow kinetics								
$\dot{Q}_m$ τ	0.87	21.18	0.20	2.80	0.87	25.62	0.20	2.78
$\dot{V}O_{2m}$ τ	0.87	23.42	0.20	2.79	0.87	23.38	0.20	2.79

Table parameters: $\dot{Q}$ denotes blood flow. The subscripts 'tot' and 'm' denote total and muscle components, respectively. [a]The remainder of the baseline $\dot{V}O_{2p}$ (and $\dot{Q}_{tot}$) comes from (and goes to) the body compartment.

Table 5: Sensitivity analysis results to identify parameters that have an influence on the ramp model

	Minus 10%				Plus 10%			
		$\dot{V}O_2$				$\dot{V}O_2$		
	Baseline (L/min)	**τ** (s)	**Slope** (L/min/min)	**Peak** (L/min)	**Baseline** (L/min)	**MRT** (s)	**Slope** (L/min/min)	**Peak** (L/min)
C_aO_2	0.0	0.0	0.0	0.0	0.0	0.0	0.0	0.0
Venus volumes								
Muscle	0.0	-0.1	0.0	0.0	0.0	0.2	0.0	0.0
Body	0.0	0.0	0.0	0.0	0.0	0.0	0.0	0.0
Mixed	0.0	-0.5	0.0	0.0	0.0	0.5	0.0	0.0
Baseline (unloaded pedalling) values								
$\dot{V}O_{2A}$	-10.3	0.9	0.0	-3.2	10.3	-1.0	0.0	3.2
Fraction from muscle[a]	0.0	0.2	0.0	0.0	0.0	-0.2	0.0	0.0
$\dot{Q}_{tot}$	0.0	-1.2	0.0	0.0	0.0	0.9	0.0	0.0
Fraction to muscle[a]	0.0	-0.3	0.0	0.0	0.0	0.2	0.0	0.0
Exercise $\dot{V}O_2$ and $\dot{Q}$ parameters								
$\Delta\dot{V}O_{2m}$ / ΔWR	0.0	0.9	-10.0	-6.8	0.0	-0.7	10.0	6.8
$\Delta\dot{Q}$ / ΔWR	0.0	1.9	0.0	0.0	0.0	-1.6	0.0	0.0
Muscle $\dot{V}O_2$ and blood flow kinetics								
$\dot{Q}_m\,\tau$	0.0	-9.5	0.0	0.4	0.0	9.5	0.0	-0.4
$\dot{V}O_{2m}\,\tau$	0.0	0.1	0.0	0.0	0.0	-0.1	0.0	0.0

Table parameters: $\dot{Q}$ denotes blood flow. The subscripts 'tot' and 'm' denote total and muscle components, respectively. [a]The remainder of the baseline $\dot{V}O_{2p}$ (and $\dot{Q}_{tot}$) comes from (and goes to) the body compartment. Values highlight in red indicate any parameters that caused changes of greater than 1% in baseline $\dot{V}O_2$, $\dot{V}O_2$ kinetics, $\dot{V}O_2$/WR slope, or $\dot{V}O_{2,peak}$.

This process yielded post-optimisation best fit parameters (Table 6). Figure 22 shows model output with best fit parameters (averaged in the same manner as experimental data) superimposed with the experimental data, and Figure 13 shows second-by-second best fit model values superimposed with averaged experimental values post optimisation.

Table 6: Individual subject best fit parameters following model optimisation

Parameter	**Subject**				
	1	**2**	**3**	**4**	**5**
$\dot{Q}_{b\ (L/min)}$	13.04	21.98	13.57	14.37	12.50
$\Delta\dot{V}O_2/\Delta WR$ (L/min/W)	0.01	0.01	0.01	0.01	0.01
$\Delta\dot{V}O_2/\Delta\dot{Q}$	7.62	4.44	7.61	7.61	7.62
$\tau\dot{V}O_{2m\ (s)}$	13.81	21.45	13.81	13.81	13.81
$\tau\dot{Q}$ (s)	18.23	28.28	12.35	11.70	11.99

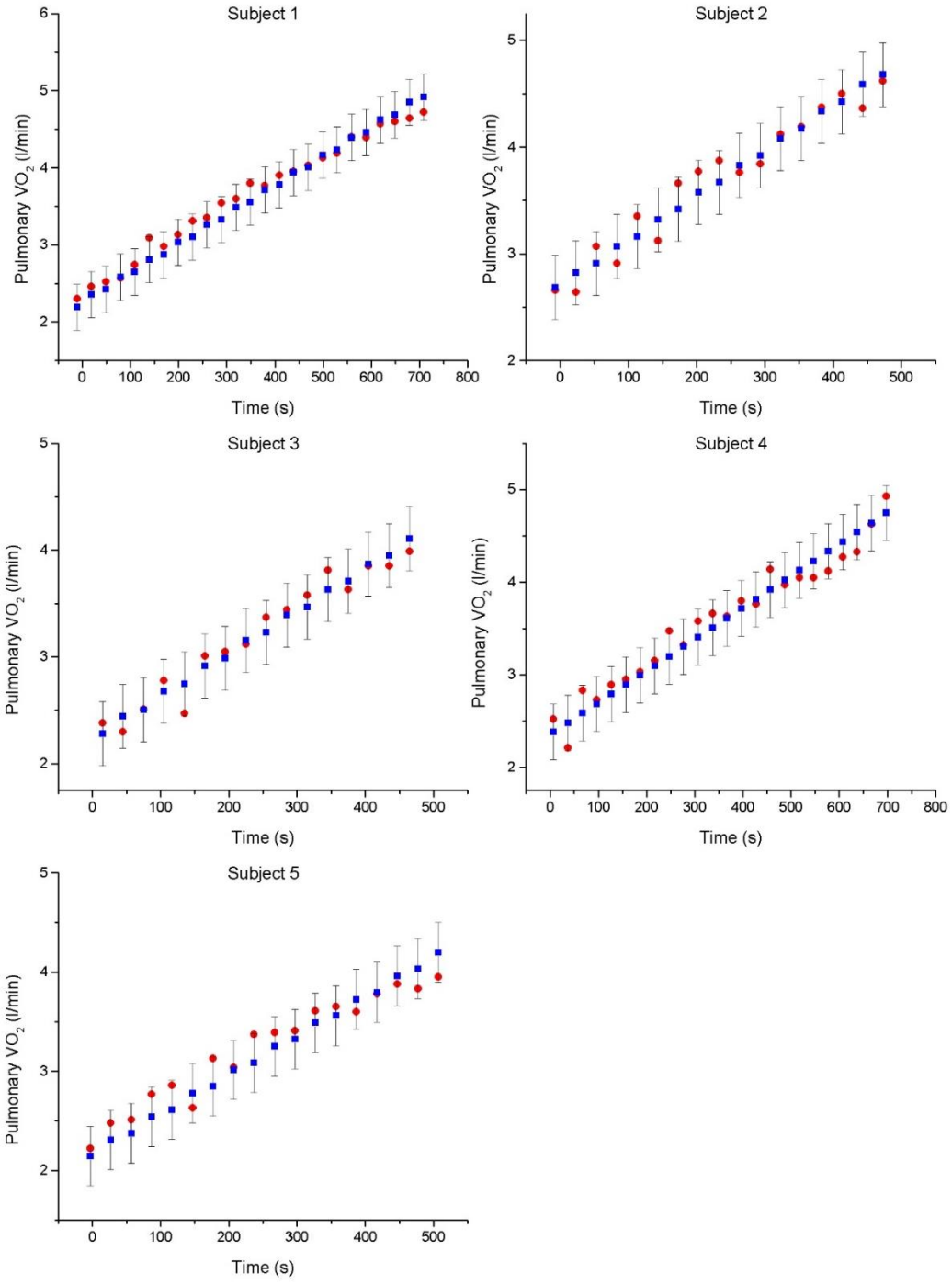

Figure 22: Averaged pre-optimised model $\dot{V}O_{2p}$ values (black triangles) with y-error bars marking 3 standard deviations from the mean, superimposed on experimental data (red circles)

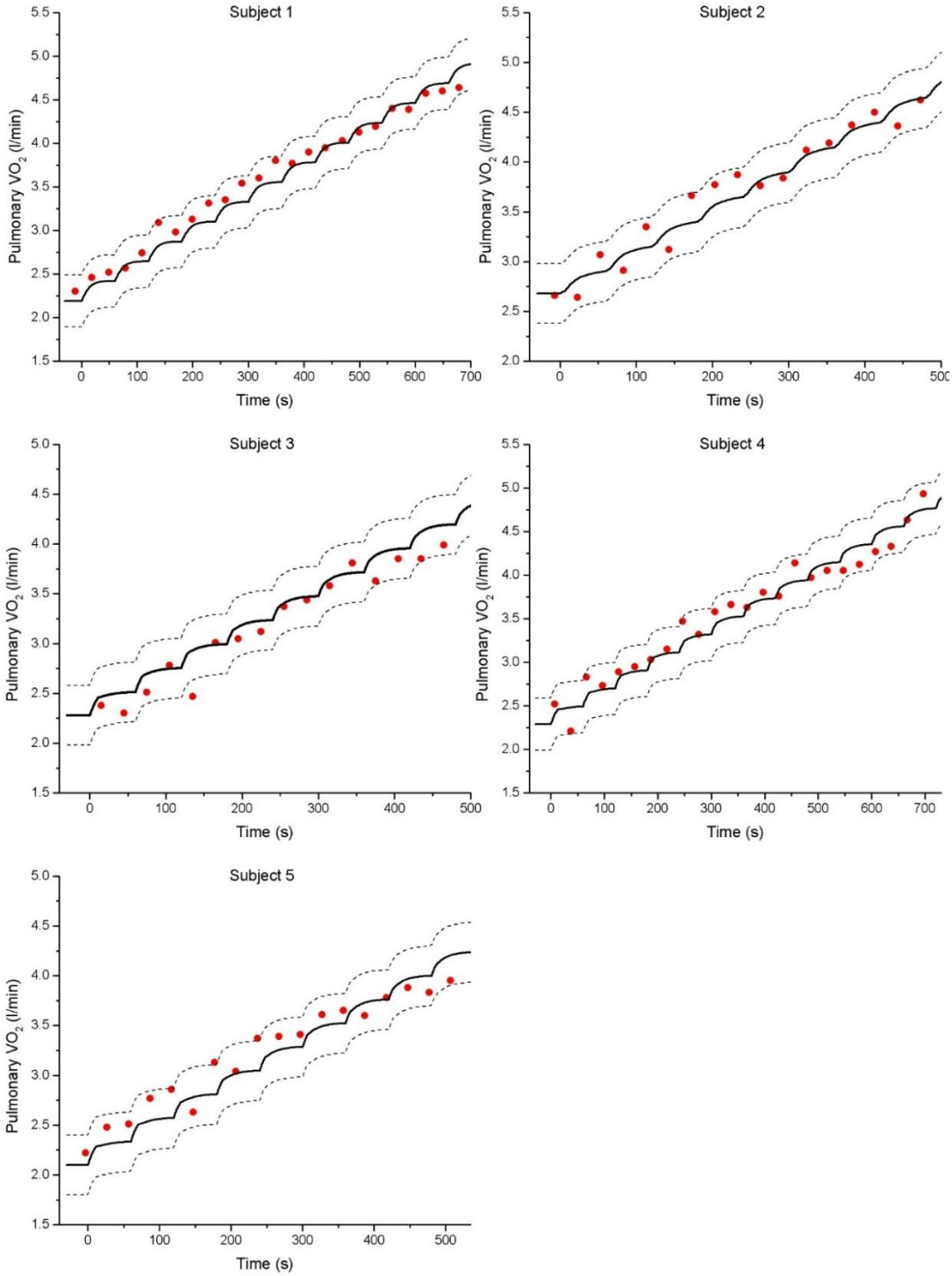

Figure 23: Time series pre-optimised model (solid black line) with 99% prediction bands (dashed black lines) superimposed with 30s averaged experimental $\dot{V}O_{2p}$ data.

The post-optimisation best fit parameters give $\dot{V}O_{2p}$ values in which 100% of values lie within ± 3 SDs of $\dot{V}O_2$ noise (i.e. 99% prediction bands) for all 5 subjects at all time points. Therefore, it can be concluded that normal variation in parameters provide a model that fits the experimental data, thus validating the MCM_{inc}. Average best fit parameters (i.e. the post-optimsation MCM_{inc} values) for the MCM_{inc} model are shown in Table 7.

Table 7: Pre and post optimisation parameter values for the MCM_{inc} model

Parameter	MCM values	
	Pre-optimisation	**Post-optimisation**
C_aO_2 (L O2/ L blood)	0.20	0.20
Venus volumes (L)		
Muscle	0.70	0.70
Body	0.10	0.10
Mixed	2.30	2.30
Baseline (unloaded pedalling) values		
$\dot{V}O_{2A}$, (L/min)	0.87	2.31
Fraction from muscle[a]	0.57	0.57
$\dot{Q}_{tot}$, (L/min)	8.89	15.09
Fraction to muscle[a]	0.57	0.57
Exercise $\dot{V}O_2$ and $\dot{Q}$ parameters		
$\Delta\dot{V}O_{2m}/\Delta$WR, (L/min/W)	0.01	0.01
$\Delta\dot{Q}$ / $\Delta\dot{V}O_{2m}$	6.00	6.98
Muscle $\dot{V}O_2$ and blood flow kinetics		
$\tau\dot{Q}_m$ (s)	24.00	15.30
$\tau\dot{V}O_{2m}$ (s)	22.00	16.50

Table parameters: $\dot{Q}$ denotes blood flow. The subscripts 'tot' and 'm' denote total and muscle components, respectively. [a]The remainder of the baseline $\dot{V}O_{2p}$ (and $\dot{Q}_{tot}$) comes from (and goes to) the body compartment. Note these are averaged values from the experimentally collected data (Grassi et al., 1996). Standard deviations have been removed for clarity.

Note the large differences in some of the parameters (baseline $\dot{V}O_2$, baseline $\dot{Q}_{tot}$, $\Delta\dot{V}O_2$ and $\Delta\dot{Q}$ relationship and $\dot{V}O_2$ and $\dot{Q}$ kinetics) following optimisation. One of the possible reasons for these differences is likely from the different unloaded pedalling work rates. For the incremental exercise protocol baseline pedalling in the elite amateur cyclists was 150 W. A higher baseline work rate will elevate baseline $\dot{V}O_2$ and cardiac output, thereby increasing the $\dot{V}O_2/\dot{Q}$ slope. The difference in the kinetics is also likely a consequence of the higher $\dot{V}O_2$ and $\dot{Q}$. This is because the model does not take into account baseline work rate (i.e. all model simulations were simulated from a 0 W baseline) thereby requiring faster kinetics to meet $\dot{V}O_2$ demands.

Model limitations

Computational models are simplified versions of complex systems. The MCM_{inc} presented here, is a relatively simplified model of circulatory and oxygen transport dynamics with a lumped “exercising muscle”, “non-exercising muscle,” and “lung” compartment. The MCM_{inc} assumes homogenous muscle compartments however, during exercise transitions there is substantial heterogeneity of fibre types with differing $\dot{V}O_2/\dot{Q}$ ratios distributed within bodily tissues, between exercising and non-exercising muscles (Ferreira, McDonough, et al., 2006), and within different locomotor muscles engaged in exercise (Armstrong and Laughlin, 1985; Piiper et al., 1985; McDonough et al., 2005; Koga et al., 2007, 2014; Laaksonen et al., 2010). This balance between $\dot{V}O_2$ and $\dot{Q}$ is important as it sets the microvascular (or capillary) PO_2 and thus the upstream driving pressure for blood-myocyte O_2 flux as well as influencing metabolic control via the impact on intramyocyte PO_2 and $\dot{V}O_2$ kinetics. Consequently, the heterogeneities in these compartments may influence model predictions. For example, areas with a low $\dot{Q}/\dot{V}O2$ ratio will have a high fractional O_2 extraction and consequently, a microvascular PO_2 so low that blood-myocyte O_2 flux will be impaired compromising mitochondrial control. Benke et al. (2003) and McDonough et al. (2005) showed that the kinetic profile of microvascular PO_2 and its absolute levels during contractions vary markedly in the soleus muscle compared with either the peroneal or gastrocnemius. In the peroneal and gastrocnemius muscles, microvascular PO_2 was shown to fall much faster and to a lower level that in the soleus muscle. As the model assumes homogenous muscle compartment, the variable $\dot{V}O_2/\dot{Q}$ ratios within the exercising muscle are not represented and the muscle oxygen extraction

response is based on a homogenous $\dot{V}O_2/\dot{Q}$ ratio such that any variance in the $\dot{V}O_2/\dot{Q}$ ratio within the muscle compartments in the model are not accounted for. The overall oxygen extraction response may therefore be under or overestimated depending on the fibre type composition and blood flow distribution in the muscle of interest. Model predictions may be improved further by creating a model compartment in which the $\dot{V}O_2/\dot{Q}$ ratio can be altered depending on the fibre type composition of the exercising muscle and its $\dot{V}O_2/\dot{Q}$ ratio.

The model is also simplified with the exclusion of any complex energetic systems, such as the breakdown of phosphocreatine, which has been demonstrated to influence the $\dot{V}O_{2p}$ phase II (i.e. $\dot{V}O_{2p}$ kinetics) response (Geer et al., 2002; Rossiter et al., 2002; Forbes et al., 2009). For example, inhibition of creatine kinase (the enzyme which catalyses the reversible transfer of high energy phosphates between phosphocreatine and ADP), at exercise onset, accelerates $\dot{V}O_2$ kinetics (Grassi et al., 2011). Furthermore, during high intensity exercise (i.e. during the later stages of the incremental exercise test) approximately 90% of the magnitude of the $\dot{V}O_2$ slow component is reflected within the exercising muscle by its PCr response (Rossiter et al., 2002).

One of the consequences of not including more complex energetic systems is that the model cannot predict some of the subtleties of the $\dot{V}O_{2p}$ response, such as the lactate threshold (one of the key parameters determined from incremental exercise testing). The model can, however, produce a $\dot{V}O_{2p}$ mean response time (the sum of the kinetics of phase I and phase II), another important parameter determined from incremental exercise. Despite its importance, the $\dot{V}O_{2p}$ mean response time is not typically used for kinetic analysis in healthy individuals due to the inability to dissociate phase I and phase II. Because of this, much less attention has been paid to the $\dot{V}O_{2p}$ mean response time (relative to phase II $\dot{V}O_{2p}$ kinetics), especially in health. The $\dot{V}O_{2p}$ mean response time, however, is more commonly used in heart failure patients, where distinguishing between phase I and phase II is more complex (this will be explored in more detail in Chapter 3). The incremental model can be used to probe in more detail, the mean response time, and in particular explore its significance in heart failure.

Additionally, the model is not able to predict any plateaus in $\dot{V}O_{2p}$ which were seen experimentally towards the end of the ramp in some subjects. The plateau in $\dot{V}O_2$ has been used to as criteria during an incremental test, to determine if the individual has achieved a true $\dot{V}O_2$ max. However, the $\dot{V}O_2$ plateau is inconsistent across individuals (Beltz et al., 2016). For example, a plateau in the $\dot{V}O_2$ response to incremental exercise has been reported in as low as 20% of some subjects (Niemelä et al., 1980; Myers et al., 1990) to as high as 94% in others (Taylor et al., 1955). Furthermore, this plateau is dependent on many factors: for example, Zuniga et al. (2012) compared the incidence of a $\dot{V}O_2$ plateau during incremental ramp exercise with incremental step exercise. During the ramp incremental protocol, they found that 64% of subjects exhibited a $\dot{V}O_2$ plateau compared to 36% during the step incremental protocol. This is interesting given that it has been shown that there are no significant differences in lactate threshold, $\dot{V}O_{2max}$, or $\Delta\dot{V}O_2/\Delta WR$ relationship as long as the overall increase in work rate remained the same (Zhang et al., 1991), and in fact, a 1-min step incremental test was indistinguishable from a ramp incremental test (Zhang et al., 1991). It has also been demonstrated that training status may affect the $\dot{V}O_2$ plateau incidence: for example, in a group of elite cyclists 47% exhibited $\dot{V}O_2$ plateau, compared to 24% untrained (Lucia et al., 2006). The authors of the latter study suggested that this was possibly due to trained cyclists having higher pain threshold than their untrained counterparts. Other variables effecting the $\dot{V}O_2$ plateau incidence are age (Astorino et al., 2000), testing modality i.e treadmill vs cycle ergometer exercise (Gordon et al., 2012), and the methodology in which $\dot{V}O_{2p}$ data are processed (Astorino, 2008). Given that the (patho)physiological mechanisms underlying the $\dot{V}O_{2p}$ plateau remain to be elucidated, adding unknown components to the model, so that it can predict plateaus in $\dot{V}O_{2p}$ (even phenomenologically), would be speculation and is beyond the scope of this study. However, it needs to be recognised that the inability of the model to predict $\dot{V}O_{2p}$ plateaus is potentially a limitation. Nevertheless, despite the potential influence of these factors, the model is still able to predict the $\dot{V}O_{2p}$ response with good accuracy.

3.5 Conclusion

The data presented here provide a version of the MCM_{step} adapted for incremental exercise. The model is, to our knowledge, the first to accurately predict $\dot{V}O_{2p}$ responses to incremental exercise, from knowledge of

circulatory and respiratory interactions measured directly from healthy individuals. This was achieved by the addition of a muscle fibre compartment in which separate muscle fibres, with their own $\dot{V}O_2$ gain, could be recruited sequentially according to the increase in work rate. Additionally, the profile of the $\dot{V}O_2$ and $\dot{Q}$ responses were modelled to increase with a short exponential phase followed by a linear phase, to replicate the $\dot{V}O_2$ response to incremental exercise.

The model can be used to explore some of the subtleties of the kinetics of the $\dot{V}O_{2p}$ response for incremental exercise, the mean response time. This will be addressed in Chapter 3. In addition, the model will be further developed in Chapter 4, to include a 'muscle oxygenation' output, which will be used to further explore the mechanisms of exercise tolerance in heart failure patients, the model will be used in this context to inform experimental data presented in Chapter 5.

Chapter 4 Investigating muscle oxygenation dynamics by computational modelling and near infrared spectroscopy

4.1 Introduction

Whole body measurements of pulmonary oxygen uptake can be measured during a cardiopulmonary exercise test, with good precision at the mouth ($\dot{V}O_{2p}$), and have been shown to be a close representation of oxygen uptake at the skeletal muscle ($\dot{V}O_{2m}$) in healthy humans (Grassi et al., 1996). However, there are limitations associated with this measurement technique, including the inability to discriminate between exercising and whole-body measurements (i.e. there is a small but significant change in oxygen uptake in the non-exercising muscles, which influences whole body oxygen uptake) as well as between different muscles engaged in the exercise (Benson et al., 2013). In addition, the presence of O_2 stores between the site of O_2 exchange and the measurement site complicate data interpretation during exercise transitions (Cerretelli and Di Prampero, 1987). Another way of measuring $\dot{V}O_{2m}$ in humans is the direct Fick method (Grassi et al., 1996; Bangsbo et al., 2000). However, this method is highly invasive and complex. Furthermore, sampling the venous effluent of the exercising muscle without contamination of venous blood from other muscles remains a technical limitation in humans (Grassi and Quaresima, 2016). Consequently, NIRS has been utilised as a non-invasive method of measuring muscle oxygenation dynamics (i.e. balance between oxygen delivery and utilisation) due to its ability to provide information on key physiological and pathophysiological mechanisms relevant in the evaluation of exercise tolerance in healthy and patient populations (Grassi and Quaresima, 2016).

Modelling studies have also been utilised to investigate key relationships related to convective and diffusive O_2 delivery, and their effects on $\dot{V}O_2$ kinetics. Spires et al. (2013) showed that when O_2 delivery is limited, the permeability surface area (a key determinant of oxygen diffusion) increases at a greater rate than $\dot{Q}$ to enhance O_2 diffusion rates between blood and

tissue. Additionally, Lai et al. (2009) developed a model of O_2 transport and metabolism to determine the contribution of myoglobin to the NIRS signal under conditions of normoxia and hypoxia. The latter study demonstrated that Mb contribution to the NIRS signal was significant under normoxic conditions, and becomes even more substantial during hypoxia, and therefore may play a role in changing the muscle oxygenation signal under conditions of normoxia and hypoxia (Lai et al., 2009). The latter study used experimentally derived NIRS along with $\dot{V}O_2$ and hemodynamic measurements as inputs to the model, to determine the factors (relative contributions of haemoglobin and myoglobin, effects of muscle blood volume etc.) that may modify the NIRS signal. However, no model has used knowledge of O_2 utilisation and transport dynamics to simulate a 'NIRS output'; that is, to predict the NIRS output for any given simulated "subject" and exercise protocol. Such a model would be a useful research tool as it will allow insight into the mechanisms that cause inter- and intra-subject/patient variability in measured NIRS signals and may provide a tool that can be translated to the clinic to determine the locus of any O_2 transport/utilisation limitation.

The aim of this study was to (i) develop a computational model of oxygen transport and circulatory dynamics (Benson et al., 2013) to include a NIRS output (deoxygenated haemoglobin + myoglobin, oxygenated haemoglobin + myoglobin, total heme, and tissue oxygenation index) for both constant work rate (step) and incremental (ramp) exercise; (ii) validate the model using experimentally collected NIRS (deoxygenated haemoglobin and myoglobin, oxygenated haemoglobin and myoglobin, tissue oxygenation index, total heme), pulmonary gas exchange measurements ($\dot{V}O_2$) and directly measured muscle $\dot{V}O_2$ and $\dot{Q}$ data obtained from healthy individuals; (iii) to explore, mechanistically, whether any of the key variables that play a role in determining muscle oxygenation in the model may explain the different NIRS responses seen in healthy individuals and those with heart failure. As with the model in Chapter 3 the model was developed collaboratively with Dr Al Benson. Contributions as follows: Sophie Hampson; model development & formulation of equations, data collection, data analysis, model validation, and all write up. Dr Al Benson: model development & formulation of equations, all model coding. The new components of the model are detailed in equations 28-52 (see below in section 'New NIRS development') which

breakdown the steps in creating an additional muscle NIRS compartment for the model.

4.2 Methods

Experimental data collection is described in the general methods section under sub-heading ‘Protocol 2’

Computational methods

4.2.1 New NIRS model development

The newly developed NIRS model (described below) is the only computational model (so far and to our knowledge) that can produce NIRS outputs (specifically oxygenated haemoglobin, deoxygenated haemoglobin, total haemoglobin and tissue oxygenation index). It takes simulated arterial and venous O_2 concentrations from the O_2 transport model (described in Chapter 1) as inputs and calculates the corresponding muscle NIRS signals. A schematic of the muscle compartment of the NIRS model is shown in Figure 24. It was assumed that the muscle is homogeneous, such that the concentrations (e.g. of oxy and deoxy haemoglobin and myoglobin) in the small muscle region investigated by NIRS (i.e. the “muscle compartment” in the NIRS model) are representative of those throughout the rest of the exercising muscle.

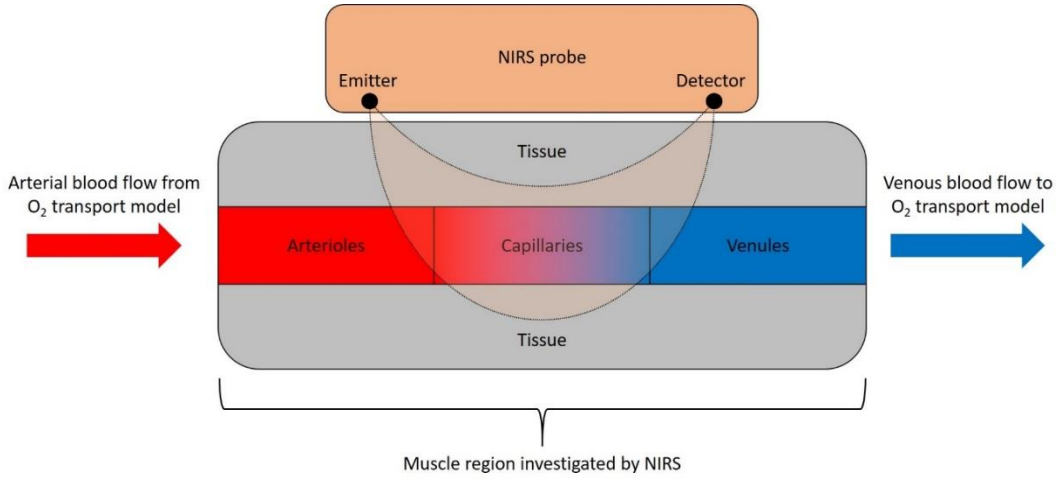

Figure 24: Schematic of the muscle compartment of the NIRS model.

Note the following volume relationships: The muscle compartment is composed of a blood compartment and a tissue (or “intracellular”) compartment, such that:

$$\text{muscle volume } (V_m) = \text{blood volume } (V_b) + \text{tissue volume } (V_i)$$

$$\text{blood fraction in muscle } (f_b) = \frac{V_b}{V_m} = \frac{V_b}{V_b + V_i}$$

$$\text{tissue fraction in muscle } (f_i) = \frac{V_i}{V_m} = \frac{V_i}{V_b + V_i}$$

and therefore $f_b + f_i = 1.0$

The blood compartment in the muscle is composed of arterial[1], capillary and venous[1] compartments, such that:

$$\text{blood volume } (V_b) = \text{arterial volume } (V_a) + \text{capillary volume } (V_c) + \text{venous volume } (V_v)$$

$$\text{arterial fraction in muscle blood } (f_a) = \frac{V_a}{V_b} = \frac{V_a}{V_a + V_c + V_v}$$

$$\text{capillary fraction in muscle blood } (f_c) = \frac{V_c}{V_b} = \frac{V_c}{V_a + V_c + V_v}$$

$$\text{venous fraction in muscle blood } (f_v) = \frac{V_v}{V_b} = \frac{V_v}{V_a + V_c + V_v}$$

---

[1] Throughout this section, “arterial” refers to blood in the arterioles of the muscle microcirculation, and has the same O_2 concentration as blood in the arteries of the O_2 transport model. Similarly, “venous” refers to the blood in the venules of the muscle microcirculation, which has the same O_2 concentration as the venous effluent leaving the exercising skeletal muscle in the O_2 transport model, i.e. before it travels along the “muscle venous system” and mixes with blood from “non-exercising” muscles.

and therefore $f_a + f_c + f_v = 1.0$

Initial pre-exercise volume fractions

Initial (pre-exercise) arterial, capillary and venous fractions in muscle blood were set to be f_a = 0.06, f_c = 0.84 and f_v = 0.1, according to measurements made in skeletal muscle (Poole et al., 1995). Note the large difference in these initial values, particularly the capillary and venous fractions, compared to those in Lai et al. (2009) (f_a = 0.1, f_c = 0.15 and f_v = 0.75) which are likely to reflect vascular volumes in the brain rather than skeletal muscle (Davis and Barstow, 2013). Any change in muscle blood volume during exercise is assumed to be proportional to the change in muscle blood flow, and takes place in the capillaries, with the arterial and venous volumes in the muscle (V_a and V_v) remaining constant. After derivation of the NIRS model equations, the developed NIRS model was optimised to: (i) determine the proportionality constant linking change in capillary volume to change in muscle blood flow; and (ii) determine the contributions of haemoglobin and myoglobin to the NIRS signal, which are reflected in the blood and tissue fractions in the muscle (f_b and f_i): see "Model optimisation" below.

Calculate total O_2 concentration in capillary blood

O_2 concentration in the capillary is spatially-varying, i.e. changes with distance along the capillary. It was assumed that the drop in capillary O_2 concentration along the length of the capillary is linear. The mean capillary O_2 concentration (over the whole muscle) is therefore given by the mean of the arterial and venous O_2 concentrations:

$$C_cO_2 = (C_aO_2 + C_vO_2)/2 \quad (28)$$

When calculating venous O_2 concentration, any blood transit times in the small total capillary volume in the exercising muscle of ~100 ml can initially

be ignored.[2] That is to say, any change in mean capillary O_2 concentration will be instantly reflected in an equal change in venous O_2 concentration.

Calculate oxygenated and deoxygenated haemoglobin concentrations in arterial, capillary and venous blood

Haemoglobin concentration in the blood, [Hb], has a value of 150 g Hb/L blood in healthy adult humans. This concentration can be converted from units of g/L to molar units (M) by dividing by the molar mass of haemoglobin[3], M_{Hb}, then multiplying by 1000 to give more useable units of mM:

$$[\mathrm{Hb}](\mathrm{mM}) = \frac{1000 \times [\mathrm{Hb}](\mathrm{g/L})}{M_{\mathrm{Hb}}} \tag{29}$$

where M_{Hb} = 65000 g/mol. Therefore, [Hb] = 150 g/L = 2.308 mM. Regardless of the units used for Hb concentration, the amount of haemoglobin that is oxygenated was required: that is, haemoglobin O_2 saturation (S_xO_2; given as a fraction, and where the subscript x denotes arterial, capillary or venous blood) was required. In order to do this, equations linking total O_2 concentration in the blood (C_xO_2; known from the O_2 transport model) and S_xO_2 were needed. The 'oxygen content equation' states that total O_2 concentration is the sum of the Hb-bound and free O_2 concentrations:

$$C_xO_2 = C_xO_{2,\mathrm{bound}} + C_xO_{2,\mathrm{free}} \tag{30}$$

where, as before, the subscript x denotes arterial, capillary or venous blood. The Hb-bound O_2 concentration is given by

---

[2] Assume body mass of 75 kg. Then, from values given in Lai et al. (2009) active muscle volume is "13% of body mass" (presumably swapping units from kg to L), so 9.75 L; muscle blood volume is 7% of muscle volume, so 682.5 ml; and capillary volume is 15% of muscle blood volume, so 102.375 ml.

[3] Molar mass used to be termed "molecular weight", and is sometimes given in units of daltons (Da), where 1 Da = 1 g/mol.

$$C_xO_{2,bound} = C_{Hb}\,[Hb]\,S_xO_2 \tag{31}$$

where C_{Hb} = 0.00134 L O_2/g Hb is Hüfner's constant defining the maximum O_2 binding capacity of haemoglobin, and [Hb] (in units of g Hb/L blood) and S_xO_2 have been defined above. From Henry's law, the free O_2 concentration is given by

$$C_xO_{2,free} = \alpha_b P_xO_2 \tag{32}$$

where α_b = 0.000031 L O_2/mmHg O_2/L blood is the solubility coefficient of O_2 in blood, and P_xO_2 is the partial pressure of O_2 (mmHg). By substituting equations 31 and 32 into equation 30, total O_2 concentration in the blood is given by

$$C_xO_2 = C_{Hb}\,[Hb]\,S_xO_2 + \alpha_b P_xO_2 \tag{33}$$

The model now has an equation linking C_xO_2 and S_xO_2. However, both S_xO_2 and P_xO_2 in equation 33 are unknowns, precluding calculation of S_xO_2 from C_xO_2 using equation 33. Therefore, to get only one unknown, one unknown can be substituted for the other. The two unknowns, S_xO_2 and P_xO_2, are related through the oxygen-haemoglobin dissociation curve, which can be described by Severinghaus (1979):

$$S_xO_2 = \frac{1}{\left[\left(\frac{1}{P_xO_2{}^3 + 150\,P_xO_2}\right)23400\right] + 1} \tag{34}$$

Unfortunately, equation 34 cannot be rearranged to make P_xO_2 the subject of the equation, due to the cubic term. Although Severinghaus (1979) provided an alternative equation describing the oxygen-haemoglobin dissociation curve with P_xO_2 on the left-hand-side of the equation, as needed, it is accurate only for values of S_xO_2 lower than 0.965; therefore the equation above was used which is accurate over the entire oxygen-haemoglobin dissociation curve. So, substituting equation 34 into equation 31 gave

$$C_xO_{2,bound} = \frac{C_{Hb}\,[Hb]}{\left[\left(\frac{1}{{P_xO_2}^3 + 150\,P_xO_2}\right)23400\right] + 1} \tag{35}$$

and , from equations 32, 35 and 37,

$$C_xO_2 = \frac{C_{Hb}\,[Hb]}{\left[\left(\frac{1}{{P_xO_2}^3 + 150\,P_xO_2}\right)23400\right] + 1} + \alpha_b P_xO_2 \tag{36}$$

Equation 36 now had only one unknown, P_xO_2. P_xO_2 could therefore be calculated using equation 36, and the resultant values plugged into equation 34 which gave S_xO_2. (This was needed to calculate P_xO_2 anyway, as it was needed for calculating myoglobin saturation below, so this was not a "wasted" step.) However, as with equation 34, equation 36 could not be directly solved for P_xO_2 (i.e. it is not possible to rearrange the equation to get P_xO_2 on the left-hand-side) due to the cubic term. Instead, a "brute-force search" was used to find the solution, by varying P_xO_2 until the right-hand side of the equation matches the value of C_xO_2 the O_2 transport model has produced. Practically, this can be achieved using a "lookup table" containing pre-calculated solutions to the equation for different values of P_xO_2 at a suitable resolution: one finds the closest C_xO_2 value in the table to the O_2 transport model's current C_xO_2 value and reads off the corresponding P_xO_2 value, then S_xO_2 can be calculated by substituting this value for P_xO_2 into equation 34. The concentration of oxygenated haemoglobin in arterial, capillary or venous blood, $[HbO_{2,x}]$, is then calculated as the product of the haemoglobin concentration and the haemoglobin saturation:

$$[HbO_{2,x}] = [Hb]\,S_xO_2 \tag{37}$$

using units of g/L or mM for $[HbO_{2,x}]$ and [Hb], as seemed fit. It follows that the remainder of the haemoglobin is deoxygenated: deoxygenated haemoglobin concentration in arterial, capillary or venous blood, $[HHb_x]$, is therefore given by

$$[HHb_x] = [Hb]\,(1 - S_xO_2) = [Hb] - [HbO_{2,x}] \tag{38}$$

Calculate oxygenated and deoxygenated myoglobin concentrations the tissue

Myoglobin concentration, [Mb], in the tissue has a value of 4.08 g Mb/L tissue[4]. Again, this concentration was converted from units of g/L to molar units (M) by dividing by the molar mass of myoglobin, M_{Mb}, then multiplying by 1000 to give more useable units of mM:

$$[\mathrm{Mb}](\mathrm{mM}) = \frac{1000 \times [\mathrm{Mb}](\mathrm{g/L})}{M_{\mathrm{Mb}}} \tag{39}$$

where M_{Mb} = 17000 g/mol. Therefore, [Mb] = 4.08 g/L = 0.24 mM. Again, regardless of the units used for Mb concentration, the amount of myoglobin that is oxygenated needed to be determined: that is, myoglobin O_2 saturation (S_iO_2; given as a fraction, and where the subscript i denotes the tissue compartment) was needed. The oxygen-myoglobin dissociation curve can be described by

$$\mathrm{S_iO_2} = \frac{\mathrm{P_iO_2}}{\mathrm{P_{50}} + \mathrm{P_iO_2}} \tag{40}$$

where P_iO_2 is the partial pressure of O_2 (mmHg) in the tissue, and P_{50} = 3.2 mmHg is the Mb half-saturation pressure (Richardson et al., 2006). Experimental evidence (Hirai et al., 2018) has shown that the absolute value of the PO_2 gradient between the capillary and the tissue (ΔPO_2, and where $\Delta PO_2 = P_cO_2 - P_iO_2$) remains relatively constant throughout a rest-contraction protocol, with values of ΔPO_2 = 19.2 ± 9.4 mmHg and ΔPO_2 = 17.3 ± 6.5 mmHg reported at rest and during steady-state contractions, respectively, with a brief drop to approximately ΔPO_2 = 14.4 ± 7.9 mmHg during the initial 30 s of contractions (see Figure 3 in; Hirai et al. (2018)). It was therefore assumed that ΔPO_2 remained constant at 17.3 mmHg (the mean of the data presented in Figure 3 in Hirai et al. (2018), and so P_iO_2 is given as

$$\mathrm{P_iO_2} = \mathrm{P_cO_2} - 17.3 \tag{41}$$

---

[4] The mean Mb concentration and Mb molar mass (molecular weight) reported in Duteil et al. (2005) was 0.24 mM and 17 kDa, respectively. Concentration in units of g/L is given by multiplying concentration in mM by molecular weight in kDa, so 0.24 mM × 17 kDa = 4.08 g/L.

with P_iO_2 constrained to be ≥3.1 mmHg (Richardson et al., 2006), and where P_cO_2 is known from equation 36. The value for P_iO_2 obtained from equation 41 can be plugged into equation 40 to give a value for S_iO_2. The concentration of oxygenated myoglobin in in the tissue, $[MbO_{2,i}]$, is then calculated as the product of the myoglobin concentration and the myoglobin saturation:

$$\left[MbO_{2,i}\right] = [Mb]\, S_iO_2 \tag{42}$$

using units of either g/L or mM for $[MbO_{2,x}]$ and [Mb], to match the units chosen for haemoglobin. It follows that the remainder of the myoglobin is deoxygenated: deoxygenated myoglobin concentration in the tissue, $[HMb_i]$, is therefore given by

$$[HMb_i] = [Mb]\,(1 - S_iO_2) = [Mb] - \left[MbO_{2,i}\right] \tag{43}$$

Calculate haem group concentrations in the muscle

The oxyhaemoglobin and deoxyhaemoglobin concentrations in arterial, capillary and venous blood, and the oxymyoglobin and deoxymyoglobin concentrations in the tissue, are given by equations 37, 38, 42 and 43. The oxy- and deoxyhaemoglobin concentrations in the entire muscle ($[HbO_2]$ and [HHb], respectively) are given by the sum of the blood compartment oxy- and deoxyhaemoglobin concentrations weighted by their compartment volume fractions in the muscle:

$$[HbO_2] = f_b\left(f_a\left[HbO_{2,a}\right] + f_c\left[HbO_{2,c}\right] + f_v\left[HbO_{2,v}\right]\right) \tag{44}$$

$$[HHb] = f_b(f_a[HHb_a] + f_c[HHb_c] + f_v[HHb_v]) \tag{45}$$

Likewise, the oxy- and deoxymyoglobin concentrations in the entire muscle ($[MbO_2]$ and [HMb], respectively) are given by the tissue oxy- and deoxymyoglobin concentrations weighted by the tissue volume fraction in the muscle:

$$[MbO_2] = f_i\left[MbO_{2,i}\right] \tag{46}$$

$$[\mathrm{HMb}] = f_{\mathrm{i}}[\mathrm{HMb_i}] \tag{47}$$

The total oxygenated and deoxygenated haem group concentrations in the muscle ([$HbMbO_2$] and [HHbMb], respectively) are given by the sum of the respective muscle haemoglobin and muscle myoglobin concentrations:

$$\begin{aligned}[\mathrm{HbMbO_2}] &= [\mathrm{HbO_2}] + [\mathrm{MbO_2}] \\ &= f_{\mathrm{b}}\left(f_{\mathrm{a}}\left[\mathrm{HbO_{2,a}}\right] + f_{\mathrm{c}}\left[\mathrm{HbO_{2,c}}\right] + f_{\mathrm{v}}\left[\mathrm{HbO_{2,v}}\right]\right) + f_{\mathrm{i}}\left[\mathrm{MbO_{2,i}}\right]\end{aligned} \tag{48}$$

$$\begin{aligned}[\mathrm{HHbMb}] &= [\mathrm{HHb}] + [\mathrm{HMb}] \\ &= f_{\mathrm{b}}(f_{\mathrm{a}}[\mathrm{HHb_a}] + f_{\mathrm{c}}[\mathrm{HHb_c}] + f_{\mathrm{v}}[\mathrm{HHb_v}]) + f_{\mathrm{i}}[\mathrm{HMb_i}]\end{aligned} \tag{49}$$

where the concentrations in equations 44-49 are in units of g/mol or, more commonly, mM.

Calculate NIRS signals

Haemoglobin molecules contain four haem units that each bind one oxygen molecule, whereas myoglobin contains only one haem unit that binds a single oxygen molecule. An oxygenated haemoglobin molecule therefore absorbs four times as much light as an oxygenated myoglobin molecule, and this affects their relative contributions to the NIRS signals (Davis and Barstow, 2013). Near infrared spectroscopy cannot differentiate between light absorption due to haemoglobin and myoglobin, and gives a lumped "oxygenated haem" signal ($HbMbO_2$) and a lumped "deoxygenated haem" signal (HHbMb). Therefore, a scaling factor was applied to [HbO_2] in order to accurately reflect the contributions of the different haem groups to these two NIRS signals:

$$\begin{aligned}\mathrm{HbMbO_2} &= [\mathrm{HbO_2}]/4 + [\mathrm{MbO_2}] \\ &= f_{\mathrm{b}}\left(f_{\mathrm{a}}\left[\mathrm{HbO_{2,a}}\right] + f_{\mathrm{c}}\left[\mathrm{HbO_{2,c}}\right] + f_{\mathrm{v}}\left[\mathrm{HbO_{2,v}}\right]\right)/4 + f_{\mathrm{i}}\left[\mathrm{MbO_{2,i}}\right]\end{aligned} \tag{50}$$

$$\begin{aligned}\mathrm{HHbMb} &= [\mathrm{HHb}] + [\mathrm{HMb}] \\ &= f_{\mathrm{b}}(f_{\mathrm{a}}[\mathrm{HHb_a}] + f_{\mathrm{c}}[\mathrm{HHb_c}] + f_{\mathrm{v}}[\mathrm{HHb_v}]) + f_{\mathrm{i}}[\mathrm{HMb_i}]\end{aligned} \tag{51}$$

Note that NIRS signals were differentiated from actual haem group concentrations by the absence of square brackets for the NIRS signals. Many experimental NIRS systems do not give absolute units for $HbMbO_2$ and HHbMb and instead use arbitrary units. In such cases, the NIRS signals are usually normalised ("norm"), as a percentage, to their starting values ("t = 0") and their values at the end of the exercise protocol ("t = end"):

$$HbMbO_{2,norm} = 100 \times \left(1 - \frac{HbMbO_{2,t=0} - HbMbO_2}{HbMbO_{2,t=0} - HbMbO_{2,t=end}}\right) \quad (52)$$

$$HHbMb_{norm} = 100 \times \frac{HHbMb - HHbMb_{t=0}}{HHbMb_{t=end} - HHbMb_{t=0}} \quad (53)$$

such that $HbMbO_{2,norm}$ = 100% at the start of exercise and 0% at the end of exercise, while $HHbMb_{norm}$ = 0% at the start of exercise and 100% at the end of exercise. This normalises the signals to conditions at the end of the exercise protocol (i.e. to $\dot{V}O_{2,peak}$ during a ramp protocol, or to steady-state $\dot{V}O_2$ during a step protocol) and allows any under- or overshoots in the $HbMbO_2$ and HHbMb signals during the exercise protocol to be identified. Alternatively, the NIRS signals can be given as a change (Δ) from their starting values, as in Lai et al. (2009):

$$\Delta HbMbO_2 = 100 \times \frac{HbMbO_2 - HbMbO_{2,t=0}}{HbMbO_{2,t=0}} \quad (54)$$

$$\Delta HHbMb = 100 \times \frac{HHbMb - HHbMb_{t=0}}{HHbMb_{t=0}} \quad (55)$$

The individual oxy- and deoxy- haemoglobin and myoglobin concentrations in the muscle (equations 44-47) can be normalised using the same methods. Finally, the tissue oxygenation index (TOI) is the ratio of the oxygenated haem concentration to the total (oxygenated and deoxygenated) haem concentration, as a percentage:

$$TOI = 100 \times \frac{[HbO_2]/4 + [MbO_2]}{[HbO_2]/4 + [MbO_2] + [HHb] + [HMb]} \quad (56)$$

where the divisor 4 is as described for equation 50.

4.2.2 Model optimisation

Change to capillary blood volume during exercise

Any change in muscle blood volume during exercise is assumed to be proportional to the change in muscle blood flow ($\dot{Q}_m$), and takes place in the capillaries, with the arterial and venous volumes in the muscle remaining constant. Thus $\Delta V_c \propto \Delta \dot{Q}_m$, and so

$$V_c = kV_{c,t=0}\,\dot{Q}_m/\dot{Q}_{m,t=0} \quad (57)$$

where k is a proportionality constant scaling the change in muscle blood flow to the change in capillary volume, and $V_{c,t=0}$ and $\dot{Q}_{m,t=0}$ are capillary volume and muscle blood flow at the start of exercise (i.e. at t = 0 s), respectively. In the NIRS model, capillary volume is constrained to only increase, and to increase to a maximum of five times its pre-exercise value, such that $V_{c,t=0} \leq V_c \leq 5V_{c,t=0}$.

Contributions of haemoglobin and myoglobin to the NIRS signal

There is debate about the contributions of haemoglobin and myoglobin to the NIRS signal (Davis and Barstow, 2013; Grassi and Quaresima, 2016), with these relative contributions likely to be due to the volumes of blood and tissue, respectively, that the NIRS probe interrogates.

Model optimisation

The likely value of the proportionality constant k and the fractions of blood (f_b) and tissue (f_i) in the muscle volume interrogated by NIRS were investigated, by optimising the NIRS model developed here (combined with the previously-validated O_2 transport model; see Chapter 3) against experimental data of simultaneously-measured pulmonary O_2 uptake ($\dot{V}O_{2p}$), cardiac output ($\dot{Q}$) and NIRS (specifically TOI) during ramp incremental exercise. Values for baseline $\dot{V}O_{2p}$, baseline $\dot{Q}$, muscle $\dot{V}O_2$ kinetics (back-calculated from experimentally-measured $\dot{V}O_{2p}$ kinetics), blood flow kinetics, $\dot{V}O_2$ gain and the slope of the $\dot{Q}/\dot{V}O_2$ relationship were obtained from the experimental data and used as inputs to the model, on a subject-by-subject basis, along with details relating to the ramp exercise protocol (ramp work rate and total duration) – see Table 2. The NIRS model parameters k and f_b (and therefore f_i) were then modified, using a custom alternating variable

search (see Chapter 3 for details), until the NIRS model TOI output matched the experimentally recorded TOI as closely as possible. For each optimisation, initial parameter values were set to k = 1.0 and f_b = 0.5 (and therefore f_i = 0.5). Because altering f_b (and therefore f_i), changes the contributions made to the NIRS signals (including TOI) by haemoglobin and myoglobin, altering these variables also alters baseline TOI in the model. Therefore, to ensure that the model baseline TOI matched the experimental baseline TOI, fractional blood flow distribution to the muscle ($f_{Q,mus}$) in the O_2 transport model was altered to ensure the balance of oxygenated and deoxygenated haemoglobin and myoglobin gave a model baseline TOI that was within ±2.5% (approximately ±4 standard deviations of the noise on TOI measured by NIRS) of the experimental baseline TOI. While doing this, $f_{Q,mus}$ was constrained to not drop so low as to completely drain O_2 in the muscle venous effluent during the ramp protocol, and not increase so much that O_2 in the "body" compartment venous effluent was completely drained. This was successfully achieved with modelling data obtained from nine of the 10 subjects. With data from the remaining subject, f_b and $f_{Q,mus}$ could not be balanced to give a model baseline TOI within ±2.5% of the experimental baseline TOI: as such, baseline TOI was not constrained for this subject.

4.3 Results and discussion

Peak pulmonary oxygen uptake during the ramp exercise test was (mean ± SD) 3.57 ± 0.97 (L/min), with a peak work rate of 290 ± 75 (W). Minimum and maximum tissue oxygenation during the ramp incremental exercise test was 60 ± 8 (%) and 75 ± 3 (%) respectively. Figure 25 shows individual subject model predicted tissue oxygenation index (red line) and experimentally (NIRS) derived tissue oxygenation index (black circles).

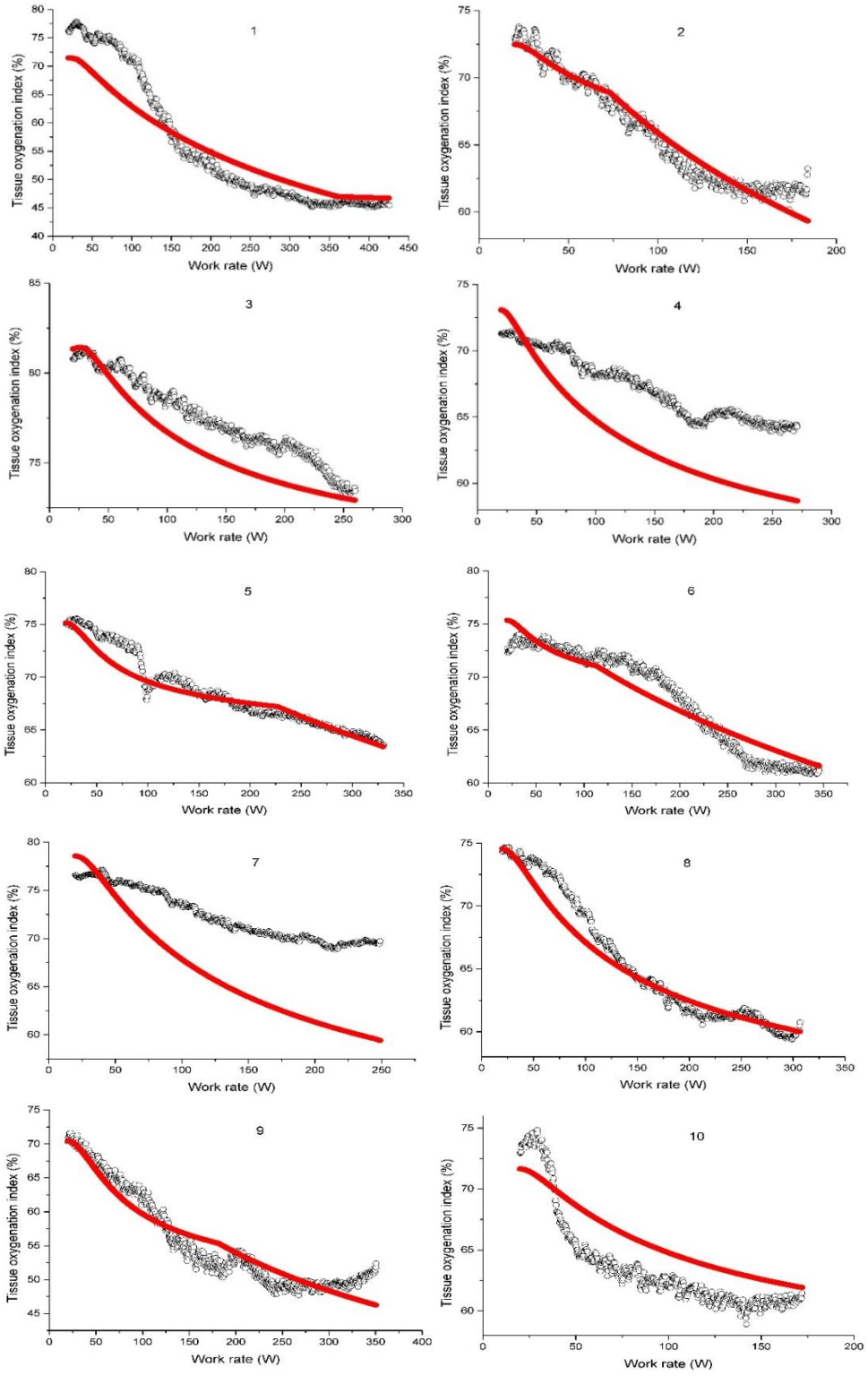

Figure 25: Individual subject tissue oxygenation index response during ramp incremental exercise (black circles) overlaid on model predicted tissue oxygenation index response (red line).

There was no significant difference between model predicted, and experimentally derived, minimum TOI ($p>0.05$), maximum TOI ($p>0.05$), and TOI amplitude ($p>0.05$; see Table 8 and Figure 26.

Table 8: Individual subject tissue oxygenation values determined during ramp incremental exercise

Subject	TOI minimum (%)		TOI maximum (%)		TOI Amplitude (%)	
	Exp	**Model**	**Exp**	**Model**	**Exp**	**Model**
1	45.5	46.7	76.3	71.5	30.8	24.8
2	63.6	59.3	72.9	72.4	9.30	13.1
3	73.4	72.9	80.8	81.3	7.40	8.4
4	64.2	58.6	71.0	73.0	6.80	14.4
7	63.5	63.4	75.0	75.1	11.5	11.7
8	61.1	61.6	72.0	75.0	10.9	13.4
9	69.9	59.4	76.5	78.6	6.60	19.2
10	60.7	60	74.5	74.3	13.8	14.3
11	52.4	46.2	70.3	70.4	17.9	24.2
12	61.7	61.9	72.9	71.6	11.2	9.70

TOI tissue oxygenation index; Exp experimental data

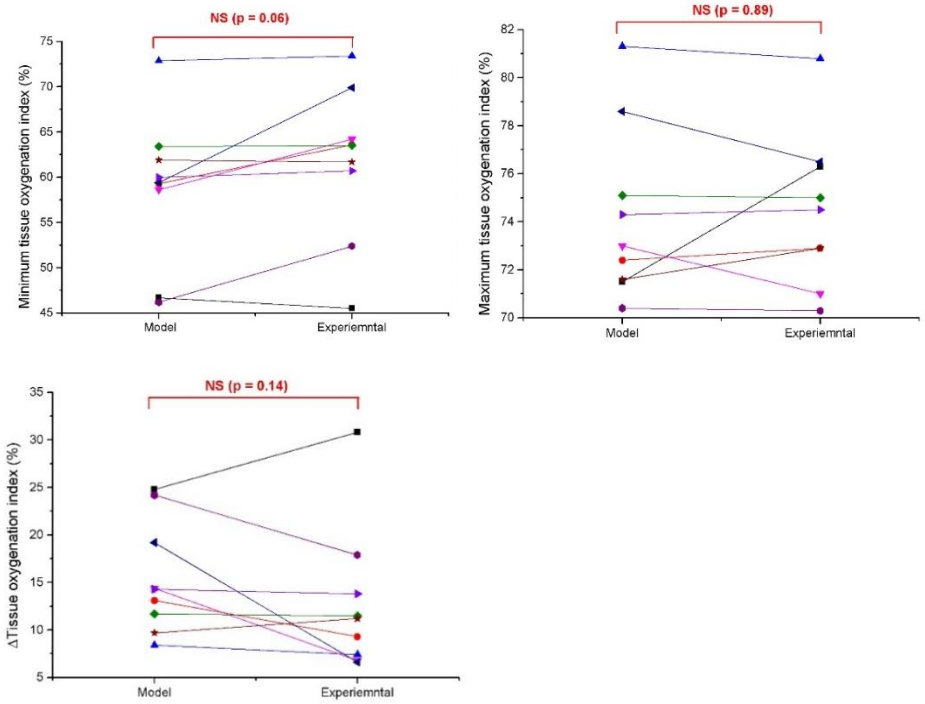

Figure 26: Top panel: (left) minimum model predicted TOI and experimentally derived TOI, (right) maximum model predicted TOI and experimentally derived TOI. Bottom panel: Model predicted TOI amplitude and experimentally derived TOI amplitude.

Individual differences between model predicted TOI start, TOI end and delta TOI shown below (Table 9). The mean overall discrepancy between model predicted TOI and experimentally derived TOI was 0.2-2.9%.

Table 9: Individual subject differences between model predicted, and experimentally derived tissue oxygenation index at the start of exercise, the end of exercise, and change in TOI (delta) during the ramp incremental test.

Subject	Starting TOI difference (%)	End TOI difference (%)	Delta TOI difference (%)
1	1.2	4.8	6.0
2	4.3	0.5	3.8
3	0.5	0.5	1.0
4	5.6	2.0	7.6
5	0.1	0.1	0.2
6	0.5	3.0	2.5
7	10.5	2.1	12.6
8	0.7	0.2	0.5
9	6.2	0.1	6.3
10	0.2	1.3	1.5
Mean	**2.6**	**0.1**	**2.7**

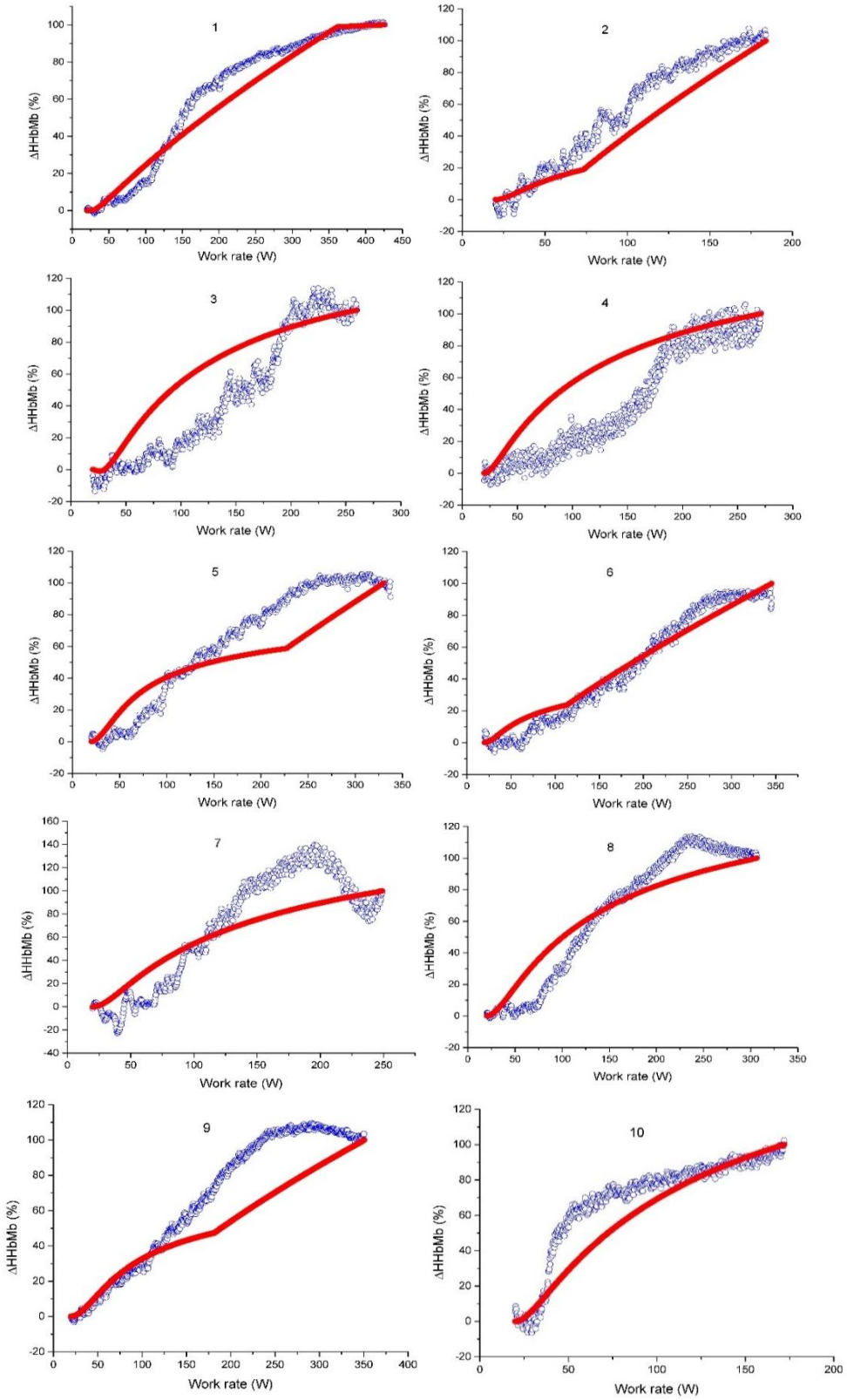

Figure 27: Individual subject model predicted ΔHHbMb (red line) and experimentally measured ΔHHbMb (blue circles).

Figures 25 and 27 show individual model predicted TOI and ΔHHbMb superimposed with experimentally measured TOI and ΔHHbMb. For the TOI In subjects 2, 5, and 9 the breakpoint (i.e. deviation from linearity) in the model output matches the breakpoint in the experimental data closely. However, the overall fit of the model is poor. The breakpoint may represent sudden changes in the local balance between $\dot{V}O_2$ and $\dot{Q}$, and these changes in the muscle oxygenation response profile may be reflected in whole body physiological responses. In healthy subjects, studies have shown the breakpoint in deoxygenated haemoglobin myoglobin to occur at 75-90% of $\dot{V}O_{2,max}$. Given the intensity at which the breakpoint occurs, the breakpoint has been related to other physiological markers of exercise intensity such as the respiratory compensation point, maximal lactate steady state, and/ or critical power (Osawa et al., 2011; Bellotti et al., 2013; Murias et al., 2013; Racinais et al., 2014; Boone et al., 2015, 2016; Fontana et al., 2015; Keir et al., 2015). However, it has been questioned whether these parameters are physiologically linked, due to the individual variance found between these parameters (Broxterman et al., 2015; Craig et al., 2015). As such, it remains to be determined whether the breakpoints and the physiological markers of exercise intensity are mechanistically linked (Boone et al., 2016). Nevertheless, the breakpoint in the ΔHHbMb response has been shown to be strongly correlated to $\dot{V}O_{2,peak}$ (Boone et al., 2009; Murias et al., 2013) showing that, in those subjects with a higher $\dot{V}O_{2,peak}$, the breakpoint occurred later on in the ramp test. The mechanisms for this shift are yet to be elucidated. The model sensitivity analysis (see section *$\Delta\dot{V}O_2/\Delta WR$* below) showed that a 10% reduction in the $\dot{V}O_2$ gain (i.e. from 0.1 to 0.09) caused a ~20% increase in the location of the normalised ΔHHbMb breakpoint (i.e. the breakpoint occurred later in the ramp simulation). This finding is consistent with experimental data where endurance trained athletes, tend to express a high $\dot{V}O_2$/WR slope (~11-12 L/min/W) (Riley et al., 1996; Boone et al., 2008) compared to heart failure or vascular disease patients who often have a low $\dot{V}O_2$/WR slope of ~9-11L/min/W (Hansen et al., 1987; Jones et al., 1998; Hsia et al., 2009). One possible explanation for the lower $\dot{V}O_2$/WR slope in HF patients may be as a consequence of a reduced blood flow to the periphery muscles, thereby, resulting in a greater contribution to energy transfer from anaerobic sources. However, this is not consistent with exercise below lactate threshold where contribution from anaerobic sources is minimal (Rossiter, 2011). Another possible explanation is that O_2 utilisation in patients is less able to keep pace

with the demands of ramp exercise, this explanation is consistent with slowed $\dot{V}O_2$ kinetics in patients (Wasserman et al., 2011).

The model predicted TOI responses show clear breakpoints in some subjects, whilst in others the TOI response follows a more fluid profile, making it harder to accurately determine the breakpoint in these subjects. From the TOI responses of subjects 2, 5, and 9, the breakpoint can be clearly identified and the model predicts these breakpoints closely . In subjects 1 and 6 there is also a clear breakpoint in the data, however, the model predicted breakpoint is slightly delayed in subject 1 and slightly premature in subject 6. Except for subject 5, these subjects display a 'typical' sigmoidal response, which is why the model may be better at estimating TOI breakpoints in these subjects. In contrast, subject 7 and 10 had untypical responses (almost linear and exponential, respectively). In these subjects the model was unable to predict the TOI response profiles. This suggests that the model is more able to predict typical TOI responses, but is less able to predict TOI response profiles when the response does not follow a typical sigmoidal pattern.

For the TOI data, in subjects 3, 4, 7 and 10 the model predicted NIRS responses are poorly predictive of the experimental data. For the HHbMb data the model predicted NIRS responses are poorly predictive of the experimental data in all subjects, as the model was optimised against TOI data. This variable and poor model fit to the experimental data suggests that the model in its current state is not an accurate representation of the NIRS oxygenation response and therefore needs more development and iterations before it can be utilised fully. This may need to include the addition of more complex systems such as a heterogenous fibre type compositions, more accurate measures of capillary, venous and arterial O_2 concentrations (at rest and during exercise) and varying venous volume sizes. A sensitivity analysis was subsequently performed on the model however due to its poor accuracy in predicting the NIRS response any potential physiological mechanisms should be interpreted with extreme caution.

To investigate the potential mechanistic determinants of the muscle oxygenation response, a sensitivity analysis was performed on the NIRS model for both step and ramp exercise. Table 10 shows model input parameters +/- 10% for the sensitivity analysis. Note that each parameter

was changed on an individual basis and therefore only one parameter was changed at a time for each simulation.

Table 10: Experimentally derived (mean) model input parameters (middle column) with minus 10% (left) and plus 10% (right).

Parameter	Parameter value		
	Minus 10%	Model input	Plus 10%
C_aO_2 (L O_2/ L blood)	0.18	0.20	0.22
Venus volumes, litres			
Muscle	0.63	0.70	0.77
Body	0.09	0.10	0.11
Mixed	2.07	2.30	2.53
Baseline (unloaded pedalling) values			
$\dot{V}O_{2p}$, L/min	0.87	0.96	1.06
Fraction from muscle[a]	0.51	0.57	0.63
$\dot{Q}_{tot}$, L/min	7.62	8.47	9.32
Fraction to muscle[a]	0.51	0.57	0.63
Exercise $\dot{V}O_2$ and $\dot{Q}$ parameters			
$\Delta\dot{V}O_{2m}/\Delta$WR, (L/min/W)	0.009	0.01	0.011
$\Delta\dot{Q}$ / $\Delta\dot{V}O_{2m}$	4.89	5.43	5.97
Muscle $\dot{V}O_2$ and blood flow kinetics			
$\dot{V}O_{2m}\tau$ (s)	23.90	26.56	29.21
$\dot{Q}_m\tau$ (s)	26.66	29.63	32.59

Table parameters: $\dot{Q}$ denotes blood flow. The subscripts 'tot' and 'm' denote total and muscle components, respectively. [a]The remainder of the baseline $\dot{V}O_{2p}$ (and $\dot{Q}_{tot}$) comes from (and goes to) the body compartment. CaO_2 and venous volumes are taken from the experimental data described in methods protocol 1. All other values were measured experimentally as described in methods protocol 2. Note that all values are means (standard deviations have been excluded for clarity).

Sensitivity analysis results are shown in Table 11, Table 12 and Table 13. Table 11 shows model output values (phase 1 amplitude, phase 1 duration, and phase II τ) during step exercise simulations. Although NIRS was the primary interest in the sensitivity analysis, the model also gives information regarding $\dot{V}O_2$ dynamics. As such, $\dot{V}O_2$ outputs were also investigated for completeness, the results of which are shown in table 11. The parameters

that had the most impact on $\dot{V}O_2$ dynamics were baseline $\dot{Q}$ and $\dot{V}O_2$ values and $\dot{V}O_2$ and $\dot{Q}$ kinetics. Table 12 shows the tissue oxygenation index results for both step and ramp simulations. The parameter that caused the biggest change in TOI was the $\dot{V}O_2$/WR slope: where reducing the slope by 10% caused a 31% change in delta TOI (compared to 7% delta for the original experimental input values). Table 13 shows model output values ($\dot{V}O_{2p}$ mean response time) for ramp model simulations. These simulations revealed no significant change in $\dot{V}O_2$ mean response time when each parameter was changed by ± 10%.

Table 11: Model output values (phase I amplitude, phase I duration and phase II time constant) for step exercise simulations for mean ± 10%

	Minus 10%			Plus 10%		
	θ1 amplitude (%)	**θ1 duration** (s)	**$\theta 2\ \tau$** (s)	**θ1 amplitude** (%)	**θ1 duration** (s)	**$\theta 2\ \tau$** (s)
Mean:	**29.71**	**21.30**	**20.65**	**29.71**	**21.30**	**20.65**
C_aO_2	29.62	20.90	20.58			
Venus volumes, litres						
Muscle	29.24	20.40	20.83	30.50	21.90	20.53
Body	29.57	20.90	20.58	29.73	21.30	20.64
Mixed	28.64	19.70	20.94	30.91	22.50	20.32
Baseline (unloaded pedalling) values						
$\dot{V}O_2$	26.51	20.90	20.83	33.21	21.30	20.95
Fraction from muscle[a]	27.58	20.90	20.30	31.77	21.30	20.93
$\dot{Q}_{tot}$	35.08	22.60	20.25	25.35	19.80	21.00
Fraction to muscle[a]	32.32	21.58	20.58	27.63	20.70	20.73
Exercise $\dot{V}O_2$ and $\dot{Q}$ parameters						
$\Delta\dot{V}O_{2m}$ / ΔWR	20.10	11.80	22.06	29.59	20.93	20.51
$\dot{V}O_2$-$\dot{Q}$ slope	27.07	21.20	20.46	32.73	20.90	20.81
Muscle $\dot{V}O2$ and blood flow kinetics						
$\dot{Q}_m\ \tau$	32.24	20.60	22.20	27.70	21.50	19.53
$\dot{V}O_{2m}\ \tau$	29.24	20.90	16.81	30.03	21.30	24.51

Table parameters: θ1 amplitude phase I amplitude; θ1 duration phase I duration; $\theta 2\ \tau$ phase II time constant. $\dot{Q}$ denotes blood flow. The subscripts 'tot' and 'm' denote total and muscle components, respectively. [a]The remainder of the baseline $\dot{V}O_{2p}$ (and $\dot{Q}_{tot}$) comes from (and goes to) the body compartment; τ time constant

Table 12: Model derived tissue oxygenation values for both step (left) and ramp (right) exercise

	Tissue oxygenation index (%)											
	Step						**Ramp**					
	10%			**-10%**			**10%**			**-10%**		
	Min	Max	Change	Min	Max	Change	Min	Max	Change	Min	Max	Change
Mean:	**64.8**	**71.8**	**7.0**	**64.8**	**71.8**	**7.0**	**59.2**	**71.9**	**12.7**	**59.2**	**71.9**	**12.7**
C_aO_2				56.6	64.4	7.8				50.9	64.5	13.6
Venus volumes, litres												
Muscle	64.7	71.8	7.1	64.5	71.8	7.3	59.2	71.9	12.7	59.2	71.9	12.7
Body	64.7	71.8	7.1	64.5	71.8	7.3	59.2	71.9	12.7	59.2	71.9	12.7
Mixed	64.7	71.8	7.1	64.4	71.9	7.5	59.2	71.9	12.7	59.2	71.9	12.7
Baseline (unloaded pedalling) values												
$\dot{V}O_{2b}$	63.7	69.7	6.0	65.3	73.9	8.6	58.4	69.7	11.3	59.9	73.9	14.0
Fraction from muscle[a]	63.7	69.6	5.9	65.5	74.1	8.6	58.4	70.0	11.6	60.0	74.1	14.1
$\dot{Q}_{tot}$	66.0	73.8	7.8	62.6	69.5	6.9	60.9	73.8	12.9	57.3	69.5	12.2
Fraction to muscle[a]	66.1	73.9	7.8	62.5	69.4	6.9	61.0	73.9	12.9	57.2	69.4	12.2
Exercise $\dot{V}O_2$ and $\dot{Q}$ parameters												
$\Delta\dot{V}O_{2m}/\Delta WR$	64.4	71.9	7.5	40.8	71.8	31.0	58.2	71.9	13.7	60.3	71.9	11.6
$\dot{V}O_2$-$\dot{Q}$ slope	66.2	71.9	5.7	63.0	71.9	8.9	60.6	71.9	11.3	57.9	71.9	14.0
$\dot{Q}_m\,\tau$	64.7	71.8	7.1	64.4	71.9	7.5	59.3	71.9	12.6	59.1	71.9	12.8
$\dot{V}O_{2m}\,\tau$	64.7	71.8	7.1	64.4	71.9	7.5	59.1	71.9	12.8	59.3	71.9	12.6

Table parameters: $\dot{Q}$ denotes blood flow. The subscripts 'tot' and 'm' denote total and muscle components, respectively. [a]The remainder of the baseline $\dot{V}O_{2p}$ (and $\dot{Q}_{tot}$) comes from (and goes to) the body compartment; τ time constant.

Table 13: Model output values for ramp incremental exercise simulations

Ramp model	Mean response time (s)	
	Parameter -10%	Parameter +10%
Mean experimentally derived input value:	**28.03**	**28.03**
C_aO_2	28.03	
Venus volumes, litres		
Muscle	28.00	28.06
Body	28.03	28.03
Mixed	29.90	28.17
Baseline (unloaded pedaling) values		
$\dot{V}O_{2A}$	28.28	27.76
Fraction from muscle[a]	28.09	27.97
$\dot{Q}_{tot}$	27.71	28.30
Fraction to muscle[a]	27.94	28.10
Exercise $\dot{V}O_2$ and $\dot{Q}$ parameters		
$\Delta\dot{V}O_{2m}/\Delta WR$	28.23	27.85
$\dot{V}O_2$-$\dot{Q}$ slope	28.44	27.62
Muscle $\dot{V}O2$ and blood flow kinetics		
$\dot{Q}_m\ \tau$	25.34	30.71
$\dot{V}O_{2m}\ \tau$	28.05	28.00

Table parameters defined above

Previous studies (Murgatroyd et al., 2011; Bowen et al., 2012) that have looked at the reproducibility of $\dot{V}O_2$ kinetics have produced 95% confidence intervals, and SD of 3.1 ± 0.9 s respectively in healthy individuals (Murgatroyd et al., 2011) and 5.0 ± 2.0 s respectively in heart failure patients (Bowen et al., 2012). Therefore, any changes greater than 3.0 s were taken as significant, as these changes are likely to be detectable, and reproducible, in a laboratory. For muscle oxygenation indexes minimum, maximum, and the change in TOI were looked at, as well as the presence of any undershoots/overshoots in step protocol, and the breakpoint in HHbMb during the ramp protocol.

Arterial O_2 content

Changing arterial O_2 content did not have any significant effect on $\dot{V}O_2$ kinetics during both step and ramp exercise. Furthermore, as C_aO_2 is relatively unchanged during exercise (Grassi et al., 1996) changing this parameter does not affect the kinetics of $\dot{V}O_{2p}$. The TOI profile during step

and ramp exercise was not altered with a 10% increase or decrease in C_aO_2 however, the absolute TOI (i.e. the oxygenation level of the tissue) was shifted downwards (Figure 28) in both ramp and step exercise protocol.

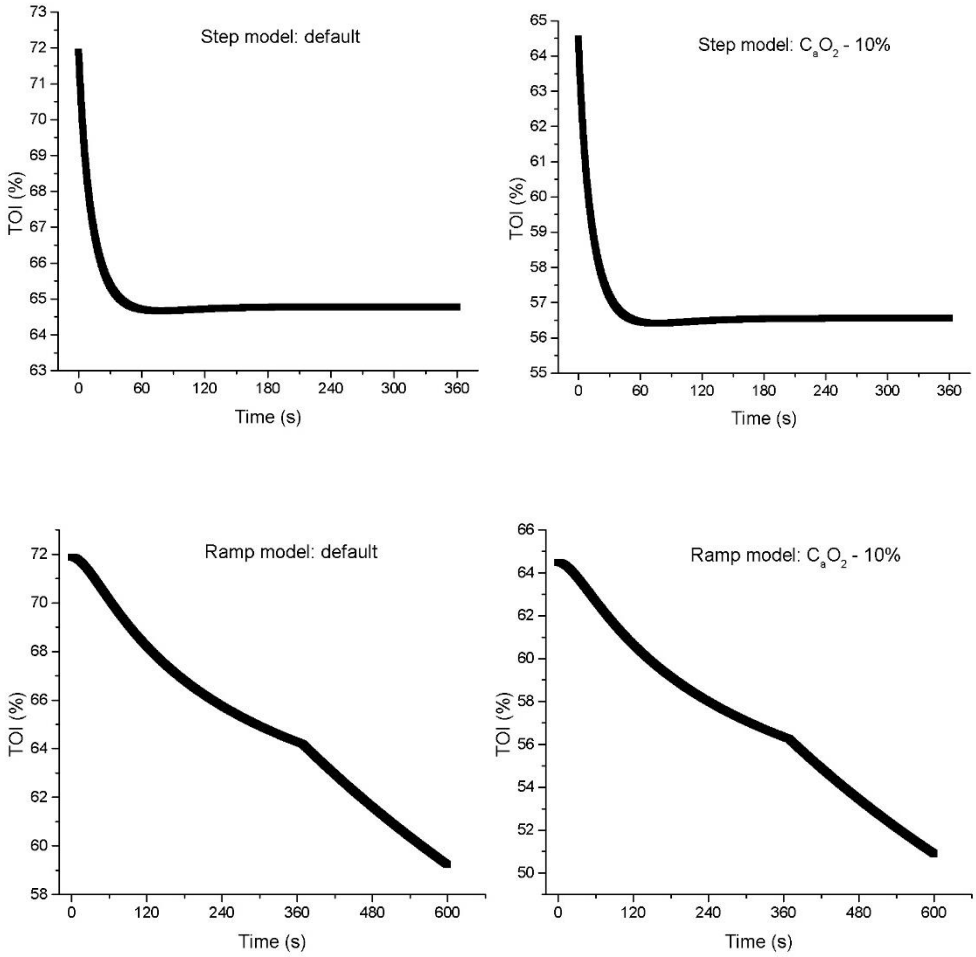

Figure 28: Top panel shows TOI response during a step exercise simulation with model mean (experimentally derived) values (left) and model mean values with a 10% reduction in arterial O_2 content (right). TOI is shifted downwards by ~7%. Bottom panels show the same effect, for ramp exercise.

In this scenario (i.e. where $\dot{Q}$ is not limiting) a 7% reduction in muscle oxygenation availability does not cause a significant change in $\dot{V}O_2$ kinetics, and therefore would be unlikely to affect exercise tolerance. However, this may become a limiting factor in a heart failure patient with anaemia (Coats, 2004).

Venous Volumes

Increasing and/or decreasing the venous volume by 10% had no significant effect on $\dot{V}O_2$ kinetics, or the TOI profile, in both step and ramp exercise protocols. It has previously been shown that venous volume size influences limb-to-lung transit delay, which can alter the $\dot{V}O_2$ signal measured by breath by breath gas exchange however, it is likely that only a 10% change is too small to induce any detectable and/or physiologically significant changes in $\dot{V}O_2$ kinetics.

Unloaded pedalling (baseline) parameters

Baseline $\dot{V}O_2$: For step exercise, no significant changes in phase II $\dot{V}O_{2p}$ kinetics were observed with a 10% increase or decrease in baseline $\dot{V}O_2$, although for ramp exercise there was a small change in phase I amplitude (3.5% increase) when $\dot{V}O_2$ baseline was increased by 10%, resulting in a 0.5s speeding of the $\dot{V}O_2$ mean response time.

Baseline cardiac output: When cardiac output was increased for step exercise (i.e. a higher baseline blood flow) this slowed phase II $\dot{V}O_{2p}$ kinetics, and when it was decreased (i.e. a lower baseline blood flow), this reduced (i.e. made faster) phase II $\dot{V}O_{2p}$ kinetics. Previous modelling studies have shown that increasing baseline cardiac output at unloaded pedalling reduces the reduction seen in venous O_2 concentration and increases the steady state oxygenation level (i.e. a smaller reduction in oxygen extraction). Despite this it is accompanied by slightly slower phase II $\dot{V}O_{2p}$ kinetics. This raises the possibility that solely raising the muscle perfusion during unloaded pedalling would result in phase II $\dot{V}O_{2p}$ kinetics that were slowed to a small degree (Benson et al., 2013). Although this difference is small (less than half a second), somewhere along the O_2 transport system, the increased blood flow is then manifested as a slowed phase II $\dot{V}O_{2p}$. Although a 10% change from mean values were not large enough to elicit a undershoot in TOI, a higher steady state value was seen when baseline cardiac output was increased compared to when it was decreased (66.0 % vs 62.6% respectively).

Muscle $\dot{V}O_2$ and blood flow kinetics: The greatest effect on the phase II $\tau\dot{V}O_{2p}$ was seen by changing the time constant of τ $\dot{V}O_2$ at the muscle for step exercise. Faster τ $\dot{V}O_{2m}$ values were manifested as a faster phase II $\tau\dot{V}O_{2p}$. When $\dot{V}O_{2m}$ kinetics are faster than muscle blood flow, the fall in

muscle oxygenation is accelerated. This could be a result of the poor matching of oxygen delivery and oxygen consumption, necessitating a higher fractional oxygen extraction to sustain a given metabolic rate. In this situation, muscle blood flow lags $\dot{V}O_{2m}$ so that the $\dot{V}O_2/\dot{Q}$ ratio is altered. This causes an O_2 delivery/utilisation mismatch: consequently, TOI transiently undershoots its steady state value (Figure 29). This profile has been demonstrated experimentally in heart failure patients previously (Sperandio et al., 2009; Bowen et al., 2012). These findings are in agreement with experimental data, and highlight the importance of the resting conditions on O_2 extraction dynamics, and how changes in the $\dot{Q}_m/\dot{V}O_{2m}$ relationship can alter the dynamics of the $\dot{V}O_2$ response (Ferreira et al., 2005; Benson et al., 2013).

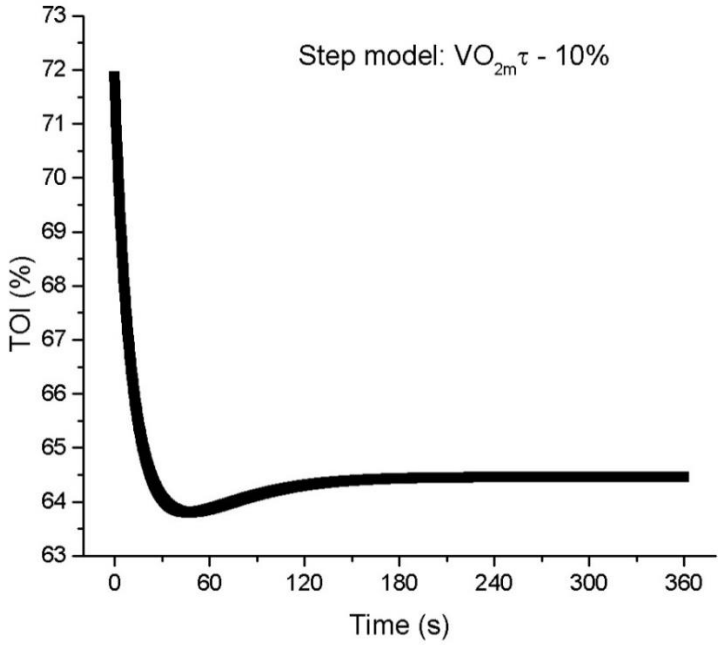

Figure 29: Tissue oxygenation response when muscle $\dot{V}O_2$ kinetics are faster relative to blood flow (Q) kinetics. In this simulation, when $\dot{V}O_{2m}$ kinetics are speeded and $\dot{Q}$ kinetics unchanged, tissue oxygenation transiently undershoots its steady state value.

Although the undershoot observed computationally is relatively small, it is important to note that the change in $\dot{V}O_2$ kinetics that elicited the undershoot was also very small i.e. from 26.6s to 23.9s, meaning the mismatch between $\dot{V}O_2$ and $\dot{Q}$ was just 5.7s (i.e. $\dot{Q}\tau$ = 29.6 and $\dot{V}O_2\tau$ = 23.9s). The larger the discrepancy between $\dot{V}O_2$ and $\dot{Q}$ kinetics was, the larger the undershoot in TOI was.

$\dot{V}O_2/\dot{Q}$ *slope*

Changing the $\dot{V}O_2/\dot{Q}$ slope by 10% had only a very small effect on phase II $\dot{V}O_2$p kinetics (i.e. less than a second) for both an increase and decrease in $\dot{V}O_2/\dot{Q}$ slope for step exercise. When the $\dot{V}O_2/\dot{Q}$ slope was increased (i.e. for a given $\dot{V}O_2$ blood flow is higher) the change in TOI was decreased (from 7% change to 5.7% change). Decreasing the $\dot{V}O_2$-$\dot{Q}$ slope (i.e. less blood flow per 1 L change in $\dot{V}O_2$) caused a greater reduction in TOI (from 7% change to 8.9% change). This is likely because more blood flow per litre change in $\dot{V}O_2$ means more O_2 rich blood being delivered to the muscles, whereas a reduced blood flow per 1 L change in $\dot{V}O_2$ would mean less O_2 delivery to the muscles, and therefore a greater reliance on O_2 extraction.

$\Delta\dot{V}O_2/\Delta$WR ($\dot{V}O_2$ gain)

The parameter that had the most significant influence on step model TOI response was the $\Delta\dot{V}O_{2m}$ /ΔWR. Although mean (experimentally derived) values plus 10% produced no significant effects on TOI response, when simulating mean values -10%, the TOI response was altered, from a 7% total reduction in TOI during step exercise (model mean values) to a 30% total reduction in TOI during the same protocol (Figure 30). Note that all other parameters were kept the same as mean experimentally derived values.

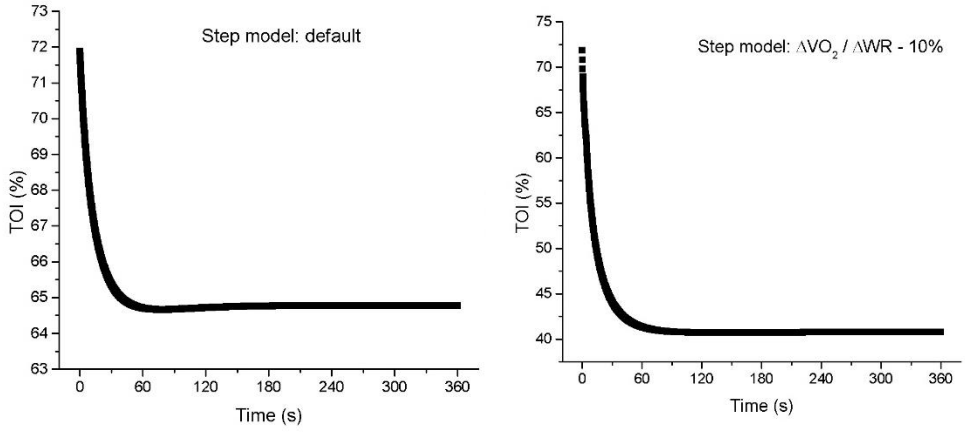

Figure 30: Simulated model outputs for step exercise for mean experimentally derived parameters (left) and mean parameters with a reduced $\Delta\dot{V}O_2$ /ΔWR (from 10 L/min/W to 9 L/min/W). When $\Delta\dot{V}O_2/\Delta$WR was lower, TOI amplitude was increased from a 7% absolute change to a 30% absolute change.

$\dot{V}O_2$ gain is typically 10 mL/min/W during cycle ergometer exercise but can vary in-between individuals 9-12 mL/min/W (Hansen et al., 1988; Riley et al., 1996; Boone et al., 2008). The model suggests that a small change in gain (i.e. from 0.01 L/min/W to 0.09 L/min/W) during step exercise can have a significant effect on tissue oxygenation index, and therefore O_2 availability at the tissue. This was accompanied with a 9% reduction in phase I amplitude and a 10 s decrease in the phase I duration, but only a very small change in phase II kinetics (i.e. from 20.7 s to 22.1 s). A smaller and shorter phase I response would indicate less O_2 being delivered, and therefore a larger reliance on O_2 extraction. Despite this, reducing total blood flow in the step model by 10% did not cause a large change in TOI from model mean parameters, however it is possible that a 10% decrease in total blood flow (i.e. 8.47 to 7.63 L/min) was not large enough to cause any changes.

For the ramp exercise simulations, changing $\Delta\dot{V}O_2/\Delta WR$ also influenced the location at which the breakpoint in HHbMb occurred. For example, a 10% reduction in $\Delta\dot{V}O_{2m}$ /ΔWR from its mean values resulted in the breakpoint occurring at ~60% of normalised HHbMb, at roughly 400 seconds into the ramp. Whereas, a 10% increase in $\Delta\dot{V}O_2/\Delta WR$ resulted in a breakpoint occurring at ~40% of normalised HHbMb, roughly 360 seconds into the ramp. As mentioned earlier, the breakpoint in HHbMb is strongly correlated to peak $\dot{V}O_2$, such that a higher breakpoint is associated with a higher $\dot{V}O_{2,peak}$ and thus a better exercise tolerance, and a lower breakpoint

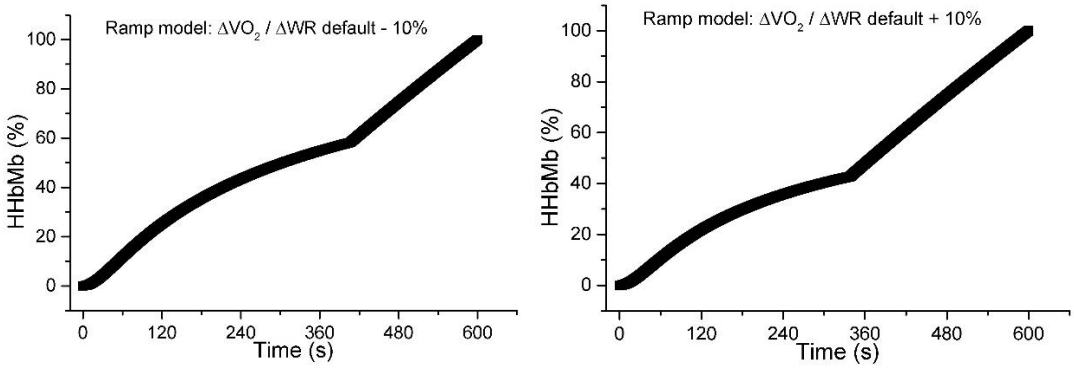

Figure 31: Model simulations for ramp exercise with a reduced gain (left) and increased gain (right). When gain is lower the breakpoint in the HHbMb response occurs later on in the ramp and at a higher HHbMb. Conversely when gain is increased the breakpoint occurs 40s (~400 vs. 360 s) sooner in the ramp and at a lower HHbMb.

Other inferences from the model

Of the parameters which elicited a change in the muscle oxygenation response ($\Delta\dot{V}O_2/\Delta WR$, baseline $\dot{Q}$, arterial O_2 content and $\dot{V}O_{2m}\tau$), the slope of the HHbMb response was looked at during the ramp exercise simulations; **Table 14** shows HHbMb slopes for each parameter. Each HHbMb response was divided into two sections and fit with a linear regression to determine the slope of the response. The initial portion of the response (slope a) corresponds to the onset of exercise until the breakpoint in HHbMb. The latter portion of the response (slope b) corresponds to first breakpoint in HHbMb until end exercise.

Table 14: HHbMb slopes

	Slope a	**Slope b**
Mean	**0.15**	**0.21**
CaO_2		
-10%	0.15	0.21
Baseline $\dot{Q}$		
-10%	0.13	0.22
+10%	0.15	0.20
$\Delta\dot{V}O_2/\Delta WR$		
-10%	0.15	0.22
+10%	0.13	0.22
$\dot{V}O_{2m}\,\tau$		
-10%	0.14	0.21
+10%	0.15	0.21

There were no large changes in the slope of the HHbMb response of any of the parameters. Altering arterial O_2 content shifted the absolute amount of tissue oxygenation downwards during step and ramp exercise simulations, but seemingly does not affect the slope of the response. Decreasing baseline cardiac output (baseline $\dot{Q}$) resulted in a lower steady state TOI during step exercise. However, this was associated with only a 0.02 % decrease in the HHbMb slope. Decreasing $\Delta\dot{V}O_2/\Delta WR$ by 10% caused a greater TOI amplitude during step exercise, however, only caused a 0.01% decrease in the HHbMb slope during the latter part of the ramp test. Finally, slightly speeding $\dot{V}O_{2m}\tau$ (i.e. reducing mean values by 10%) caused an undershoot in TOI during step exercise however, only caused a 0.01% reduction the slope of the HHbMb response. It has been suggested that the

slope of the HHbMb response is related to the level of oxygen extraction in the exercising muscle (Barroco et al., 2017). In this regard, an undershoot in TOI during constant work rate exercise (representative of increased O_2 extraction at exercise onset due to $\dot{V}O_2/\dot{Q}$ mismatch) would result in a corresponding increase in the HHbMb slope during incremental exercise. The NIRS model did not detect such changes. There are a few possible reasons for this i) due to the dynamic nature of ramp the body is more able to cope with small changes in these parameters and therefore, a 10% change is too small to detect changes in the HHbMb slope or ii) the NIRS model is not sensitive enough to detect these changes during ramp exercise.

4.3.1 Model limitations, implications and confidence

NIRS measurements can be influenced by several different factors including i) heterogeneity of blood flow and oxygen uptake, leading to non-uniform muscle oxygenation ii) capillary recruitment iii) adipose tissue thickness, and IV) relative contributions of haemoglobin and myoglobin to the NIRS signal.

Heterogeneity of blood flow and muscle oxygenation

As with the MCM Ramp incremental model (Chapter 3), it was assumed that the NIRS model contained a homogenous muscle compartment, such that, both blood flow and muscle $\dot{V}O_2$ were distributed uniformly throughout the muscle. However, the skeletal muscle is not a homogenous compartment. There is substantial heterogeneity in muscle blood flow (Laughlin and Armstrong, 1982; Piiper, 2000; Russell S. Richardson et al., 2001), and in muscle fibre types (with differing $\dot{V}O_2/\dot{Q}$ ratios and different metabolic capacities (Crow and Kushmerick, 1982) distributed within bodily tissues, between exercising and non-exercising muscles (Ferreira, McDonough, et al., 2006), and within different locomotor muscles engaged in exercise (Armstrong and Laughlin, 1985; Piiper et al., 1985; McDonough et al., 2005; Koga et al., 2007, 2014; Laaksonen et al., 2010). It is therefore uncertain whether the NIRS model output provides an accurate assessment of the heterogenous blood flow and $\dot{V}O_2$ relationships within the muscle. The implications of this simplified approach to predicting NIRS responses is that the NIRS response will be different depending on the fibre type and distribution. Type I highly oxidative fibres have faster kinetics than type II fibres which are less oxidative thereby altering the oxygen extraction

response and in a muscle containing more type I fibres oxygen extraction will be higher (and faster) compared to a muscle type with a greater proportion of type II (less oxidative fibres). Therefore, in muscle with a more type I fibres the NIRS response may show a steeper HHbMb slope This simplification of the NIRS model may explain some of the discrepancies seen between model output and experimental data and may account for the models inability to detect subtleties in the NIRS response, such as the breakpoint and slope of the NIRS response. This may be even more important during ramp exercise where type II fibres are increasingly recruited as exercise intensity increases.

Capillary recruitment

During muscle contraction, intravascular volume increases by vasodilation, with recruitment of new microvascular vessels and/or increase of capillary surface area (Renkin et al., 1966; Baker and Davis, 1974). The model assumes that blood volume change occurs in the capillaries, and not in arterioles or venules which were kept constant. According to Poole and Mathieu-Costello (1989), capillaries contribute to >90% of the total blood volume in muscle and furthermore, they proposed that the storage of blood in veins would mainly occur externally to the muscle. As such, the vascular component of the NIRS signal would predominantly come from the capillaries, and so NIRS oxygenation changes are likely to mainly reflect changes in capillary and intracellular O_2 levels. The model also assumes that any change in capillary blood flow is proportional to a change in cardiac output, however, as discussed above, blood flow to the exercising muscle is not homogenous and therefore, the model may not be an accurate representation of changes in oxygenation within different regions and across different muscles.

Adipose tissue thickness

NIR light must travel through the skin and subcutaneous fat layers to reach the underlying skeletal muscle, acting to “contaminate” the signal of interest (i.e. the signal coming from the skeletal muscle). While algorithms have been developed for adipose tissue correction (Niwayama et al., 2000; Geraskin et al., 2007) these are not included in most commercial instruments (Ferrari et al., 2011). The NIRS model presented in this chapter is a simplified version of a NIRS device in that, it does not account for the effects of light scattering or absorption due to adipose tissue thickness. As

such, the NIRS model might not reliably replicate NIRS signals in populations with high adipose tissue thickness. One of the advantages of this, however, is it may potentially be able to provide important information of local muscle oxygenation, in patients who are excluded from NIRS studies due to obesity.

Relative contributions of Hb and Mb to the NIRS signal

Data examining the contribution of haemoglobin and myoglobin to the NIRS signal is conflicting. Some studies have reported that the contribution of myoglobin to the NIRS signal is minimal, around 10% with the remaining 90% coming from haemoglobin (Seiyama et al., 1988; Mancini et al., 1994). Mancini et al. (1994) found using magnetic resonance spectroscopy that during submaximal exercise there was no desaturation of Mb, despite an increase NIRS desaturation. In addition, Seiyama et al. (1988) found the contribution of Myoglobin to the NIRS signal in hindlimb rats to be less than 10%. However, as suggested by Davis and Barstow (2013), the type of muscle used in the study (rat white vastus hindlimb) contains only a small amount of myoglobin, therefore, this muscle may not be representative of NIRS myoglobin contribution in the human vastus muscle (Davis and Barstow, 2013). Other studies have shown myoglobin contribution to the NIRS signal to be much more significant (Tran et al., 1999; Richardson et al., 2001; Spires et al., 2011). Recently, Davis and Barstow (2013) determined the contribution of myoglobin to be greater than ≥50% in human muscles. In the model, one of the assumptions affecting the contribution of myoglobin to the NIRS signal is that myoglobin in the intercellular space is 4.08g per litre of intracellular space (Duteil et al., 2005). This study utilised nuclear magnetic resonance imaging and was carried out in the human calf muscles of endurance trained and sprint trained athletes; a key finding from this study was that myoglobin concentration was increased in the endurance trained athletes (i.e. those with high oxidative capacity). With this in mind, the NIRS model may not be an accurate representation of NIRS signals in other muscles (i.e. that contain different fibre types and quantities), and also across untrained or diseased populations. Another assumption of the NIRS model is that intracellular partial pressure of oxygen remains constant throughout the exercise protocol and is ~17.3mmHg lower than the capillary partial pressure of O_2. This assumption is based on a study by Hirai et al. (2018), which is the only study to date to measure partial pressure of oxygen across the interstitial space in the skeletal muscle microcirculation during

exercise contractions. This was achieved by utilising phosphorescence quenching in exposed male rat spinotrapezius muscle. As such, it is uncertain whether these assumptions hold true in human muscles.

Other factors

The NIRS HHbMb signal is normalised from baseline to peak exercise (0-100%). Whilst baseline and peak HHbMb values were taken as 30s unloaded pedalling (baseline) and final HHbMb (peak) in order to retain the overall profile of the response (i.e. by taking the final HHbMb rather than the peak value throughout the ramp, the NIRS output will show any undershoot/overshoots relative to the final value) the slope of the response may be altered. This may partially explain why undershoots in the TOI response (in response to changing input parameter) were not associated with 'reciprocal' changes in the NIRS HHbMb response for ramp exercise. In addition, the NIRS model was only optimised against TOI data, so any inferences taken from the HHbMb data should be interpreted with caution.

Model input parameters were derived from experimental data in healthy young individuals. Baseline cardiac output and cardiac output kinetics were measured by photoplethysmography, which utilises measures of finger blood pressure to estimate stroke volume, heart rate and cardiac output. While this method has been shown to correlate well with intra-arterial BP measurements (Gomides et al., 2010), it is less reliable during exercise transitions and higher exercise intensities (Waldron et al., 2017). During exercise testing in this current study, in some subjects at the onset of exercise or in the latter stages of ramp exercise calibration was lost. As such, absolute values were only used when derived during unloaded pedalling (i.e. low intensity steady state exercise), or to measure the *change* in cardiac output during moderate intensity exercise transitions. Additionally, data were discarded if calibration was lost during unloaded pedalling or the exercise transient. Cardiac output kinetics were determined using the same kinetic analysis technique as pulmonary $\dot{V}O_2$ data (see methods), however, determining $\dot{V}O_2$ kinetics from pulmonary $\dot{V}O_2$ data is done often, with vigorous procedures. This method of measuring cardiac output kinetics has not, however, gone through the same process. Given this, the cardiac output data (and $\dot{V}O_2/\dot{Q}$ relationship data) inputted into the model may not be an accurate estimation of the actual cardiac output. Despite this, it is worth noting that the values obtained from this method lie within the 'expected

normal' range for healthy individuals (De Cort et al., 1991). Finally, $\dot{V}O_2$ kinetics from step exercise were used as model inputs from ramp exercise. This may influence the model predictions as the $\dot{V}O_2$ response varies according to the exercise protocol so that kinetics measured from step exercise may not exactly match those measured from ramp exercise.

4.4 Conclusion

The model presented is the first, to our knowledge, to predict NIRS responses during ramp incremental and step exercise from knowledge of circulatory, respiratory, and oxygen uptake dynamic interactions. With respect to the muscle oxygenation dynamics, the model shows that alterations in the $\dot{V}O_2/\dot{Q}$ relationship, including its kinetics, slope and absolute values, all affected the muscle oxygenation response. When $\dot{V}O_2$ kinetics are faster relative to $\dot{Q}$ kinetics TOI transiently undershoot its steady state value. Similarly, if baseline cardiac output becomes limiting to $\dot{V}O_2$, or there is a reduction in $\dot{Q}$ per litre change in $\dot{V}O_2$, TOI will undershoot its steady state response. Additionally, the model suggests muscle oxygenation responses are also sensitive to changes in the $\Delta\dot{V}O_{2m}/\Delta WR$ relationship. Specifically reducing this relationship caused a greater reliance on O_2 extraction. The model, however, could not detect any changes in the slope of the HHbMb response during ramp exercise.

The newly developed NIRS model, overall, was not able to accurately predict the muscle oxygenation response to ramp exercise. Despite no significant differences in the change in muscle oxygenation from the start to end of exercise, the model could not predict breakpoint in the data nor the slopes of the oxygenation responses. Therefore, further development and validation of the model is necessary before its clinical utility can be realised.

Chapter 5 Assessment of oxygen uptake kinetics measurements during ramp incremental exercise in heart failure patients

5.1 Introduction

The underlying principles of $\dot{V}O_2$ kinetics, and the $\dot{V}O_2$ response to exercise of different intensities, and of varying protocols (i.e. constant work rate [step] and incremental [ramp]) of have been described in Chapter 1. Briefly, the $\dot{V}O_2$ response to moderate intensity step exercise includes a three-phase response. Phase I reflects an increase in pulmonary blood flow, phase II represents an increase in $\dot{V}O_2$ at the exercising muscle and phase three indicates $\dot{V}O_2$ has reached a steady state. In heart failure, both phase I and phase II of the $\dot{V}O_2$ response may be impacted (Sietsema et al., 1986) indicating a failure to increase total blood flow (phase I), and muscle $\dot{V}O_2$ (phase II). Accordingly, $\dot{V}O_2$ kinetics are impaired (slowed) in diseased states when compared with healthy individuals. This has been reported as early as 1927, when Meakins and Long, (1927) observed slower O_2 kinetics in a patient with circulatory failure, compared with a healthy subject. Slower $\dot{V}O_2$ kinetics in heart failure are important to consider, as the demands of a given task in healthy versus heart failure patients do not differ, so for any given metabolic transition, the heart failure patient gains a higher O_2 deficit. Given this, it is not surprising that $\dot{V}O_2$ kinetics are strongly correlated to exercise tolerance in heart failure (Sperandio et al., 2009), as well as highly predictive of morbidity and mortality (Schalcher et al., 2003). However, it remains unclear what underlying mechanisms are responsible for exercise intolerance in heart failure. Specifically, whether the underlying mechanisms for the reduction in exercise capacity and slowed $\dot{V}O_2$ kinetics is due to a limitation in convective O_2 transport, and/or diffusive O_2 transport is a topic of much debate. Resolving this issue may be useful for the development of treatments and improved classification of these patients, allowing for more

appropriate treatment selection (Kemps et al., 2009). Moreover, as resting indices of cardiac function (Faggiano et al., 2001) and the level of perceived exercise tolerance (Wilson et al., 1995) poorly correlate with exercise capacity in heart failure patients, exercise testing with breath by breath gas exchange has become a pivotal tool in the evaluation and monitoring of HF patients. One of the limitations of breath-by-breath gas exchange measurements is that it represents a 'whole body' measurement and, as discussed by Poole et al. (2012), the scientific utility of breath by breath gas exchange measurements are dependent on rigorous demonstration that relate meaningfully to events occurring within the exercising muscle.

A study by Sperandio et al. (2009) observed that during phase II of the $\dot{V}O_2$ response, microvascular O_2 flow was impaired in optimally treated HF patients compared to age matched controls at the onset of heavy intensity exercise. They observed a transient overshoot in the deoxygenated haemoglobin + myoglobin (qualitatively similar to the undershoot in capillary PO_2) signal by near infrared spectroscopy, implying that estimated fractional O_2 extraction increased above the steady state level because of impaired blood flow relative to $\dot{V}O_2$. This response is thought to be related to the transient lowering of capillary PO_2 that appears large enough to reduce the diffusion gradient from capillary to mitochondria, causing impaired O_2 flux and limiting the rate of increase in muscle $\dot{V}O_2$.

Similar features have been observed in HF rats. Diederich et al. (2002), investigated the dynamics of PO_2 in contracting skeletal muscle of rats with HF. In the control rats, at the onset of contractions PmO_2 fell to a steady state value and there was no undershoot in P_mO_2 observed. Conversely, in rats with moderate Left Ventricular Systolic Dysfunction (LVSD), there was a more rapid fall in P_mO_2, which was associated with a transient undershoot below its steady state value. As P_mO_2 is representative of the relationship between $\dot{Q}m$ and $\dot{V}O_2$, these results are suggestive of a slowed microvascular blood flow response compared with that of $\dot{V}O_2$. Humans studies in support of this have demonstrated that the delay in $\dot{V}O_2$ kinetics at the onset of submaximal exercise in HF patients is correlated with a delay in cardiac output increase (Koike et al., 1994).

Furthermore, Kemps et al. (2010) demonstrated that $\dot{V}O_2$ onset kinetics during exercise below LT, and recovery are prolonged in HF patients, and examined the physiological background of this delay in moderately impaired

HF patients by comparing the kinetics of cardiac output ($\dot{Q}$) to $\dot{V}O_2$ (Kemps et al., 2010). They found there were no significant differences between the time constant of $\dot{Q}$ to $\dot{V}O_2$ during exercise onset or recovery, indicating that O_2 delivery was not in excess of metabolic demands in the HF patients. As studies with a similar approach in healthy individuals reported faster onset kinetics of $\dot{Q}$ compared to $\dot{V}O_2$ (Lador et al., 2006), they postulated that the delayed O_2 onset and recovery kinetics at submaximal exercise in moderately impaired HF patients are limited by an impairment in O_2 delivery rather than O_2 utilisation.

Using a different approach Mezzani et al. (2013) found that light to moderate intensity aerobic exercise training in HF patients speeded pulmonary $\dot{V}O_2$ kinetics and increased peak peripheral oxygen extraction, supporting the hypothesis that microcirculatory O_2 delivery impairment is a key factor in determining exercise intolerance in HF patients.

These data indicate that disturbances in cardio-circulatory (blood flow) responses play a prominent role in limiting $\dot{V}O_{2p}$ kinetics and tolerance to heavy intensity exercise. Nevertheless, it has been demonstrated that $\dot{Q}$ kinetics adjust faster relative to $\dot{V}O_2$ kinetics, at least in health (Grassi et al., 1996; MacDonald et al., 1998; Bangsbo et al., 2000). This is the first line of evidence that $\dot{Q}$ is *not* limiting to $\dot{V}O_2$. Grassi et al. (1997) examined metabolic and cardiovascular adjustments in 82 heart transplant recipients (HTR), and the effects of different exercise protocols on metabolic and cardiovascular variables. They found that in heart transplant recipients a priming exercise bout, despite speeding O_2 flow to the muscles, did not affect the $\dot{V}O_2$ on kinetics, implying that the slower $\dot{V}O_2$ on kinetics in heart transplant recipients are attributable to peripheral factors (Grassi et al., 1997). In addition, the $\dot{V}O_2$ recovery kinetics were slower in heart transplant recipients than in the control group, indicating a greater O_2 deficit in heart transplant recipients and hence, a sluggish muscle $\dot{V}O_2$ adjustment.

Grassi et al. (1998) was able to directly determine muscle O_2 delivery and muscle $\dot{V}O_2$ kinetics by using isolated in situ dog gastrocnemius preparation. Despite eliminating any delay in O_2 muscle delivery from rest to contraction (60-70% $\dot{V}O_{2,peak}$), there were no significant effect on $\dot{V}O_{2m}$ kinetics, indicating that the $\dot{V}O_2$ on kinetics were not limited by O_2 delivery to the muscle, but were presumably determined by the intracellular control of O_2 utilisation (Grassi et al., 1998).

In support of this hypothesis, Grassi et al. (1996) demonstrated in a unique study, via an adapted constant-infusion thermodilution technique (Andersen and Saltin, 1985), that at transition from light to moderate intensity exercise, the increase in the $\dot{V}O_2$ kinetics at the leg muscle was less marked when compared to the $\dot{V}O_2$ at the lungs. This finding indicates that the significant increase in O_2 delivery to the leg muscle within this period, was largely offset by a reduction in O_2 extraction, suggesting that $\dot{V}O_2$ at the leg muscle is not limited by bulk O_2 delivery. These findings are important to consider because for those patients who are limited by O_2 utilisation, interventions that are aimed to solely increase cardiac output (for example cardiac resynchronization therapy) may not be completely effective in patients with O_2 utlilsation impairments.

5.2 Assessment of oxygen uptake kinetics

The assessment of oxygen uptake kinetics in healthy individuals is well established and has been described in detail in Chapter 1. Briefly, oxygen uptake kinetics are typically determined from breath-by-breath gas exchange measurements made during moderate intensity constant work-rate step exercise, where the phase II “fundamental phase” of the $\dot{V}O_{2p}$ response is isolated and fit with an exponential function. However, this method of determining oxygen uptake kinetics has limitations when applied to determining oxygen uptake kinetics in heart failure patients. One such limitation is the poor accuracy of the exponential fit to the $\dot{V}O_2$ data, due to high signal to noise ratio. This is because a lower lactate threshold in heart failure patients results in a lower $\dot{V}O_2$ amplitude which, in turn, increases the signal-to-noise ratio thereby lessening the accuracy of the exponential fit to the $\dot{V}O_2$ data (Lamarra et al., 1987). Additionally, oscillations in oxygen uptake and CO_2 production that are common in heart failure patients may worsen the accuracy of the exponential fit further (Francis et al., 1999). Furthermore, as phase I represents an increased blood flow, it is questionable whether sluggish cardiac function may prolong phase I, thereby confounding the accurate isolation of the fundamental phase. In Chapter 3, a sensitivity analysis of the MCM_{inc} model showed that a 10% reduction in total blood flow had the effect of prolonging phase I by 1.3 seconds, giving an indication that removing, up to, the first 20 seconds [as in health (Benson et al., 2017)] in order to isolate the fundamental phase may not always be

sufficient in heart failure patients, meaning the phase II response could be 'diluted' by phase I. Although it is not known if this is enough to cause physiological alterations and is yet to be confirmed experimentally.

Given the above limitations, some investigators have sought to characterise oxygen uptake kinetics by using the mean response time. There are several ways in which this can be done (Sietsema et al., 1986, 1994; Hepple et al., 1999; Schalcher et al., 2003). One such way utilises an algebraic method where the cumulative sum of $\dot{V}O_2$, in excess of baseline (or resting) $\dot{V}O_2$ is subtracted from the theoretical $\dot{V}O_2$ requirement such that:

$$t \cdot \Delta\dot{V}O_2 - \Sigma\dot{V}O_2 = \text{oxygen deficit} \quad (58)$$

where t is the test duration, $\Delta\dot{V}O_2$ is the change in the steady state $\dot{V}O_2$, and $\Sigma\dot{V}O_2$ is the cumulative sum of $\dot{V}O_2$ in excess of baseline $\dot{V}O_2$. The mean response time is then calculated by dividing the oxygen deficit by the theoretical $\dot{V}O_2$ requirement such that:

$$\text{MRT} = \text{oxygen deficit} / \Delta\dot{V}O_2 \quad (59)$$

Whilst this method has been utilised in research settings (Sietsema et al., 1994; Hepple et al., 1999; Schalcher et al., 2003; Bowen et al., 2012), due to the relatively complex nature of the data analysis process, it may not be easily applicable to clinical settings. In addition to this, constant work rate exercise bouts are not commonly used as standard care in clinic unlike ramp incremental tests. Furthermore, despite its inability to separate out total blood flow from changes in muscle oxygen uptake dynamics, it has been demonstrated to represent and even better predictor of mortality than $\dot{V}O_{2,peak}$ in heart failure patients [Figure 32 (Schalcher et al., 2003)].

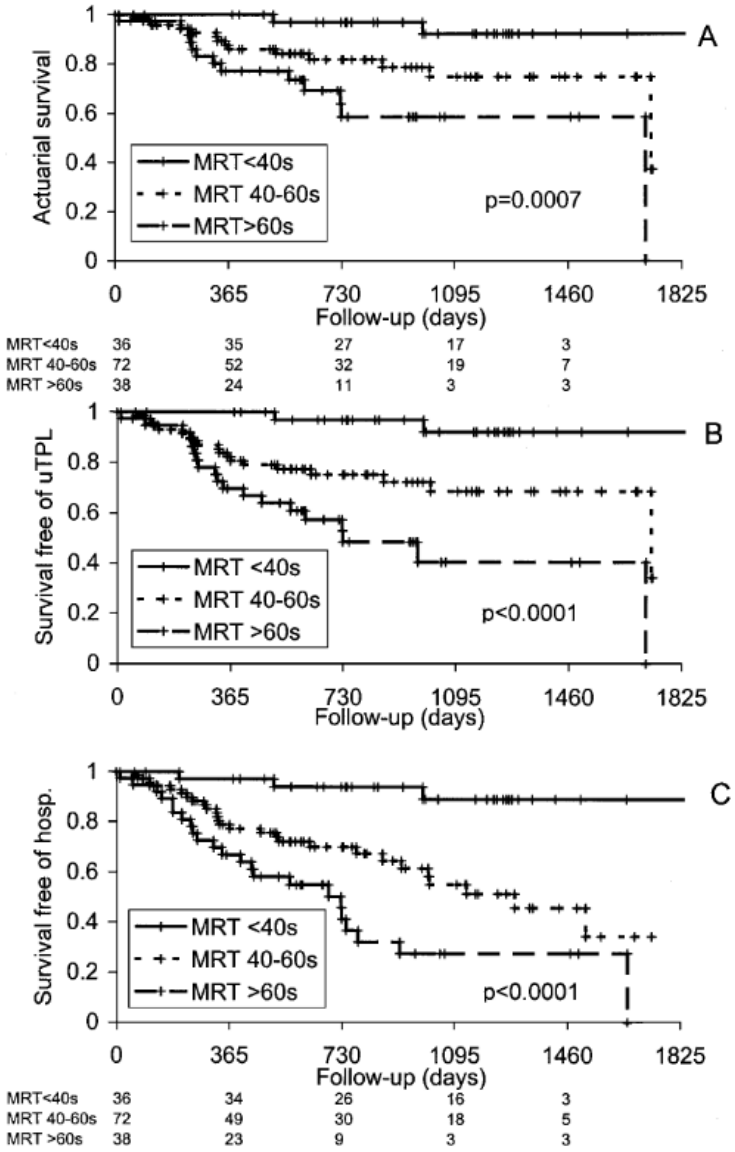

Figure 32: Kaplan-Meier plots of cardiac survival (top,A), cardiac survival free of urgent transplantation (uTPL) [middle, B],and survival free of hospitalization (hosp) [bottom, C] for the following three categories of MRT: 60s, 40 to 60 s, and 40 s. The table between top, A, and middle, B, denotes the number of patients in each category of MRT at baseline, and after 1, 2, 3, and 4 years with respect to cardiac survival and cardiac survival free of urgent transplantation, respectively. The table below bottom, C, denotes the number of patients with respect to cardiac survival free of hospitalization. Taken from Schalcher et al. (2003).

The mean response time can also be obtained from ramp incremental exercise (which is often carried out as a part of standard care in clinical assessment of heart failure patients) and represents time taken for the $\dot{V}O_2$ response to increase in a linear fashion. It is typically quantified as the time interval between the onset of the ramp exercise, and the intersection of the extrapolation of the baseline $\dot{V}O_2$ and the backwards extrapolation of the linear $\dot{V}O_2$/time relationship (Figure 33).

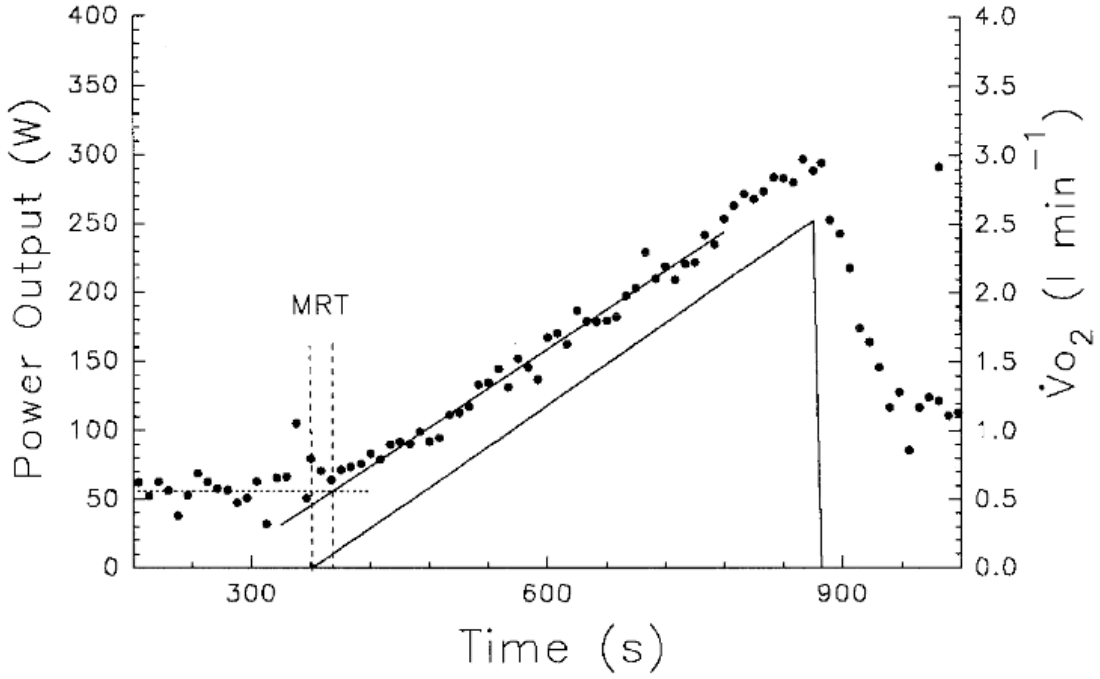

Figure 33: A typical $\dot{V}O_2$ response to ramp incremental exercise of a representative normal subject. The mean response time (MRT) of the $\dot{V}O_2$ response is calculated as the time from the onset of the ramp exercise to the point of the intersection of baseline $\dot{V}O_2$ and a linear back extrapolation of the $\dot{V}O_2$ vs time slope. Taken from Barstow et al. (2000)**.**

Until the development of the ramp protocol both a constant work rate step exercise test and a ramp test were required to obtain the four key parameters of exercise tolerance (i.e. $\dot{V}O_{2,max}$, lactate threshold, time constant for oxygen uptake kinetics and work efficiency). Whipp et al. (1981), showed that the ramp incremental test could be used as an alternative to two tests to accurately determine these parameters, based on the principle that $\dot{V}O_2$ operates with first-order linear dynamics. However, similar to constant work rate exercise, the mean response time derived from

ramp incremental exercise incorporates both phase I and phase II of the $\dot{V}O_2$ response. Therefore, it is not clear if the MRT is a true representation of muscle oxygen uptake kinetics, especially in heart failure patients where impairments in the O_2 transport system can derange these parameters. Therefore, the aims of this chapter were (i) to establish if *pulmonary* $\dot{V}O_2$ kinetics measured during step exercise are an accurate reflection of *muscle* oxygen uptake kinetics in heart failure patients (i.e. $\dot{V}O_{2p}\tau$ vs $\dot{V}O_{2m}\tau$) and; (ii) if the mean response time measured from ramp incremental exercise is equal to muscle $\dot{V}O_2$ kinetics determined from step exercise in heart failure patients (i.e. $\dot{V}O_{2p,MRT}$ *vs* $\dot{V}O_{2m}\tau$).

5.3 Methods

Experimental data collection, measurements, exercise protocol and data analysis are described in the general methods section under sub-heading "Protocol 2" for healthy participants, and "Protocol 4" for heart failure patients.

Model simulations

The MCM_{inc} and MCM step models were utilised and individualised on a patient-by-patient basis. Model input parameters (baseline $\dot{V}O_2$, $\dot{V}O_2$ gain, cardiac output kinetic, oxygen uptake kinetics and baseline cardiac output) were determined experimentally from ramp and step exercise tests. For each participant/patient, and each protocol (i.e step or ramp) muscle oxygen uptake kinetics were adjusted in the model until the model $\dot{V}O_{2p}$ phase II output (for step exercise) or $\dot{V}O_{2p}$ mean response time (for ramp exercise) matched the experimentally derived $\dot{V}O_2$ kinetics in a given individual, thereby providing model predicted ("muscle") muscle $\dot{V}O_2$ kinetic and experimentally measured ("lung") muscle $\dot{V}O_2$ kinetics.

Previous studies (Murgatroyd et al., 2011; Bowen et al., 2012) that have examined the reproducibility of $\dot{V}O_2$ kinetics have produced 95% confidence intervals, and SD of 3.1 ± 0.9 s in healthy individuals (Murgatroyd et al., 2011) and 5.0 ± 2.0 s in heart failure patients (Bowen et al., 2012). Therefore, any changes greater than 3.0 s for healthy participants and 5 seconds for heart failure patients were taken to be physiologically significant, as these changes are likely to be detectable, and reproducible, in a laboratory.

Statistical analysis

Model predicted, and experimentally measured, oxygen uptake kinetics were compared using paired *t*-tests. Significance was accepted as $p < 0.05$.

5.4 Results and discussion

Results are presented as mean ± standard deviation unless otherwise stated. Heart failure patients achieved a $\dot{V}O_{2,peak}$ of 1.16 ± 0.46 L/min, which corresponded to a peak work rate of 81 ± 31 W. This was lower than healthy patients who achieved a $\dot{V}O_2$ peak of 3.57 ± 1.02 L/min and peak work rate of 290 ± 79 W. $\dot{V}O_2$ gain was lower in heart failure patients than healthy individuals (0.009 L/min/W vs 0.012 L/min/W respectively).

Figure 34 shows $\dot{V}O_2$ responses to step and ramp incremental exercise in a representative HF patient and healthy individual. Oxygen uptake kinetics were significantly slower in heart failure patients than controls (step ($\dot{V}O_2\tau$): 24.0 s ± 7.2 s vs 50.4 s ± 17.8 s, p = 0.006 respectively; ramp ($\dot{V}O_{2,MRT}$): 45.5 s ± 8.8 s vs 81.3 s ± 27.0 s, p = 0.01 respectively).

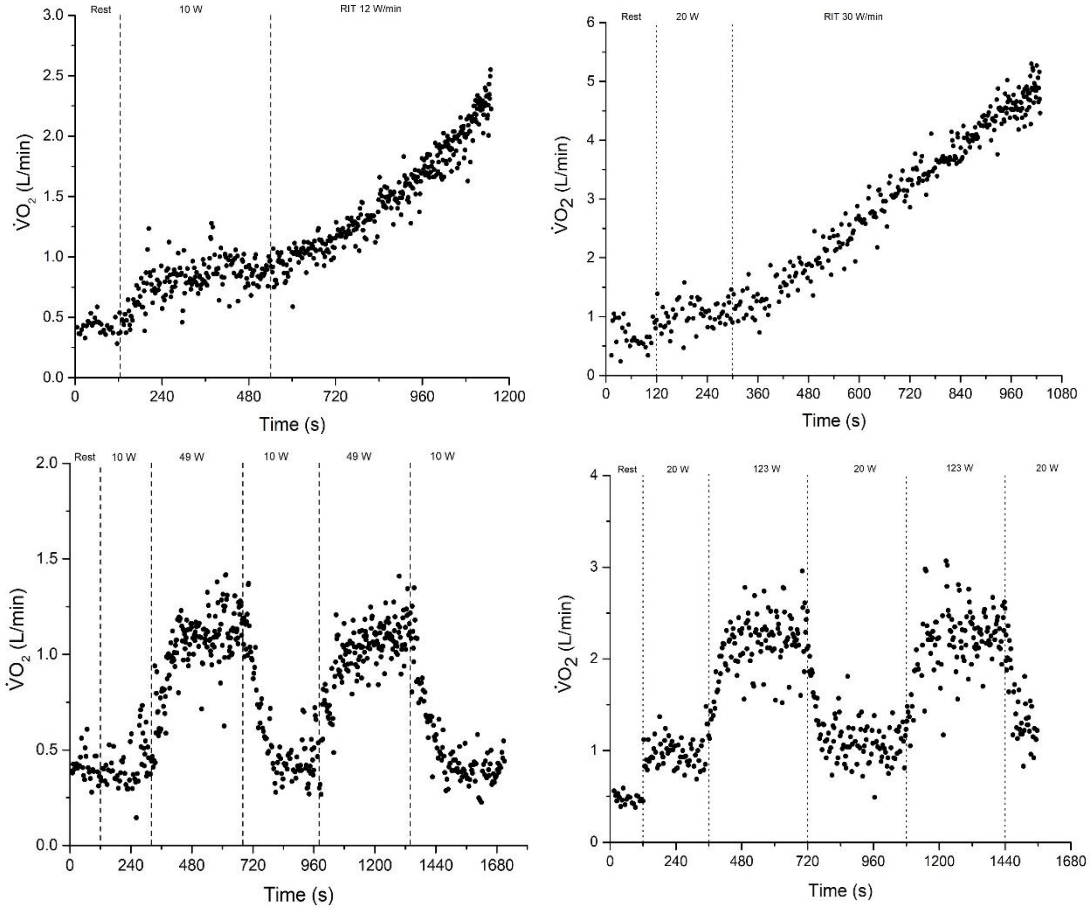

Figure 34: Oxygen uptake responses ($\dot{V}O_2$ L/min) plotted as a function of time during ramp incremental exercise (top panels) and constant work rate step exercise (bottom panels) in a representative heart failure patient (left panels) and healthy participant (right panels).

Individual model input parameters are shown below in Table 15 (healthy participants) and Table 16 (heart failure patients). Model output parameters and experimentally derived muscle and pulmonary oxygen uptake kinetics are shown in tables 17-20. Figure 35 shows a summary of these findings.

Table 15: Individual model input parameters from ramp and step exercise heart failure patient

Subject	$\dot{V}O_2$ baseline (L/min)	$\dot{Q}$ baseline (L/min)	$\dot{V}O_{2p}\tau$ (s)	$Q\tau$ (s)	Gain (L/min/W)	$\dot{V}O_2$ MRT (ramp)	ramp WR (W/min)	ramp duration (s)
1	0.24	3.52	47.7	54.0	0.007	48.00	4.00	579.00
2	0.31	4.43	27.9	19.0	0.007	75.00	12.00	737.00
3	0.29	4.14	83.9	113.0	0.010	144.00	5.00	437.00
4	0.29	4.15	42.9	43.0	0.011	94.00	8.00	424.00
5	0.24	3.47	57.2	46.0	0.010	67.00	4.00	829.00
6	0.32	4.62	64.9	59.0	0.089	67.00	5.00	927.00
7	0.38	5.45	26.1	55.0	0.013	86.00	5.00	609.00
8	0.40	5.83	52.5	42.0	0.011	69.00	14.00	449.00
Mean	0.31	4.45	50.39	54.00	0.009	81.25	7.13	623.88
SD	0.06	0.84	19.06	26.88	0.002	28.84	3.87	190.66

$\dot{V}O_2$ baseline was taken as final 60s UP during ramp test; $\dot{Q}$ baseline = $\dot{V}O_2$ baseline x 14.5 (see methods); $\dot{V}O_2p\ \tau$ was measured from step exercise; $\dot{Q}\tau$ was assumed from HR kinetics measured from step exercise, Gain was measured from ramp exercise; $\dot{V}O_2$ MRT was measured from ramp exercise. For more detail on data analysis see general methods section.

Table 16: Individual model input parameters from ramp and step exercise in healthy participants

Subject	$\dot{V}O_2$ baseline (L/min)	$\dot{Q}$ baseline (L/min)	$\dot{V}O_{2p}\,\tau$ (s)	$Q\tau$ (s)	Gain (L/min/W)	$\dot{V}O_2$ MRT (ramp)	Ramp rate (W/min)	Ramp duration (s)
1	1.05	6.19	26.25	22.20	0.013	39.00	33.00	732.00
2	0.69	6.17	21.03	24.00	0.013	35.00	15.00	657.00
3	0.78	8.70	19.97	11.32	0.012	43.00	20.00	718.00
4	0.91	7.80	18.96	24.91	0.013	45.00	20.00	755.00
5	1.11	11.55	20.08	41.77	0.012	60.00	30.00	636.00
6	1.44	9.59	20.62	35.36	0.013	47.00	25.00	783.00
7	0.70	8.40	17.82	14.95	0.013	31.00	25.00	552.00
8	1.04	9.48	40.84	68.03	0.014	52.00	25.00	796.00
9	0.95	8.55	30.63	29.01	0.011	54.00	15.00	608.00
Mean	0.96	8.49	24.02	30.17	0.013	45.11	23.11	11.55
SD	0.23	1.69	7.48	17.00	0.001	9.32	6.19	1.40

$\dot{V}O_2$ baseline was taken as final 60s UP during ramp test; $\dot{Q}$ baseline was measured experimentally during moderate intensity step exercise; $\dot{V}O_2p\ \tau$ was measured from step exercise; $\dot{Q}\tau$ was measured from moderate intensity step exercise, Gain was measured from ramp exercise; $\dot{V}O_2$ MRT was measured from ramp exercise. For more detail on data analysis see general methods section.

Ramp exercise

The experimentally measured pulmonary $\dot{V}O_2$ mean response time was significantly different from the predicted muscle $\dot{V}O_2$ kinetics in heart failure and health during ramp exercise ($p = 0.0001$; $p = 0.002$ respectively). It is worth noting that, although significantly different, the average MRT for the model predicted and mean experimentally derived values for healthy individuals, was only 1 second different (44s vs 45s, respectively). This one second difference is unlikely to be detectable when $\dot{V}O_2$ kinetics are measured experimentally in a laboratory (Murgatroyd et al., 2011). For HF patients, experimentally measured MRT was 9 seconds longer than model predicted $\dot{V}O_{2m}$. There was no correlation between MRT duration and baseline $\dot{V}O_2$ in healthy ($r^2 = -0.1$; $p > 0.05$) or in heart failure ($r^2 = 0.1$; $p > 0.05$), nor was there any correlation between mean response time and baseline $\dot{V}O_2$ in either the healthy or heart failure ($r^2 = -0.1$; $p > 0.05$; $r^2 = 0.5$; $p > 0.05$ respectively).

Table 17: model predicted muscle $\dot{V}O_2$ kinetics and experimentally measured mean response time (MRT) in 8 heart failure patients for ramp exercise

Subject	MRT (s) experimental	$\dot{V}O_{2m}\tau$ (s) model predicted
1	48	33
2	75	70
3	133	122
4	94	84
5	67	57
6	67	60
7	86	76
8	69	64
Mean	80	71
SD	25	26

Table 18: model predicted muscle $\dot{V}O_2$ kinetics and experimentally measured mean response time (MRT) in 9 healthy individuals for ramp exercise

Subject	MRT (s) experimental	$\dot{V}O_{2m}\tau$ (s) model predicted
1	39	39
2	33	35
3	42	43
4	44	45
5	59	60
6	47	47
7	30	31
8	51	52
9	52	54
Mean	44	45
SD	9	9

Step exercise

The experimentally measured muscle $\dot{V}O_2$ kinetics (i.e. phase II $\dot{V}O_{2p}$) and model predicted muscle $\dot{V}O_2$ kinetics from step exercise was significantly different in heart failure patients and in health ($p = 0.001$; $p = 0.2$ respectively). Despite this statistically significant difference, the average difference between model predictions and experimental data was only 3 seconds different in health (24s vs 27s) which as described above is unlikely to be physiologically detectable (Murgatroyd et al., 2011). In heart failure patients there was a 6 second difference between the two parameters (51s for experimental vs 57s for model predicted). which would be detectable in an exercise test (Bowen et al., 2012).

Table 19: Model predicted muscle $\dot{V}O_2$ kinetics and experimentally measured pulmonary $\dot{V}O_2$ kinetics in 8 heart failure patients for step exercise

Subject	$\dot{V}O_{2p}\tau$ (s) experimental	$\dot{V}O_{2m}\tau$ (s) model predicted
1	48	55
2	28	29
3	84	95
4	43	50
5	57	62
6	65	71
7	26	36
8	53	55
Mean	51	57
SD	19	21

Table 20: Model predicted muscle $\dot{V}O_2$ kinetics and experimentally measured pulmonary $\dot{V}O_2$ kinetics in 9 healthy individuals for step exercise

Subject	$\dot{V}O_{2p}\tau$ (s) experimental	$\dot{V}O_{2m}\tau$ (s) model predicted
1	26	26
2	21	25
3	20	18
4	19	24
5	20	26
6	21	27
7	18	19
8	41	49
9	31	32
Mean	24	27
SD	8	9

Furthermore, despite some significant differences there were good correlations between experimentally measured $\dot{V}O_{2p}$ MRT and model predicted $\dot{V}O_{2m}\tau$ in heart failure patients and healthy individuals (r^2 = 0.98 and 0.99 respectively) and also between experimentally measured $\dot{V}O_{2p}\tau$ and model predicted $\dot{V}O_{2m}\tau$ (r^2 = 0.97 and 0.88 respectively) in both heart failure patients and healthy individuals (Figure 36) suggesting that for the ramp protocol $\dot{V}O_{2p}$ measured experimentally is similar to $\dot{V}O_{2m}$ kinetics predicted by the model and that for step exercise $\dot{V}O_{2p}$ kinetics measured experimentally are representative of $\dot{V}O_{2m}$ kinetics predicted by the model.

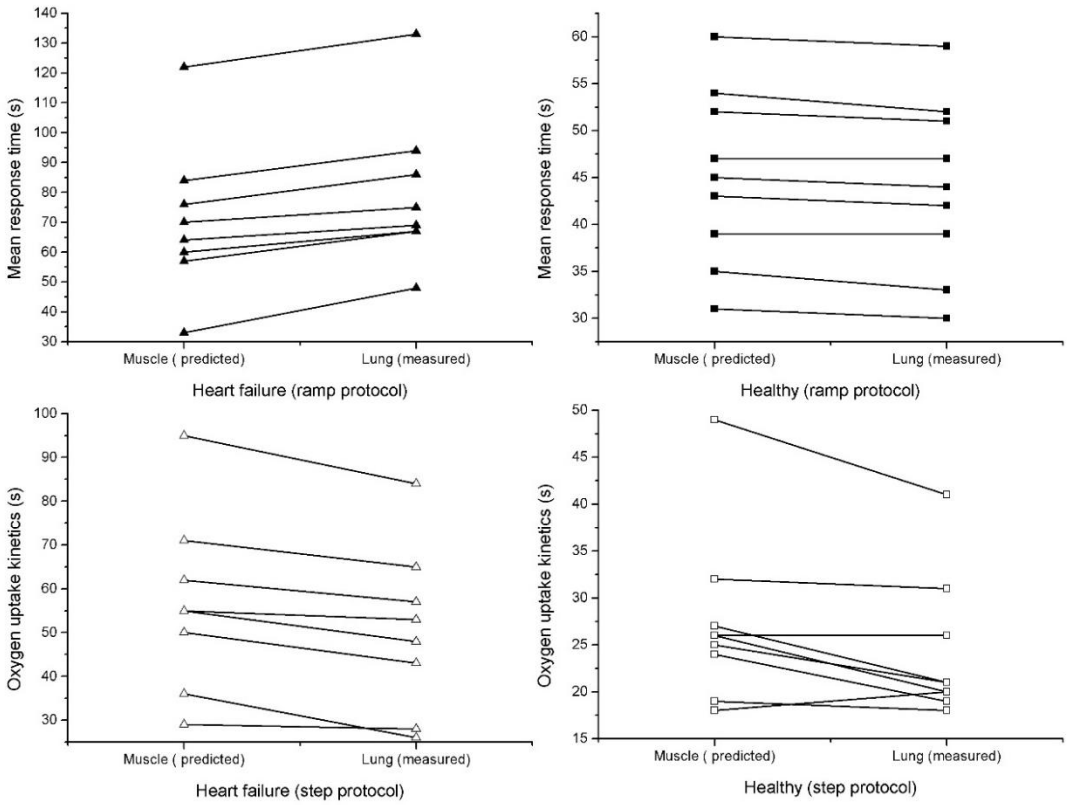

Figure 35: Top panel: Mean response determined by breath-by-breath gas exchange measurements (“lung”) and model predictions (“muscle”) in heart failure patients (left) and healthy participants (right) during ramp incremental exercise. Bottom panel: Muscle oxygen uptake kinetics determined from breath-by-breath gas exchange measurements (“lung”) and model predictions (“muscle”) during constant work rate step exercise. In all conditions (i.e. step vs ramp, heart failure vs healthy) the oxygen uptake kinetics measured at the lung were significantly different from the predicted oxygen uptake at the muscle.

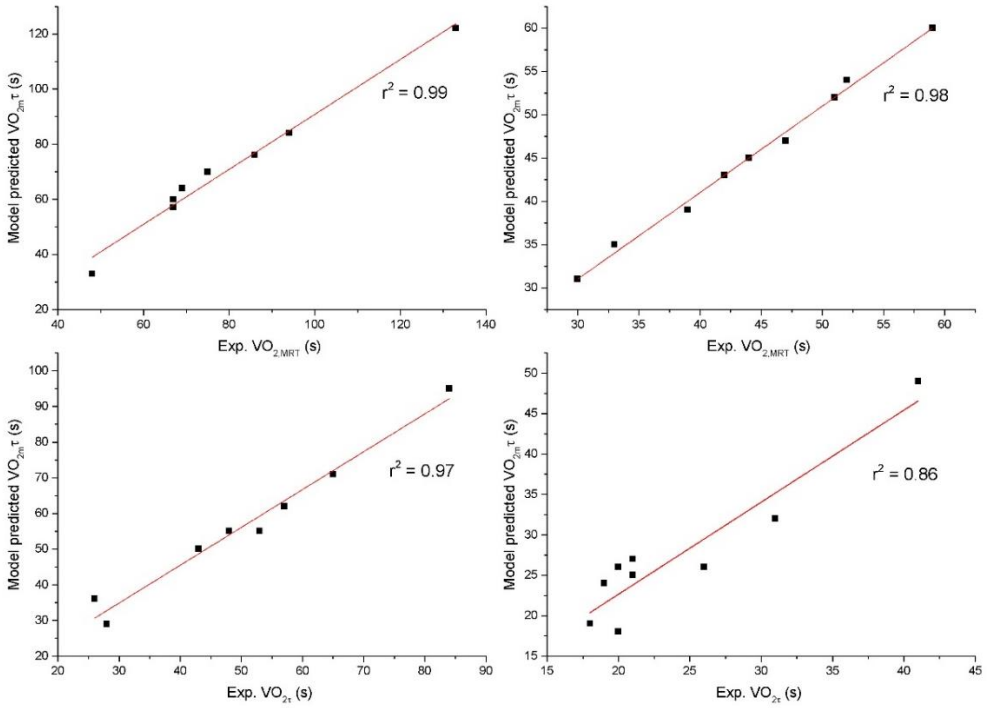

Figure 36: Top panel: correlations between experimentally measured $\dot{V}O_{2p}$ MRT and model predicted $\dot{V}O_{2m}\boldsymbol{\tau}$ in heart failure patients (left) and healthy individuals (right). Bottom panel: correlations between experimentally measured $\dot{V}O_{2p}\boldsymbol{\tau}$ and model predicted $\dot{V}O_{2m}\boldsymbol{\tau}$.

Mean response time: step vs ramp exercise

Experimentally derived mean response time values determined from ramp incremental exercise and constant work rate step exercise are shown in Table 21. Mean response time was on average, 19 seconds longer when determined from ramp incremental exercise when compared to step exercise. However, the individual difference varied between patients. In 3/8 patients MRT was slower when determined from ramp exercise whereas in the remaining 5 patients MRT was slower when determined from ramp exercise than step exercise.

Table 21: Experimentally derived mean response time (MRT) from ramp incremental and step exercise in heart failure patients

Subject	MRT (s) (Ramp)	MRT (s) (Step)	Difference (s)
1	48	72	-24
2	75	35	40
3	144	100	44
4	94	40	54
5	67	72	-5
6	67	75	-8
7	86	44	42
8	69	60	9
Mean	**81**	**62**	**19**
SD	**27**	**21**	**7**

The experimental data and model simulations show good correlations between experimentally measured $\dot{V}O_{2p}$ MRT and model predicted $\dot{V}O_{2m}\tau$, and experimentally measured $\dot{V}O_{2p}\tau$ and model predicted $\dot{V}O_{2m}\tau$ in both heart failure patients and healthy individuals suggesting that *pulmonary* $\dot{V}O_2$ kinetics measured during step exercise are an accurate reflection of *muscle* oxygen uptake kinetics in heart failure patients (i.e. $\dot{V}O_{2p}\tau$ vs $\dot{V}O_{2m}\tau$). However, when comparing methods of measuring MRT, when measured from ramp exercise, mean response time was on average 19 seconds faster when measured from step exercise suggesting that the mean response determined by different methods and from different protocols are not equal.

In healthy individuals only a 1 second difference was found between experimentally measured MRT and predicted muscle $\dot{V}O_2$ kinetics whereas an average of a 9 second difference was observed in the heart failure group. Given that MRT is a summation of phase I and phase II of the $\dot{V}O_2$ response, and phase I typically lasts ~15-20 seconds, it might be expected that MRT would be longer $\dot{V}O_{2p}\tau$ in healthy individuals. One possible explanation for this could be because of the sensitivity of the mean response time to the paraments quantifying the $\dot{V}O_2$ response to exercise. For example, Boone et al. (2008) showed that MRT was influenced by the baseline that the ramp exercise was initiated from as well as the steepness of the ramp protocol. A lower baseline $\dot{V}O_2$ was associated with shorter MRT as were steeper ramp slopes. Because of this, it is recommended that baseline work rate should be 50 W or above however, this may not be

feasible in heart failure patients due to low exercise tolerance. For example, mean peak work rate during ramp exercise in this study was 81 W however, the lowest peak work rate achieved was 46 W. Additionally, starting the ramp exercise from a higher baseline may limit the number of data points obtained in a low-moderate intensity work rate. In this study, lower baselines were observed in the HF patients, as was steeper ramp slopes in health. Despite this there was no strong correlation between MRT and slope steepness or baseline $\dot{V}O_2$ in either group suggesting that MRT was not affected by these variables.

A consistent finding was that oxygen uptake kinetics were significantly slower in heart failure patients than healthy individuals, regardless of the exercise protocol used, or the method of determining its kinetics. As oxygen uptake kinetics depend on the rate of tissue oxygenation (O_2 delivery), and the ability to utilise O_2, derangements of O_2 delivery and/or O_2 utilisation may be responsible for the prolongation of O_2 kinetics in HF (Kemps et al., 2010). These derangements in O_2 delivery and/or O_2 utilisation are still not completely understood and furthermore, it is unclear which of the impairments (i.e. O_2 delivery or O_2 utilisation, or both) are the primary cause of exercise intolerance in heart failure.

It is possible that the primary limiting factor (i.e O_2 delivery or O_2 utilisation) could vary between individuals. For example, Bowen et al. (2012) looked at $\dot{V}O_2$ kinetics and muscle oxygenation dynamics in heart failure patients before and after priming (i.e. to increase cardiac output) exercise. They found that the dynamics of microvascular O_2 delivery-to-utilisation relationship in the skeletal muscles of HF patients to be impaired (this was manifested as an overshoot in muscle deoxygenation at exercise onset). However, they also observed that, although resting muscle oxygenation was increased and $\dot{V}O_2$ kinetics were speeded following priming exercise in all patients, in the patients with the slowest $\dot{V}O_2$ kinetics (and lower resting muscle oxygenation and worse symptoms), $\dot{V}O_2$ kinetics remained slow (>40 s), and the rate of muscle deoxygenation actually declined after priming exercise. This suggests that the patients with slower $\dot{V}O_2$ kinetics were less able to ‘make use’ of the increase in oxygen delivery. This finding indicates that the patients in with slower $\dot{V}O_2$ kinetics (and more severe symptoms), may have been limited by some intracellular pathology, and the patients with less severe HF were able to gain more benefit from the increased $\dot{Q}_m$ and therefore are not limited by O_2 utilisation (Bowen et al., 2012).

Given that the severity of heart failure and prolongation of oxygen uptake kinetics at the skeletal muscle may be related to the locus of impairments in the O_2 transport system (Bowen et al., 2012), it is of the upmost importance that determining $\dot{V}O_2$ kinetics at the skeletal muscle are done accurately, with care and precision. Although a ramp incremental test is more widely used in clinics, the results from this current study suggest that the pulmonary oxygen uptake kinetics gained from ramp incremental exercise cannot be reliably used to determine muscle oxygen uptake kinetics in heart failure patients alone as, according to the modelling predictions, they vary considerably depending on the chosen method of data collection and data analysis. Other non-invasive methods that can be applied more specifically at a skeletal muscle level (such as near infrared spectroscopy) may aid measurements in this context.

It is also important to consider that, although the model has been validated against experimental $\dot{V}O_2$ data, it was not validated against ramp $\dot{V}O_2$ MRT (as these data were not available) and, therefore, it is not a given that the model is more accurate than the experimental data when comparing the two. Furthermore, there are limitations that should be considered with the model. One such limitation is that the venous volumes in the model remain constant between individuals and different exercise protocols/intensities, and are based on measurements made in healthy, amateur cyclists. This may affect model $\dot{V}O_2$ predictions as altering venous capacitances affects the amplitude and duration of phase I (i.e. the time delay) of the $\dot{V}O_2$ response. The influence of this time delay is that on reaching the lung, the muscular venous effluent incorporated into C_VO_2 is associated with a higher blood flow value than that which contributed to its determination (i.e. the instantaneous pulmonary blood flow is raised by a proportion related to the intervening transit time). Sluggish circulatory dynamics (e.g. in heart failure patients) may affect the venous volume during exercise and the exercise transient.to an even larger extent than in healthy individuals This may alter the time delay of the $\dot{V}O_2$ response and therefore subsequent kinetic coupling (Benson et al., 2013). Therefore, it is not known if these values are relevant in the heart failure population.

5.5 Conclusion

In conclusion, the data and model simulations presented in this chapter show that, according to the model predictions, muscle oxygen uptake kinetics are strongly correlated to pulmonary oxygen uptake measurements in heart failure patients. However, the mean response time may differ within the same patient depending on the exercise protocol and method of data analysis used such that, the mean response time determined from step exercise is not equal to the mean response in the same patient when determined from ramp incremental exercise. Therefore, for ramp incremental exercise to be used to its full clinical utility, additional measurements may be needed alongside breath-by-breath measurements to identify patients in whom skeletal muscle dysfunction is a limiting factor in exercise tolerance.

Chapter 6 Characterising muscle oxygenation dynamics measured by near infrared spectroscopy in heart failure

6.1 Non-invasive estimation of the matching of muscle O_2 delivery to O_2 utilisation

Direct measurement of the $\dot{V}O_{2m}/\dot{Q}_m$ dynamics in humans is technically and practically challenging. As such, skeletal muscle O_2 uptake ($\dot{V}O_{2m}$) is often estimated from measurements of pulmonary O_2 uptake ($\dot{V}O_{2p}$) during cardiopulmonary exercise testing. However, it is known that pulmonary $\dot{V}O_2$ kinetics dissociates from muscle $\dot{V}O_2$ kinetics during the exercise transient, partly due to intervening circulatory dynamics (Barstow et al., 1990; Lai et al., 2006; Benson et al., 2013). In addition, skeletal muscle blood flow has been estimated from measurements of cardiac output; however, these are complicated by variability of blood flow redistribution and vasodilatory capacity (Musch et al., 2004; Harper et al., 2008; Sperandio et al., 2012). Investigating muscle oxygenation dynamics provides an alternative approach to investigating $\dot{V}O_{2m}$-$\dot{Q}_m$ dynamics. For example, modelling studies have shown that reducing $\dot{V}O_{2m}$ relative to $\dot{Q}_m$ slows and reduces the extent of the decrease in muscle oxygenation during exercise transients (Barstow et al., 1990) whereas reducing $\dot{Q}_m$ relative to $\dot{V}O_{2m}$ accelerates and increases transient decrease in muscle oxygenation. Moreover, a lower pre-exercise $\dot{Q}_m$ amplifies the latter response (Benson et al., 2013).

Muscle oxygenation dynamics can be measured non-invasively in humans using NIRS. The principles of NIRS are discussed in detail in Chapter 1. Briefly, NIRS allows non-invasive and continuous measurement of local muscle oxidative metabolism at rest and during exercise, based on the principle that the NIR light absorption characteristics of haemoglobin (Hb) and myoglobin (Mb) depend on their oxygen saturation (Grassi et al., 2003). Of the NIRS derived parameters, relative changes in deoxygenated

haemoglobin and myoglobin (HHbMb) can be considered a proxy for the arterio-venous O_2 difference (i.e. proportional to $C_aO_2 - C_vO_2$), and thus microvascular O_2 extraction (DeLorey et al., 2003; Grassi et al., 2003).

The use of NIRS in heart failure studies have predominantly been investigated during constant work rate exercise (DeLorey et al., 2003; Grassi et al., 2003; Sperandio et al., 2009; Bowen et al., 2012). A key finding from studying NIRS during constant work rate exercise is the presence of a transient overshoot in deoxygenated Hb and Mb (HHbMb), or a reciprocal undershoot in the tissue oxygenation index (TOI) signal by NIRS, implying that estimated fractional O_2 extraction increases above the steady state level because of impaired O_2 delivery relative to O_2 requirements at the onset of exercise (Sperandio et al., 2009; Bowen et al., 2012). However, during daily life humans hardly experience prolonged periods of metabolic steady state (Boone et al., 2016). As such, studying *dynamics* of $\dot{V}O_{2m}$-$\dot{Q}_m$ during the *non-steady state* is highly relevant to understanding key aspects of metabolic and vascular control. The typical NIRS deoxygenated haemoglobin and myoglobin response to ramp exercise in healthy humans has been described in Chapter 1. In the context of this chapter, there is some uncertainty as to the most accurate and useful method of characterising and quantifying the HHbMb response profile. A linear relationship between $\dot{Q}_m$ and $\dot{V}O_{2m}$ would result in a hyperbolic oxygen extraction profile (Whipp et al., 1982; Ferreira et al., 2006). However, so far the NIRS HHbMb response to incremental exercise has been best characterised with a sigmoidal function (Ferreira et al., 2007; Boone et al., 2009, 2012; DiMenna et al., 2010; Chin et al., 2011) or more recently, a double linear function (Spencer et al., 2012). Figure 37 shows a schematic representation of both the sigmoid and double linear functions.

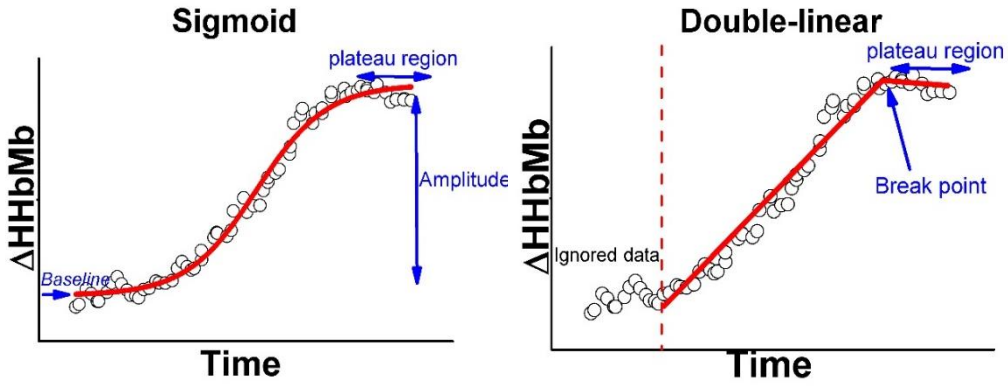

Figure 37: A schematic representation of a sigmoidal fit (left) and a double-linear fit (right), the blue arrows indicate key parameters that each function generates. Data redrawn from (Ferreira *et al.*, 2007).

A sigmoidal response suggests that the dynamics of $\dot{V}O_{2m}$ and $\dot{Q}_m$ are not linear during ramp exercise but are exercise intensity dependent such that, at lower exercise intensities $\dot{Q}_m$ kinetics are faster relative to $\dot{V}O_{2m}$ kinetics, but as exercise intensity increases, $\dot{Q}_m$ kinetics get progressively slower, until $\dot{V}O_{2m}$ and $\dot{Q}_m$ kinetics become well matched (Ferreira et al., 2007). Ferreira et al. (2007) demonstrated this by modelling the $\dot{V}O_{2m}/\dot{Q}_m$ relationship from knowledge of deoxygenated haemoglobin and myoglobin response in a healthy subject (Figure 38). The linear portions of the $\dot{V}O_{2m}/\dot{Q}_m$ relationship correspond to the flat areas of the arterio-venous O_2 content difference ($[a\text{-}v]O_2$), indicating good matching between $\dot{V}O_{2m}$ and $\dot{Q}_m$ and therefore stable oxygen extraction. Whereas where Q_m kinetics appear to be slow, and $\dot{V}O_{2m}$ kinetics appear to be fast, $(a\text{-}v)O_2$ difference increases steeply, indicating greater oxygen extraction.

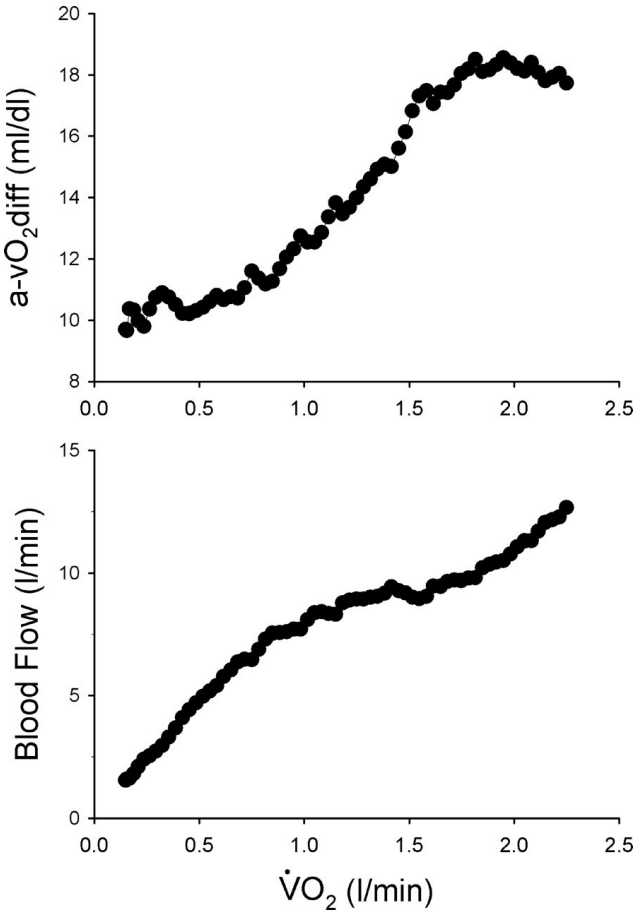

Figure 38: Schematic representation of the relationship between arteriovenous O_2 difference [a-vO_2diff or (a-v)O_2] and muscle $\dot{V}o_2$ (top) and blood flow and muscle $\dot{V}o_2$ (bottom). (a-v)O_2 was estimated from the profile of the deoxygenated haemoglobin and myoglobin response. Taken from Ferreira et al. (2007).

However, issues with the sigmoidal characterisation of the deoxygenated haemoglobin and myoglobin response arise from the lack of a physiological reasoning for the symmetrical upper and lower curves implied by a sigmoidal function (i.e. symmetrical upper and lower curves imply that the relationship is identical at exercise onset and at peak exercise). Furthermore, it has been argued that characterising the whole response may compromise the accuracy of the fit to other portions of the response (Spencer et al., 2012).

The double-linear characterisation of the HHbMb response has been shown to provide a more accurate fit to the HHbMb response during ramp exercise when compared to the sigmoidal function. Similar to the sigmoid function, the double-linear function also suggests that the dynamic relationship between $\dot{V}O_{2m}$ and $\dot{Q}_m$ is exercise intensity dependent, where during

increasing exercise intensity, $\dot{Q}_m$ kinetics increase slower relative to $\dot{V}O_{2m}$ kinetics resulting in greater O_2 extraction and thus an increase in HHbMb. This is until HHbMb reaches a 'break-point' where $\dot{Q}_m$ and $\dot{V}O_{2m}$ increase at a similar rate and the HHbMb signal plateaus. This approach of characterising the muscle deoxygenation response focuses on the location of the breakpoint of the NIRS HHbMb response however, it remains to be elucidated whether these breakpoints in the NIRS response are mechanistically linked to physiological markers of exercise intensity (Boone et al., 2016). Furthermore, the double-linear function disregards the initial portion of the HHbMb response at the onset of the ramp exercise (i.e. it fits from the point of systematic increase in HHbMb). It is questionable whether the advantages of a better fit to a portion of the data justifies the removal of the NIRS HHbMb response at the start of the ramp (which represents transitions in metabolic activity) and is arguably the area in which most day to day activities are performed; and therefore, where insights into the dynamic balance between $\dot{V}O_{2m}$ and $\dot{Q}_m$ at exercise onset may be obtained.

More recently, Barroco et al. (2017) proposed a simplified method of characterising the muscle deoxygenation response to ramp exercise by NIRS, by comparing the slope of the HHbMb response in heart failure patients to aged match healthy controls. They showed that the slope of HHbMb was steeper in HF than healthy controls and that, towards peak exercise the HHbMb response increased in HF compared to a decreasing or flattening HHbMb in healthy controls. In addition, the slope of the HHbMb was significantly correlated to peak work rate in the HF group (i.e. a steeper slope was associated with a lower peak work rate). This simpler approach to characterising the HHbMb NIRS derived response may prove valuable in clinical settings, to quantify impairments in O_2 delivery in HF patients. The main limitation to this approach is that it disregards both the initial and final portion of the response. Therefore, as with the double linear function, disregarding portions of the response may mean important information regarding oxygen delivery and utilisation are essentially ignored.

Resolving the issue of accurately and fully quantifying the HHbMb response to ramp incremental exercise has mechanistic implications for understanding the control of O_2 delivery and utilisation. Furthermore, a simpler approach (i.e. one that does not require the need for complex mathematical sigmoidal functions) may aid the use of NIRS as an evaluative tool in a clinical setting.

The aims for this study were to: (i) use a simplified approach (by fitting the linear portion of the HHbMb response) to characterise the HHbMb NIRS derived response to ramp incremental exercise in HF patients; (ii) compare and determine which function (sigmoidal or double linear) fits the NIRS HHbMb data the best according to the Akaike Information Criterion in a small subset of patients and; (iii) determine if NIRS deoxygenated haemoglobin + myoglobin responses can be utilised to identify the locus of exercise intolerance in heart failure patients. Aim iii is briefly addressed in this chapter by considering the profile of the NIRS HHbMb responses but is primarily addressed in the case study presented at the end of this chapter, by exploring the HHbMb and TOI responses in one patient prior to and post cardiac resynchronisation therapy.

As NIRS measurements are indirect, there are some assumptions associated with this method (this will be discussed in more detail in the 'limitations' section of this chapter). Briefly, it was assumed that (i) the ΔHHbMb profile is a proxy for oxygen extraction in the tissue sampled by the NIRS probe, and; (ii) the relative contributions of haemoglobin and myoglobin to the deoxygenated ΔHHbMb signal is unknown, and that contributions from Mb do not affect the relationship between ΔHHbMb and $(a\text{-}v)O_2$. These assumptions are inherent with the indirect NIRS technique however, due to the non-invasiveness of the technique, it can be applied relatively easily in clinical settings. With these assumptions in mind, NIRS ΔHHbMb measurements can potentially provide unique non-invasive insights into control mechanisms governing the $\dot{V}O_{2m}$-$\dot{Q}_m$ relationship.

6.2 Methods

Experimental data collection, measurements, exercise protocol and data analysis are described in the general methods section under sub-heading "Protocol 2" for healthy participants, and "Protocol 5" for heart failure patients.

6.3 Results

$\dot{V}O_2$ responses

During incremental ramp exercise, $\dot{V}O_{2,peak}$ was higher in healthy controls than heart failure patients (53.5 ± 14.8 mL/kg/min vs 15.8 ± 4.0 mL/kg/min

respectively). This was associated with higher peak work rates in healthy controls than heart failure patients (314 ± 70 W vs 95 ± 31 W respectively).

NIRS responses

Three distinct skeletal muscle deoxygenation (normalised HHbMb) responses to ramp incremental exercise were identified. These response types were identified by visual inspection only (Figure 39,Figure 40 and Figure 41). Response 1 is a sigmoidal type response, where at exercise onset O_2 delivery is adequate to meet O_2 utilisation demands. This is demonstrated by a flat or shallow initial deoxygenation response. Following this initial stage, as exercise intensity begins to increase, muscle oxygen delivery lags muscle oxygen demand, demonstrated by an increase in the deoxygenation response. Towards peak exercise, oxygen delivery “catches up” to oxygen utilisation demand and the deoxygenation response begins to plateau. This pattern of response was identified in 18 out of 31 HF patients, and all healthy controls. Response 2 is characterised by a slowing exponential-like muscle deoxygenation response. At exercise onset there is an immediate increase in muscle deoxygenation, indicating that muscle oxygen delivery is not adequate to meet oxygen utilisation demands, necessitating an increased reliance on oxygen extraction. As exercise continues, oxygen delivery and oxygen demand gradually become better matched, and muscle deoxygenation starts to plateau. This pattern was identified in 5 out of 31 patients. Response 3 can be characterised by a ‘two-phase’ response. In this response, there is no slowing or plateauing of muscle deoxygenation at exercise onset or towards peak exercise. Instead muscle deoxygenation increases at exercise onset and continues to increase towards peak exercise. In patients manifesting this type of response, muscle oxygen delivery lags muscle oxygen demand throughout the exercise protocol, and towards peak exercise this oxygen delivery-oxygen utilisation mismatch becomes worse. This pattern was identified in 8 out of 31 patients.

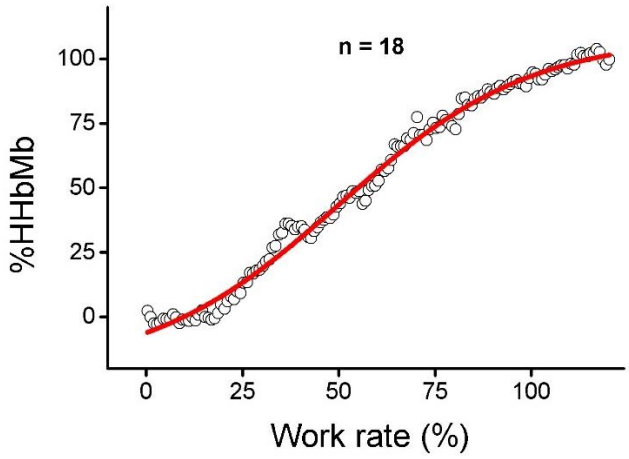

Figure 39: RESPONSE 1 (*n* = 18) Similar to healthy individuals: at exercise onset O_2 delivery is adequate to meet demands of O_2 utilisation. As exercise intensity increases O_2 delivery 'lags' behind O_2 utilisation, until HHbMb begins to plateau, indicating O_2 delivery and utilisation are better matched. Open squares show patient data, red line was produced using a sigmoid function although its main purpose is to aid the reader by highlighting the response profile.

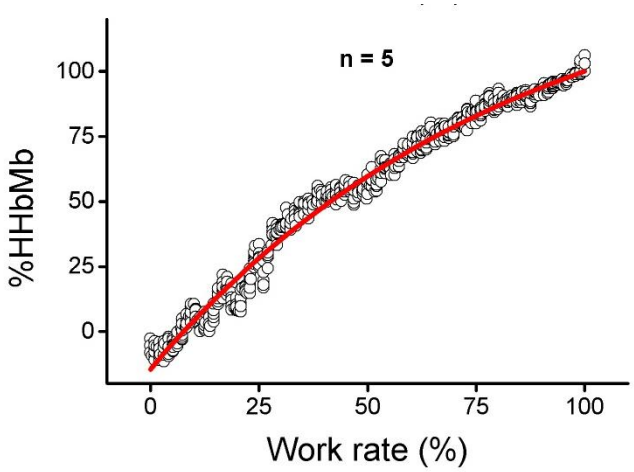

Figure 40: RESPONSE 2 (*n* = 5) At exercise onset, an instantaneous rise in HHbMb, indicating O_2 delivery is inadequate to meet demands of O_2 utilisation. As exercise intensity increases, O_2 delivery 'catches up' and the HHbMb response begins to plateau, indicating improved matching of O_2 delivery to O_2 utilisation. Open circles show patient data, red line was produced with an exponential function to illustrate the response pattern and aid the reader.

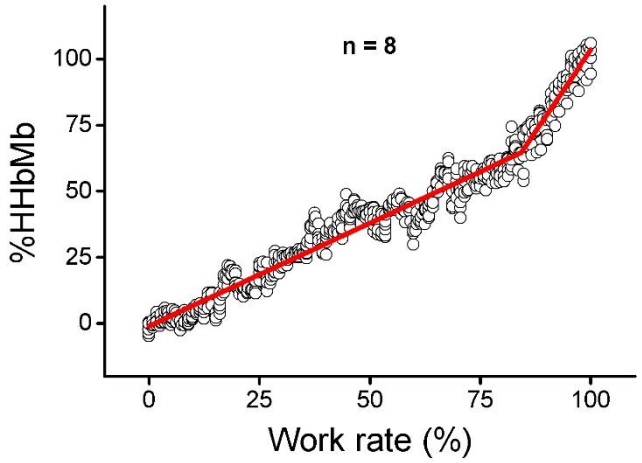

Figure 41: RESPONSE 3 (*n* = 8) Two phases, with no plateau or slowing of HHbMb at exercise onset or towards peak exercise, highlighting an immediate O_2 delivery limitation, which is exacerbated as exercise intensity increases in these patients, indicating a progressive O_2 delivery O_2 utilisation mismatch. Open circles show patient HHbMb data, the red line was produced using a double-linear function and is there to aid the reader by highlighting the response pattern.

Table 22 shows key parameters identified from the NIRS muscle deoxygenation responses during ramp exercise. Average $\dot{V}O_{2,peak}$ was highest in response 2 (14.69 mL/kg/min), as was the slope of the deoxygenation response (1.83 %W). The lowest mean $\dot{V}O_{2,peak}$ was in response 1 (14.69 mL/kg/min), but had the largest percentage change in muscle deoxygenation (23.88 %). Peak work rate was similar across each response (range 97-77 W). Response 3 had the lowest average deoxygenation slope (1.41 %W), but the highest average break point in muscle deoxygenation (point B; 82 W). Time to limit of tolerance was 654 s for response 1, 555 s for response 2, and 597 s for response 3.

Table 22: Key parameters derived from the NIRS deoxygenation response, separated by response profile in HF patients

	Response 1	Response 2	Response 3
Point "A" (W)	23.76	18.00	23.38
Point "B" (W)	75.65	68.00	82.13
Point "C" (W)	96.59	99.00	98.63
deoxy-HbMb slope (%W)	1.65	1.83	1.41
delta deoxy-HbMb (%)	23.88	18.20	22.13
$\dot{V}O_{2,peak}$ (mL/kg/min)	14.69	18.53	15.03

6.3.1 Characterising the data using a simplified approach

Figure 42 shows the NIRS HHbMb response in a representative healthy control (top panel) and heart failure patient (bottom panel). Points A, B and C all occurred at lower work rates in heart failure patients than healthy controls. The mid-exercise HHbMb slope on average was steeper in heart failure than controls, and the HHbMb difference between points B and C was greater in heart failure than controls. These values are summarised below in Table 23.

Table 23: Key variables of the NIRS HHbMb response in healthy controls and heart failure patients.

Variables	Healthy (n = 10)	Heart failure (n = 31)
Point "A" (W)	37 ± 10	23 ± 8
Point "B" (W)	243 ± 56	75 ± 22
Point "C" (W)	314 ± 75	97 ± 31
HHbMb slope (%W)	0.56 ± 0	1.7 ± 1
delta HHbMb (%)	3 ± 16	23 ± 11

Table parameters: Point A, work rate at initial increase in HHbMb; point B, point as which HHbMb deviates from linearity; Point C, peak work rate; HHbMb slope, the linear portion of the muscle deoxygenation response; delta HHbMb, overall change in the muscle deoxygenation response from exercise onset until peak exercise. Data are reported as means ± SD.

Steeper HHbMb- work rate slopes were significantly associated with lower peak work rates (r^2 = -0.8, $p < 0.05$), and a lower $\dot{V}O_{2,peak}$ (r^2 = -0.7, $p < 0.05$) in patients (Figure 43).

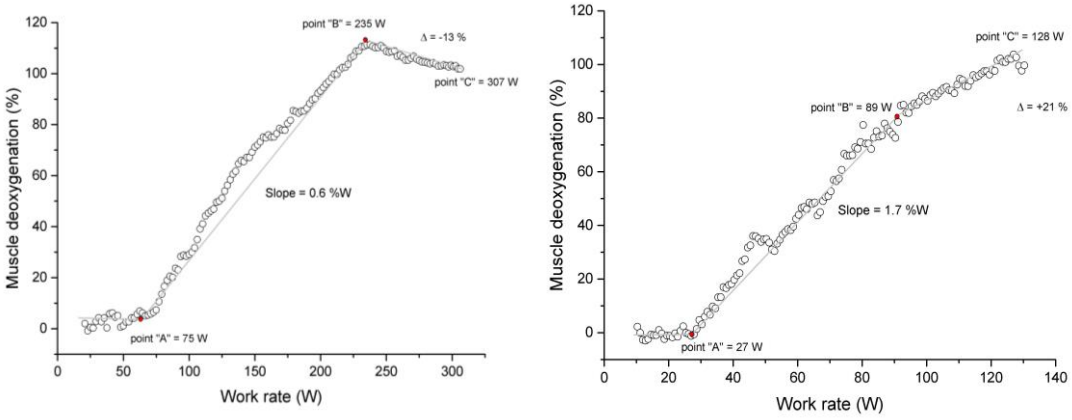

Figure 42: Normalised deoxygenated haemoglobin-myoglobin (ΔHHbMb %) response to ramp incremental exercise plotted as a function of increasing work rate (W) exercise in a representative healthy control (left) and heart failure patient (right). Point A corresponds to the point at which ΔHHbMb begins to systematically increase. Point B represents ΔHHbMb departure from linearity and point C corresponds to peak work rate. Note that data was normalised to the final HHbMb value (not the peak value) in order to maintain the profile of the response. Because of this, in some subjects (where the final HHbMb value was lower than the peak HHbMb value) normalised HHbMb exceeded 100%.

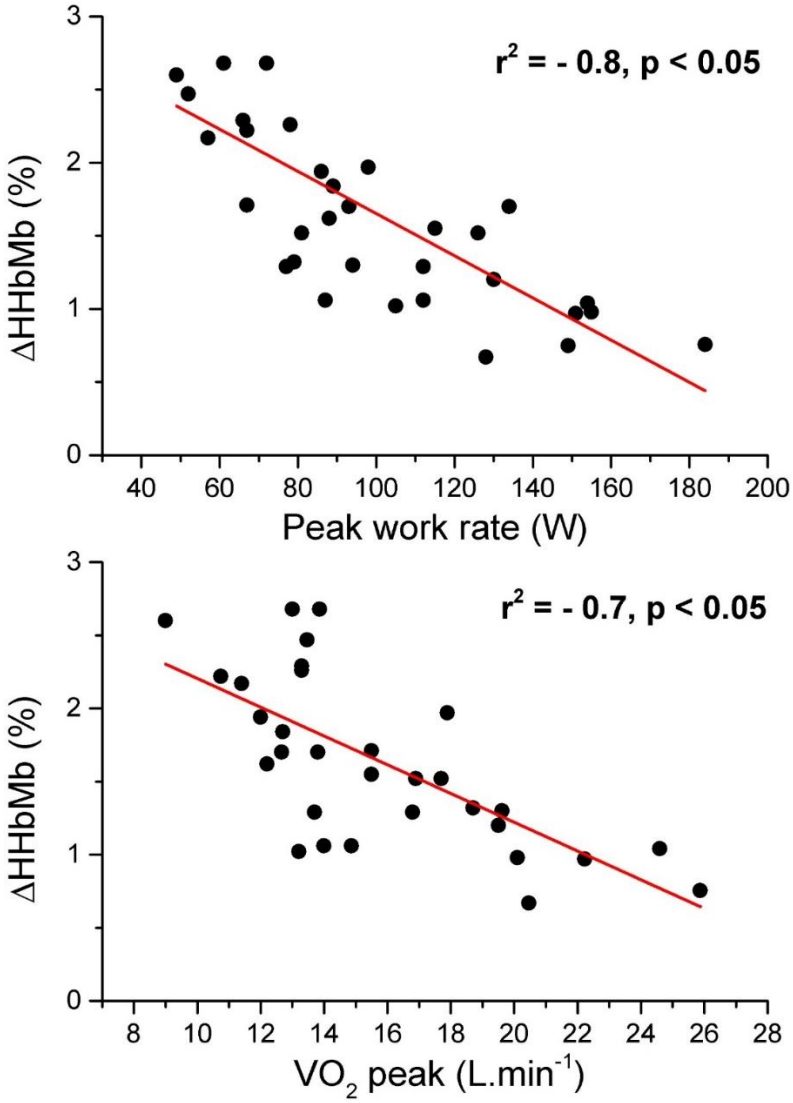

Figure 43: Correlation between ΔHHbMb-work rate slope and peak work rate (top), and $\dot{V}O_2$ peak (bottom) in patients.

6.3.2 Comparing sigmoid and double linear functions

For a small subset of patients, NIRS HHbMb responses were fit with both a sigmoidal and a double linear function and these fits were then compared. Individual and mean patient responses from the ramp incremental exercise test for these patients (n=8) are summarised in Table 24. In these patients, peak work rate was (mean ± SD) 106 ± 35 W, which yielded a $\dot{V}O_{2,peak}$ of 18.84 ± 5.65 mL/kg/min. Peak work rate was positively correlated with absolute $\dot{V}O_{2,peak}$ (r^2 = 0.89, p < 0.05), normalised $\dot{V}O_{2,peak}$ (r^2 = 0.86, p < 0.05) and HR rise (r^2 = 0.77, p < 0.05). However, there was no significant correlation between HR rise [a potential index of an increase in cardiac output; (Davies *et al.*, 1972)] and $\dot{V}O_{2,peak}$ when expressed as an absolute

value (L/min^{-1}; r^2 = 0.4, p > 0.05) or normalised to body mass (mL/min/kg; r^2 = 0.46, p > 0.05). Furthermore, there was no significant correlation between $\dot{V}O_{2,peak}$ and the amplitude of the NIRS ΔHHbMb response (r^2 = -0.46, p > 0.05 and r^2 = -0.47, p > 0.05 for absolute and normalised $\dot{V}O_{2,peak}$ values, respectively).

There was no significant correlation between the peak work rate and slope 1 (double linear function), but there was a significant correlation between work rate peak and slope 2 (r^2 = -0.56, p > 0.05 and r^2 = -0.76, p < 0.05 respectively). Similarly, for absolute $\dot{V}O_{2,peak}$ (L/min), there was no significant correlation between slope 1, but there was a significant correlation between slope 2 and $\dot{V}O_{2,peak}$ (r^2 = -0.55, p > 0.05 and r^2 = -0.88, p < 0.05 respectively).

Table 24: Individual subject parameters from the ramp incremental exercise test

Subject	Peak WR (watts)	HR Rise (bpm)	$\dot{V}O_{2,peak}$ (L/min)	$\dot{V}O_{2,peak}$ (mL/min/kg)
1	136.00	135.00	1.79	20.46
2	51.00	49.00	0.93	13.46
3	98.00	95.00	1.59	17.89
4	106.00	102.00	1.53	19.62
5	93.00	88.00	1.20	12.66
6	154.00	148.00	1.82	24.59
7	74.00	33.00	1.02	13.60
8	139.00	67.00	2.37	28.42
Mean	106.00	90.00	1.53	18.84
SD	35.00	40.00	0.48	5.65

Figure 44 shows the second-by-second response of the change in deoxygenated haemoglobin and myoglobin (ΔHHbMb), oxygenated haemoglobin and myoglobin (Δ$HbMbO_2$), and total haemoglobin and myoglobin (ΔHb_{total}), and tissue oxygenation index (TOI%) from the onset of the ramp incremental exercise to the end of the ramp exercise in a representative subject. The sigmoidal and the double-linear function fits to deoxygenated haemoglobin and myoglobin for this representative subject are shown in Figure 45. This patient displayed a muscle deoxygenation profile of response 1 where HHbMb shows a brief period of relatively unchanging HHbMb, followed by progressive increase in the HHbMb signal, until, towards peak exercise, the slope of the HHbMb signal becomes

shallower, (although there is no pronounced plateau region in this patient). Out of the subset HF group (n = 8) 4 patients displayed this response profile (response 1), 2 patients showed slowing exponential-like responses (response 2), and the remaining 2 patients showed an immediate linear increase in HHbMb at the onset of the ramp until around 75% of peak work rate, where there was an upward inflection of HHbMb (response 3). This pattern was also preserved in the oxygenated haemoglobin profile, although appears to be more affected by changes in the $\Delta HbMb_{total}$ signal (see Figure 44). For example, in this representative subject, mid-way through the exercise there is a distinct sharp spike in $\Delta HbMb_{total}$ which is associated with reciprocal changes in the oxygenated haemoglobin profile but is much less pronounced in the HHbMb response.

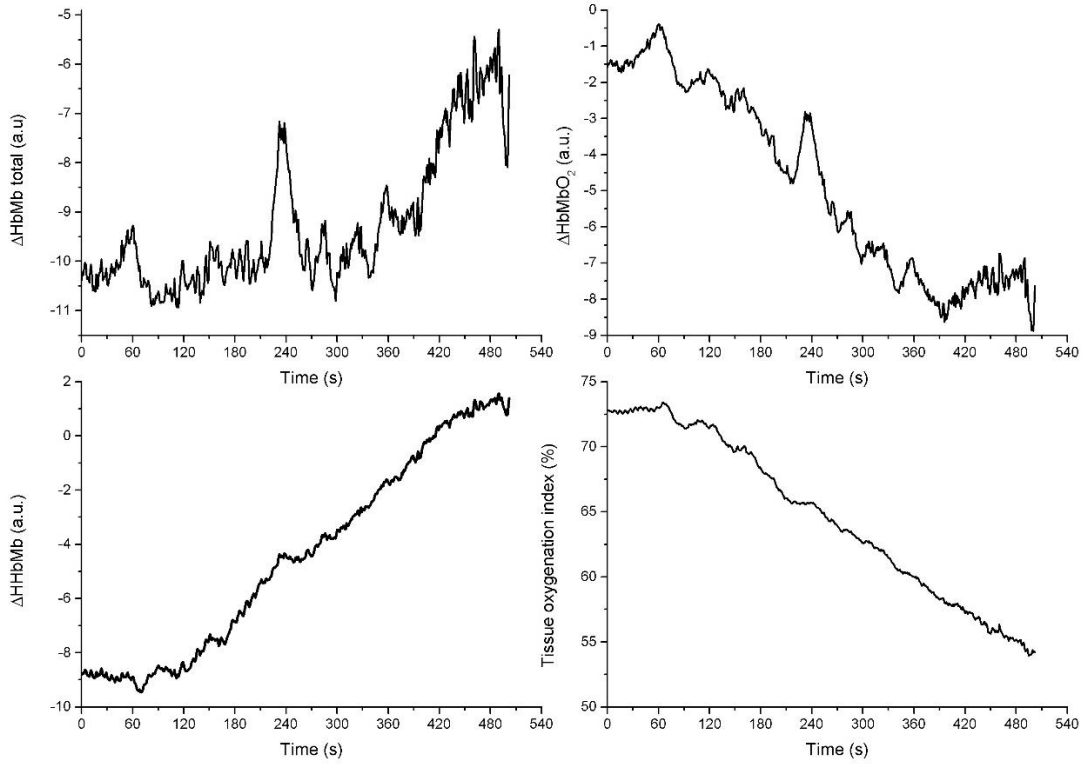

Figure 44: Second-by-second responses of total haemoglobin and myoglobin (top left); oxygenated haemoglobin and myoglobin (top right); deoxygenated haemoglobin and myoglobin (bottom left) and tissue oxygenation index (bottom right) during ramp incremental cycling in a representative subject.

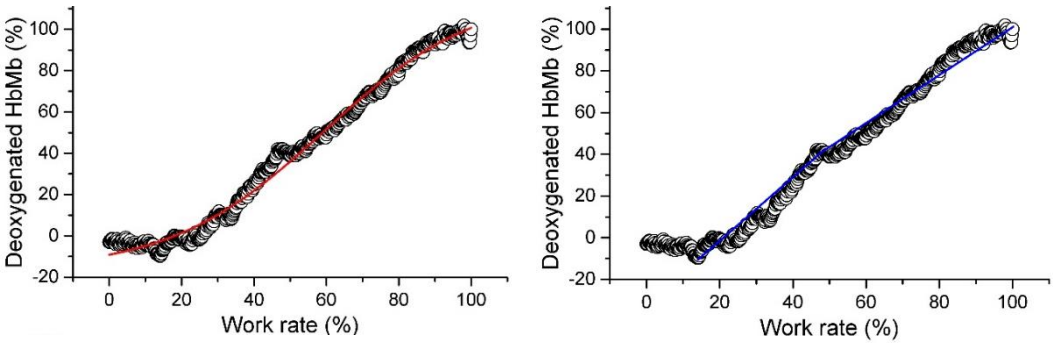

Figure 45: Sigmoidal fit (left) and double linear fit (right) of the deoxygenated haemoglobin and myoglobin response plotted as a function of normalised work rate in a representative subject.

For the 8 patients, individual deoxygenated haemoglobin and myoglobin data was plotted as a function of normalised and absolute work rate and fit with both the sigmoidal and the double-linear functions. Group mean parameter estimates for both fitted functions are shown in

Table **25**. The breakpoint in the double-linear function occurred at 67 ± 24 W (absolute WR), and 57 ± 13 % (normalised WR). For the double linear function, in 6 out of 8 subjects, slope 1 was steeper than slope 2 (1.76 ± 0.7 vs 1.14 ± 0.5 respectively; absolute WR) and (1.54 ± 0.5 vs 0.96 ± 0.3 respectively; normalised WR), indicating a slowing of the muscle deoxygenation response towards peak exercise. Conversely, in 2 out of 8 patients the slope 1 of the double-linear function was shallower than slope 2 (0.62 ± 0.1 vs 1.90 ± 0.8 respectively; absolute WR) and (0.53 ± 0.2 vs 1.13 ± 0.8 respectively; normalised WR), indicating a speeding of muscle deoxygenation towards the end of exercise. Furthermore, in the patients displaying a markedly sharp increase in the ΔHHbMb towards the end of exercise (response 3) a robust fit of the sigmoid function was not possible. As such, these subjects were excluded from the sigmoidal model fitting averages. None of the patients displayed a distinct plateau towards the end of the ramp exercise, as is seen in healthy subjects (Ferreira et al., 2007). The c/d point (representing the x value at 50% of the total amplitude) was 51.8 ± 19 W (absolute WR) and 44.3 ± 12 % (normalised WR).

Table 25: Group mean parameter estimates for the sigmoid and double-linear model of the deoxygenated haemoglobin and myoglobin response profile (for all response types) plotted as a function of absolute work rate and normalised work rate.

Sigmoid	y_0	A	d	xc	c
Absolute WR	-7.69	128.21	0.08	64.8	3.63
Normalised WR	-7.69	128.2	0.07	53.22	2.89

Double-linear	BP (W)	b_1	m_1	b_2	m_2
Absolute WR	67.64	-28.66	1.48	-26.33	1.33
Normalised WR	57.08	-13.89	1.29	-0.66	1.01

Sigmoid model parameters: y_0, baseline; A, amplitude; c is a constant dependant on d, the slope of the sigmoid, where c/d gives the x value corresponding to 50% of the total amplitude. Double linear parameters: BP, break point; b_1, slope 1; m_1, intercept 1; b_2, slope 2, m_2 intercept 2.

Individual ΔAIC_C values for normalised ΔHHbMb are shown in Table 26. When plotted as a function of absolute work rate or normalised work rate, the double-linear model provided the best characterisation of the underlying HHbMb response in all subjects, indicated by a positive ΔAIC_C score. 100% of data points were considered for the sigmoid function, whereas a mean of 90% (range 81 – 100 % amongst subjects) of data points were considered for the double-linear function (for both absolute work rate and normalised work rate). Based on a positive ΔAIC_C score, the results suggest that a double-linear function provides the best model fit of the ΔHHbMb response to ramp incremental exercise in heart failure patients, compared to the sigmoid function.

Table 26: Individual ΔAIC_C values derived from comparisons between the double linear and sigmoid functions for normalised muscle deoxygenation (%ΔHHbMb) plotted as a function of absolute and normalised WR. Positive scores favour the double-linear function.

	ΔAIC_C values for %ΔHHbMb	
Subject	**Absolute WR**	**Normalised WR**
1	328.77	334.73
2	315.07	315.08
3	1221.68	1110.16
4	878.06	878.05
5	805.94	804.99
6	198.75	198.75
7	1519.43	606.24
8	1043.99	1043.99

6.4 Discussion

NIRS responses

Three distinct responses from the NIRS deoxygenated haemoglobin and myoglobin signal were identified. Response 1 followed a sigmoidal-*like* response, which was demonstrated in 58% of HF patients. It is important to note that, although oxygen extraction slowed towards peak exercise, no patients showed a distinct plateau, similar to the response observed in healthy individuals (Figure 46). Overall, patients with response 1 had the lowest mean $\dot{V}O_{2,peak}$ but the highest mean oxygen extraction. This is interesting to consider as, throughout this thesis, a higher oxygen extraction has been associated with a lower oxygen delivery. However, it is the *profile* of the oxygen extraction (rather than the overall amount) that may be the bigger determinant of exercise tolerance. For example, if a high amount of O_2 is extracted in a very short space of time, this may drain the muscle of oxygen which, in turn, would transiently lower the microvascular partial pressure and inhibit O_2 flux. However, if the oxygen is extracted in a stable but consistent manner over a prolonged period of time, O_2 doesn't become limiting (providing adequate O_2 delivery is maintained), O_2 flux is maintained, and exercise can be sustained for longer so that over the period of exercise, a larger amount of oxygen can be extracted and a higher $\dot{V}O_2$ achieved. Previous findings in healthy subjects have shown that a higher $\dot{V}O_{2,peak}$ has been associated with higher oxygen extraction (Boone et al., 2009). However, in HF patients displaying this response, the (mean) higher oxygen extraction was not associated with the (mean) highest $\dot{V}O_2$. Furthermore, the highest (mean) $\dot{V}O_2$ was in patients who displayed response 2, which had the lowest overall O_2 extraction. On average though, patients with response 1 were able to exercise for longer than in those with responses 2 (654 vs 555 s respectively). These findings are somewhat conflicting, as both $\dot{V}O_{2,peak}$ and time to limit of tolerance are markers of exercise capacity, so it is logical to expect that the group who exercised longer would achieve a higher $\dot{V}O_{2,peak}$. However, this is not the case in the data presented in this chapter. From the data presented in this study, response 1 cannot provide any specific insights into the delivery vs utilisation limitation debate further than a sigmoidal response is typically seen in healthy individuals.

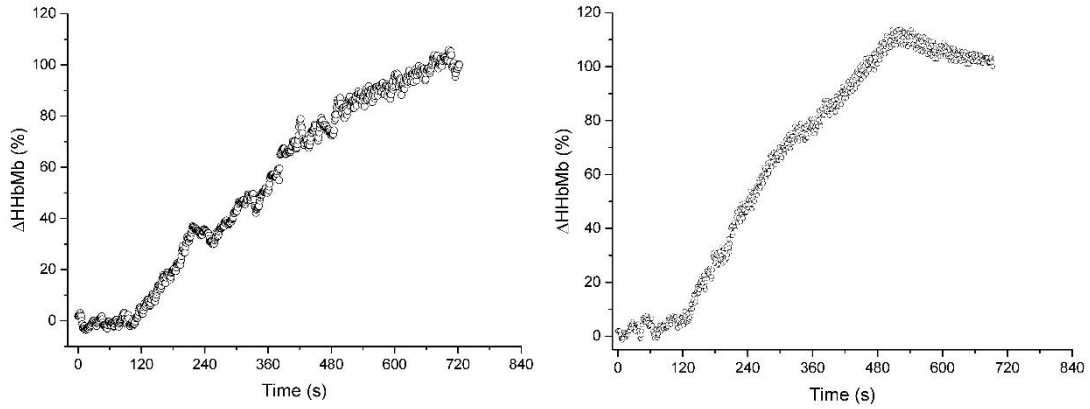

Figure 46: Response 1 in a representative HF patient (left) and healthy control (right). In HF patients displaying a sigmoidal-like response (response 1) deoxygenated haemoglobin and myoglobin (ΔHHbMb %) did not show a distinct plateau in like that seen in healthy subjects, where ΔHHbMb % either plateaued or decreased slightly towards peak exercise.

Response 2 followed a similar profile as response 1, with the exception that at the onset of exercise, HHbMb increased immediately (i.e. there was no flat or shallow HHbMb seen at exercise onset). This indicates that in these patients at the onset of exercise, there is an immediate increase in oxygen demand, that cannot be met with oxygen supply, causing an increased reliance on oxygen extraction. However, as exercise intensity increases, this mismatch between oxygen supply and demand decreases, and oxygen extraction follows a similar profile to response 1 until the end of exercise. In patients displaying this response, mean $\dot{V}O_{2,peak}$ was higher than in the other two groups (i.e response 1 and 3), and % change in oxygen extraction was the lowest overall. Despite this, total ramp time was the shortest in this group [555 s vs 654 s (response 1) and 592 s (response 3)]. This may be because oxygen was depleted at a *faster* rate over a shorter period (represented by a steeper HHbMb slope) earlier on in exercise in those with response 2, thereby causing a greater reliance on anaerobic energy sources. A greater reliance on anaerobic energy sources contributes to an increased fatigue and therefore, earlier exercise termination. From the data presented in this study, the information gained from response 2 is that these patients are limited by oxygen delivery at exercise onset (i.e. they have a slow initial response) but are able to meet O_2 delivery demands during exercise.

Response 3 was characterised by an immediate increase in HHbMb at exercise onset (as with response 2), and an increasing HHbMb towards

peak exercise (instead of a decreasing increase in HHbMb towards peak exercise seen in responses 1 and 2). This indicates a progressive and increasing reliance on oxygen extraction in these patients. The mean $\dot{V}O_{2,peak}$ in patients displaying response 3 was lower than those displaying response 2, but slightly higher than those with response 1. In addition, the % change in HHbMb was higher than response 2, and slightly lower than response 1. The response seen in these patients indicates that throughout the whole of the ramp exercise, oxygen delivery is lagging oxygen demand (due to the continuously increase HHbMb). Furthermore, in some patients this worsened towards peak exercise. Given this, it might be reasonable to expect these patients to have the lowest exercise capacity. However, patients in this group exercised on average for 43 seconds longer than those displaying response 2 (but 62 s less than response 1 group). These findings highlight the importance of considering the *profile* of the oxygen extraction (i.e. the steep at which oxygen is extracted) as well as the total amount of oxygen being extracted. The key information gained from response 3 is that patients with this response are primarily O_2 delivery limited at exercise onset and throughout exercise.

One possible reason for the inconsistency in the data could simply be a result of having different representative group sizes for each response. Especially considering that when the data was evaluated as a whole (i.e. not spilt into respective responses) there was a strong correlation found between these factors mentioned above (see next section below). However, more patients displaying responses 2 and 3 are needed to evaluate these responses reliably, and as separate entities. This part of this studies shows an alternative approach to characterising the NIRS HHbMb data as opposed to just fitting the data with a statistical function, as in previous studies. Although on its own it cannot provide definite conclusions regarding O_2 delivery vs O_2 utilisation limitations, it may represent a useful additional tool in characterising the overall response type and deciding what function is more suitable to use when characterising the data.

Simplified fit

Heart failure vs healthy controls

A simplified method of characterising the NIRS HHbMb data was applied to all heart failure patients and healthy controls, regardless of the profile of the response. Overall, heart failure patients demonstrated steeper deoxygenation-work rate slopes in addition to increasing (instead of stable or

decreasing) deoxygenation towards peak exercise. This finding is consistent with, and therefore, supports, the notion that impaired skeletal muscle perfusion causes $\dot{V}O_{2m}/\dot{Q}_m$ mis-match and a greater reliance on oxygen extraction during steady state exercise transitions (Sperandio et al., 2009; Bowen et al., 2012) and incremental exercise (Wilson et al., 1989; Barroco et al., 2017) in heart failure patients.

Healthy controls displayed a non-linear (sigmoidal) response to ramp exercise, consistent with previous studies investigating muscle deoxygenation dynamics during ramp exercise in healthy individuals, which is indicative of a non-linear $\dot{V}O_{2m}/\dot{Q}_m$ relationship (Ferreira et al., 2007; Boone et al., 2009, 2012; DiMenna et al., 2010; Spencer et al., 2012; Barroco et al., 2017). There have been several mechanisms proposed for the s-shaped (i.e. non-linear $\dot{V}O_{2m}$-$\dot{Q}_m$ relationship) muscle deoxygenation (ΔHHbMb) response to ramp exercise in health. The initial unchanging or relatively flat response in ΔHHbMb at the start of the ramp (phase 1) has been attributed to the mechanical effects of muscle contraction at exercise onset (i.e. muscle pump and rapid vasodilation), that contribute to rapid $\dot{Q}_m$ kinetics during light exercise, and which become progressively less important during higher work rates. In addition, parasympathetic withdrawal in the early stages of the ramp exercise results in an increase in cardiac output, which progressively slows as work rate increases (Stringer et al., 2005; Ferreira et al., 2007). Following this initial slow response, ΔHHbMb increases more steeply (phase 2), indicating that fractional O_2 extraction is greater than the increase in $\dot{Q}_m$ during higher work rates. This may be related to changes in the parasympathetic-sympathetic balance (Ferreira et al., 2007), as well as muscle fibre type and recruitment. Muscle comprised of slow twitch fibres [which are preferentially recruited at the start of ramp incremental exercise (Koga et al., 2014)] demonstrate faster adjustments of $\dot{Q}_m$ relative to $\dot{V}O_{2m}$, and better $\dot{V}O_{2m}$ to $\dot{Q}_m$ coupling when compared to fast twitch fibres [which are recruited later during the ramp (Jones et al., 2004)] (Behnke et al., 2003; McDonough et al., 2005). Ramp exercise is characterised by a shift from predominantly slow twitch fibres, to an increase in fast-twitch muscle fibre recruitment (Jones et al., 2004; Koga et al., 2014). As such, this may partially explain the slowing of $\dot{Q}_m$ towards peak exercise (Ferreira et al., 2007; Boone et al., 2010). Additionally, Stringer et al. (2005) reported a non-linear increase in cardiac output during ramp exercise (i.e. a less pronounced increase in cardiac output at higher work rates). A non-linear cardiac output response may also contribute to the non-linear $\dot{V}O_{2m}$-

$\dot{Q}_m$ relationship at the microvascular level. The plateau in ΔHHbMb towards the end of the ramp (phase 3) indicates a matching between the rate of increase in $\dot{Q}_m$ relative to $\dot{V}O_{2m}$. It has been argued that the plateau indicates that fractional extraction has reached it upper limit (Boone et al., 2016). In this context, in heart failure patients, steeper deoxygenation slopes were interpreted as an increased reliance on O_2 extraction due to slower $\dot{Q}_m$ relative to $\dot{V}O_{2m}$ (i.e. impaired $\dot{Q}_m$), which gets progressively worse towards peak exercise, as indicated by an increasing (instead of stable or decreasing) ΔHHbMb slope. Although this simplified method of characterising the muscle deoxygenation response excludes the initial and final portions of the ramp, evaluating the slope of the ramp can provide useful information. This is because a steeper ΔHHbMb-work rate slope was associated with a lower peak work rate and a lower $\dot{V}O_{2,peak}$ in heart failure patients. This may be related to an increased reliance on oxygen extraction due to insufficient oxygen delivery, and/or greater recruitment of type II fibres, which are less oxidative and fatigue faster. In addition, by excluding the initial and latter stages, the slope of the deoxygenation response obtained is not influenced by the quality of the function fit to the rest of the data. For example, by measuring the slope of the deoxygenation response with a sigmoidal and/or double linear function, the fit to the linear portion of the response will be adjusted in order to get the best overall fit to the whole response (sigmoidal) or the middle and end portion (double-linear). Another advantage of using this simplified method is that it is avoids the need for applying complex functions, making it more accessible in clinical settings where access to, and knowledge of, statistical programs may be limited.

Sigmoid function vs double linear function

For sigmoid and double linear functions (in a sub-set of 8 patients) individual normalised muscle deoxygenation (%ΔHHbMb) responses were fitted with either a sigmoid function (which considers the overall response) or a piecewise double-linear function (which considers the predominant increase in ΔHHb and the following plateau region). Based on a positive ΔAIC score, the double-linear function provided the best characterisation the %ΔHHbMb response to ramp incremental exercise in all patients, relative to the sigmoid function. However, the AIC_c score is limited in that it is relative (i.e. it only compares one model fit to another), so although it demonstrates that the double-linear fit was better than the sigmoidal fit, it doesn't give any

information regarding the physiological implications of this. Furthermore, it does not give information regarding the quality of the fit overall. For example both could be extremely poor fits but the AICc score would still provide an assessment of which of the two poor fits is the better out of the two.

Physiological implications of the double-linear function: It is important to note that the %ΔHHbMb response profile in all of the HF patients did *not* display a discernible plateau region as seen in healthy individuals (Spencer et al., 2012), and in some patients the response became steeper at the end of the ramp incremental test. As the double-linear function is based on characterising (i) the slope of the HHbMb response and (ii) the *plateau* towards peak exercise, it is questionable whether the model, despite proving an overall better characterisation of the muscle deoxygenation response when compared to a sigmoidal function, has any physiological meaning. Nonetheless, in all patients there was a discernible breakpoint when fitting the double-linear function, indicating a relative change in the $\dot{V}O_{2m}/\dot{Q}_m$ relationship. The break point in the HHbMb response, where the HHbMb response levels off, indicates a change in the $\dot{V}O_{2m}/\dot{Q}_m$ relationship and possibly that microvascular O_2 extraction has reached some upper limit (Boone et al., 2015). The underlying mechanisms for this breakpoint, however, are yet to be elucidated, but have been related to the critical power, maximum lactate steady state, and respiratory compensation point (Bellotti et al., 2013; Murias et al., 2013; Racinais et al., 2014; Keir et al., 2015). This is based on the assumptions that (i) the critical power and the maximum lactate steady state demarcate the highest work rate that can be sustained for long periods of time and (ii) that the breakpoint in HHbMb may represent some upper limit of oxygen extraction. Therefore, these thresholds and the breakpoint in HHbMb may be related due to similar underlying physiology such that, they both reflect a common level of aerobic metabolism beyond which there is a progressive loss of homeostasis (Keir et al., 2015). In healthy individuals the break point in the HHbMb signal occurs between 75-90% of $\dot{V}O_{2,max}$ (Boone et al., 2016); however, the breakpoint in the HF data occurred much lower (~60% of normalised work rate, which corresponded to a range of ~35-85% $\dot{V}O_{2,peak}$). Whether this is a true reflection of the underlying physiology or is simply caused by limitations in the fitting of the double-linear function is difficult to ascertain. Furthermore, the double-linear function is fit from the point of a systematic increase in ΔHHbMb above baseline, observed during the middle portion of exercise onwards. This fit, however, excludes the initial phase 1 portion of the

ΔHHbMb response, meaning information regarding the balance between O_2 delivery and O_2 utilisation at the onset of exercise (possibly the intensity at which most activities of daily living are performed) is ignored (Boone et al., 2016). This is a possible limitation of using this function to characterise muscle deoxygenation. Therefore, although the double linear function provided a superior fit to the data, according to the AIC_C score, it is important to consider whether the function is accurately describing the underlying physiological response Furthermore, it also important to consider whether a better fit that characterises a portion of the response is more desirable than a slightly worse fit that characterise the whole response.

Physiological implications of the sigmoid function: The sigmoidal model indicates that, at very low work rates, $\dot{Q}_m$ kinetics are faster than $\dot{V}O_{2m}$ kinetics (that is, O_2 is delivered to the muscle faster than it is utilised), resulting in a slower increase in fractional O_2 extraction. Potential mechanisms for this response have been described above.

In the heart failure patients, none displayed a pronounced plateau, and in some patients the muscle deoxygenation actually increased towards end-exercise. This lack of a plateau in ΔHHbMb may have contributed to the less superior sigmoidal function fit (according to the $AIC_{C\ score}$); and may be indicative of a muscle blood flow limitation (i.e. when the ΔHHbMb response profile is flat, $\dot{V}O_{2m}$ and $\dot{Q}_m$ are well matched; however, an increasing ΔHHbMb indicates that the increase in fractional O_2 extraction is greater relative to the increase in $\dot{Q}_m$ and therefore, that O_2 delivery is not sufficient to meet the demands of O_2 utilisation at that moment). This is especially evident in those patients in whom the slope of the ΔHHbMb response became steeper following the breakpoint in indicating that fractional O_2 extraction is greater than the increase in ΔHHbMb, suggesting that these patients are still heavily reliant on O_2 extraction as exercise progresses towards peak exercise. This is unlike in healthy subjects (Spencer et al., 2012), where most patients displayed a plateau, indicating that $\dot{V}O_{2m}$ and $\dot{Q}_m$ are well coupled (Spencer et al., 2012). Furthermore, the sigmoid function, in most cases, underestimated the reliance on O_2 extraction in later exercise in this study. So, despite ΔHHbMb being normalised, the projected baseline and peak values either fell short (i.e. below 0%; in one subject the baseline value was consistently under -50% regardless of being expressed as a function of absolute work rate, or normalised work rate) or exceeded the 100% peak value, which may result in the sigmoid function being unable to accurately identify baseline and end-exercise values.

Ferreira et al., (2007) proposed that the sigmoidal function could be used as a tool to detect changes in the $\dot{V}O_{2m}/\dot{Q}_m$ relationship due to changes in microvascular function (i.e. a slow cardiac response necessitates a higher reliance on O_2 extraction, causing the slope of the ΔHHbMb response to be steeper, and to increase at an earlier stage in exercise) and thus, predicted that disease-related changes in microvascular function may shift the sigmoid to the left, whereas exercise training and interventions to improve vascular function might shift the sigmoid to the right. Boone et al. (2009) demonstrated the latter by comparing the ΔHHb responses to cycle exercise in trained cyclists and physically active students and found a rightward shifting of the sigmoid in the trained group, suggesting that aerobic fitness status affects the $\dot{V}O_{2m}/\dot{Q}_m$ relationship. In an effort to mimic disease related changes in microvascular function, DiMenna et al. (2010) investigated the influence of supine cycle ergometer exercise in comparison to upright cycle ergometer exercise on the ΔHHbMb response profile. The authors found that the slope of the ΔHHbMb profile was steeper during supine cycling when compared to upright cycling, consistent with the notion that the reduced muscle perfusion (due to the supine position) necessitates a higher fractional O_2 extraction (Ferreira et al., 2007). However, the c/d point of the sigmoid (at which 50% of the total amplitude was reached) was not significantly altered [unlike in Boone et al. (2009)], suggesting that there was no leftward shifting of the sigmoid. This, however, could be a reflection of how much the supine position actually mimics disease related changes in microvascular function. In the present study, the c/d point occurred at a lower absolute work rate in heart failure patients than controls (52 W vs 136 W respectively) however, when work rate was normalised the c/d point was only 1% different between heart failure patients and healthy controls (44% vs 45% respectively), suggesting no leftward shift of the sigmoid in heart failure patients compared to young healthy controls in this study.

6.5 Summary

The double-linear function provided a better fit to the data compared to the sigmoid function according to the AIC_c score. Fitting the data with a double linear function provides us with a breakpoint, indicating a change in the $\dot{V}O_{2m}/\dot{Q}_m$ relationship however, it is not clear if the breakpoint is physiologically significant, nor if it gives us useful information on what is

happening at the muscle during exercise. The double linear function also gives two slopes (slope 1 representing the linear portion of the response and slope 2 representing the plateau towards peak exercise), however the accuracy of these slopes may be compromised, by the function trying to get the best fit to *both* parts of the response. Slope 2 of the response is supposed to represent a plateau in muscle deoxygenation, although there were no distinct plateaus in HF patients seen in this study. Therefore, it is possible that this compromised the accuracy of the fit and as such, may have had an influence on the results. This may explain why there was no significant correlation between peak work rate and peak $\dot{V}O_2$ with slope 1 (i.e. the linear portion of the response) with the double linear function.

The sigmoid function characterises the whole of the muscle deoxygenation response, unlike the double linear function and simplified linear fit. This is advantageous in that information can be obtained regarding all stages of exercise. On the other hand, this may be partly why it provided a less superior fit to the data when compared to double linear function. Furthermore, in heart failure the responses were variable, and (unlike in healthy subjects) did not display a discernible plateau either at the beginning and/or at the end of exercise. Although the sigmoid function seems to describe the data well in health, the variable responses in heart failure patients may mean that the sigmoidal function does not always fit well to the data in HF, and therefore, the resultant information gained from this fit may not be accurate. For example, the c/d point (which is unique information that cannot be gained from the double linear of simplified linear functions), was not different between heart failure patients and healthy controls when muscle deoxygenation was plotted as a function of normalised work rate.

Separating the NIRS derived deoxygenation into distinct responses may be useful to identify patients who are O_2 delivery limited. However, more data is needed to reliably quantify the separate responses and their corresponding physiological meaning.

The simplified linear fitting approach provides information on the slope of the response. Unlike the double linear function, the fitting of the linear regression is not dependent on any other portions of the response (as these are disregarded), meaning that the slope of the response is more likely to be a reliable representation of muscle deoxygenation. This may explain why the slope of the response using this approach was significantly correlated to peak work rate and peak $\dot{V}O_2$. In addition, using this method means there is

no need for complex functions. The major disadvantages of the simplified fit are that it disregards the initial and final portions of response of the muscle deoxygenation response, which are arguably, the most important areas of the test. Nevertheless, this simplified linear function provides important and useful information that is related to exercise tolerance. Given this, along with its ease of use and understanding may be the most useful tool to evaluate muscle deoxygenation dynamics in clinical setting.

6.6 Study limitations

As NIRS is an indirect measurement, there are inherent limitations that must be considered in this study. Two major assumptions of the study are that: (i) ΔHHbMb responses reflect microvascular oxygen extraction in the portion of the muscle being investigated; and (ii) the contribution of myoglobin to the NIRS signal is unknown, therefore ΔHHbMb reflects both haemoglobin and myoglobin contributions, and this does not affect the relationship between ΔHHbMb and oxygen extraction. Other important limitations inherent with all NIRS studies include: the effect of the relatively small (and superficial) sample of muscle tissue sampled on the NIRS signal, and the effect of changes in blood volume on the NIRS signal.

HHbMb as a surrogate of oxygen extraction

While this relationship is yet to be validated directly in humans (partly due to the difficulty in sampling venous blood from the exercise muscle without contamination from other muscles/tissue) studies in the dog gastrocnemius have found good, and very good, correlation between HHbMb and venous O_2 saturation (Grassi et al., 2002; Goodwin et al., 2011; Wüst et al., 2014; Sun et al., 2016). Sun et al. (2016) found a highly linear correlation between NIRS derived HHbMb and C_vO_2 in the dog gastrocnemius muscle (r^2 = 0.89 $\pm$ 0.06), indicating NIRS HHbMb accurately reflects mean venous O_2 saturation in the interrogated muscle tissue. Similarly, Wust et al. (2014) found a good correlation between venous O_2 saturation and HHbMb in the dog gastrocnemius muscle in conditions of spontaneous blood flow (r^2 = 0.69 $\pm$ 0.12; $p > 0.001$) and a very good correlation during conditions of constant blood flow (r^2 = 0.93 $\pm$ 0.06). Furthermore, indirect studies in exercising humans have demonstrated similar HHbMb kinetics to the (a-v)O_2 time course in human limb and isolated in situ dog muscle, intracellular PO_2

in single amphibian muscle fibres and microvascular PO_2 in rat muscle [(Grassi, 2005) Figure 47].

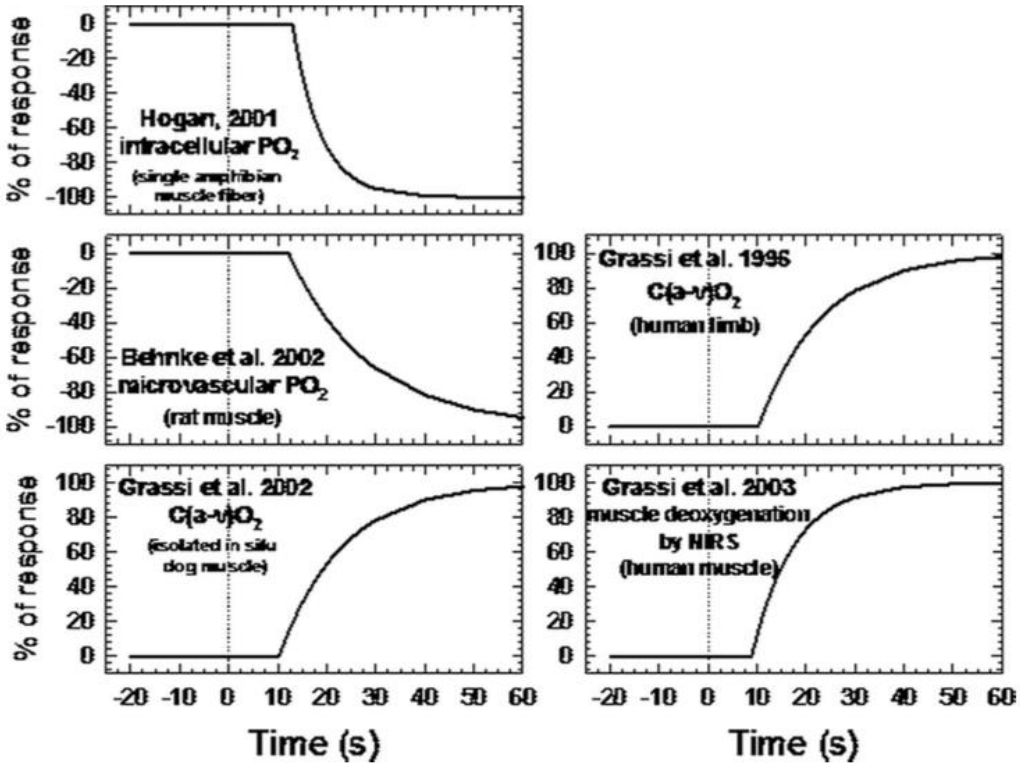

Figure 47: Kinetics of different variables related to O_2 extraction upon a step increase in metabolic demand, as determined in studies conducted by utilising different techniques and experimental models (Grassi et al., 1996, 2002, 2003; Hogan, 2001; Behnke et al., 2002). Note that an increased O_2 extraction is reflected by an increased muscle deoxygenation by NIRS, by an increased $C(a\text{-}v)O_2$, but by a decreased microvascular or intracellular PO_2. The vertical broken lines (time = 0) indicate the time at which the metabolic demand was increased. All variables show a quite similar "biphasic" response, that is, an early phase lasting around 10 seconds in which no significant change vs the baseline value is observed, followed by the monoexponential increase (or decrease) to the asymptotic value. Taken from Grassi (2005).

Contribution of Hb and Mb to the NIRS signal

Due to similar absorption spectra, it is not possible to distinguish between haemoglobin and myoglobin. As such, the relative contributions of Hb and Mb to the NIRS signal are unknown. As discussed in detail earlier, there is a debate regarding the relative contributions of Hb and Mb to the NIRS signal,

and evidence is conflicting. Some authors have suggested that the Mb contribution to the NIRS signal is small (Seiyama et al., 1988; Mancini et al., 1994), although other studies has found the contribution much higher (Tran et al., 1999; Richardson et al., 2001; Spires et al., 2011). Davis and Barstow (2013) determined the contribution of myoglobin to be greater than ≥50% in human muscles. Regardless, the time course for the desaturation of Mb and Hb has been found to be similar (Davis & Barstow, 2013); therefore, a greater contribution of Mb to the NIRS signal would not invalidate the interpretation that changes in this signal reflect fractional O_2 extraction (Grassi & Quaresima, 2016). For the purpose of this study it is recognised that the muscle deoxygenation signal by NIRS is derived from both Hb and Mb contributions.

Small volume muscle tissue sampled by NIRS probe

It is well known that adipose tissue thickness can have a confounding influence on NIRS measurements (van Beekvelt et al., 2001), as NIRS instruments can only interrogate a relatively small and superficial volume of skeletal muscle (Chance et al., 1988). To anticipate the possible influence of adipose tissue thickness, the ΔHHb signal was normalised to the amplitude of the response, and NIRS measurements were not collected in patients with large body mass. Furthermore, muscle activation, metabolism and blood flow are heterogeneously distributed; as such, the area of muscle under investigation may not be an accurate representation of the whole muscle (Grassi & Quaresima, 2016)

Changes in blood volume

While interpretation of the oxygenated NIRS signal ($HbMbO_2$) is dependent on changes in muscle blood flow, the deoxygenated signal (HHbMb) appears to be less influenced by changes in blood volume, as it is primarily dependent on O_2 extraction (Grassi et al., 2003; Goodwin et al., 2011; Grassi and Quaresima, 2016). As described above, there is an association between NIRS derived muscle deoxygenation and femoral O_2 saturation, however, it has been shown that this is not the same for oxygenated haemoglobin and myoglobin. This has been demonstrated by Grassi et al. (2003) who observed the following relationships during cycle ergometry exercise: at the onset of exercise for ~10 s all NIRS oxygenation variables remained constant (phase a in Figure 48) compared with the unloaded pedalling baseline. After this initial period, oxygenated haemoglobin and myoglobin (i.e. Δ[oxy(Hb + Mb)] in Figure 48) and deoxygenated

haemoglobin and myoglobin (Δ[deoxy(Hb + Mb)] in Figure 48) decreased and increased, respectively (phase b in Figure 48) and reached a steady-state level in ~60 s. As a consequence of the Δ[oxy(Hb + Mb)] and Δ[deoxy(Hb + Mb)] time courses during phase b, the sum of the two variables, i.e., Δ[oxy(Hb + Mb) + deoxy(Hb + Mb)] (indicating the total Hb + Mb volume in the region of interest) remained substantially constant, whereas Δ[oxy(Hb + Mb) - deoxy(Hb + Mb)] decreased exponentially and reached a steady state in ~60 s. After the initial 60 s, Δ[deoxy(Hb + Mb)] remained constant to the end of the exercise, whereas Δ[oxy(Hb + Mb)] increased (phase c in Figure 48). This increased muscle oxygenation during constant-load exercise was observed by MacDonald, (1999) and it did not correlate with the simultaneously determined oxygenated haemoglobin and myoglobin saturation in the vein draining from the exercising muscle.

This observation is possibly due to an increased blood flow to the skin (Grassi et al., 2003). The deoxygenated Hb + Mb may not be affected by the increase in blood volume, since an enhanced blood flow is unlikely to be associated with an increase in gas exchange (Koga et al., 2015). In addition, the TOI% response is also less sensitive to changes in skin perfusion as it is presented as a ratio of (HbO_2/Hbtotal). However, as it is still dependent on HbO_2, may be more sensitive than ΔHHb.

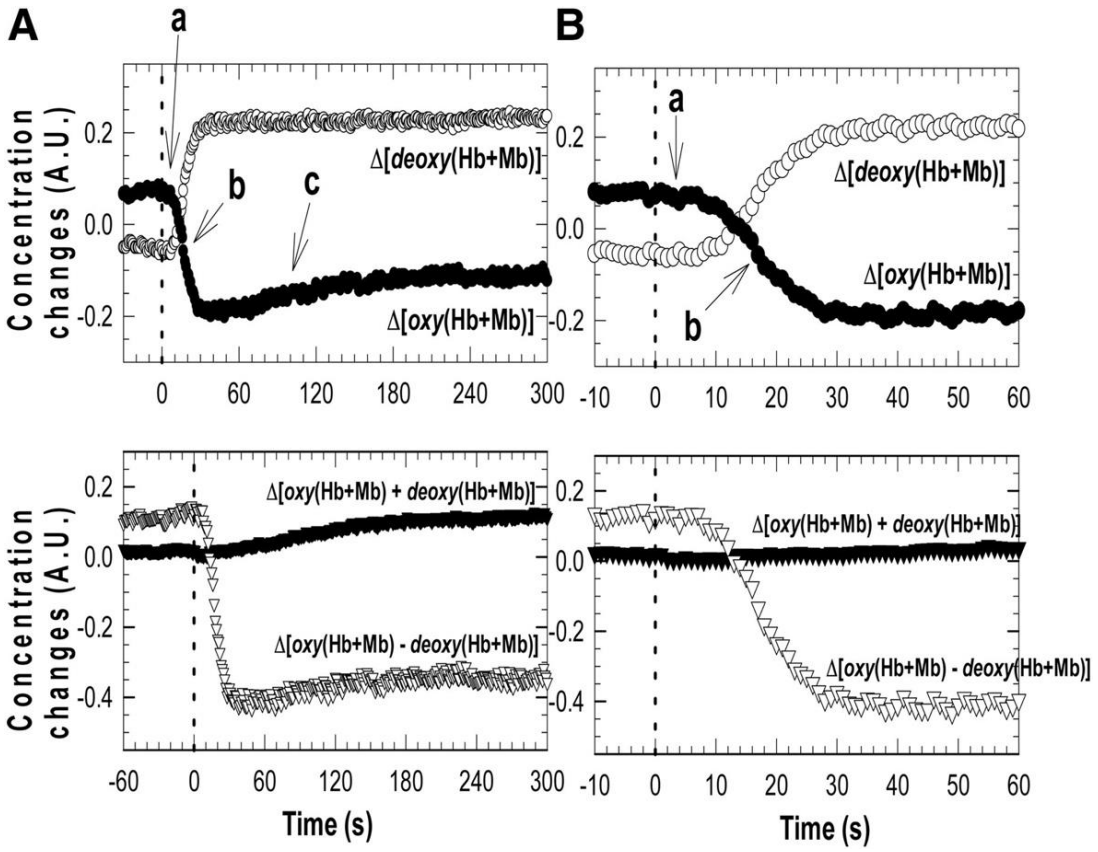

Figure 48: (A) time courses of vastus lateralis Δ[oxy(Hb + Mb)], Δ[deoxy(Hb + Mb)], Δ[oxy(Hb + Mb) + deoxy(Hb + Mb)], and Δ[oxy(Hb + Mb) - deoxy(Hb + Mb)] in a typical subject during transition (at *time 0*, vertical dashed line) from unloaded pedaling to moderate intensity constant-load exercise. (B*)*: same data shown in A, with abscissa expanded to allow a better appreciation of time courses of variables during the early phase of the transition. Different phases of the response are represented by a, b, and c. Taken from Grassi et al. (2003).

6.7 Conclusions

The present study demonstrates that in heart failure (NYHA II-III) patients the deoxygenated haemoglobin and myoglobin response to ramp incremental is variable between individuals but can be classified into three distinct responses according to the skeletal muscle O_2 delivery dynamics during ramp incremental exercise. A simplified linear fit to the mid portion of the deoxygenation response gave valuable insights into the $\dot{V}O_{2m}/\dot{Q}_m$

relationship in heart failure patients. A steeper increase in muscle deoxygenation was related to lower peak work rates and a lower $\dot{V}O_{2,peak}$, indicating that patients with steeper deoxygenation slopes had a greater reliance on oxygen extraction due to limited oxygen delivery.

In a small subset of patient's muscle deoxygenation responses were characterised by a double linear function and a sigmoid function. According to the AIC_C score, the double-linear function provided a better fit to the data than a sigmoidal function. However, the lack of any discernible plateau in HHbMb towards the end of exercise causes a problem for both functions and, therefore, parameter estimates, and their physiological implications must be considered when judging model quality. As the data was highly variable between patients and given the three distinct response types shown fitting all or most of the response may not always be possible and/or appropriate with a 'one fits all' approach.

As such, a simplified linear function that is fit to the just the linear portion of the HHbMb response may provide the most useful insights into the $\dot{V}O_{2m}/\dot{Q}_m$ relationship, that can be applied across variable responses, and does not require complex mathematical functions.

6.8 Case study

6.8.1 Introduction

It has been shown that small increases in resting muscle blood flow have marked benefits for maintaining muscle O_2 availability during exercise, predicting improved exercise tolerance. For example, Benson et al. (2013) showed that small increases in blood flow at rest not only increases the steady state (resting and exercising) muscle oxygenation values, but also reduces the characteristic undershoot in muscle oxygenation seen in heart failure patients (Sperandio et al., 2009), thereby giving a 'double benefit' effect. Furthermore, experimental data (Bowen et al., 2012) have shown that a priming exercise bout in heart failure patients (to increase baseline blood flow) also resulted in a reduction of the undershoot in muscle oxygenation seen at the onset of exercise in some patients. Based on this, it is reasonable to predict that increasing resting blood flow will have a profound effect on the *dynamics* of the muscle oxygenation response during a subsequent increase in work rate, thereby reducing the undershoot in muscle oxygenation. This is particularly pertinent for individuals with blood flow and O_2 delivery problems, such as heart failure patients.

The development of cardiac resynchronisation therapy (CRT) has been a major breakthrough in the treatment of HF (Auricchio and Prinzen, 2011), in which the primary aim is to improve cardiac output by synchronsing the pumping action of the ventricles. This is achieved via implantation of a biventricular pacemaker, which has three leads that sit in the heart (one in the right atria, and a lead in each (the left and right) ventricle). In some cases, CRT has been shown to improve quality of life, exercise tolerance, and left ventricular ejection fraction (LVEF) in HF patients (Birnie and Tang, 2006; Tomczak et al., 2012). Despite these advances, however, it has been reported that up to 30 % of patients that receive CRT therapy do not show any improvement in symptoms; these patients are often referred to as CRT 'non-responders' (Saxon and Ellenbogen, 2003; Birnie and Tang, 2006). One hypothesis to explain CRT 'non-responders' is that the extra cardiac output generated from CTR isn't being distributed to the exercising muscle and is instead being distributed elsewhere in the body, while a second hypothesis is that the extra cardiac output is being distributed to the exercising muscles but there is a problem with O_2 utilisation at a skeletal muscle level (e.g. mitochondrial dysfunction) that means they are unable to

use the extra O_2 being delivered (Bowen et al., 2012). As such, interventions aimed solely at improving cardiac output (i.e. CRT) might not be completely effective in patients who also have dysfunction at a skeletal muscle level. Additionally, when it comes to assessing the efficacy of CRT, important effects on the functional status of the patient are difficult to quantify objectively (i.e. by patients NYHA class and quality of life score), and very significant placebo effects can be seen with this type of intervention. Functional assessments therefore need to be performed in conjunction with less subjective measurements of ventricular performance and exercise capacity, pre- and post-CRT (Fox et al., 2005). With this in mind, non-invasive methods of determining the *primary* locus of exercise intolerance in HF patients (i.e. impaired O_2 delivery and/or impaired O_2 utilisation) could prove useful in targeting individual therapeutic intervention (i.e. exercise training in patients with poor skeletal muscle function). As discussed in detail throughout this thesis, muscle oxygenation dynamics during exercise, measured noninvasively using near infrared spectroscopy, can provide insights into O_2 delivery/utilisation matching. NIRS could therefore provide information on the locus (central/peripheral) of the exercise intolerance, which in turn may assist in guiding or quantifying the effectiveness of treatment. The aim of this case study was to measure muscle oxygenation dynamics non-invasively before and after CRT in a heart failure patient with reduced ejection fraction.

6.8.2 Methods

Participants and protocols

One heart failure patient (age 76 years; BMI 24; LVEF 12 %; NYHA II) volunteered to take part in the study and provided informed written consent. The investigation was approved by the National Institute for Health Research, Leeds Clinical Facility research committee.

The patient attended Leeds Clinical Research facility on two occasions. On both occasions, the patient performed a symptom limited ramp incremental exercise test to the limit of tolerance. Each test was preceded and followed with at least 4 minutes of unloaded pedalling at 10 W. Ramp rates (15 W/min) was individually targeted to produce a test duration of 8-12 minutes and kept the same on both tests. The patient was instructed to keep the RPM between 70-80 on both tests. The test was terminated when the pedal

cadence could no longer be maintained above 50 rpm despite strong verbal encouragement. The first test took place prior to CRT implantation and the second test took place 6 weeks following CRT.

Equipment and measurements

Data was analysed in the same manner described in the general methods sections under sub-heading protocol 2.

6.8.3 Results

Results from the ramp incremental test are shown in Table 27. Peak work rate and time to limit of tolerance both improved by 9% and 17% respectively following CRT (185 to 202 W and 910 to 1060 s, respectively), despite a 41% *decrease* in HHbMb. The tissue saturation index was significantly increased post CRT. $\dot{V}O_{2,peak}$ on the first test before CRT was 1.34 mL/min/kg however, due to a leak in the mask towards the end of the second exercise test it was not possible to obtain an accurate $\dot{V}O_{2,peak}$.

Table 27: Key variables derived from ramp incremental exercise test

Test	Ramp rate (W/min)	Ramp duration (s)	$\dot{V}O_{2,peak}$ (mL/min/kg)	WR peak (W)	HR rise (bpm)	HHbMb amplitude (a.u.)
Pre	15.0	910.0	1.34	185.0	40.0	20.1
Post	15.0	1060.0	N/A	202.0	39.0	11.8

Figure 49 shows the muscle deoxygenation (HHbMb) pre and 6 weeks post CRT (top) and tissue oxygenation index (bottom). In addition to the decrease in the change in muscle deoxygenation, the profile of the muscle deoxygenation also changed, such that, at the onset of exercise, muscle deoxygenation increased at a slower rate than before CRT. This is also reflected in the tissue oxygenation index profile.

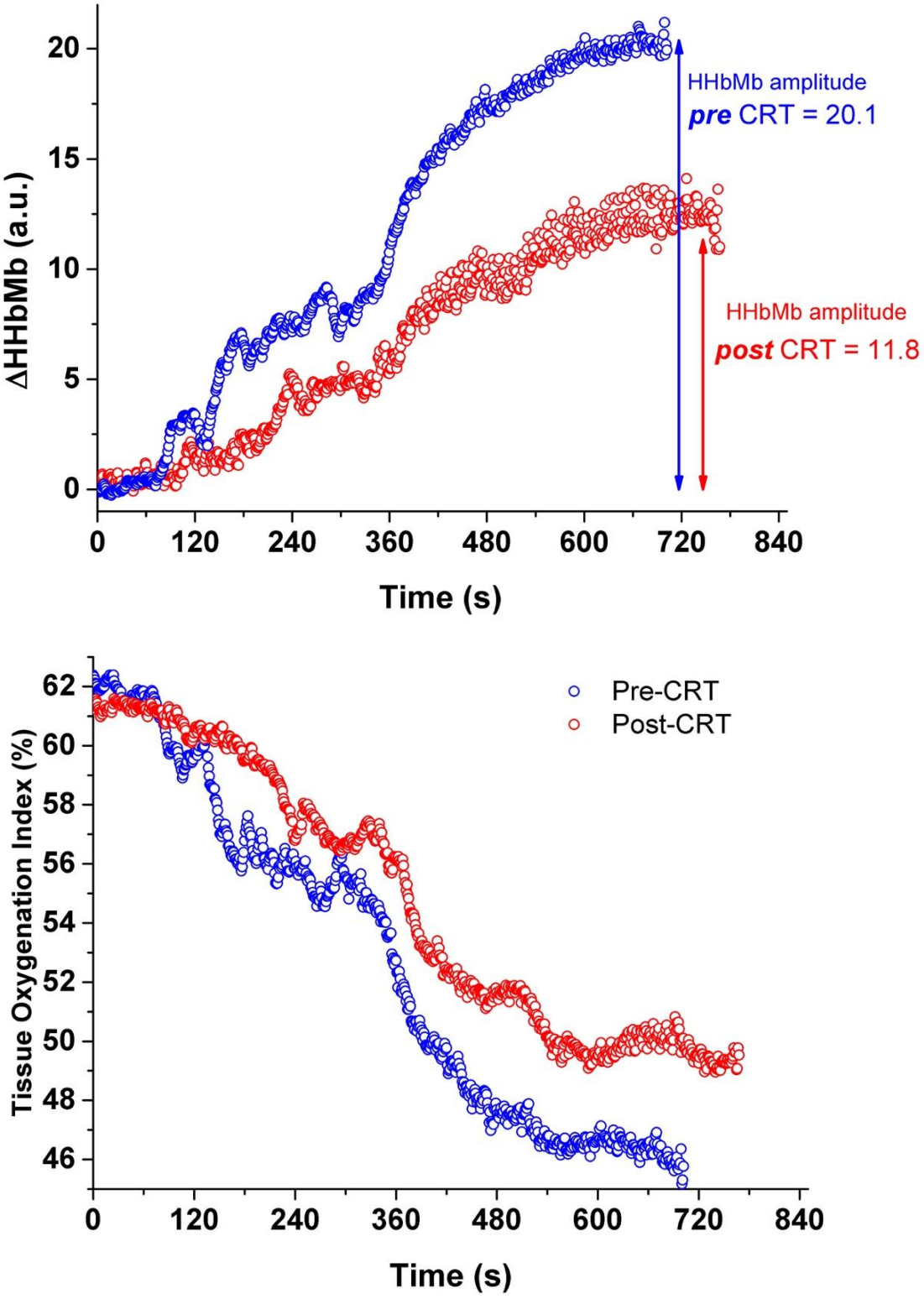

Figure 49: NIRS deoxygenated haemoglobin and myoglobin (top) and tissue oxygenation index (bottom) response before and after cardiac resynchronisation therapy in a heart failure patient.

6.8.4 Discussion

In the case study presented, exercise capacity (time to limit of tolerance and peak work rate) was improved in one patient following CRT. Additionally, the overall amount of muscle oxygen extraction (assessed by NIRS deoxygenated and haemoglobin and myoglobin, and tissue oxygenation index) was reduced, suggesting increased blood flow to the vastus lateralis muscle following CRT improved the matching between $\dot{V}O_{2m}/\dot{Q}_m$, and decreased the reliance on oxygen extraction during ramp incremental exercise in this heart failure patient. This is the first study to demonstrate this these changes following CRT by NIRS, although a larger subject number is needed to confirm this. Previous studies have shown that most patients will improve their exercise capacity by 1-2 mL/min/kg in $\dot{V}O_{2,max}$ and improvements in exercise duration to be around 30-60 s (Saxon and Ellenbogen, 2003) following CRT. While the changes in $\dot{V}O_{2,max}$ in this patient cannot be evaluated, exercise duration was increased by 57 s, in agreement with previous studies, and indicating that exercise capacity has been improved following CRT. This improvement can be attributed to improvements in cardiac structure and function (Cazeau et al., 2001; Auricchio et al., 2002). The mechanisms responsible for this are still not completely understood, but it is thought that the electrical resynchronisation of the heart can reduce the left bundle branch block-induced dyssynchrony between the left and right ventricle and the intraventricular dyssynchrony within the left ventricle (Abraham and Hayes, 2003). This acts to improve left ventricular filling time, decrease septal dyskinesis and reduce mitral regurgitation, improving central haemodynamics (Kass et al., 1999; Auricchio et al., 2002). Figure 50 shows changes in left ventricular ejection fraction following CRT from key clinical trials and studies (Auricchio et al., 1999; Cleland et al., 2001; Linde et al., 2002, 2008; Higgins et al., 2003; Young et al., 2003; Abraham et al., 2004; Bristow et al., 2004; Moss et al., 2005).

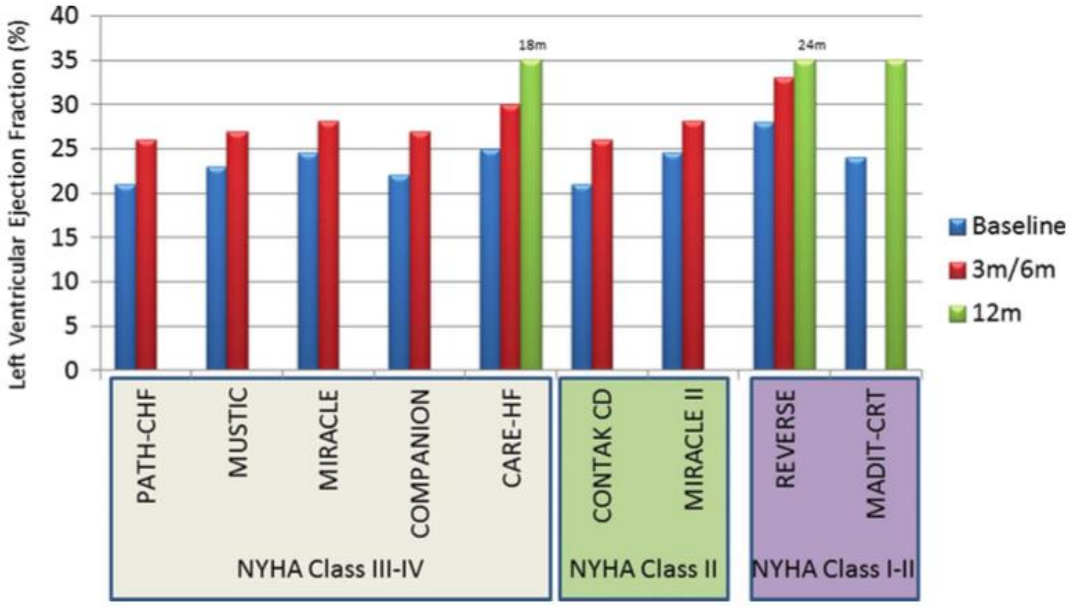

Figure 50: Change in left ventricular ejection fraction (LVEF) after cardiac resynchronisation therapy (CRT) in heart failure patients with different functional classes (New York Heart Association; NYHA), in comparison to LVEF before CRT (blue bars), and 3-6 months CRT (red bars), or 12-24 months (green bars). Taken from Auricchio and Prinzen (2011).

Despite this improvement in cardiac haemodynamics, there is still a portion of patients (around 30%) classed as CRT “non-responders”. Non-responders can be classed as: those who do not see an improvement in symptoms, but continue to live as an effect of therapy; and those who experience relief from symptoms but have poor outcomes (Auricchio and Prinzen, 2011). Possible central explanations for the variability in response to CRT include variability in the patterns of mechanical dyssynchrony, the site of LV stimulation, and the etiology of heart failure (Birnie and Tang, 2006). However, as mentioned earlier, indices of cardiac function do not relate well to exercise tolerance. As such, it is pertinent to consider what is happening peripherally. One possibility is that the extra cardiac output generated from CRT does not reach the exercising muscle but is diverted elsewhere (i.e. a blood flow redistribution problem), while another is that the extra cardiac output is reaching the exercising muscle, but some patients are unable to utilise the extra cardiac output (and therefore oxygen) being delivered. This may be attributed to a plethora of skeletal muscle adaptations that have been observed in heart failure patients (Figure 51) including a shift in fibre type from type I oxidative fibres, to type II glycolytic fibres; a reduction in

mitochondrial density and mitochondrial volumes; muscle wasting and muscle fibre atrophy; and increases apoptosis. Accordingly, several studies have observed a significant relationship between skeletal muscle abnormalities (such as those listed above and in Figure 51), and exercise tolerance (Wiener et al., 1986; Mancini et al., 1989, 1992; Sullivan et al., 1990; Minotti et al., 1991; Drexler et al., 1992; Clark et al., 1996; Massie et al., 1996; Nagai et al., 2004; Middlekauff, 2010).

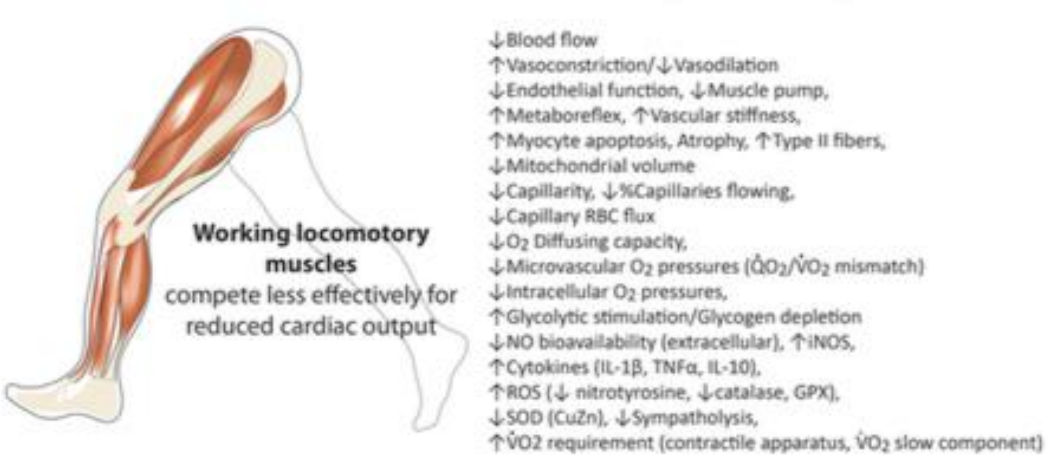

Figure 51: Effects of heart failure on the skeletal muscle. Taken from Poole et al. (2011).

Wilson et al. (1984), demonstrated the presence of skeletal muscle dysfunction by (invasively) simultaneously measuring cardiac haemodynamics and peripheral blood flow in 11 heart failure patients, with and without dobutamine infusion. Without dobutamine, patients were limited by fatigue and had reduced oxygen uptake, as well as markedly elevated leg muscle oxygen extraction at peak exercise, consistent with a blood flow limitation. With dobutamine infusion, cardiac output was significantly increased, as was leg blood flow. Despite this, there was no significant change in maximal exercise duration or peak $\dot{V}O_2$. Whereas, leg muscle oxygen extraction significantly decreased (85 ± 2 % to 80 ± 2%, $p < 0.01$), suggesting that even with increased oxygen delivery, the skeletal muscle may not extract the extra oxygen being delivered.

The results from the present case study are similar to those found by Wilson et al. (1984), in that following intervention (to improve cardiac output),

muscle blood flow appeared to be increased but muscle oxygen extraction was decreased. This supports the conclusion that an increased blood flow reduced the reliance on O_2 extraction, presumably by improving the matching of the $\dot{V}O_{2m}/\dot{Q}_m$ ratio. Unlike in Wilson et al. (1984), in the current case study, exercise duration and peak work rate was improved, indicating that CRT may result in some improvement in exercise tolerance (although as this case study is only in one patient it is unclear whether this result would be seen in other HF patients). Unfortunately, the patient was not followed up in the present study, therefore, it is not known if the patient presented in this case study was deemed a responder or non-responder.

The slight improvement in exercise capacity would suggest a response to therapy. However, this patient did not their increase oxygen extraction which is more indicative of a non-responder. It is logical to think that if oxygen delivery to the exercising muscle is improved, then oxygen extraction rates would be increased in order to “take advantage” of the increased oxygen delivery in order to facilitate an improvement exercise capacity however, oxygen extraction was *decreased* in this patient. It is therefore possible to interpret these results such that, prior to CRT the patient was primarily limited by oxygen delivery however following CRT this primary limitation appears to have moved towards an oxygen utilisation limitation. This raises several questions: (i) has this patient improved tolerance to exercise following CRT (and therefore is a “responder”) despite skeletal muscle abnormalities, and does this depend on the degree of the improvement in oxygen delivery (i.e. is it enough to override a poor oxygen utilisation response? (ii) Did muscle oxygen extraction not increase in an attempt to keep the $\dot{V}O_{2m}/\dot{Q}_m$ relationship stable, such that O_2 delivery is well matched to O_2 utilisation (i.e. would an even larger increase oxygen delivery be met with a larger increase in oxygen extraction? These questions highlight one of the limitations in using NIRS in this way i.e. it is only possible to assess the balance between oxygen delivery and oxygen utilisation such that it is not always possible to distinguish if changes in the NIRS oxygenation response are a result of a change in oxygen delivery and/or a change in oxygen utilisation. One possible way to overcome this limitation is to eliminate the influence of one of these factors (i.e. the influence of oxygen delivery). This concept is addressed in the next chapter.

6.8.5 Conclusion

This data presented in this case study suggests that NIRS may be a useful and objective way to assess CRT effectiveness, by demonstrating improvement in skeletal muscle oxygen delivery. Furthermore, NIRS may have the potential to identify the locus of the O_2 delivery/utilisation limitation underlying exercise tolerance in a given heart failure patient, so that those who are likely to be CRT non-responders may be identified before undergoing invasive surgery (see future considerations section for discussion).

Chapter 7 Assessing the reproducibility of muscle oxidative capacity measured by near infrared spectroscopy in healthy humans

7.1 Introduction

A major symptom of heart failure is poor exercise tolerance. Although exercise intolerance does not correlate to the degree of cardiovascular dysfunction (Witte et al., 2004), it represents one of the best predictors of mortality (Clark et al., 1996). Abnormal skeletal muscle metabolism in HF may, in part, account for this dissociation between cardiac function and exercise intolerance (Massie et al., 1987; Mancini et al., 1994; Clark et al., 1996; Bowen et al., 2012). In the skeletal muscle, three energy pathways are responsible for ATP regeneration: the breakdown of phosphocreatine (PCr), which results in the formation of inorganic phosphate (Pi); glycolysis/glycogenolysis, which produces lactate and H^+; and oxidative phosphorylation, by the coupling of oxygen use to the phosphorylation of adenosine diphosphate (ADP) in the mitochondria (Baker et al., 2010). The mitochondria generate most of the ATP required to support muscle contraction. As such, mitochondrial functioning and/or density is related to exercise capacity (Holloszy, 1967; Holloszy et al., 1970; Gollnick et al., 1973). Accordingly, impairments in the mitochondria, such as reductions in mitochondrial function and/or density, are associated with ageing (Conley et al., 2000) and diseases including diabetes (Joseph et al., 2012) and heart failure (Clark et al., 1996).

During recovery from exercise, NIRS measurements during repeated arterial occlusions have been utilised in order to determine the kinetics of the recovery of muscle oxygen consumption ($m\dot{V}O_2$). The purpose of the occlusions is to achieve brief periods of ischemia, such that $m\dot{V}O_2$ is isolated from the influence of circulatory and pulmonary interactions (i.e. in the absence of blood flow, muscle deoxygenation occurs solely by O_2 consumption). The time-course of the $m\dot{V}O_2$ recovery follows an exponential time-course and is directly related to oxidative capacity [in single frog muscle

fibres (Wüst et al., 2013)]. The m$\dot{V}O_2$ recovery rate constant (*k*) is therefore considered to be an index of mitochondrial function (Motobe et al., 2004; Ryan et al., 2012, 2013, 2014; Brizendine et al., 2013; Adami et al., 2017). In humans the recovery kinetics of m$\dot{V}O_2$ determined by NIRS have been shown to be closely correlated with the kinetics of PCr recovery determined by 31^{P}MRS following exercise (Ryan et al., 2013) and by muscle biopsy (Ryan et al., 2014).

This NIRS method for assessing oxidative capacity relies on two competing assumptions: i) that exercise is sufficiently intense enough to activate mitochondrial oxidative enzymes and elicit a sufficient increase in m$\dot{V}O_2$; and ii) that O_2 availability is not limiting to *k* (Haseler et al., 2004; Adami and Rossiter, 2017). In addition, there should be no change in blood volume (represented by changes in total haemoglobin + myoglobin in the NIRS signal) during occlusions for this method to be valid, as changes in blood volume could confound the slope of the recovery m$\dot{V}O_2$ (Ryan et al., 2012). The latter issue has been addressed by Ryan et al. (2012) who developed a method for correcting for blood volume changes. Meeting the other two conditions is largely dependent on the researcher correctly carrying out the test and have been addressed in detail in the discussion section.

The principles of NIRS have been described in detail in Chapter 1. In the context of this chapter, the rate of decrease in tissue oxygenation index (TOI) or oxygenated haemoglobin and myoglobin (HbMbO2; or, conversely, the rate of increase in deoxygenated haemoglobin and myoglobin, HHbMb) during the intermittent arterial occlusions is considered an estimate of muscle oxygen consumption. The relatively low cost of NIRS and ease of application on human participants have made NIRS an attractive tool to use in both research and clinical settings (Wolf et al., 2007). Despite this there are few published studies reporting the reproducibility of the oxidative capacity assessment (Ryan et al., 2012; Southern et al., 2013; Adami et al., 2017). Furthermore, of these reports, the techniques used to elicit a rise in m$\dot{V}O_2$ have varied from electrical stimulation (Ryan et al., 2012), pneumatic ergometer (Southern et al., 2013), resistance bands (Southern et al., 2013) and running (Buchheit et al., 2011) in healthy populations, and manually applied (hand) resistance (Adami et al., 2017) in chronic obstructive pulmonary disease (COPD) patients. It is worth noting, however, that in the few studies that have been published good reproducibility was reported

regardless of the method used for exercise (i.e. coefficient of variance of ~10%).

Throughout this thesis, the importance of utilising non-invasive methods of assessing skeletal muscle function (i.e. O_2 uptake/consumption at the skeletal muscle) has been discussed. In chapters 3 and 4 computational approaches were used to investigate muscle $\dot{V}O_2$ dynamics, and in chapter 5, 6 and 7 experimental approaches (i.e. gas exchange and NIRS) were utilised to investigate the same. The experimental NIRS measurements made so far in this thesis have been reflective of both oxygen delivery and oxygen utilisation, thereby giving important insights into the *balance* between oxygen delivery and oxygen utilisation. This chapter will focus on a novel technique developed to investigate muscle oxygen consumption at the exercising muscle *solely* by NIRS (Hamaoka et al., 1996; Motobe et al., 2004). This technique may present a non-invasive method of detecting skeletal muscle abnormalities, *without the confounding effects of O_2 delivery*. If this technique is reproducible it may represent a useful tool to identify individuals who have an oxygen utilisation limitation at the skeletal muscle level regardless of their blood flow status. The aim of this study was to test the reproducibility (assessed by coefficient of variance and intraclass correlation) of this oxidative capacity assessment technique (see methods) in young healthy individuals, to include tests conducted on the same day, and tests conducted across on two different days. Manual resistance was applied for the exercise portion of the test (see methods) in order to keep the test simple and inexpensive, so that it in future studies it could be applied in heart failure patients in a clinical setting.

7.2 Methods

Methods are described in the general methods section under sub-heading "Protocol 5".

7.3 Results

Participants

All participants tolerated the sustained and intermittent arterial occlusions well and completed the whole protocol. In two subjects $m\dot{V}O_2$ k or τ could not be confidently resolved for all four oxidative capacity assessments, and

in one subject, m$\dot{V}O_2$ *k* or τ could not be confidently resolved in two oxidative capacity assessments (see discussion section for possible explanations). In these subjects the data did not fall in an exponential manner, rather, the data was highly variable such that fitting an exponential function was either not possible, or fitting an exponential function returned unphysiological results (e.g. τ of 430 s). As such, these tests were excluded from further analysis.

Physiological normalisation

Physiological normalisation revealed the maximum physiological range calculated from the minimum and maximum NIRS signal values during and after the sustained arterial occlusion. Values ranged from a minimum TOI of (mean ± SD) 45 ± 11% (day 1) and 42 ± 8% (day 2) to a maximum TOI of 73 ± 2% (day 1) to 72 ± 3% (day 2), giving a mean range of 28 ± 10% (day 1) and 30 ± 7% (day 2). There were no significant differences between minimum or maximum TOI between either same day bouts or different day bouts ($p > 0.05$).

Muscle oxidative capacity

Subject test-retest reliability variables are presented in Table 28. A total of 44 m$\dot{V}O_2$ recovery kinetics assessments were performed for the study. Individual test re-rest reliability of τ within the same day was CV = 6.7, ICC = 0.92 (day 1) and CV = 12.6, ICC = 0.08 (day 2). Individual test re-rest reliability of rate constant *k* within the same day was CV = 10.3, ICC = 0.98 (day 1) and CV = 12.47, ICC = 0.26 (day 2). Figure 52 shows the NIRS signal during the oxidative capacity assessment and the resultant m$\dot{V}O_2$ kinetics in a representative subject. Figure 53 shows comparisons of *k* and τ across bouts 1 and 2 on days 1 and 2. Bland-Altman limit of agreement analysis revealed 95% confidence intervals of (-1.2, 0.7 *k* day 1; -0.5, 0.9 *k* day 2; -6.1, 1.8 τ day 1; -8.6, 9.5 τ day 2), and no order effect was detected. Figure **54** shows Bland Altman limit of agreement plots for repeated *k* and τ measurements between *same day* bouts.

Table 28: Test-retest reproducibility and coefficient of variant (CV) of gastrocnemius muscle oxidative capacity assessed by near infrared spectroscopy in young healthy participants

	τ (s)				*k* (min-1)			
	Bout 1	**Bout 2**	**CV**	**ICC**	**Bout 1**	**Bout 2**	**CV**	**ICC**
Day 1	26.4 ± 8	28.6 ± 11	6.70	0.92	2.7 ± 1.5	2.9 ± 2.5	10.32	0.98
Day 2	28.3 ± 9	27.8 ± 7	12.60	0.08	2.4 ± 0.9	2.2 ± 0.2	12.47	0.26

Data are presented as mean ± SD. *k* = proportional to muscle oxidative capacity; CV = coefficient of variation; ICC Intraclass correlation coefficient

Table 29 shows the test-retest reproducibility and coefficient of variance of oxidative capacity assessment where tests were performed on *separate days*.

Table 29: Test-retest reproducibility and coefficient of variance (CV) of gastrocnemius muscle oxidative capacity assessed by near infrared spectroscopy in young healthy participants on separate days

	day 1	**day 2**	**CV**	**ICC**
***τ* (s)**	25.7 ± 11	28.0 ± 2	14.0	0.55
***k* (min-1)**	2.8 ± 2	2.15 ± 0.1	7.1	0.28

Data are presented as mean ± SD. *k* = proportional to muscle oxidative capacity; CV = coefficient of variation; ICC Intraclass correlation coefficient

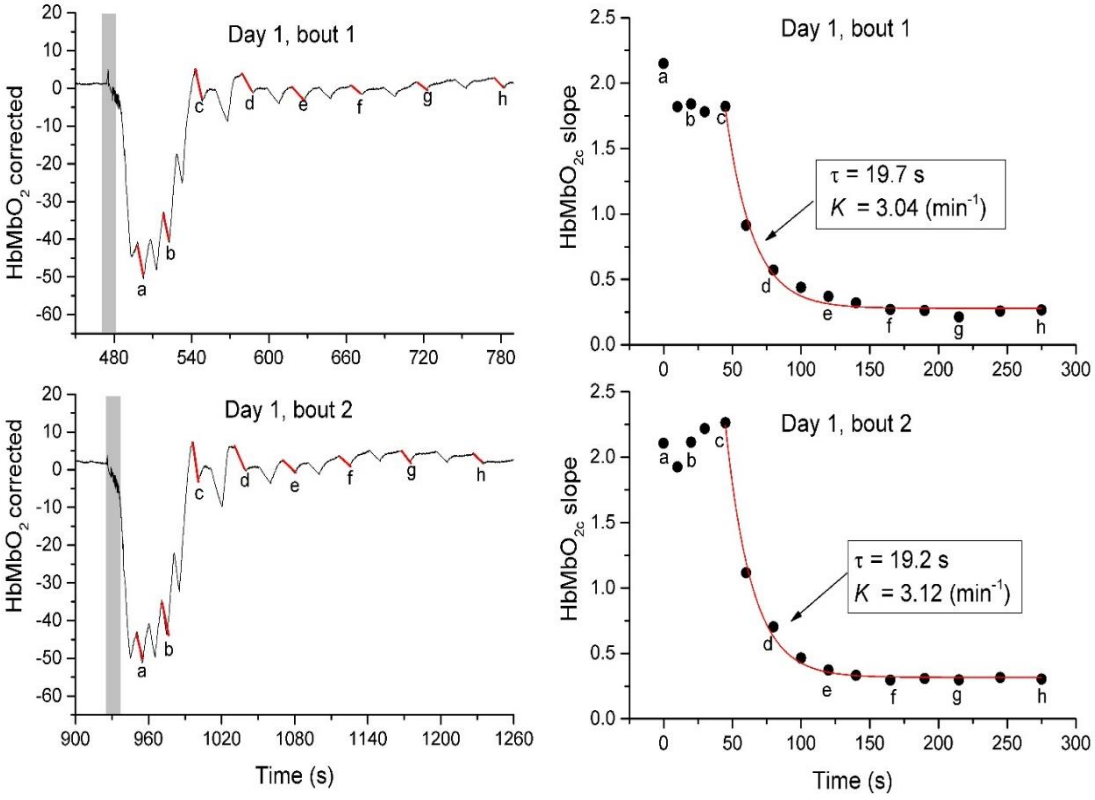

Figure 52: $HbMbO_2$ changes during the oxidative capacity protocol for a representative subject on day 1. The left panels show the $HbMbO_2$ (corrected for changes in blood volume) during dynamic exercise (grey shaded area) and intermittent arterial occlusion during recovery. Right panels show calculated muscle $\dot{V}O_2$ recovery profile *k* $m\dot{V}O_2$ (red line). The letters (a-h) are given to illustrate how corresponding $m\dot{V}O_2$ values are derived from the negative linear HbMbO2c slopes during intermittent occlusions. τ (s) is the $m\dot{V}O_2$ time constant determined by non-linear least squares regression analysis. *k*, is the rate constant, which is linearly related to muscle oxidative capacity ($k = (1 / \tau) \cdot 60$, min^{-1}).

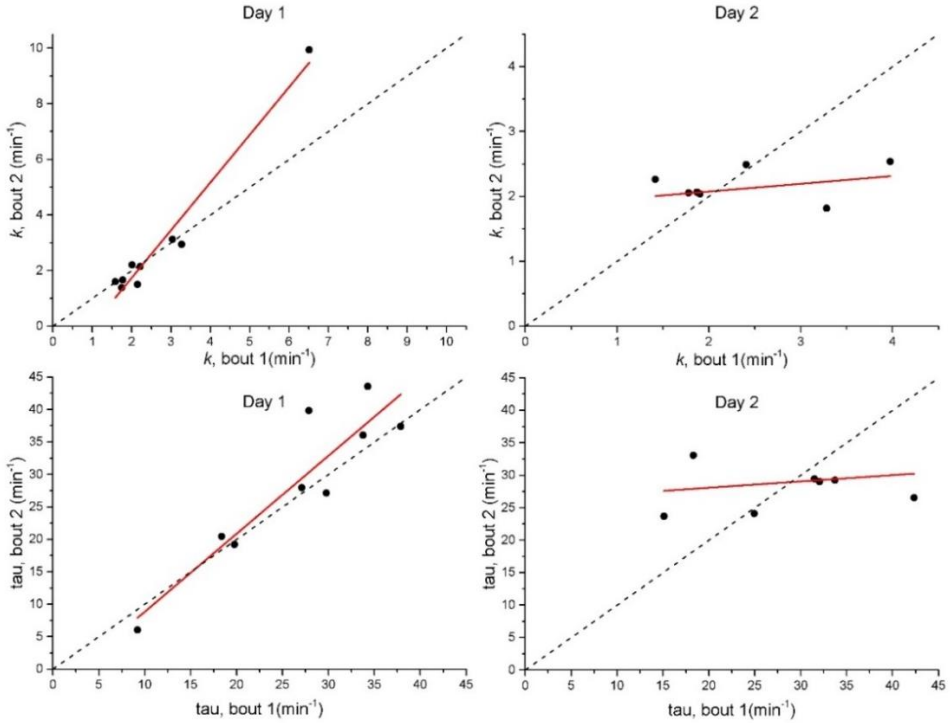

Figure 53: Muscle oxidative capacity and *k* (top panels) τ (bottom panels) test-retest analysis on day 1 and day 2. Red line shows linear regression, dotted line show line of identity (x = y)

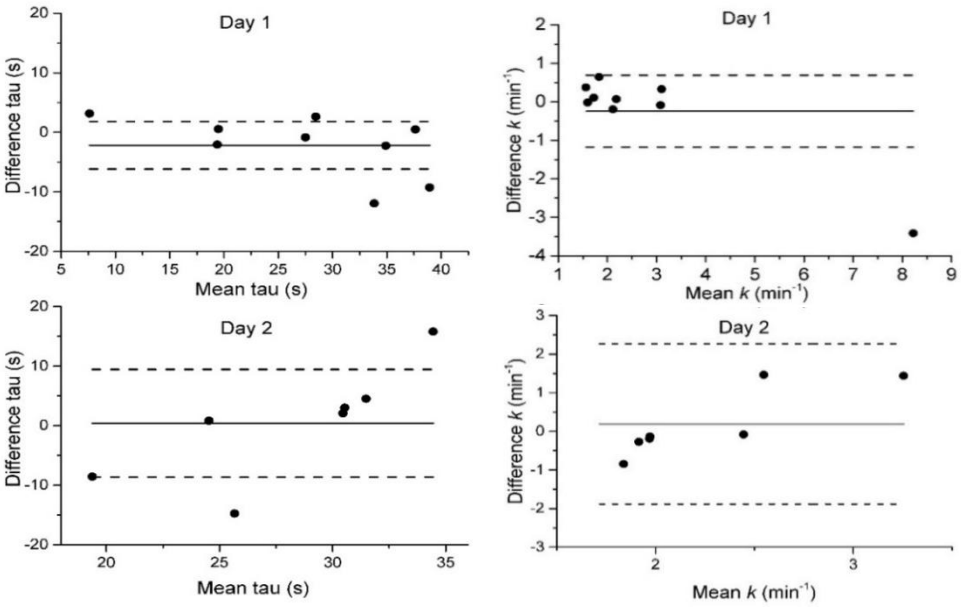

Figure 54: Bland-Altman plots of agreements between repeated measurements of muscle $\dot{V}O_2$ τ (left) and recovery rate constant (*k*, right). Dashed lines show 95% limits of agreement.

7.4 Discussion

This study found that the $m\dot{V}O_2$ recovery rate constant *k* (an index of mitochondrial function), and time constant τ measured by NIRS is reproducible in healthy subjects. The within subject variability in this study (mean CV for τ = 9% and for *k* = 11%) was consistent with the results of other studies using similar techniques (CV 10-11%; Southern et al., 2014), (CV 9.4%; Buchheit et al., 2011), (CV 10.6%; Ryan et al., 2012), and (CV 9.8%; Adami et al., 2017). Furthermore, the time constants reported in this study (mean τ 25.7 s day 1; 28.0 s day 2) were similar to those reported in similar populations (Ryan et al., 2012), and also to those measured in the same participants, by pulmonary oxygen uptake measurements which were reported in chapter two (mean τ 24.4 s). In addition, time constants were also similar to the recovery time constant of PCr kinetics measured by MRS in the gastrocnemius muscle (Yoshida and Watari, 1993; McCully et al., 1994; Larson-Meyer et al., 2000; van den Broek et al., 2007). The finding from the present study supports the use of NIRS assessment in determining mitochondrial oxidative capacity in healthy subjects.

Factors influencing variability and reproducibility of the NIRS muscle oxidative test

The two major conditions of the oxidative capacity test are i) that exercise is sufficient to activate mitochondrial oxidative enzymes and an increase in $m\dot{V}O_2$ and ii) that oxygen is not limiting to *k*. Care needs to be taken during the oxidative capacity tests that both these conditions are met. For example, experiments on isolated single muscle fibers have shown that maximal activation of mitochondrial enzymes might not be achieved when contraction frequency is too low (Wüst et al., 2013). However, higher order PCr recovery kinetics have been reported during recovery from very high intensity exercise performed in vivo (Forbes et al., 2009). In addition, strong activation of muscle fibers may limit O_2 availability and slow PCr recovery kinetics (Haseler et al., 2004). However, the point at which to stop exercise during the oxidative capacity test has varied between different researchers. In some studies, physiological normalisation was completed after the oxidative capacity assessment, so the level of O_2 desaturation was not measured and scaled to the maximum physiological range during the exercise (Ryan et al., 2012, 2013, 2014). Others have used a percentage of maximal work intensity determined from prior exercise tests. For example,

Motobe et al. (2004) measured m$\dot{V}O_2$ recovery in the forearm following 60 s dynamic handgrip exercise at 40% of participants' maximal voluntary contraction, and Buchheit et al. (2011) measured m$\dot{V}O_2$ following running at 40% and 60% of (pre-determined) maximal running speeds. Recently, Adami et al. (2017) used a modified version of the protocol proposed by Ryan et al. (2012), by completing the physiological normalisation maneuver prior to the oxidative capacity assessment. This allowed determination of the maximal physiological range of each subject (in older adults and chronic obstructive pulmonary disease patients) prior to the oxidative capacity assessment, to avoid reaching a critical low intramuscular PO_2 level induced by the exercise. In addition to good reproducibility Adami et al. (2017), showed that exercise stimuli that resulted in a small increase in m$\dot{V}O_2$ and small reduction in saturation was associated with poor test-retest reproducibility. Consequently, it was suggested that the risk to NIRS test validity of under stimulating the muscle during dynamic exercise was greater than the risk of O_2 limiting deoxygenation caused by contractions that are too intense or sustained. The authors therefore recommended that exercise desaturation should reach a value in 30-50% of the physiological normalization range in order to ensure test quality (Adami et al., 2017).

In this current study, the mean 30-50% physiological normalisation range was 64% (for 30% desaturation) and 58% (for 50% desaturation). The mean actual desaturation for all 11 participants was 57%. Excluding the two participants in which it was not possible to confidently estimate kinetic parameters changed this by only 1% (i.e. a mean of 58%). As such, participants in this current study were at the maximum (50%) range of desaturation on average of that suggested by Adami et al. (2017). This is of interest, as in all but two tests, the m$\dot{V}O_2$ recovery did not follow a strictly exponential profile. Rather, after an initial 'slowed' m$\dot{V}O_2$ response, the response profile then fell exponentially. This suggests that in this group of healthy participants, a target of 50% PN is too high (i.e. O_2 was desaturated to an extent in which O_2 availability became limiting to m$\dot{V}O_2$). This is demonstrated in Figure 55. In this individual, minimum TOI was 36% and maximum TOI was 74%, therefore the 50% PN muscle desaturation target is 74 - [(74-36)/2] = 55%. As can be seen, exercise was stopped at a level of 59%, which was 4% above the 50% target value (this equates to ~40% of PN range). Despite this, the first 4 m$\dot{V}O_2$ recovery slopes were uncharacteristically slow, before they began to fall exponentially. This slow initial response is suggestive of O_2 delivery being limited (Adami et al.,

2017). This pattern (i.e. initial slow m$\dot{V}O_2$ recovery slopes) was observed in all but two oxidative capacity assessments. Consequently, the exponential was fitted to the data from the point at which the data points began to fall in an exponential manner (determined by visual inspection). Estimating the parameters in this way may have influenced curve fitting (i.e. because the point at which to start the fitting is subjective to the person conducting the analysis). Therefore, this may explain some of the variability in measurements. In addition, removing these first data points from analysis means that the initial mechanisms of the muscle recovery phase are essentially ignored. This raises the possibility that by removing the first few data points means missing out on quantifying some physiological mechanism.

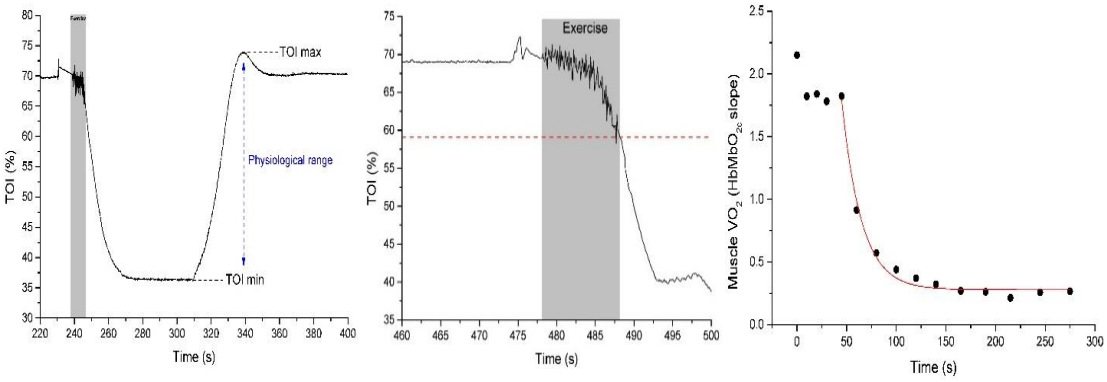

Figure 55: NIRS traces from a representative subject during a single visit. Left: The PN manoeuvre identifies the maximal physiological range (blue line), determined from the minimum TOI (TOI min) at the end of the sustained arterial occlusion, and the maximum TOI (TOI max) at the end of the reactive hyperaemia. Middle: the start of the oxidative capacity assessment. Grey shaded area indicates brief plantar flexion exercise. The red dotted line shows where plantar flexion exercise was stopped (~59%). Target desaturation determined by the PN was 55% (i.e. 4% lower than were exercise was stopped, equating to ~40% PN range). Right: resulting m$\dot{V}O_2$ recovery response profile. Circles show slope of $HbMbO_2$ recovery. Red line is non-linear regression fit to estimate rate constant k and τ.

Southern et al. (2013) tested the reproducibility of the oxidative capacity test during different exercise modalities in healthy individuals. In this study PN was performed before the oxidative capacity test. In both exercise protocols (resistance band vs ergometer) muscle desaturation for the oxidative capacity test was capped at 30% of the PN range. The authors reported no deviations from an exponential response in the $m\dot{V}O_2$ recovery and concluded $m\dot{V}O_2$ time constants were reproducible in both exercise modalities. As the study by Adami et al. (2017) was in older and chronic obstructive pulmonary disease patients, it is possible that a higher level of exercise was needed to activate oxidative enzymes and produce a sufficient $m\dot{V}O_2$ response (which may be due to a smaller muscle mass and lower muscle respiratory capacity) compared to healthy populations (Coggan et al., 1993; Maltais et al., 2000).

Additionally, in two of the subjects, it was not possible confidently determine time constants from the $m\dot{V}O_2$ recovery slopes (which were erroneously low). Consequently, possible explanations for this were explored. Figure 56 shows the physiological normalisation maneuver (top panels) and the corresponding first bout of exercise (bottom panels) in the two participants where kinetics parameters could not be confidently estimated. As can be seen, in both participants the muscle was desaturated beyond the 50% PN target. As such, in these participants it is likely that O_2 became limiting to *k* and therefore confounded the slopes of the $m\dot{V}O_2$ recovery.

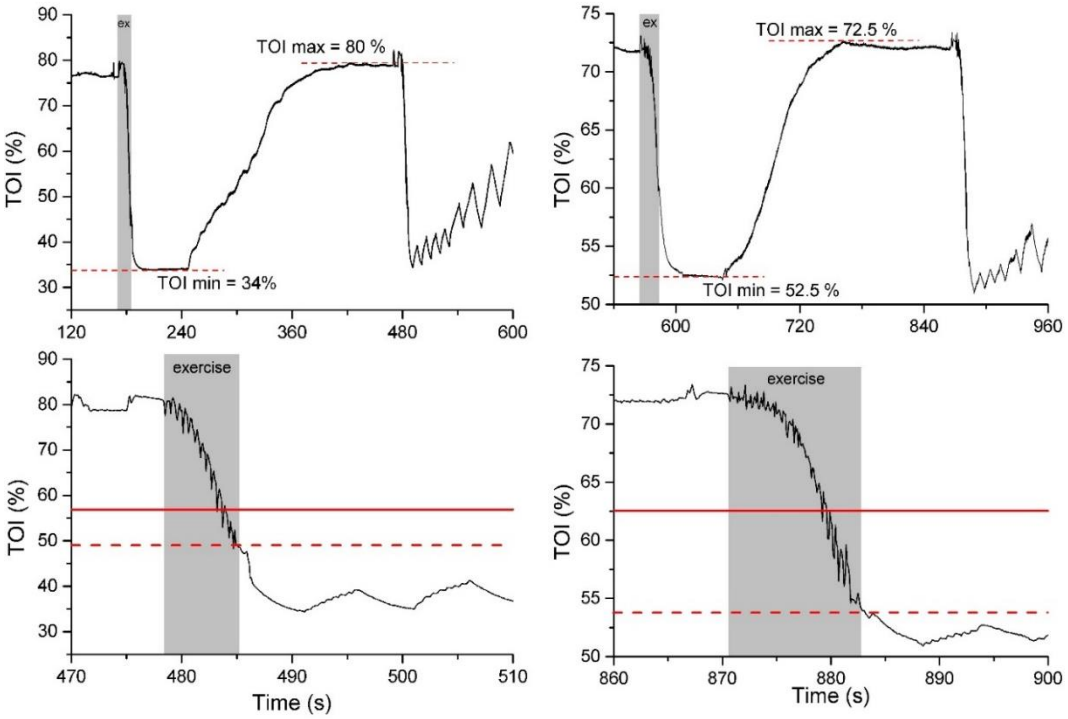

Figure 56: TOI profiles during PN manoeuvre (top panels) and oxidative capacity assessment (bottom panels) in the two subjects in whom recovery kinetics could not be confidently estimated. For subject x (left panels) TOI min was 34%, and TOI max was 80%. Target muscle desaturation therefore is 80 – ((80 – 34)/2) = 57%. The solid red line shows where exercise should have been stopped (i.e. 57%) and the dotted red lie shows where exercise was actually stopped (i.e. 49%). For subject y (right panels) TOI min was 52.5%, and TOI max was 72.5%. Target muscle desaturation therefore is 72.5 – ((72.5 – 52.5)/2) = 62.5%. The solid red line shows where exercise should have been stopped (i.e. 62.5%) and the dotted red lie shows where exercise was actually stopped (i.e. 53%).

It is also important to consider the possible consequences of completing the physiological normalisation manoeuvre before the oxidative assessment, as this essentially creates an ischemic preconditioning effect (Crisafulli et al., 2011), which could influence the assumptions inherent with the oxidative capacity technique (i.e. sufficient oxygen availability). The effects of this on mitochondrial functioning and the resultant *k* rate constant remain largely unknown (Adami et al., 2017). However, it has been argued that due to a strong correlation between NIRS derived oxidative capacity and high-resolution respirometry, O_2 availability is not problematic when measuring

oxidative capacity with NIRS in healthy individuals (Chung et al., 2018). On average, in the current study, the muscle was depleted to 50% of the physiological normalisation range. Despite overall reproducible results, as described above, there was an initial lag before $m\dot{V}O_2$ recovery fell exponentially, suggesting a cut-off point of 30% of physiological normalisation might be a more suitable value in healthy participants to minimise errors and disparities in curve fitting, and supporting the notion that O_2 availability *is* important to consider when performing the oxidative capacity assessment.

Changes in blood flow

In order for the oxidative capacity test to be valid, there should be no change in blood volume (represented in the NIRS signal as tHbMb) such that there should be symmetrical changes in $HbMbO_2$ and HHbMb (Ryan et al., 2012). However, it has been suggested that during occlusions there is a blood volume change that can mask changes in the NIRS signals due to oxygen consumption (Ryan et al., 2013) and consequently, may act to confound the slope measurements for oxygen consumption (De Blasi et al., 1997; Van Beekvelt et al., 2001). The cause of the blood volume change during arterial occlusion has been attributed to the movement of haem concentrations from larger vessels undetectable by NIRS, to microvascular beds detected by NIRS, which is caused by residual pressure gradients (Ryan et al., 2013). To overcome this, a blood volume correction algorithm was applied, and fitted the linear regression analysis to the corrected NIRS signals. This method of correcting for blood volume has been shown to provide good reliability of $m\dot{V}O_2$ recovery (CV = 10%) and produced similar coefficients of variance to PCr recovery kinetics (Ryan et al., 2012).

Influence of adipose tissue thickness (ATT)

Near infrared light must cross the skin and subcutaneous fat in order to reach the underlying skeletal muscle tissue, Therefore, the amount of adipose tissue can influence the NIRS signal (i.e. high ATT values act to dampen the NIRS signal). This is important to consider when testing obese populations. In this study participants were young, healthy and relatively lean, so it is anticipated that the effects of ATT to be lessened. Furthermore, the NIRS device used (continuous wave spectrometer) is unable to calculate the path length of near infrared light and therefore absolute concentrations of

O_2 consumption are not possible. In order to account for this, the data was scaled to the maximal physiological calibration (ischemic calibration). This method allows for comparisons between individuals with varying amounts of ATT overlying the muscle of interest. Whilst time domain and frequency domain devices estimate path length and better estimate absolute values, these devices are still influenced by ATT (Koga et al., 2011). As such, this additional information will not influence the calculation of the rate constant *k* for the recovery of $m\dot{V}O_2$ (Ryan et al., 2013). Therefore, compared to previous studies, the results from this study suggest that the physiological normalisation range may vary depending on the population being studied and therefore needs to be considered when determining methods and that, in young healthy individuals the PN range may be smaller, and target desaturation be lower (i.e. closer to the 30% mark rather than 50%).

Finally, other factors such as variability in NIRS placement, NIRS movement artifact, and day-to-day variability in participants could contribute to the overall variability in this study.

7.5 Conclusion

The NIRS oxidative capacity assessment test-retest reliability was found to be reproducible within the same day, and between different days. However, the $m\dot{V}O_2$ recovery response profile did not follow a strictly exponential response possible influencing curve fitting and the resultant $m\dot{V}O_2$ recovery kinetics. With this in mind, it is important that the person administering the test has a thorough understanding of the methodological limitations and constraints of the test, as well as the ability to respond to the results ‘on screen’ during the test, in order to satisfy the main assumptions of the test. Consequently, strict and specific guidelines that could be adopted and adhered to in clinical practice would be essential if the test was to become a mainstream clinical tool. Furthermore, the NIRS oxidative capacity test may be useful to identify the presence of skeletal muscle dysfunction, independent of blood flow. This is important as, in patients with skeletal muscle dysfunction, improving blood flow and oxygen delivery to the muscle may not give way to any improvements in symptoms or exercise tolerance, as the skeletal muscle can’t ‘make use’ of the extra oxygen being delivered. This is pertinent in patients that meet the current criteria for cardiac

resynchronisation therapy (which does not include any measure of skeletal muscle function). If a heart failure patient is identified to have skeletal muscle dysfunction, interventions such as exercise training can be implemented to improve to efficacy of cardiac resynchronisation therapy. Therefore, despite its inherent limitations, NIRS represent an important technique that is valuable and practical in research and clinical settings.

Chapter 8 Conclusions and future considerations

There were two major aims of this thesis: (i) to develop and validate a computational model of circulatory and oxygen uptake dynamics, that is able to predict oxygen uptake measurements that are experimentally measured at the lungs (i.e. pulmonary oxygen uptake), and at the skeletal muscle (i.e. muscle oxygen uptake) for ramp incremental exercise and; (ii) to test the clinical utility of using near infrared spectroscopy as a non-invasive tool to determine the locus of exercise intolerance in heart failure patients.

To fulfil the first aim, a model of circulatory and oxygen uptake and dynamics for ramp incremental exercise was developed and validated. The new components of the ramp incremental model included adding a muscle fibre recruitment component in which individual muscle fibres, with their own $\dot{V}O_2$ gain, can be gradually recruited throughout the exercise. Other additions to the model included modelling to $\dot{V}O_2$ and $\dot{Q}$ responses to rise with an initial short exponential phase followed by a linear phase for the rest of the ramp in order to mimic the $\dot{V}O_2$ response to ramp exercise. This is the first model to predict the pulmonary $\dot{V}O_2$ response (typically measured by gas exchange measurements) to ramp exercise *which has been validated against $\dot{V}O_2$ and $\dot{Q}$ measurements measured directly (Fick method) in healthy humans*. The model was developed specifically for ramp incremental exercise so that it is transferable into clinical settings. This is because the standard exercise test heart failure patients undergo is an incremental exercise test. However, to date, much of the research undertaken has focused on constant work rate exercise, where the oxygen uptake response is different. The model was developed even further in Chapter 4 to include a NIRS output (specifically oxygenated haemoglobin and myoglobin, deoxygenated haemoglobin and myoglobin, tissue oxygenation index and total haemoglobin and myoglobin). This involved the addition of a NIRS compartment, within the muscle compartment that takes simulated arterial and venous O_2 concentrations from the validated O_2 transport model (described in Chapter 3) as inputs and calculates the corresponding muscle NIRS signals. The development of a muscle oxygenation response was motivated by the need for a deeper understanding of the relationship between oxygen delivery and oxygen

utilisation in heart failure patients. The new ramp model and NIRS model were able to simulate experimental data to provide insights into muscle oxygen utilisation dynamics to ramp exercise. Based on the model simulations the following conclusions can be drawn: (i) breath-by-breath gas exchange measurements, on their own, are not a reliable estimate of *muscle* oxygen uptake kinetics and (ii) alterations in the oxygen delivery-to-oxygen utilisation relationship, including its kinetics, the slope of the oxygenation response and its baseline absolute values, all have an influence on the muscle oxygenation response. Specifically, when $\dot{V}O_2$ kinetics are faster relative to $\dot{Q}$ kinetics the tissue oxygenation index transiently undershoots its steady state value. Similarly, if baseline cardiac output becomes limiting to $\dot{V}O_2$, or there is a reduction in $\dot{Q}$ per litre change in $\dot{V}O_2$, tissue oxygenation will undershoot its steady state response. Additionally, a novel finding from the model simulations is muscle oxygenation responses are sensitive to changes in the oxygen uptake-to-work rate relationship. Specifically, reducing this relationship by 10% caused a greater reliance on O_2 extraction as demonstrated by a steeper HHbMb slope.

The model presented in chapter 4 is the first of its kind to predict muscle oxygenation responses by near infrared spectroscopy during ramp incremental and step exercise from knowledge of circulatory, respiratory, and oxygen uptake dynamic interactions. However, the newly developed NIRS model, overall, could not accurately predict the muscle oxygenation response (tissue oxygenation index and deoxygenated haemoglobin and myoglobin) to ramp exercise. There were no significant differences in the change (delta) in the muscle tissue oxygenation index from the start to end of exercise, however, the model could not predict breakpoint in the data nor the slopes of the oxygenation responses. Given the poor fits to the data, further development and validation of the model is necessary before its clinical utility can be realised, and before inferences can be made regarding mechanisms of exercise intolerance.

For the second aim, a variety experimental approaches were utilised. Chapter 5 aimed to determine whether breath-by-breath pulmonary gas exchange measurements from ramp exercise alone can provide a reliable estimation of skeletal muscle oxygen uptake kinetics in heart failure patients. This was based on the need for a method of determining muscle $\dot{V}O_2$ kinetics more easily in a clinical setting. The model simulations and experimental data presented in this chapter show that, according to the

model predictions, muscle oxygen uptake kinetics were strongly correlated to pulmonary oxygen uptake measurements in heart failure patients during ramp exercise. However, the pulmonary mean response time (that encompasses both phase I and phase II of the $\dot{V}O_2$ response) may differ within the same patient depending on the exercise protocol (i.e. ramp vs step) and method of data analysis used such that, the mean response time determined from step exercise is not equal to the mean response in the same patient when determined from ramp incremental exercise. Although these findings are based on modelling predictions, they highlight the importance of carefully considering methodological strategies when making non-invasive measurements in heart failure patients. Given these findings, for ramp incremental exercise to be used to its full clinical utility, additional measurements may be needed alongside breath-by-breath measurements to identify patients in whom skeletal muscle dysfunction is a limiting factor in exercise tolerance. As such, for the next chapter near-infrared spectroscopy was implemented during a range of exercise protocols and conditions. The aim of Chapter 6, was to characterise the NIRS deoxygenated haemoglobin and myoglobin response to ramp incremental exercise in heart failure patients. A simplified approach to doing so proved the most useful in regard to the information gained from the test, as well as the method that could be most easily transferred into a clinical setting. Using this simplified method, the following conclusions were derived: (i) in heart failure patients, the deoxygenated haemoglobin and myoglobin response to ramp incremental is variable between individuals but can be classified into three distinct responses according to the skeletal muscle O_2 delivery dynamics during ramp incremental exercise and; (ii) a simplified linear fit to the mid portion of the deoxygenation response gave valuable insights into the $\dot{V}O_{2m}/\dot{Q}_m$ relationship in heart failure patients. Specifically, a steeper increase in muscle deoxygenation was related to lower peak work rates and a lower $\dot{V}O_{2,peak}$, indicating that patients with steeper deoxygenation slopes had a greater reliance on oxygen extraction due to limited oxygen delivery. This is the first study to date, to directly compare the different methodological approaches to characterising NIRS data from ramp incremental exercise in heart failure patients. It is also the first use the response type profile (i.e. in this study three distinct profiles were identified) to characterise NIRS responses. These responses may be useful in future studies to assist characterising the NIRS response and identify patients who are limited by skeletal muscle O_2 delivery based on their response type.

Furthermore, the near infrared spectroscopy and oxygen uptake data presented in the short case study presented at the end of the chapter suggests that NIRS may be a useful and objective way to assess the effectiveness of cardiac resynchronisation therapy. In the case study, following intervention to increase cardiac output, muscle blood flow appeared to be increased (indicated by a higher baseline TOI) however overall muscle oxygen extraction was decreased (indicated by a smaller delta) indicating that an increased blood flow reduces the reliance on O_2 extraction, presumably by improving the matching of the $\dot{V}O_{2m}/\dot{Q}_m$ ratio. This shows the potential utility of NIRS for future studies, in distinguishing between patients in whom exercise tolerance is mediated primarily by oxygen delivery and in those whom it is mediated primarily by limitations in oxygen utilisation (i.e. in the presence skeletal muscle dysfunction), so that those who are likely to be cardiac resynchronisation therapy non-responders may be identified before undergoing invasive surgery. With the right exercise protocol, it would be possible to use NIRS to determine changes to these factors described above. (0or example, by utilising a RISE protocol) with measurements of breath-by-breath gas exchange and near infrared spectroscopy, performed at various stages of their treatment plan (i.e. before and at intervals following CRT) the following outcomes could be demonstrated: (i) exercise tests that include NIRS can distinguish between patients in whom exercise intolerance is mediated primarily by oxygen delivery, and those in whom this is mediated primarily by limitations in oxygen utilisation (i.e. skeletal muscle dysfunction) (ii) CRT increases both central cardiac output and skeletal muscle blood flow, and describe the time course of these changes. This can be demonstrated by performing echocardiography measurements (for central haemodynamics) and by assessing baseline blood flow by utilising near infrared spectroscopy measurement from the warm up and step portions of the RISE test (iii) in those in whom the exercise test results suggest exercise intolerance is primarily a consequence of a limitation in oxygen utilisation, there is a reduction in the magnitude of improvement in CHF symptoms following CRT (this could be assessed by subjective questions, such as ‘ratings of perceived exertion’ charts as well as their clinical response to the therapy (IV) describe the time course of any increase in exercise tolerance following CRT, and gain insight into the mechanisms of any improvement (further insights could also be gained from developing and utilising the NIRS model) and finally (V) if the tests are repeated at intervals following CRT (i.e. 1

week, 6 weeks, and 6 months) these data could be used to describe the time course of any increase in exercise tolerance following CRT. The advantage of this test is that, echocardiography measurements and a ramp incremental exercise test are standard clinical assessments for CRT patients as such, the addition of NIRS and an extension of the standard ramp test to include a short constant work rate bout following the ramp are relatively simple and non-invasive additions. The study would, however, require more visits to the research lab for the patients.

The technique presented in Chapter 7 demonstrates another method for determining the presence of skeletal muscle dysfunction. Although it is yet to be validated in heart failure patients it represents a promising non-invasive method of identifying, by NIRS, skeletal muscle dysfunction (if present) without the influence of blood flow. The advantages of this technique are that it does not require maximal, or even a high amount of, effort on behalf of the individual completing the test. The disadvantages of this test are it requires the person administering the test to have a thorough understanding of the methodological limitations and constraints of the test, as well as the ability to respond to the results 'on screen' during the test, in order to satisfy the main assumptions of the test. Regardless, it was found that the NIRS oxidative capacity assessment test-retest reliability was reproducible within the same day, and between different days in young healthy individuals. Furthermore, the results from this study contribute to other studies in determining what the physiological normalisation range should be. Other studies have suggested 30-50% however this study showed that in some cases, 50% was too large of a decrease in muscle oxygenation and a value closer to 30% may be more appropriate in young healthy individuals. Future studies testing the reproducibility and validity of this technique in heart failure patients is the logical next step in determining a non-invasive way to detect skeletal muscle dysfunction in heart failure patients.

To conclude, computational models are simplifications of complex systems, nevertheless, they can provide useful insights into the normal and physiological functioning of such complex systems that cannot be gained through experimental work, either due to technical limitations or ethical issues. A sufficiently detailed model, which has been validated under a wide range of physiological and pathological conditions, may be able to relate skeletal muscle oxygenation dynamics to exercise intolerance mechanisms in heart failure. Consequently, the models presented in this thesis could

assist in tailoring interventional treatments and in assessing the efficacy of such treatments. As such, their continued development and verification are an important direction for future research. In addition, although the applications of near infrared spectroscopy presented in this thesis have several limitations, this is inherent with all non-invasive investigations, and has the advantage of being relatively easily to apply in clinical settings. Therefore, despite its inherent limitations, near infrared spectroscopy represents an important technique that is valuable and practical in research and clinical settings.

Reference list

Abraham, W. T. and Hayes, D. L. (2003) 'Cardiac Resynchronization Therapy for Heart Failure.' *Circulation*, 108(21) pp. 2596–2603.

Abraham, W. T., Young, J. B., León, A. R., Adler, S., Bank, A. J., Hall, S. A., Lieberman, R., Liem, L. B., O'Connell, J. B., Schroeder, J. S. and Wheelan, K. R. (2004) 'Effects of Cardiac Resynchronization on Disease Progression in Patients With Left Ventricular Systolic Dysfunction, an Indication for an Implantable Cardioverter-Defibrillator, and Mildly Symptomatic Chronic Heart Failure.' *Circulation*, 110(18) pp. 2864–2868.

Adami, A., Cao, R., Porszasz, J., Casaburi, R. and Rossiter, H. B. (2017) 'Reproducibility of NIRS assessment of muscle oxidative capacity in smokers with and without COPD.' *Respiratory Physiology & Neurobiology*, 235, January, pp. 18–26.

Adami, A. and Rossiter, H. (2017) 'Principles, Insights and Potential Pitfalls of the Non-Invasive Determination of Muscle Oxidative Capacity by Near-Infrared Spectroscopy.' *Journal of Applied Physiology*, 124, July, pp. 245–248.

Allen, D. G., Lamb, G. D. and Westerblad, H. (2008) 'Skeletal muscle fatigue: cellular mechanisms.' *Physiological Reviews*, 88(1) pp. 287–332.

Armstrong, R. B. and Laughlin, M. H. (1985) 'Rat muscle blood flows during high-speed locomotion.' *Journal of Applied Physiology (Bethesda, Md.: 1985)*, 59(4) pp. 1322–1328.

Astorino, T. A. (2008) 'Alterations in VO2max and the VO2 plateau with manipulation of sampling interval.' *Clinical Physiology and Functional Imaging*, 29(1) pp. 60–67.

Astorino, T. A., Robergs, R. A., Ghiasvand, F., Marks, D. and Burns, S. (2000) 'Incidence of the oxygen plateau at VO2max during exercise testing to volitional fatigue.' *Journal of Exercise Physiology Online*, 3 pp. 1–12.

Auricchio, A. and Prinzen, F. W. (2011) 'Non-Responders to Cardiac Resynchronization Therapy.' *Circulation Journal*, 75(3) pp. 521–527.

Auricchio, A., Stellbrink, C., Sack, S., Block, M., Vogt, J., Bakker, P., Huth, C., Schöndube, F., Wolfhard, U., Böcker, D., Krahnefeld, O., Kirkels, H. and Pacing Therapies in Congestive Heart Failure (PATH-CHF) Study Group (2002) 'Long-term clinical effect of hemodynamically optimized cardiac resynchronization therapy in patients with heart failure and ventricular conduction delay.' *Journal of the American College of Cardiology*, 39(12) pp. 2026–2033.

Auricchio, A., Stellbrink, C., Sack, S., Block, M., Vogt, J., Bakker, P., Mortensen, P. and Klein, H. (1999) 'The Pacing Therapies for Congestive Heart Failure (PATH-CHF) study: rationale, design, and endpoints of a

prospective randomized multicenter study.' *The American Journal of Cardiology*, 83(5B) pp. 130D-135D.

Baker, C. H. and Davis, D. L. (1974) 'Isolated skeletal muscle blood flow and volume changes during contractile activity.' *Blood Vessels*, 11(1–2) pp. 32–44.

Baker, J. S., McCormick, M. C. and Robergs, R. A. (2010) 'Interaction among Skeletal Muscle Metabolic Energy Systems during Intense Exercise.' *Journal of Nutrition and Metabolism*, 2010.

Bangsbo, J., Krustrup, P., González-Alonso, J., Boushel, R. and Saltin, B. (2000) 'Muscle oxygen kinetics at onset of intense dynamic exercise in humans.' *American Journal of Physiology. Regulatory, Integrative and Comparative Physiology*, 279(3) pp. R899-906.

Barroco, A. C., Sperandio, P. A., Reis, M., Almeida, D. R. and Neder, J. A. (2017) 'A practical approach to assess leg muscle oxygenation during ramp-incremental cycle ergometry in heart failure.' *Brazilian Journal of Medical and Biological Research*, 50(12).

Barstow, T. J., Jones, A. M., Nguyen, P. H. and Casaburi, R. (2000) 'Influence of Muscle Fibre Type and Fitness on the Oxygen Uptake/Power Output Slope During Incremental Exercise in Humans.' *Experimental Physiology*, 85(1) pp. 109–116.

Barstow, T. J., Lamarra, N. and Whipp, B. J. (1990) 'Modulation of muscle and pulmonary O2 uptakes by circulatory dynamics during exercise.' *Journal of Applied Physiology (Bethesda, Md.: 1985)*, 68(3) pp. 979–989.

Barstow, T. J. and Molé, P. A. (1987) 'Simulation of pulmonary O2 uptake during exercise transients in humans.' *Journal of Applied Physiology (Bethesda, Md.: 1985)*, 63(6) pp. 2253–2261.

Beaver, W. L., Lamarra, N. and Wasserman, K. (1981) 'Breath-by-breath measurement of true alveolar gas exchange.' *Journal of Applied Physiology: Respiratory, Environmental and Exercise Physiology*, 51(6) pp. 1662–1675.

Behnke, B. J., Delp, M. D., McDonough, P., Spier, S. A., Poole, D. C. and Musch, T. I. (2004) 'Effects of chronic heart failure on microvascular oxygen exchange dynamics in muscles of contrasting fiber type.' *Cardiovascular Research*, 61(2) pp. 325–332.

Behnke, B. J., Kindig, C. A., Musch, T. I., Sexton, W. L. and Poole, D. C. (2002) 'Effects of prior contractions on muscle microvascular oxygen pressure at onset of subsequent contractions.' *The Journal of Physiology*, 539(Pt 3) pp. 927–934.

Behnke, B. J., McDonough, P., Padilla, D. J., Musch, T. I. and Poole, D. C. (2003) 'Oxygen Exchange Profile in Rat Muscles of Contrasting Fibre Types.' *The Journal of Physiology*, 549(2) pp. 597–605.

Belardinelli, R., Barstow, T. J., Nguyen, P. and Wasserman, K. (1997) 'Skeletal muscle oxygenation and oxygen uptake kinetics following constant work rate exercise in chronic congestive heart failure.' *The American Journal of Cardiology*, 80(10) pp. 1319–1324.

Bellotti, C., Calabria, E., Capelli, C. and Pogliaghi, S. (2013) 'Determination of Maximal Lactate Steady State in Healthy Adults: Can NIRS Help?' *Medicine & Science in Sports & Exercise*, 45(6) p. 1208.

Beltz, N. M., Gibson, A. L., Janot, J. M., Kravitz, L., Mermier, C. M. and Dalleck, L. C. (2016) 'Graded Exercise Testing Protocols for the Determination of VO2max: Historical Perspectives, Progress, and Future Considerations.' *Journal of Sports Medicine*, 2016.

Benson, A. P., Bowen, T. S., Ferguson, C., Murgatroyd, S. R. and Rossiter, H. B. (2017) 'Data collection, handling, and fitting strategies to optimize accuracy and precision of oxygen uptake kinetics estimation from breath-by-breath measurements.' *Journal of Applied Physiology*, 123(1) pp. 227–242.

Benson, A. P., Grassi, B. and Rossiter, H. B. (2013) 'A validated model of oxygen uptake and circulatory dynamic interactions at exercise onset in humans.' *Journal of Applied Physiology (Bethesda, Md.: 1985)*, 115(5) pp. 743–755.

Birnie, D. H. and Tang, A. S. (2006) 'The problem of non-response to cardiac resynchronization therapy.' *Current Opinion in Cardiology*, 21(1) pp. 20–26.

Blix, A. S. (2018) 'Adaptations to deep and prolonged diving in phocid seals.' *Journal of Experimental Biology*, 221(12) p. jeb182972.

Boone, J., Barstow, T. J., Celie, B., Prieur, F. and Bourgois, J. (2015) 'The impact of pedal rate on muscle oxygenation, muscle activation and whole-body VO2 during ramp exercise in healthy subjects.' *European Journal of Applied Physiology*, 115(1) pp. 57–70.

Boone, J., Bouckaert, J., Barstow, T. J. and Bourgois, J. (2012) 'Influence of priming exercise on muscle deoxy[Hb + Mb] during ramp cycle exercise.' *European Journal of Applied Physiology*, 112(3) pp. 1143–1152.

Boone, J., Koppo, K., Barstow, T. and Bouckaert, J. (2009) 'Pattern of deoxy[Hb + Mb] during ramp cycle exercise: Influence of aerobic fitness status.' *European journal of applied physiology*, 105, February, pp. 851–9.

Boone, J., Koppo, K., Barstow, T. and Bouckaert, J. (2010) 'Effect of exercise protocol on deoxy[Hb+Mb]: incremental step versus ramp exercise.' *MEDICINE AND SCIENCE IN SPORTS AND EXERCISE*, 42(5) pp. 935–942.

Boone, J., Koppo, K. and Bouckaert, J. (2008) 'The V˙O2 response to submaximal ramp cycle exercise: Influence of ramp slope and training status.' *Respiratory Physiology & Neurobiology*, 161(3) pp. 291–297.

Boone, J., Vandekerckhove, K., Coomans, I., Prieur, F. and Bourgois, J. G. (2016) 'An integrated view on the oxygenation responses to incremental exercise at the brain, the locomotor and respiratory muscles.' *European Journal of Applied Physiology*, 116(11–12) pp. 2085–2102.

Boushel, R., Langberg, H., Olesen, J., Gonzales-Alonzo, J., Bülow, J. and Kjaer, M. (2001) 'Monitoring tissue oxygen availability with near infrared spectroscopy (NIRS) in health and disease.' *Scandinavian Journal of Medicine & Science in Sports*, 11(4) pp. 213–222.

Boushel, R., Pott, F., Madsen, P., Rådegran, G., Nowak, M., Quistorff, B. and Secher, N. (1998) 'Muscle metabolism from near infrared spectroscopy during rhythmic handgrip in humans.' *European Journal of Applied Physiology and Occupational Physiology*, 79(1) pp. 41–48.

Bowen, T. S., Cannon, D. T., Murgatroyd, S. R., Birch, K. M., Witte, K. K. and Rossiter, H. B. (2012) 'The intramuscular contribution to the slow oxygen uptake kinetics during exercise in chronic heart failure is related to the severity of the condition.' *Journal of Applied Physiology*, 112(3) pp. 378–387.

Bredy, C., Ministeri, M., Kempny, A., Alonso-Gonzalez, R., Swan, L., Uebing, A., Diller, G.-P., Gatzoulis, M. A. and Dimopoulos, K. (2018) 'New York Heart Association (NYHA) classification in adults with congenital heart disease: relation to objective measures of exercise and outcome.' *European Heart Journal. Quality of Care & Clinical Outcomes*, 4(1) pp. 51–58.

Bristow, M. R., Krueger, S., Carson, P. and White, B. G. (2004) 'Cardiac-Resynchronization Therapy with or without an Implantable Defibrillator in Advanced Chronic Heart Failure.' *The New England Journal of Medicine* p. 11.

Brizendine, J. T., Ryan, T. E., Larson, R. D. and McCULLY, K. K. (2013) 'Skeletal Muscle Metabolism in Endurance Athletes with Near-Infrared Spectroscopy:' *Medicine & Science in Sports & Exercise*, 45(5) pp. 869–875.

van den Broek, N. M. A., De Feyter, H. M. M. L., de Graaf, L., Nicolay, K. and Prompers, J. J. (2007) 'Intersubject differences in the effect of acidosis on phosphocreatine recovery kinetics in muscle after exercise are due to differences in proton efflux rates.' *American Journal of Physiology. Cell Physiology*, 293(1) pp. C228-237.

Broxterman, R. M., Ade, C. J., Craig, J. C., Wilcox, S. L., Schlup, S. J. and Barstow, T. J. (2015) 'The relationship between critical speed and the respiratory compensation point: Coincidence or equivalence.' *European Journal of Sport Science*, 15(7) pp. 631–639.

Buchfuhrer, M. J., Hansen, J. E., Robinson, T. E., Sue, D. Y., Wasserman, K. and Whipp, B. J. (1983) 'Optimizing the exercise protocol for cardiopulmonary assessment.' *Journal of Applied Physiology: Respiratory, Environmental and Exercise Physiology*, 55(5) pp. 1558–1564.

Buchheit, M., Ufland, P., Haydar, B., Laursen, P. B. and Ahmaidi, S. (2011) 'Reproducibility and sensitivity of muscle reoxygenation and oxygen uptake recovery kinetics following running exercise in the field.' *Clinical Physiology and Functional Imaging*, 31(5) pp. 337–346.

Burnley, M., Doust, J. H., Ball, D. and Jones, A. M. (2002) 'Effects of prior heavy exercise onV˙o 2 kinetics during heavy exercise are related to changes in muscle activity.' *Journal of Applied Physiology*, 93(1) pp. 167–174.

Cahalin, L. P., Mathier, M. A., Semigran, M. J., Dec, G. W. and DiSalvo, T. G. (1996) 'The Six-Minute Walk Test Predicts Peak Oxygen Uptake and Survival in Patients With Advanced Heart Failure.' *Chest*, 110(2) pp. 325–332.

Cazeau, S., Varma, C. and Haywood, G. A. (2001) 'Effects of Multisite Biventricular Pacing in Patients with Heart Failure and Intraventricular Conduction Delay.' *The New England Journal of Medicine* p. 8.

Cerretelli, P. and Di Prampero, R. E. (1987) 'Gas exchange in exercise. In handbook of physiology. The respiratory system gas exchange.' *Section 3*, 4, January, pp. 297–339.

Cerretelli, P., Grassi, B., Colombini, A., Carù, B. and Marconi, C. (1988) 'Gas exchange and metabolic transients in heart transplant recipients.' *Respiration Physiology*, 74(3) pp. 355–371.

Chaggar, P. S., Malkin, C. J., Shaw, S. M., Williams, S. G. and Channer, K. S. (2009) 'Neuroendocrine Effects on the Heart and Targets for Therapeutic Manipulation in Heart Failure.' *Cardiovascular Therapeutics*, 27(3) pp. 187–193.

Chance, B., T Dait, M., Zhang, C., Hamaoka, T. and Hagerman, F. (1992) 'Recovery from Exercise-Induced Desaturation in the Quadriceps Muscles of Elite Competitive Rowers.' *The American journal of physiology*, 262, April, pp. C766-75.

Chin, L. M. K., Kowalchuk, J. M., Barstow, T. J., Kondo, N., Amano, T., Shiojiri, T. and Koga, S. (2011) 'The relationship between muscle deoxygenation and activation in different muscles of the quadriceps during cycle ramp exercise.' *Journal of Applied Physiology*, 111(5) pp. 1259–1265.

Chung, S., Nelson, M. D., Hamaoka, T., Jacobs, R. A., Pearson, J., Subudhi, A. W., Jenkins, N. T., Bartlett, M. F., Fitzgerald, L. F., Miehm, J. D., Kent, J. A., Lucero, A. A., Rowlands, D. S., Stoner, L., McCully, K. K., Call, J., Rodriguez-Miguelez, P., Harris, R. A., Porcelli, S., Rasica, L., Marzorati, M.,

Quaresima, V., Ryan, T. E., Vernillo, G., Millet, G. P., Malatesta, D., Millet, G. Y., Zuo, L. and Chuang, C.-C. (2018) 'Commentaries on Viewpoint: Principles, insights, and potential pitfalls of the noninvasive determination of muscle oxidative capacity by near-infrared spectroscopy.' *Journal of Applied Physiology (Bethesda, Md.: 1985)*, 124(1) pp. 249–255.

Clark, A. L., Poole-Wilson, P. A. and Coats, A. J. (1996) 'Exercise limitation in chronic heart failure: central role of the periphery.' *Journal of the American College of Cardiology*, 28(5) pp. 1092–1102.

Cleland, J. G. F., Daubert, J. C., Erdmann, E., Freemantle, N., Gras, D., Kappenberger, L., Klein, W. and Tavazzi, L. (2001) 'The CARE-HF study (CArdiac REsynchronisation in Heart Failure study): rationale, design and end-points.' *European Journal of Heart Failure*, 3(4) pp. 481–489.

Coats, A. J. S. (2004) 'Anaemia and heart failure.' *Heart*, 90(9) pp. 977–979.

Coggan, A. R., Abduljalil, A. M., Swanson, S. C., Earle, M. S., Farris, J. W., Mendenhall, L. A. and Robitaille, P. M. (1993) 'Muscle metabolism during exercise in young and older untrained and endurance-trained men.' *Journal of Applied Physiology*, 75(5) pp. 2125–2133.

Conley, K. E., Jubrias, S. A. and Esselman, P. C. (2000) 'Oxidative capacity and ageing in human muscle.' *The Journal of Physiology*, 526(1) pp. 203–210.

Costes, F., Barthelemy, J. C., Feasson, L., Busso, T., Geyssant, A. and Denis, C. (1996) 'Comparison of muscle near-infrared spectroscopy and femoral blood gases during steady-state exercise in humans.' *Journal of Applied Physiology*, 80(4) pp. 1345–1350.

Cowie, M. R. (2000) 'Survival of patients with a new diagnosis of heart failure: a population based study.' *Heart*, 83(5) pp. 505–510.

Craig, J. C., Broxterman, R. M. and Barstow, T. J. (2015) 'Considerations for Identifying the Boundaries of Sustainable Performance.' *Medicine & Science in Sports & Exercise*, 47(9) p. 1997.

Crisafulli, A., Tangianu, F., Tocco, F., Concu, A., Mameli, O., Mulliri, G. and Caria, M. A. (2011) 'Ischemic preconditioning of the muscle improves maximal exercise performance but not maximal oxygen uptake in humans.' *Journal of Applied Physiology*, 111(2) pp. 530–536.

Crow, M. T. and Kushmerick, M. J. (1982) 'Chemical energetics of slow- and fast-twitch muscles of the mouse.' *The Journal of General Physiology*, 79(1) pp. 147–166.

Davis, J. A., Whipp, B. J., Lamarra, N., Huntsman, D. J., Frank, M. H. and Wasserman, K. (1982) 'Effect of ramp slope on determination of aerobic parameters from the ramp exercise test.' *Medicine and Science in Sports and Exercise*, 14(5) pp. 339–343.

Davis, M. and Barstow, T. (2013) ‘Estimated Contribution of Hemoglobin and Myoglobin to Near Infrared Spectroscopy.’ *Respiratory physiology & neurobiology*, 186, January.

De Blasi, R. A., Almenrader, N., Aurisicchio, P. and Ferrari, M. (1997) ‘Comparison of two methods of measuring forearm oxygen consumption (VO2) by near infrared spectroscopy.’ *Journal of Biomedical Optics*, 2(2) pp. 171–175.

De Cort, S. C., Innes, J. A., Barstow, T. J. and Guz, A. (1991) ‘Cardiac output, oxygen consumption and arteriovenous oxygen difference following a sudden rise in exercise level in humans.’ *The Journal of Physiology*, 441, September, pp. 501–512.

DeLorey, D. S., Kowalchuk, J. M. and Paterson, D. H. (2003) ‘Relationship between pulmonary O2 uptake kinetics and muscle deoxygenation during moderate-intensity exercise.’ *Journal of Applied Physiology (Bethesda, Md.: 1985)*, 95(1) pp. 113–120.

Delpy, D. T., Cope, M., Zee, P. van der, Arridge, S., Wray, S. and Wyatt, J. (1988) ‘Estimation of optical pathlength through tissue from direct time of flight measurement.’ *Physics in Medicine & Biology*, 33(12) p. 1433.

Demarle, A. P., Slawinski, J. J., Laffite, L. P., Bocquet, V. G., Koralsztein, J. P. and Billat, V. L. (2001) ‘Decrease of O2 deficit is a potential factor in increased time to exhaustion after specific endurance training.’ *Journal of Applied Physiology*, 90(3) pp. 947–953.

Diederich, E. R., Behnke, B. J., McDonough, P., Kindig, C. A., Barstow, T. J., Poole, D. C. and Musch, T. I. (2002) ‘Dynamics of microvascular oxygen partial pressure in contracting skeletal muscle of rats with chronic heart failure.’ *Cardiovascular Research*, 56(3) pp. 479–486.

DiMenna, F. J., Bailey, S. J. and Jones, A. M. (2010) ‘Influence of body position on muscle deoxy[Hb+Mb] during ramp cycle exercise.’ *Respiratory Physiology & Neurobiology*, 173(2) pp. 138–145.

Drexler, H., Riede, U., Münzel, T., König, H., Funke, E. and Just, H. (1992) ‘Alterations of skeletal muscle in chronic heart failure.’ *Circulation*, 85(5) pp. 1751–1759.

Dunn, J.-O., Mythen, M. G. and Grocott, M. P. (2016) ‘Physiology of oxygen transport.’ *BJA Education*, 16(10) pp. 341–348.

Duteil, S., Bourrilhon, C., S Raynaud, J., Wary, C., S Richardson, R., Leroy-Willig, A., C Jouanin, J., Guezennec, C. and G Carlier, P. (2005) ‘Metabolic and vascular support for the role of myoglobin in humans: A multiparametric NMR study.’ *American journal of physiology. Regulatory, integrative and comparative physiology*, 287, January, pp. R1441-9.

Esaki, K., Hamaoka, T., Rådegran, G., Boushel, R., Hansen, J., Katsumura, T., Haga, S. and Mizuno, M. (2005) 'Association between regional quadriceps oxygenation and blood oxygen saturation during normoxic one-legged dynamic knee extension.' *European Journal of Applied Physiology*, 95(4) p. 361.

Faggiano, P., D'Aloia, A., Gualeni, A. and Giordano, A. (2001) 'Relative contribution of resting haemodynamic profile and lung function to exercise tolerance in male patients with chronic heart failure.' *Heart*, 85(2) pp. 179–184.

Faulkner, J., Heigenhauser, G. and Schork, M. (1977) 'The cardiac output-oxygen uptake relationship of men during graded bicycle ergometry.' *Medicine and science in sports*, 9, February, pp. 148–54.

Ferrari, M., Muthalib, M. and Quaresima, V. (2011) 'The use of near-infrared spectroscopy in understanding skeletal muscle physiology: recent developments.' *Philosophical Transactions of the Royal Society A: Mathematical, Physical and Engineering Sciences*, 369(1955) pp. 4577–4590.

Ferreira, Hageman, K. S., Hahn, S. A., Williams, J., Padilla, D. J., Poole, D. C. and Musch, T. I. (2006) 'Muscle microvascular oxygenation in chronic heart failure: role of nitric oxide availability.' *Acta Physiologica (Oxford, England)*, 188(1) pp. 3–13.

Ferreira, L. F., Koga, S. and Barstow, T. J. (2007) 'Dynamics of noninvasively estimated microvascular O2 extraction during ramp exercise.' *Journal of Applied Physiology*, 103(6) pp. 1999–2004.

Ferreira, L. F., McDonough, P., Behnke, B. J., Musch, T. I. and Poole, D. C. (2006) 'Blood flow and O2 extraction as a function of O2 uptake in muscles composed of different fiber types.' *Respiratory Physiology & Neurobiology*, 153(3) pp. 237–249.

Ferreira, L. F., Poole, D. C. and Barstow, T. J. (2005) 'Muscle blood flow–O2 uptake interaction and their relation to on-exercise dynamics of O2 exchange.' *Respiratory Physiology & Neurobiology*, 147(1) pp. 91–103.

Ferreira, McDonough, P., Behnke, B. J., Musch, T. I. and Poole, D. C. (2006) 'Blood flow and O2 extraction as a function of O2 uptake in muscles composed of different fiber types.' *Respiratory Physiology & Neurobiology*, 153(3) pp. 237–249.

Fontana, F. Y., Keir, D. A., Bellotti, C., De Roia, G. F., Murias, J. M. and Pogliaghi, S. (2015) 'Determination of respiratory point compensation in healthy adults: Can non-invasive near-infrared spectroscopy help?' *Journal of Science and Medicine in Sport*, 18(5) pp. 590–595.

Forbes, S. C., Paganini, A. T., Slade, J. M., Towse, T. F. and Meyer, R. A. (2009) 'Phosphocreatine recovery kinetics following low- and high-intensity

exercise in human triceps surae and rat posterior hindlimb muscles.' *American Journal of Physiology - Regulatory, Integrative and Comparative Physiology*, 296(1) pp. R161–R170.

Fox, D. J., Fitzpatrick, A. P. and Davidson, N. C. (2005) 'Optimisation of cardiac resynchronisation therapy: addressing the problem of "non-responders."' *Heart*, 91(8) pp. 1000–1002.

Franciosa, J. A., Park, M. and Levine, T. B. (1981) 'Lack of correlation between exercise capacity and indexes of resting left ventricular performance in heart failure.' *The American Journal of Cardiology*, 47(1) pp. 33–39.

Francis, D. (2000) 'Cardiopulmonary exercise testing for prognosis in chronic heart failure: continuous and independent prognostic value from VE/VCO2slope and peak VO2.' *European Heart Journal*, 21(2) pp. 154–161.

Francis, D. P., Davies, L. C., Willson, K., Piepoli, M., Seydnejad, S. R., Ponikowski, P. and Coats, A. J. S. (1999) 'Impact of periodic breathing on V̇O2 and V̇CO2: a quantitative approach by Fourier analysis.' *Respiration Physiology*, 118(2) pp. 247–255.

Geer, C. M., Behnke, B. J., McDonough, P. and Poole, D. C. (2002) 'Dynamics of microvascular oxygen pressure in the rat diaphragm.' *Journal of Applied Physiology*, 93(1) pp. 227–232.

Geraskin, D., Platen, P., Franke, J. and Kohl-Bareis, M. (2007) 'Algorithms for Muscle Oxygenation Monitoring Corrected for Adipose Tissue Thickness.' *In* Buzug, T. M., Holz, D., Bongartz, J., Kohl-Bareis, M., Hartmann, U., and Weber, S. (eds) *Advances in Medical Engineering*. Springer Berlin Heidelberg (Springer Proceedings in Physics), pp. 384–388.

Gerbino, A., Ward, S. A. and Whipp, B. J. (1996) 'Effects of prior exercise on pulmonary gas-exchange kinetics during high-intensity exercise in humans.' *Journal of Applied Physiology (Bethesda, Md.: 1985)*, 80(1) pp. 99–107.

Gollnick, P. D., Armstrong, R. B., Saltin, B., Saubert, C. W., Sembrowich, W. L. and Shepherd, R. E. (1973) 'Effect of training on enzyme activity and fiber composition of human skeletal muscle.' *Journal of Applied Physiology*, 34(1) pp. 107–111.

Gomides, R. S., Dias, R. M. R., Souza, D. R., Costa, L. a. R., Ortega, K. C., Mion, D., Tinucci, T. and de Moraes Forjaz, C. L. (2010) 'Finger blood pressure during leg resistance exercise.' *International Journal of Sports Medicine*, 31(8) pp. 590–595.

Goodwin, M. L., Hernández, A., Lai, N., Cabrera, M. E. and Gladden, L. B. (2011) 'V̇o2 on-kinetics in isolated canine muscle in situ during slowed convective O2 delivery.' *Journal of Applied Physiology*, 112(1) pp. 9–19.

Gordon, D., Mehter, M., Gernigon, M., Caddy, O., Keiller, D. and Barnes, R. (2012) 'The effects of exercise modality on the incidence of plateau at V·O2max.' *Clinical physiology and functional imaging*, 32, September, pp. 394–9.

Grassi, B. (2005) 'Delayed metabolic activation of oxidative phosphorylation in skeletal muscle at exercise onset.' *Medicine and Science in Sports and Exercise*, 37(9) pp. 1567–1573.

Grassi, B., Gladden, L. B., Samaja, M., Stary, C. M. and Hogan, M. C. (1998) 'Faster adjustment of O2delivery does not affect V˙o 2 on-kinetics in isolated in situ canine muscle.' *Journal of Applied Physiology*, 85(4) pp. 1394–1403.

Grassi, B., Hogan, M. C., Greenhaff, P. L., Hamann, J. J., Kelley, K. M., Aschenbach, W. G., Constantin-Teodosiu, D. and Gladden, L. B. (2002) 'Oxygen uptake on-kinetics in dog gastrocnemius in situ following activation of pyruvate dehydrogenase by dichloroacetate.' *The Journal of Physiology*, 538(Pt 1) pp. 195–207.

Grassi, B., Marconi, C., Meyer, M., Rieu, M. and Cerretelli, P. (1997) 'Gas exchange and cardiovascular kinetics with different exercise protocols in heart transplant recipients.' *Journal of Applied Physiology*, 82(6) pp. 1952–1962.

Grassi, B., Pogliaghi, S., Rampichini, S., Quaresima, V., Ferrari, M., Marconi, C. and Cerretelli, P. (2003) 'Muscle oxygenation and pulmonary gas exchange kinetics during cycling exercise on-transitions in humans.' *Journal of Applied Physiology*, 95(1) pp. 149–158.

Grassi, B., Poole, D. C., Richardson, R. S., Knight, D. R., Erickson, B. K. and Wagner, P. D. (1996) 'Muscle O2 uptake kinetics in humans: implications for metabolic control.' *Journal of Applied Physiology (Bethesda, Md.: 1985)*, 80(3) pp. 988–998.

Grassi, B. and Quaresima, V. (2016) 'Near-infrared spectroscopy and skeletal muscle oxidative function in vivo in health and disease: A review from an exercise physiology perspective.' *Journal of Biomedical Optics*, 21, July, p. 091313.

Grassi, B., Rossiter, H. B., Hogan, M. C., Howlett, R. A., Harris, J. E., Goodwin, M. L., Dobson, J. L. and Gladden, L. B. (2011) 'Faster O2 uptake kinetics in canine skeletal muscle in situ after acute creatine kinase inhibition.' *The Journal of Physiology*, 589(Pt 1) pp. 221–233.

Hamaoka, T., Iwane, H., Shimomitsu, T., Katsumura, T., Murase, N., Nishio, S., Osada, T., Kurosawa, Y. and Chance, B. (1996) 'Noninvasive measures of oxidative metabolism on working human muscles by near-infrared spectroscopy.' *Journal of Applied Physiology*, 81(3) pp. 1410–1417.

Hansen, J. E., Casaburi, R., Cooper, D. M. and Wasserman, K. (1988) 'Oxygen uptake as related to work rate increment during cycle ergometer exercise.' *European Journal of Applied Physiology and Occupational Physiology*, 57(2) pp. 140–145.

Hansen, J. E., Sue, D. Y., Oren, A. and Wasserman, K. (1987) 'Relation of oxygen uptake to work rate in normal men and men with circulatory disorders.' *The American Journal of Cardiology*, 59(6) pp. 669–674.

Harper, A. J., Ferreira, L. F., Lutjemeier, B. J., Townsend, D. K. and Barstow, T. J. (2008) 'Matching of blood flow to metabolic rate during recovery from moderate exercise in humans.' *Experimental Physiology*, 93(10) pp. 1118–1125.

Haseler, L. J., Lin, A. P. and Richardson, R. S. (2004) 'Skeletal muscle oxidative metabolism in sedentary humans: 31P-MRS assessment of O2 supply and demand limitations.' *Journal of Applied Physiology*, 97(3) pp. 1077–1081.

Heinonen, I., Koga, S., Kalliokoski, K. K., Musch, T. I. and Poole, D. C. (2015) 'Heterogeneity of Muscle Blood Flow and Metabolism: Influence of Exercise, Aging and Disease States.' *Exercise and sport sciences reviews*, 43(3) pp. 117–124.

Hepple, R. T., Liu, P. P., Plyley, M. J. and Goodman, J. M. (1999) 'Oxygen uptake kinetics during exercise in chronic heart failure: influence of peripheral vascular reserve' p. 9.

Higginbotham, M. B., Morris, K. G., Williams, R. S., McHale, P. A., Coleman, R. E. and Cobb, F. R. (1986) 'Regulation of stroke volume during submaximal and maximal upright exercise in normal man.' *Circulation Research*, 58(2) pp. 281–291.

Higgins, S. L., Hummel, J. D., Niazi, I. K., Giudici, M. C., Worley, S. J., Saxon, L. A., Boehmer, J. P., Higginbotham, M. B., De Marco, T., Foster, E. and Yong, P. G. (2003) 'Cardiac resynchronization therapy for the treatment of heart failure in patients with intraventricular conduction delay and malignant ventricular tachyarrhythmias.' *Journal of the American College of Cardiology*, 42(8) pp. 1454–1459.

Hirai, D. M., Craig, J. C., Colburn, T. D., Eshima, H., Kano, Y., Sexton, W. L., Musch, T. I. and Poole, D. C. (2018) 'Skeletal muscle microvascular and interstitial from rest to contractions.' *The Journal of Physiology*, 596(5) pp. 869–883.

Hirai, D. M., Musch, T. I. and Poole, D. C. (2015) 'Exercise training in chronic heart failure: improving skeletal muscle O2 transport and utilization.' *American Journal of Physiology-Heart and Circulatory Physiology*, 309(9) pp. H1419–H1439.

Hobbs, F. D. R., Roalfe, A. K., Davis, R. C., Davies, M. K. and Hare, R. (2007) 'Prognosis of all-cause heart failure and borderline left ventricular systolic dysfunction: 5 year mortality follow-up of the Echocardiographic Heart of England Screening Study (ECHOES).' *European Heart Journal*, 28(9) pp. 1128–1134.

Hoffmann, U., Drescher, U., Benson, A. P., Rossiter, H. B. and Essfeld, D. (2013) 'Skeletal muscle VO_2 kinetics from cardio-pulmonary measurements: assessing distortions through O_2 transport by means of stochastic work-rate signals and circulatory modelling.' *European Journal of Applied Physiology*, 113(7) pp. 1745–1754.

Hogan, M. C. (2001) 'Fall in intracellular PO(2) at the onset of contractions in Xenopus single skeletal muscle fibers.' *Journal of Applied Physiology (Bethesda, Md.: 1985)*, 90(5) pp. 1871–1876.

Holloszy, J. O. (1967) 'Biochemical adaptations in muscle. Effects of exercise on mitochondrial oxygen uptake and respiratory enzyme activity in skeletal muscle.' *The Journal of Biological Chemistry*, 242(9) pp. 2278–2282.

Holloszy, J. O., Oscai, L. B., Don, I. J. and Molé, P. A. (1970) 'Mitochondrial citric acid cycle and related enzymes: adaptive response to exercise.' *Biochemical and Biophysical Research Communications*, 40(6) pp. 1368–1373.

Hsia, D., Casaburi, R., Pradhan, A., Torres, E. and Porszasz, J. (2009) 'Physiological responses to linear treadmill and cycle ergometer exercise in COPD.' *European Respiratory Journal*, 34(3) pp. 605–615.

Hughson, R. L. (1984) 'Alterations in the oxygen deficit-oxygen debt relationships with beta-adrenergic receptor blockade in man.' *The Journal of Physiology*, 349, April, pp. 375–387.

Hughson, R. L. and Morrissey, M. (1982) 'Delayed kinetics of respiratory gas exchange in the transition from prior exercise.' *Journal of Applied Physiology: Respiratory, Environmental and Exercise Physiology*, 52(4) pp. 921–929.

Hughson, R. L., Tschakovsky, M. E. and Houston, M. E. (2001) 'Regulation of Oxygen Consumption at the Onset of Exercise.' *Exercise and Sport Sciences Reviews*, 29(3) p. 129.

Jöbsis, F. F. (1977) 'Noninvasive, infrared monitoring of cerebral and myocardial oxygen sufficiency and circulatory parameters.' *Science (New York, N.Y.)*, 198(4323) pp. 1264–1267.

Jones, A. M., Campbell, I. T. and Pringle, J. S. M. (2004) 'Influence of muscle fibre type and pedal rate on the<Emphasis Type="Italic"> V̇</Emphasis>O<Subscript>2</Subscript>-work rate slope during ramp exercise.' *European Journal of Applied Physiology*, 91(2–3) pp. 238–245.

Jones, A. M., Grassi, B., Christensen, P. M., Krustrup, P., Bangsbo, J. and Poole, D. C. (2011) 'Slow component of VO2 kinetics: mechanistic bases and practical applications.' *Medicine and Science in Sports and Exercise*, 43(11) pp. 2046–2062.

Jones, A. M. and Poole, D. C. (2005) 'Oxygen Uptake Kinetics in Sport, Exercise and Medicine.' *Journal of Sports Science & Medicine*, 4(1) p. 84.

Jones, S., Elliott, P., Sharma, S., McKenna, W. and Whipp, B. (1998) 'Cardiopulmonary responses to exercise in patients with hypertrophic cardiomyopathy.' *Heart*, 80(1) pp. 60–67.

Joseph, A.-M., Joanisse, D. R., Baillot, R. G. and Hood, D. A. (2012) *Mitochondrial Dysregulation in the Pathogenesis of Diabetes: Potential for Mitochondrial Biogenesis-Mediated Interventions*. Journal of Diabetes Research. [Online] [Accessed on 1st September 2018] https://www.hindawi.com/journals/jdr/2012/642038/.

Kass, D. A., Chen, C.-H., Curry, C., Talbot, M., Berger, R., Fetics, B. and Nevo, E. (1999) 'Improved Left Ventricular Mechanics From Acute VDD Pacing in Patients With Dilated Cardiomyopathy and Ventricular Conduction Delay.' *Circulation*, 99(12) pp. 1567–1573.

Keir, D. A., Fontana, F. Y., Robertson, T. C., Murias, J. M., Paterson, D. H., Kowalchuk, J. M. and Pogliaghi, S. (2015) 'Exercise Intensity Thresholds: Identifying the Boundaries of Sustainable Performance.' *Medicine & Science in Sports & Exercise*, 47(9) p. 1932.

Kemp, C. D. and Conte, J. V. (2012) 'The pathophysiology of heart failure.' *Cardiovascular Pathology*, 21(5) pp. 365–371.

Kemps, H. M., Schep, G., Zonderland, M. L., Thijssen, E. J., De Vries, W. R., Wessels, B., Doevendans, P. A. and Wijn, P. F. (2010) 'Are oxygen uptake kinetics in chronic heart failure limited by oxygen delivery or oxygen utilization?' *International Journal of Cardiology*, 142(2) pp. 138–144.

Kindig, C. A., Musch, T. I., Basaraba, R. J. and Poole, D. C. (1999) 'Impaired capillary hemodynamics in skeletal muscle of rats in chronic heart failure.' *Journal of Applied Physiology (Bethesda, Md.: 1985)*, 87(2) pp. 652–660.

Kitzman, D. W. and Groban, L. (2008) 'EXERCISE INTOLERANCE.' *Heart failure clinics*, 4(1) pp. 99–115.

Knight, D., Poole, D., Schaffartzik, W., J Guy, H., Prediletto, R., C Hogan, M. and D Wagner, P. (1992) 'Relationship between body and leg VO2 during maximal cycle ergometry.' *Journal of applied physiology (Bethesda, Md.: 1985)*, 73, October, pp. 1114–21.

Koga, S., Poole, D. C., Ferreira, L. F., Whipp, B. J., Kondo, N., Saitoh, T., Ohmae, E. and Barstow, T. J. (2007) 'Spatial heterogeneity of quadriceps

muscle deoxygenation kinetics during cycle exercise.' *Journal of Applied Physiology*, 103(6) pp. 2049–2056.

Koga, S., Poole, D. C., Fukuoka, Y., Ferreira, L. F., Kondo, N., Ohmae, E. and Barstow, T. J. (2011) 'Methodological validation of the dynamic heterogeneity of muscle deoxygenation within the quadriceps during cycle exercise.' *American Journal of Physiology. Regulatory, Integrative and Comparative Physiology*, 301(2) pp. R534-541.

Koga, S., Rossiter, H. B., Heinonen, I., Musch, T. I. and Poole, D. C. (2014) 'Dynamic Heterogeneity of Exercising Muscle Blood Flow and O2 Utilization.' *Medicine & Science in Sports & Exercise*, 46(5) pp. 860–876.

Koike, A., Hiroe, M., Adachi, H., Yajima, T., Yamauchi, Y., Nogami, A., Ito, H., Miyahara, Y., Korenaga, M. and Marumo, F. (1994) 'Oxygen uptake kinetics are determined by cardiac function at onset of exercise rather than peak exercise in patients with prior myocardial infarction.' *Circulation*, 90(5) pp. 2324–2332.

Krustrup, P., Jones, A. M., Wilkerson, D. P., Calbet, J. a. L. and Bangsbo, J. (2009) 'Muscular and pulmonary O2 uptake kinetics during moderate- and high-intensity sub-maximal knee-extensor exercise in humans.' *The Journal of Physiology*, 587(Pt 8) pp. 1843–1856.

Kubo, S. H., Rector, T. S., Bank, A. J., Williams, R. E. and Heifetz, S. M. (1991) 'Endothelium-dependent vasodilation is attenuated in patients with heart failure.' *Circulation*, 84(4) pp. 1589–1596.

Laaksonen, M. S., Björklund, G., Heinonen, I., Kemppainen, J., Knuuti, J., Kyröläinen, H. and Kalliokoski, K. K. (2010) 'Perfusion heterogeneity does not explain excess muscle oxygen uptake during variable intensity exercise.' *Clinical Physiology and Functional Imaging*, 30(4) pp. 241–249.

Lai, N., Camesasca, M., Saidel, G. M., Dash, R. K. and Cabrera, M. E. (2007) 'Linking Pulmonary Oxygen Uptake, Muscle Oxygen Utilization and Cellular Metabolism during Exercise.' *Annals of biomedical engineering*, 35(6) pp. 956–969.

Lai, N., Dash, R. K., Nasca, M. M., Saidel, G. M. and Cabrera, M. E. (2006) 'Relating pulmonary oxygen uptake to muscle oxygen consumption at exercise onset: in vivo and in silico studies.' *European journal of applied physiology, European journal of applied physiology*, 97, 97(4, 4) pp. 380, 380–394.

Lai, N., Zhou, H., Saidel, G., Wolf, M., Mccully, K., Bruce Gladden, L. and E Cabrera, M. (2009) 'Modeling oxygenation in venous blood and skeletal muscle in response to exercise using near-infrared spectroscopy.' *Journal of applied physiology (Bethesda, Md. : 1985)*, 106, May, pp. 1858–74.

Lamarra, N., Whipp, B. J., Ward, S. A. and Wasserman, K. (1987) 'Effect of interbreath fluctuations on characterizing exercise gas exchange kinetics.' *Journal of Applied Physiology (Bethesda, Md.: 1985)*, 62(5) pp. 2003–2012.

Larson-Meyer, D. E., Newcomer, B. R., Hunter, G. R., Hetherington, H. P. and Weinsier, R. L. (2000) '31P MRS measurement of mitochondrial function in skeletal muscle: reliability, force-level sensitivity and relation to whole body maximal oxygen uptake.' *NMR in biomedicine*, 13(1) pp. 14–27.

Laughlin, M. H. and Armstrong, R. B. (1982) 'Muscular blood flow distribution patterns as a function of running speed in rats.' *American Journal of Physiology-Heart and Circulatory Physiology*, 243(2) pp. H296–H306.

Linde, C., Abraham, W. T., Gold, M. R., St John Sutton, M., Ghio, S., Daubert, C. and REVERSE (REsynchronization reVErses Remodeling in Systolic left vEntricular dysfunction) Study Group (2008) 'Randomized trial of cardiac resynchronization in mildly symptomatic heart failure patients and in asymptomatic patients with left ventricular dysfunction and previous heart failure symptoms.' *Journal of the American College of Cardiology*, 52(23) pp. 1834–1843.

Linde, C., Leclercq, C., Rex, S., Garrigue, S., Lavergne, T., Cazeau, S., McKenna, W., Fitzgerald, M., Deharo, J.-C., Alonso, C., Walker, S., Braunschweig, F., Bailleul, C. and Daubert, J.-C. (2002) 'Long-term benefits of biventricular pacing in congestive heart failure: results from the MUltisite STimulation in cardiomyopathy (MUSTIC) study.' *Journal of the American College of Cardiology*, 40(1) pp. 111–118.

Lipkin, D. P., Jones, D. A., Round, J. M. and Poole-Wilson, P. A. (1988) 'Abnormalities of skeletal muscle in patients with chronic heart failure.' *International Journal of Cardiology*, 18(2) pp. 187–195.

Lipkin, D. and Poole-Wilson, P. (1986) 'Symptoms limiting exercise in chronic heart failure.' *British medical journal (Clinical research ed.)*, 292, May, pp. 1030–1.

Lucia, A., Rabadan, M., Hoyos, J., Hernandez-Capilla, M., Perez, M., San Juan, A. F., Earnest, C. P., Chicharro, J. L. and web-support@bath.ac.uk (2006) 'Frequency of the VO2max plateau phenomenon in world-class cyclists.' *International Journal of Sports Medicine*, 27 pp. 984–992.

MacDonald, M. J., Naylor, H. L., Tschakovsky, M. E. and Hughson, R. L. (2001) 'Peripheral circulatory factors limit rate of increase in muscle O2 uptake at onset of heavy exercise.' *Journal of Applied Physiology*, 90(1) pp. 83–89.

MacDonald, M. J., Shoemaker, J. K., Tschakovsky, M. E. and Hughson, R. L. (1998) 'Alveolar oxygen uptake and femoral artery blood flow dynamics in upright and supine leg exercise in humans.' *Journal of Applied Physiology*, 85(5) pp. 1622–1628.

MacDonald, M. J., Tarnopolsky, M. A., Green, H. J. and Hughson, R. L. (1999) 'Comparison of femoral blood gases and muscle near-infrared spectroscopy at exercise onset in humans.' *Journal of Applied Physiology*, 86(2) pp. 687–693.

Maltais, F., LeBlanc, P., Whittom, F., Simard, C., Marquis, K., Bélanger, M., Breton, M. J. and Jobin, J. (2000) 'Oxidative enzyme activities of the vastus lateralis muscle and the functional status in patients with COPD.' *Thorax*, 55(10) pp. 848–853.

Mancini, D. M., Bolinger, L., Li, H., Kendrick, K., Chance, B. and Wilson, J. R. (1994) 'Validation of near-infrared spectroscopy in humans.' *Journal of Applied Physiology (Bethesda, Md.: 1985)*, 77(6) pp. 2740–2747.

Mancini, D. M., Coyle, E., Coggan, A., Beltz, J., Ferraro, N., Montain, S. and Wilson, J. R. (1989) 'Contribution of intrinsic skeletal muscle changes to 31P NMR skeletal muscle metabolic abnormalities in patients with chronic heart failure.' *Circulation*, 80(5) pp. 1338–1346.

Mancini, D. M., Eisen, H., Kussmaul, W., Mull, R., Edmunds, L. H. and Wilson, J. R. (1991) 'Value of peak exercise oxygen consumption for optimal timing of cardiac transplantation in ambulatory patients with heart failure.' *Circulation*, 83(3) pp. 778–786.

Mancini, Donna M., Henson, D., Lamanca, J. and Levine, S. (1994) 'Evidence of reduced respiratory muscle endurance in patients with heart failure.' *Journal of the American College of Cardiology*, 24(4) pp. 972–981.

Mancini, D. M., Walter, G., Reichek, N., Lenkinski, R., McCully, K. K., Mullen, J. L. and Wilson, J. R. (1992) 'Contribution of skeletal muscle atrophy to exercise intolerance and altered muscle metabolism in heart failure.' *Circulation*, 85(4) pp. 1364–1373.

Manns, P., R Tomczak, C., Jelani, A. and Haennel, R. (2010) 'Oxygen uptake kinetics: Associations with ambulatory activity and physical functional performance in stroke survivors.' *Journal of rehabilitation medicine : official journal of the UEMS European Board of Physical and Rehabilitation Medicine*, 42, March, pp. 259–64.

Massie, B., Conway, M., Yonge, R., Frostick, S., Ledingham, J., Sleight, P., Radda, G. and Rajagopalan, B. (1987) 'Skeletal muscle metabolism in patients with congestive heart failure: relation to clinical severity and blood flow.' *Circulation*, 76(5) pp. 1009–1019.

Massie, B. M., Simonini, A., Sahgal, P., Wells, L. and Dudley, G. A. (1996) 'Relation of systemic and local muscle exercise capacity to skeletal muscle characteristics in men with congestive heart failure.' *Journal of the American College of Cardiology*, 27(1) pp. 140–145.

Matcher, S., Kirkpatrick, P., Nahid, K., Cope, M. and T. Delpy, D. (1995) ‘Absolute quantification methods in tissue near-infrared spectroscopy.’ *In Proc SPIE*, pp. 486–495.

Matsumoto, A., Itoh, H., Yokoyama, I., Aoyagi, T., Sugiura, S., Hirata, Y., Kato, M. and Momomura, S. (1999) ‘Kinetics of oxygen uptake at onset of exercise related to cardiac output, but not to arteriovenous oxygen difference in patients with chronic heart failure.’ *The American Journal of Cardiology*, 83(11) pp. 1573–1576.

McCully, K. K., Iotti, S., Kendrick, K., Wang, Z., Posner, J. D., Leigh, J. and Chance, B. (1994) ‘Simultaneous in vivo measurements of HbO2 saturation and PCr kinetics after exercise in normal humans.’ *Journal of Applied Physiology (Bethesda, Md.: 1985)*, 77(1) pp. 5–10.

McDonough, P., Behnke, B. J., Padilla, D. J., Musch, T. I. and Poole, D. C. (2005) ‘Control of microvascular oxygen pressures in rat muscles comprised of different fibre types.’ *The Journal of Physiology*, 563(3) pp. 903–913.

Meakins, J. and Long, C. N. H. (1927) ‘Oxygen consumption, oxygen debt and lactic acid in circulatory failure.’ *Journal of Clinical Investigation*, 4(2) pp. 273–293.

Mezzani, A., Grassi, B., Jones, A. M., Giordano, A., Corrà, U., Porcelli, S., Della Bella, S., Taddeo, A. and Giannuzzi, P. (2013) ‘Speeding of pulmonary VO2 on-kinetics by light-to-moderate-intensity aerobic exercise training in chronic heart failure: clinical and pathophysiological correlates.’ *International Journal of Cardiology*, 167(5) pp. 2189–2195.

Middlekauff, H. R. (2010) ‘Making the Case for Skeletal Myopathy as the Major Limitation of Exercise Capacity in Heart Failure.’ *Circulation. Heart failure*, 3(4) pp. 537–546.

Minotti, J. R., Christoph, I., Oka, R., Weiner, M. W., Wells, L. and Massie, B. M. (1991) ‘Impaired skeletal muscle function in patients with congestive heart failure. Relationship to systemic exercise performance.’ *Journal of Clinical Investigation*, 88(6) pp. 2077–2082.

Moss, A. J., Brown, M. W., Cannom, D. S., Daubert, J. P., Estes, M., Foster, E., Greenberg, H. M., Hall, W. J., Higgins, S. L., Klein, H., Pfeffer, M., Wilber, D. and Zareba, W. (2005) ‘Multicenter Automatic Defibrillator Implantation Trial–Cardiac Resynchronization Therapy (MADIT-CRT): Design and Clinical Protocol.’ *Annals of Noninvasive Electrocardiology*, 10(s4) pp. 34–43.

Motobe, M., Murase, N., Osada, T., Homma, T., Ueda, C., Nagasawa, T., Kitahara, A., Ichimura, S., Kurosawa, Y., Katsumura, T., Hoshika, A. and Hamaoka, T. (2004) ‘Noninvasive monitoring of deterioration in skeletal muscle function with forearm cast immobilization and the prevention of deterioration.’ *Dynamic Medicine*, 3(1) p. 2.

Murgatroyd, S. R., Ferguson, C., Ward, S. A., Whipp, B. J. and Rossiter, H. B. (2011) 'Pulmonary O2 uptake kinetics as a determinant of high-intensity exercise tolerance in humans.' *Journal of Applied Physiology (Bethesda, Md.: 1985)*, 110(6) pp. 1598–1606.

Murias, J. M., Keir, D. A., Spencer, M. D. and Paterson, D. H. (2013) 'Sex-related differences in muscle deoxygenation during ramp incremental exercise.' *Respiratory Physiology & Neurobiology*, 189(3) pp. 530–536.

Musch, T., E Eklund, K., Hageman, K. and Poole, D. (2004) 'Altered regional blood flow responses to submaximal exercise in older rats.' *Journal of applied physiology (Bethesda, Md. : 1985)*, 96, February, pp. 81–8.

Myers, J., Prakash, M., Froelicher, V., Do, D., Partington, S. and Atwood, J. E. (2002) 'Exercise capacity and mortality among men referred for exercise testing.' *The New England Journal of Medicine*, 346(11) pp. 793–801.

Myers, J., Walsh, D., Sullivan, M. and Froelicher, V. (1990) 'Effect of sampling variability and plateau on oxygen uptake.' *Journal of applied physiology (Bethesda, Md. : 1985)*, 68, February, pp. 404–10.

Nagai, T., Okita, K., Yonezawa, K., Yamada, Y., Hanada, A., Ohtsubo, M., Morita, N., Murakami, T., Nishijima, H. and Kitabatake, A. (2004) 'Comparisons of the skeletal muscle metabolic abnormalities in the arm and leg muscles of patients with chronic heart failure.' *Circulation Journal: Official Journal of the Japanese Circulation Society*, 68(6) pp. 573–579.

Niemelä, K., Palatsi, I., Linnaluoto, M. and Takkunen, J. (1980) 'Criteria for maximum oxygen uptake in progressive bicycle tests.' *European Journal of Applied Physiology and Occupational Physiology*, 44(1) pp. 51–59.

Nilsson, K. R., Duscha, B. D., Hranitzky, P. M. and Kraus, W. E. (2008) 'Chronic heart failure and exercise intolerance: the hemodynamic paradox., Chronic Heart Failure and Exercise Intolerance: The Hemodynamic Paradox.' *Current cardiology reviews, Current Cardiology Reviews*, 4, 4(2, 2) pp. 92, 92–100.

Niwayama, M., Lin, L., Shao, J., Kudo, N. and Yamamoto, K. (2000) 'Quantitative measurement of muscle hemoglobin oxygenation using near-infrared spectroscopy with correction for the influence of a subcutaneous fat layer.' *Review of Scientific Instruments*, 71, December, pp. 4571–4575.

O'Driscoll, B. R., Howard, L. S. and Davison, A. G. (2008) 'BTS guideline for emergency oxygen use in adult patients.' *Thorax*, 63(Suppl 6) p. vi1.

Osawa, T., Kime, R., Hamaoka, T., Katsumura, T. and Yamamoto, M. (2011) 'Attenuation of Muscle Deoxygenation Precedes EMG Threshold in Normoxia and Hypoxia.' *Medicine & Science in Sports & Exercise*, 43(8) p. 1406.

Owan, T. E., Hodge, D. O., Herges, R. M., Jacobsen, S. J., Roger, V. L. and Redfield, M. M. (2006) 'Trends in Prevalence and Outcome of Heart Failure with Preserved Ejection Fraction.' *New England Journal of Medicine*, 355(3) pp. 251–259.

Özyener, F., Rossiter, H. B., Ward, S. A. and Whipp, B. J. (2001) 'Influence of exercise intensity on the on- and off-transient kinetics of pulmonary oxygen uptake in humans.' *The Journal of Physiology*, 533(Pt 3) pp. 891–902.

Pereira, M. I. R., Gomes, P. S. C. and Bhambhani, Y. N. (2007) 'A Brief Review of the Use of Near Infrared Spectroscopy with Particular Interest in Resistance Exercise.' *Sports Medicine*, 37(7) pp. 615–624.

Piiper, J. (2000) 'Perfusion, diffusion and their heterogeneities limiting blood–tissue O2 transfer in muscle.' *Acta Physiologica Scandinavica*, 168(4) pp. 603–607.

Piiper, J., Pendergast, D. R., Marconi, C., Meyer, M., Heisler, N. and Cerretelli, P. (1985) 'Blood flow distribution in dog gastrocnemius muscle at rest and during stimulation.' *Journal of Applied Physiology (Bethesda, Md.: 1985)*, 58(6) pp. 2068–2074.

Piña, I. L., Apstein, C. S., Balady, G. J., Belardinelli, R., Chaitman, B. R., Duscha, B. D., Fletcher, B. J., Fleg, J. L., Myers, J. N. and Sullivan, M. J. (2003) 'Exercise and Heart Failure: A Statement From the American Heart Association Committee on Exercise, Rehabilitation, and Prevention.' *Circulation*, 107(8) pp. 1210–1225.

Ponikowski, P., Anker, S. D., AlHabib, K. F., Cowie, M. R., Force, T. L., Hu, S., Jaarsma, T., Krum, H., Rastogi, V., Rohde, L. E., Samal, U. C., Shimokawa, H., Budi Siswanto, B., Sliwa, K. and Filippatos, G. (2014) 'Heart failure: preventing disease and death worldwide.' *ESC Heart Failure*, 1(1) pp. 4–25.

Poole, D. C., Barstow, T. J., McDonough, P. and Jones, A. M. (2008) 'Control of oxygen uptake during exercise.' *Medicine and Science in Sports and Exercise*, 40(3) pp. 462–474.

Poole, D. C., Hirai, D. M., Copp, S. W. and Musch, T. I. (2011) 'Muscle oxygen transport and utilization in heart failure: implications for exercise (in)tolerance.' *American Journal of Physiology-Heart and Circulatory Physiology*, 302(5) pp. H1050–H1063.

Poole, D. C. and Jones, A. M. (2012) 'Oxygen uptake kinetics.' *Comprehensive Physiology*, 2(2) pp. 933–996.

Poole, D. C. and Mathieu-Costello, O. (1989) 'Skeletal muscle capillary geometry: adaptation to chronic hypoxia.' *Respiration Physiology*, 77(1) pp. 21–29.

Poole, D. C., Schaffartzik, W., Knight, D. R., Derion, T., Kennedy, B., Guy, H. J., Prediletto, R. and Wagner, P. D. (1991) 'Contribution of excising legs to the slow component of oxygen uptake kinetics in humans.' *Journal of Applied Physiology*, 71(4) pp. 1245–1260.

Poole, D. C., Wagner, P. D. and Wilson, D. F. (1995) 'Diaphragm microvascular plasma PO2 measured in vivo.' *Journal of Applied Physiology*, 79(6) pp. 2050–2057.

Press, W. H. (ed.) (2007) *Numerical recipes: the art of scientific computing*. 3rd ed, Cambridge, UK ; New York: Cambridge University Press.

Racinais, S., Buchheit, M. and Girard, O. (2014) 'Breakpoints in ventilation, cerebral and muscle oxygenation, and muscle activity during an incremental cycling exercise.' *Frontiers in Physiology*, 5, April.

Renkin, E., Hudlicka, O. and Sheehan, R. (1966) 'Influence of metabolic vasodilatation on blood-tissue diffusion in skeletal muscle.' *American Journal of Physiology-Legacy Content*, 211(1) pp. 87–98.

Richardson, R. S., Duteil, S., Wary, C., Wray, D. W., Hoff, J. and Carlier, P. G. (2006) 'Human skeletal muscle intracellular oxygenation: the impact of ambient oxygen availability.' *The Journal of Physiology*, 571(2) pp. 415–424.

Richardson, Russell S., Haseler, L. J., Nygren, A. T., Bluml, S. and Frank, L. R. (2001) 'Local perfusion and metabolic demand during exercise: a noninvasive MRI method of assessment.' *Journal of Applied Physiology*, 91(4) pp. 1845–1853.

Richardson, R. S., Newcomer, S. C. and Noyszewski, E. A. (2001) 'Skeletal muscle intracellular Po2 assessed by myoglobin desaturation: response to graded exercise.' *Journal of Applied Physiology*, 91(6) pp. 2679–2685.

Richardson, R. S., Poole, D. C., Knight, D. R., Kurdak, S. S., Hogan, M. C., Grassi, B., Johnson, E. C., Kendrick, K. F., Erickson, B. K. and Wagner, P. D. (1993) 'High muscle blood flow in man: is maximal O2 extraction compromised?' *Journal of Applied Physiology*, 75(4) pp. 1911–1916.

Richardson, R., Wary, C., Wray, D. W., Hoff, J., Rossiter, H., Layec, G. and G Carlier, P. (2015) 'MRS Evidence of Adequate O2 Supply in Human Skeletal Muscle at the Onset of Exercise.' *Medicine and science in sports and exercise*, 47, March.

Richardson, T., A Kindig, C., Musch, T. and Poole, D. (2003) 'Effects of chronic heart failure on skeletal muscle capillary hemodynamics at rest and during contractions.' *Journal of applied physiology (Bethesda, Md. : 1985)*, 95, October, pp. 1055–62.

Riley, M., Wasserman, K., Fu, P. C. and Cooper, C. B. (1996) 'Muscle substrate utilization from alveolar gas exchange in trained cyclists.'

European Journal of Applied Physiology and Occupational Physiology, 72(4) pp. 341–348.

Rossiter, H. B. (2011) 'Exercise: Kinetic considerations for gas exchange.' *Comprehensive Physiology*, 1(1) pp. 203–244.

Rossiter, H. B., Howe, F. A., Ward, S. A., Kowalchuk, J. M., Griffiths, J. R. and Whipp, B. J. (2000) 'Intersample fluctuations in phosphocreatine concentration determined by 31P-magnetic resonance spectroscopy and parameter estimation of metabolic responses to exercise in humans.' *The Journal of Physiology*, 528(2) pp. 359–369.

Rossiter, H. B., Kowalchuk, J. M. and Whipp, B. J. (2006) 'A test to establish maximum O2 uptake despite no plateau in the O2 uptake response to ramp incremental exercise.' *Journal of Applied Physiology*, 100(3) pp. 764–770.

Rossiter, H. B., Ward, S. A., Kowalchuk, J. M., Howe, F. A., Griffiths, J. R. and Whipp, B. J. (2002) 'Dynamic asymmetry of phosphocreatine concentration and O(2) uptake between the on- and off-transients of moderate- and high-intensity exercise in humans.' *The Journal of Physiology*, 541(Pt 3) pp. 991–1002.

Ryan, T. E., Brophy, P., Lin, C.-T., Hickner, R. C. and Neufer, P. D. (2014) 'Assessment of in vivo skeletal muscle mitochondrial respiratory capacity in humans by near-infrared spectroscopy: a comparison with in situ measurements.' *The Journal of Physiology*, 592(15) pp. 3231–3241.

Ryan, T. E., Erickson, M. L., Brizendine, J. T., Young, H.-J. and McCully, K. K. (2012) 'Noninvasive evaluation of skeletal muscle mitochondrial capacity with near-infrared spectroscopy: correcting for blood volume changes.' *Journal of Applied Physiology*, 113(2) pp. 175–183.

Ryan, T. E., Southern, W. M., Reynolds, M. A. and McCully, K. K. (2013) 'A cross-validation of near-infrared spectroscopy measurements of skeletal muscle oxidative capacity with phosphorus magnetic resonance spectroscopy.' *Journal of Applied Physiology*, 115(12) pp. 1757–1766.

Saltin, B., Blomqvist, G., Mitchell, J. H., Johnson, R. L., Wildenthal, K. and Chapman, C. B. (1968) 'Response to exercise after bed rest and after training.' *Circulation*, 38(5 Suppl) pp. VII1-78.

Savarese, G. and Lund, L. H. (2017) 'Global Public Health Burden of Heart Failure.' *Cardiac Failure Review*, 3(1) pp. 7–11.

Saxon, L. and Ellenbogen, K. (2003) 'Resynchronization Therapy for the Treatment of Heart Failure.' *Circulation*, 108(9) pp. 1044–1048.

Schalcher, C., Rickli, H., Brehm, M., Weilenmann, D., Oechslin, E., Kiowski, W. and Brunner-La Rocca, H. P. (2003) 'Prolonged Oxygen Uptake Kinetics During Low-Intensity Exercise Are Related to Poor Prognosis in Patients

With Mild-to-Moderate Congestive Heart Failure*.' *Chest*, 124(2) pp. 580–586.

Seiyama, A., Hazeki, O. and Tamura, M. (1988) 'Noninvasive Quantitative Analysis of Blood Oxygenation in Rat Skeletal Muscle.' *Journal of biochemistry*, 103, April, pp. 419–24.

Severinghaus, J. W. (1979) 'Simple, accurate equations for human blood O2 dissociation computations.' *Journal of Applied Physiology: Respiratory, Environmental and Exercise Physiology*, 46(3) pp. 599–602.

Sietsema, K. E., Ben-Dov, I., Yu Zhang, Y., Sullivan, C. and Wasserman, K. (1994) 'Dynamics of Oxygen Uptake for Submaximal Exercise and Recovery in Patients With Chronic Heart Failure.' *Chest*, 105(6) pp. 1693–1700.

Sietsema, K. E., Cooper, D. M., Perloff, J. K., Rosove, M. H., Child, J. S., Canobbio, M. M., Whipp, B. J. and Wasserman, K. (1986) 'Dynamics of oxygen uptake during exercise in adults with cyanotic congenital heart disease.' *Circulation*, 73(6) pp. 1137–1144.

Southern, W. M., Ryan, T. E., Reynolds, M. A. and McCully, K. (2013) 'Reproducibility of near-infrared spectroscopy measurements of oxidative function and postexercise recovery kinetics in the medial gastrocnemius muscle.' *Applied Physiology, Nutrition, and Metabolism*, 39(5) pp. 521–529.

Spencer, M. D., Murias, J. M. and Paterson, D. H. (2012) 'Characterizing the profile of muscle deoxygenation during ramp incremental exercise in young men.' *European Journal of Applied Physiology*, 112(9) pp. 3349–3360.

Sperandio, P. A., Borghi-Silva, A., Barroco, A., Nery, L. E., Almeida, D. R. and Neder, J. A. (2009) 'Microvascular oxygen delivery-to-utilization mismatch at the onset of heavy-intensity exercise in optimally treated patients with CHF.' *American Journal of Physiology-Heart and Circulatory Physiology*, 297(5) pp. H1720–H1728.

Sperandio, P. A., Oliveira, M. F., Rodrigues, M. K., Berton, D. C., Treptow, E., Nery, L. E., Almeida, D. R. and Neder, J. A. (2012) 'Sildenafil improves microvascular O2 delivery-to-utilization matching and accelerates exercise O2 uptake kinetics in chronic heart failure.' *American Journal of Physiology. Heart and Circulatory Physiology*, 303(12) pp. H1474-1480.

Spires, J., Gladden, L. B., Grassi, B., Goodwin, M. L., Saidel, G. M. and Lai, N. (2013) 'Distinguishing the effects of convective and diffusive O2 delivery on V̇o2 on-kinetics in skeletal muscle contracting at moderate intensity.' *American Journal of Physiology-Regulatory, Integrative and Comparative Physiology*, 305(5) pp. R512–R521.

Spires, J., Lai, N., Zhou, H. and Saidel, G. M. (2011) 'Hemoglobin and Myoglobin Contributions to Skeletal Muscle Oxygenation in Response to Exercise.' LaManna, J. C., Puchowicz, M. A., Xu, K., Harrison, D. K., and Bruley, D. F. (eds) *Oxygen Transport to Tissue XXXII*, 701 pp. 347–352.

Stelken, A. M., Younis, L. T., Jennison, S. H., Douglas Miller, D., Miller, L. W., Shaw, L. J., Kargl, D. and Chaitman, B. R. (1996) 'Prognostic value of cardiopulmonary exercise testing using percent achieved of predicted peak oxygen uptake for patients with ischemic and dilated cardiomyopathy.' *Journal of the American College of Cardiology*, 27(2) pp. 345–352.

Stringer, W., J Whipp, B., Wasserman, K., Porszasz, J., Christenson, P. and French, W. (2005) 'Non-linear cardiac output dynamics during ramp-incremental cycle ergometry.' *European journal of applied physiology*, 93, April, pp. 634–9.

Stringer, W. W., Hansen, J. E. and Wasserman, K. (1997) 'Cardiac output estimated noninvasively from oxygen uptake during exercise.' *Journal of Applied Physiology*, 82(3) pp. 908–912.

Sullivan, M. J., Green, H. J. and Cobb, F. R. (1990) 'Skeletal muscle biochemistry and histology in ambulatory patients with long-term heart failure.' *Circulation*, 81(2) pp. 518–527.

Sullivan, M. J., Knight, J. D., Higginbotham, M. B. and Cobb, F. R. (1989) 'Relation between central and peripheral hemodynamics during exercise in patients with chronic heart failure. Muscle blood flow is reduced with maintenance of arterial perfusion pressure.' *Circulation*, 80(4) pp. 769–781.

Sun, Y. I., Ferguson, B. S., Rogatzki, M. J., McDonald, J. R. and Gladden, L. B. (2016) 'Muscle Near-Infrared Spectroscopy Signals versus Venous Blood Hemoglobin Oxygen Saturation in Skeletal Muscle.' *Medicine and Science in Sports and Exercise*, 48(10) pp. 2013–2020.

Suzuki, S., Takasaki, S., Ozaki, T. and Kobayashi, Y. (1999) 'Tissue oxygenation monitor using NIR spatially resolved spectroscopy.' *In Optical Tomography and Spectroscopy of Tissue III*. International Society for Optics and Photonics, pp. 582–593.

Taylor, H. L., Buskirk, E. and Henschel, A. (1955) 'Maximal Oxygen Intake as an Objective Measure of Cardio-Respiratory Performance.' *Journal of Applied Physiology*, 8(1) pp. 73–80.

Thomas, C. and Lumb, A. B. (2012) 'Physiology of haemoglobin.' *Continuing Education in Anaesthesia Critical Care & Pain*, 12(5) pp. 251–256.

Tran, T.-K., Sailasuta, N., Kreutzer, U., Hurd, R., Chung, Y., Mole, P., Kuno, S. and Jue, T. (1999) 'Comparative analysis of NMR and NIRS measurements of intracellular P O 2 in human skeletal muscle.' *American Journal of Physiology-Regulatory, Integrative and Comparative Physiology*, 276(6) pp. R1682–R1690.

Treacher, D. F. and Leach, R. M. (1998) 'Oxygen transport—1. Basic principles.' *BMJ*, 317(7168) pp. 1302–1306.

Van Beekvelt, M. C. P., Colier, W. N. J. M., Wevers, R. A. and Van Engelen, B. G. M. (2001) 'Performance of near-infrared spectroscopy in measuring local O2 consumption and blood flow in skeletal muscle.' *Journal of Applied Physiology*, 90(2) pp. 511–519.

Vogiatzis, I., Habazettl, H., Louvaris, Z., Andrianopoulos, V., Wagner, H., G Zakynthinos, S. and D Wagner, P. (2015) 'A method for assessing heterogeneity of blood flow and metabolism in exercising normal human muscle by near infrared spectroscopy.' *Journal of applied physiology (Bethesda, Md. : 1985)*, 118, January, p. jap.00458.2014.

Wagner, P. D. (1996) 'Determinants of Maximal Oxygen Transport and Utilization' p. 32.

Waldron, M., Jeffries, O. and Patterson, S. D. (2017) 'Inter-day reliability of Finapres® cardiovascular measurements during rest and exercise.'

Wasserman, K., Hansen, J., Sue, D. Y., Stringer, W., Sietsema, K. E., Sun, X.-G. and Whipp, B. J. (2011) *Principles of exercise testing and interpretation: Including pathophysiology and clinical applications: Fifth edition*.

Wasserman, K., Whipp, B. J., Koyl, S. N. and Beaver, W. L. (1973) 'Anaerobic threshold and respiratory gas exchange during exercise.' *Journal of Applied Physiology*, 35(2) pp. 236–243.

Weber, K. T., Kinasewitz, G. T., Janicki, J. S. and Fishman, A. P. (1982) 'Oxygen utilization and ventilation during exercise in patients with chronic cardiac failure.' *Circulation*, 65(6) pp. 1213–1223.

Weber, K. T., Wilson, J. R., Janicki, J. S. and Likoff, M. J. (1984) 'Exercise testing in the evaluation of the patient with chronic cardiac failure.' *The American Review of Respiratory Disease*, 129(2 Pt 2) pp. S60-62.

Weisman, I., M. (2003) 'ATS/ACCP Statement on Cardiopulmonary Exercise Testing.' *American Journal of Respiratory and Critical Care Medicine*, 167(2) pp. 211–277.

Whipp (1994) 'The slow component of O2 uptake kinetics during heavy exercise.' *Medicine & Science in Sports & Exercise*, 26(11) pp. 1319–1326.

Whipp, B. J., Davis, J. A., Torres, F. and Wasserman, K. (1981) 'A test to determine parameters of aerobic function during exercise.' *Journal of Applied Physiology: Respiratory, Environmental and Exercise Physiology*, 50(1) pp. 217–221.

Whipp, B. J., Ward, S. A., Lamarra, N., Davis, J. A. and Wasserman, K. (1982) 'Parameters of ventilatory and gas exchange dynamics during exercise.' *Journal of Applied Physiology: Respiratory, Environmental and Exercise Physiology*, 52(6) pp. 1506–1513.

Whipp, B. J., Ward, S. A. and Wasserman, K. (1986) ‘Respiratory markers of the anaerobic threshold.’ *Advances in Cardiology*, 35 pp. 47–64.

Whipp, B. J. and Wasserman, K. (1972) ‘Oxygen uptake kinetics for various intensities of constant-load work.’ *Journal of Applied Physiology*, 33(3) pp. 351–356.

Whipp, B. and Ward, S. (1992) *Pulmonary Gas Exchange Dynamics and the Tolerance to Muscular Exercise: Effects of Fitness and Training*.

Wiener, D. H., Fink, L. I., Maris, J., Jones, R. A., Chance, B. and Wilson, J. R. (1986) ‘Abnormal skeletal muscle bioenergetics during exercise in patients with heart failure: role of reduced muscle blood flow.’ *Circulation*, 73(6) pp. 1127–1136.

Williams, S. G., Cooke, G. A., Wright, D. J., Parsons, W. J., Riley, R. L., Marshall, P. and Tan, L. B. (2001) ‘Peak exercise cardiac power output; a direct indicator of cardiac function strongly predictive of prognosis in chronic heart failure.’ *European Heart Journal*, 22(16) pp. 1496–1503.

Wilson, J. R., Mancini, D. M., McCully, K., Ferraro, N., Lanoce, V. and Chance, B. (1989) ‘Noninvasive detection of skeletal muscle underperfusion with near-infrared spectroscopy in patients with heart failure.’ *Circulation*, 80(6) pp. 1668–1674.

Wilson, J. R., Martin, J. L., Schwartz, D. and Ferraro, N. (1984) ‘Exercise intolerance in patients with chronic heart failure: role of impaired nutritive flow to skeletal muscle.’ *Circulation*, 69(6) pp. 1079–1087.

Wilson, J. R., Rayos, G., Yeoh, T. K., Gothard, P. and Bak, K. (1995) ‘Dissociation between exertional symptoms and circulatory function in patients with heart failure.’ *Circulation*, 92(1) pp. 47–53.

Witte, K. K., Nikitin, N. P., De, R. S., Cleland, J. G. and Clark, A. L. (2004) ‘Exercise capacity and cardiac function assessed by tissue Doppler imaging in chronic heart failure., Exercise capacity and cardiac function assessed by tissue Doppler imaging in chronic heart failure.’ *Heart (British Cardiac Society), Heart*, 90, 90(10, 10) pp. 1144, 1144–1150.

Wolf, M., Ferrari, M. and Quaresima, V. (2007) ‘Progress of near-infrared spectroscopy and topography for brain and muscle clinical applications.’ *Journal of Biomedical Optics*, 12(6) p. 062104.

Wüst, R. C. I., Laarse, W. J. van der and Rossiter, H. B. (2013) ‘On–off asymmetries in oxygen consumption kinetics of single Xenopus laevis skeletal muscle fibres suggest higher-order control.’ *The Journal of Physiology*, 591(3) pp. 731–744.

Wüst, R. C. I., McDonald, J. R., Sun, Y., Ferguson, B. S., Rogatzki, M. J., Spires, J., Kowalchuk, J. M., Gladden, L. B. and Rossiter, H. B. (2014) ‘Slowed muscle oxygen uptake kinetics with raised metabolism are not

dependent on blood flow or recruitment dynamics.' *The Journal of Physiology*, 592(8) pp. 1857–1871.

Yoshida, T. and Watari, H. (1993) '31P-nuclear magnetic resonance spectroscopy study of the time course of energy metabolism during exercise and recovery.' *European Journal of Applied Physiology and Occupational Physiology*, 66(6) pp. 494–499.

Young, J. B., Abraham, W. T., Smith, A. L., Leon, A. R., Lieberman, R., Wilkoff, B., Canby, R. C., Schroeder, J. S., Liem, L. B., Hall, S., Wheelan, K. and Investigators, for T. M. I. I. R. C. E. (MIRACLE I. T. (2003) 'Combined Cardiac Resynchronization and Implantable Cardioversion Defibrillation in Advanced Chronic Heart Failure: The MIRACLE ICD Trial.' *JAMA*, 289(20) pp. 2685–2694.

Zelis, R., Flaim, S. F., Liedtke, A. J. and Nellis, S. H. (1981) 'Cardiocirculatory dynamics in the normal and failing heart.' *Annual Review of Physiology*, 43 pp. 455–476.

Zelis, R., Longhurst, J., Capone, R. J. and Mason, D. T. (1974) 'A comparison of regional blood flow and oxygen utilization during dynamic forearm exercise in normal subjects and patients with congestive heart failure.' *Circulation*, 50(1) pp. 137–143.

Zelis, R., Mason, D. T. and Braunwald, E. (1968) 'A comparison of the effects of vasodilator stimuli on peripheral resistance vessels in normal subjects and in patients with congestive heart failure.' *The Journal of Clinical Investigation*, 47(4) pp. 960–970.

Zelis, R., Sinoway, L., Musch, T. and Davis, D. (1988) *The peripheral distribution of cardiac output in heart failure*.

Zhang, C. Johnson, M., Chow, N. and Wasserman, K. (1991) 'Effect of exercise testing protocol on parameters of aerobic function.' *Medicine and science in sports and exercise*, 23, June, pp. 625–30.

Zhou, H., Lai, N., Saidel, G. M. and Cabrera, M. E. (2008) 'Multi-scale model of O2 transport and metabolism: response to exercise.' *Annals of the New York Academy of Sciences*, 1123, March, pp. 178–186.

Zuniga, J., J Housh, T., Camic, C., Bergstrom, H., Traylor, D., Schmidt, R. and O Johnson, G. (2012) 'Metabolic parameters for ramp versus step incremental cycle ergometer tests.' *Applied physiology, nutrition, and metabolism = Physiologie appliquee, nutrition et metabolisme*, 37, September.